



United Nations
Educational, Scientific and
Cultural Organization



International
Hydrological Programme
of UNESCO

Uncertainties in the 'monitoring-conceptualisation- modelling' sequence of catchment research

**11th Conference of the Euromediterranean Network of
Experimental and Representative Basins (ERB)
Luxembourg, 20 – 22 September 2006**

*Convened by:
Public Research Center – Gabriel Lippmann (Luxembourg) and
ERB, UNESCO/IHP (NE FRIEND Project 5)*

PROCEEDINGS

Edited by L. Pfister and L. Hoffmann

**Published in 2007 by the International Hydrological Programme (IHP) of the
United Nations Educational, Scientific and Cultural Organization (UNESCO)**
1 rue Miollis, 75732 Paris Cedex 15, France

**IHP-VI Technical Document in Hydrology N°81
UNESCO Working Series SC-2007/WS/54**

© UNESCO/IHP 2007

The designations employed and the presentation of material throughout the publication do not imply the expression of any opinion whatsoever on the part of UNESCO concerning the legal status of any country, territory, city or of its authorities, or concerning the delimitation of its frontiers or boundaries.

This publication may be reproduced in whole or in part in any form for education or nonprofit use, without special permission from the copyright holder, provided acknowledgement of the source is made. As a courtesy the authors should be informed of any use made of their work. No use of this publication may be made for commercial purposes.

Publications in the series of *IHP Technical Documents in Hydrology* are available from:

IHP Secretariat | UNESCO | Division of Water Sciences
1 rue Miollis, 75732 Paris Cedex 15, France
Tel: +33 (0)1 45 68 40 01 | Fax: +33 (0)1 45 68 58 11
E-mail: ihp@unesco.org
<http://www.unesco.org/water/ihp>

(SC-2007/WS/54)

UNCERTAINTIES IN THE 'MONITORING-CONCEPTUALISATION-MODELLING' SEQUENCE OF CATCHMENT RESEARCH

International conference, Luxembourg, September 20-22, 2006

Convened by:

European Network of Experimental and Representative Basins (ERB)
UNESCO IHP Northern European FRIEND Project 5

Organised by:

Centre de Recherche Public – Gabriel Lippmann, Belvaux (Luxembourg)

International Scientific Committee

- Piet Warmerdam, ERB international coordinator, Wageningen, The Netherlands
- Mitja Brilly, Ljubljana, Slovenia
- Wojciech Chelminski, Krakow, Poland
- François De Troch, Ghent, Belgium
- Francesc Gallart, Barcelona, Spain
- George Ivanov Gergov, Sofia, Bulgaria
- Ladislav Holko, Liptovsky Mikulas, Slovakia
- Hubert Holzmann, Vienna, Austria
- Jarmo Linjama, Helsinki, Finland
- Ian Littlewood, Wallingford, United Kingdom
- Franca Maraga, Torino, Italy
- Pavol Miklanek, Bratislava, Slovakia
- Pompiliu Mita, Bucharest, Romania
- Laurent Pfister, Belvaux, Luxembourg
- Manfred Spreafico, Bern, Switzerland
- Miroslav Tesar, Stachy, Czech Republic
- Stefan Uhlenbrook, Germany
- Daniel Viville, Strasbourg, France
- Sergei Zhuravin, St. Petersburg, Russia

International Organizing Committee

- Piet Warmerdam, International coordinator ERB
- Mike Bonell, IHP representative
- Ladislav Holko, NE FRIEND 5 coordinator
- Ian Littlewood, PUB representative
- Laurent Pfister, Local organizing committee chair
- Stefan Uhlenbrook, PUB representative

Local Organizing Committee at CRP-Gabriel Lippmann

- Rudi van den Bos
- Elisabeth Clot
- Hugo Hellebrand
- Lucien Hoffmann
- Jean-François Iffly
- Andreas Krein
- Olivier Marquis
- Patrick Matgen
- Bernard Perbal
- Laurent Pfister

Previous ERB conferences and proceedings

- October 1986 : Aix en Provence (France)
- October 1988 : Perugia (Italy)
Erosion and sediment transport.
European Network of Representative and Experimental Basins, 2nd General Meeting, Perugia. Associazione Italiana di Idronomia, Publ. No. 9, Padova, 1989, 203 pp.
- September 1990 : Wageningen (The Netherlands)
Hydrological research basins and the environment.
TNO Comm. on Hydrol. Res., Proc. and Informat. No. 44, The Hague, 347 pp.
- September 1992 : Oxford (United Kingdom)
Methods of hydrological basin comparison.
Institute of Hydrology Rep. No. 120, Wallingford, 198 pp.
- September 1994 : Barcelona (Spain)
Assessment of hydrological temporal variability and changes.
Acta Geol. Hisp., (Special Issue), vol. 28, no. 2-3, Barcelona, 1995, 138 pp.
- September 1996 : Strasbourg (France)
Ecohydrological processes in small basins.
Technical Documents in Hydrology 14, IHP UNESCO, Paris, 1997, 199 pp.
- September 1998 : Liblice (Czech Republic)
Catchment hydrological and biochemical processes in a changing environment.
Technical Documents in Hydrology 37, IHP UNESCO, Paris, 2000, 296 pp.
- September 2000 : Ghent (Belgium)
Monitoring and modelling catchment water quantity and quality.
Technical Documents in Hydrology 66, IHP UNESCO, Paris, 2003, 112 pp.
- September 2002 : Demänovská dolina (Slovakia)
Interdisciplinary approaches in small catchment hydrology: monitoring and research.
Technical Documents in Hydrology 67, IHP UNESCO, Paris, 2003, 256 pp.
- October 2004 : Torino (Italy)
Progress in surface and subsurface water studies at plot and small basin scale.
Technical Documents in Hydrology 77, IHP UNESCO, Paris, 2005, 194 pp.

PREFACE

The ERB network organises scientific conferences in the field of catchment hydrology every 2 years. During the ERB General Assembly that took place in September 2004 in Torino (Italy), the CRP-Gabriel Lippmann had been selected for organising the 2006 edition of the biennial conference cycle.

At a very early stage of the conference preparation process, it was decided to set the conference under the umbrella of the IAHS (International Association of Hydrological Sciences) initiative ‘PUB (Prediction in Ungauged Basins) decade’ and the UNESCO IHP Northern European FRIEND Project 5. Thanks to the financial support received from the FNR (National Research Fund) Luxembourg, the UNESCO-IHP (International Hydrological Programme), and private companies (OTT-Messtechnik, VWR, Campbell Scientific, ELSCOLAB, ARIAS), the organising committee had the opportunity to plan high quality keynote lectures on the one hand, and to financially help young scientists and researchers from East European countries to attend the ERB conference. By doing so, the organising committee already fulfilled one of the main goals of the ERB conferences, which is to bring young scientists and confirmed well-known researchers together.

Finally, a total of 115 registered participants from 25 countries attended the conference. In the book of abstracts a total of 87 contributions were included and distributed to each participant.

The conference programme was built around the general topic of uncertainties in hydrological sciences. Three sessions were dealing with uncertainties in the monitoring-conceptualisation-modelling sequence of catchment research. A fourth session was focusing on new developments in catchment hydrology, mainly with respect to the observation of hydrological processes. The fifth session was related to the PUB initiative of the IAHS.

The programme was built around five keynote lectures, given by invited speakers:

- Session 1 on ‘Uncertainties in hydro-climatological measurements’:

F. Gallart (Institute of Earth Sciences 'Jaume Almera', Barcelona, Spain), ‘Sediment measurement errors in relationship with temporal and spatial scales’.

- Session 2 on ‘Reduction of uncertainties in model concepts using experimental data’:

H.H.G. Savenije (TU Delft, Delft, The Netherlands), ‘Reducing model uncertainty in river basins by atmospheric convergence data and gravity observations from space’.

- Session 3 on ‘Calibration of hydrological models: coping with concept shortcomings and data uncertainties’:

B. Ambroise (Institut de Mécanique des Fluides et des Solides, Université de Strasbourg, France), ‘Some issues in the calibration of hydrological models: coping with concept shortcomings and data uncertainties’.

- Session 4 on ‘New ideas, developments and experiences in small basin research’:

T. Bogaard (Utrecht University, Utrecht, The Netherlands), ‘(Un)certain problems, ideas and developments in catchment hydrology’.

- Session 5 on ‘PUB – Prediction in Ungauged Basins’:

G. Blöschl (TU Wien, Vienna, Austria), ‘Rainfall-runoff modelling in ungauged basins’.

In total, 46 oral presentations and 41 poster presentations were given by the conference participants during the three days of the event.

For the poster presentations, special sessions were organised in order to give the scientists the opportunity to present their posters during 3 minutes to the audience. During the conference, session

discussions had been led in such a way that clear objectives previously defined by the ERB scientific committee had to be addressed and commented on with respect to the oral and poster presentations given. At the end of the conference, a final roundtable discussed to what extent the conference had helped making progress in the assessment and mitigation of uncertainties in catchment hydrology.

A half-day excursion to the Attert basin allowed the organisers to present the experimental catchments with their measuring devices operated in this Luxembourgish catchment, which is part of the ERB network.

This volume contains a wrap-up of the roundtable discussions, the papers related to 24 selected oral presentations, as well as the list of posters exhibited during the conference.

The editors are very grateful to the reviewers for their devotion and important scientific review work they have accomplished in the very large range of topics of the 11th ERB conference. The organisers of the conference would also like to thank the ERB coordinator, Piet Warmerdam, for his organisational support and scientific help throughout the preparation phase of the conference. The organisers are particularly grateful to UNESCO-IHP for having accepted to publish the proceedings in their series 'Technical documents in hydrology'.

These proceedings of the 11th ERB conference are dedicated to our late colleague and national ERB correspondent from Bulgaria, George Gergov.

CONFERENCE SYNTHESIS

The following provides a synthesis of the outcomes of the discussions that took place at the end of each conference session.

SESSION 1: 'UNCERTAINTIES IN HYDRO-CLIMATOLOGICAL MEASUREMENTS'

Objectives: Identify problems in obtaining accurate measurements and propose new approaches to tackle those difficulties.

Issues raised:

Precipitation measurements:

- Errors in rainfall measurements are a major issue (evolution of instrument accuracy, location, etc.). How then accurately determine spatial and temporal variability of rainfall, also with respect to climate change.
- Could meteorological radar measurements improve rainfall measurement accuracy? Currently, there is no other way than to couple radar measurements to ground measurements.

Groundwater modelling:

- The issue of transition probabilities in Markov chain techniques: High spatial density of field measurements is necessary for a better guessing of transition probabilities in the horizontal direction.
- Boreholes could be a way to investigate vertical probabilities to move from one soil type to another.

Conclusions:

A well-known problem in hydro-climatological measurements persists: how to get accurate and representative data?

Accuracy is a technical problem (instrument design, quality, location, etc.), while representativity is a strategic problem:

- what representativity are we looking for (spatial and temporal scales)?
 - what processes are relevant at what time and what scale? So, which processes to study?
- Use representative data to generalise (regionalise, transpose, etc.)? How to get from point to area?
- by multiplying measurements? What about representativity then?
 - by applying models, transposition techniques, interpolation, etc.

SESSION 2: 'REDUCTION OF UNCERTAINTIES IN MODEL CONCEPTS USING EXPERIMENTAL DATA'

Objectives: How to use experimental field data to elaborate and improve model concepts, as well as the consistency of model structures?

Issues raised:

Use of experimental data for the reduction of uncertainties in hydrological modelling:

Are uncertainties reduced or increased using orthogonal or additional data? The results of the GRACE project suggest: the accuracy of additional data cannot be guaranteed; thus, its use must be considered with restrictions and care.

A good approach could be to look at a model from different angles, i.e. which are the best data, the best configurations, etc. for the study site considered.

Input data quality:

Maybe output quality differences may also be the result of erroneous model structures, configurations, not only input data quality..., although the latter may be the most influential one.

If you have different catchments with similar characteristics then your parameter sets may also be similar, what happens if areas are very different?

How to regionalize input data effectively? Thiessen polygons in mountainous areas, is it successful? Yes, if the areas in the region are very similar, i.e. if the area is more or less homogeneous.

Uncertainties can be expressed in terms of the R determination coefficient but what about using MONTE CARLO simulations?

Comparing different models:

Care must be taken to keep model results close to observations while incorporating experimental data elements that are important for process simulation and thus to reduce uncertainties more effectively.

Conclusions:

When building model concepts, the following questions should always be asked: What should be measured? What are the collected data for?

It is essential to first understand ongoing processes, and provide related data to modelers. But field experimentalists and modellers do not have necessarily the same needs! There should be a better coordination between field experimentalists and conceptual hydrologists/modellers. On too many occasions there is a large discrepancy between the modellers' needs and the measurements they can rely on.

What is the impact of unknown data accuracy and spatio-temporal representativity on the modelling process?

Instead of trying out hundreds of model concepts and uncertainty assessment techniques, should we not rethink the interaction chain between field hydrologists (hydrologists, hydro-chemists, hydro-geologists) and modellers? In other words, the following questions should always be addressed :

- What does the modeller want to model?
- What processes does he need to model (or what process groups)?
- What does the modeller need in order to assess efficiently the internal consistency of his model?
- What can the field hydrologist offer him? What should he change in his experimental set-up?

We need to tighten the links between field hydrologists and modellers!

SESSION 3: 'CALIBRATION OF HYDROLOGICAL MODELS: COPING WITH CONCEPT SHORTCOMINGS AND DATA UNCERTAINTIES'

Objectives: Identify the problems linked with the use of 'uncertain data' in model development and calibration. The propagation of errors in the monitoring-conceptualisation-modelling sequence of catchment research is of particular relevance.

Issues raised:

Reducing uncertainties (what is needed):

Assessing uncertainty is needed no matter which kind of data or how much data there is. It is particularly needed for risk assessment. Experimental work is also critical. If we have a good idea and view on processes, it is possible to use simple, less complex models.

Likewise, there is a need for improved instrument calibration and improved identifiability of parameters.

What about sensitivity and inter-correlation of parameters that may hamper the model calibration? This is not an important issue in the case of simple models. Sensitivity analysis helps to get an idea on inter-correlation and thus reduces the issue.

Equifinality and GLUE are important concepts and tools.

Calibration in other domains (spectral) is useful: use of short (or old) time series to derive periodicity characteristics (esp. suitable for ungauged basins). Certain questions remain as to the invariability of the statistical characteristics.

Modellers should always be aware that climate change may require new model structures, concepts. Event intensities will change and maybe shorter time intervals should thus be worked on.

Conclusions:

Uncertainty assessment is an important issue in fundamental studies (new modelling approaches), as well as in applied research (for example risk assessment).

With climate variability/change becoming an important issue in hydrological studies, uncertainty assessment is of major importance. Are our data sets and modelling tools adapted to climate change studies ...?

Uncertainty assessment (both on data and model results) and internal model consistency assessment should both be a priority and pursued in parallel.

SESSION 4: 'NEW IDEAS, DEVELOPMENTS AND EXPERIENCES IN SMALL BASIN RESEARCH'

Objectives: Present the latest approaches and studies applied to small experimental basins. The ultimate goal of these studies is a better understanding of the components of the hydrological cycle (both in terms of runoff generation and of water acting as a vector for sediments, pollutants, etc.).

Issues raised:

Experimental hydrolog:

There is a clear need to adapt field measurements to back-up modelling at different scales.

It is important to identify model shortcomings: new observations can show limitations of model concepts and structures. In other words: model consistency should be assessed via field observations.

The identification of relevant runoff producing processes is essential: one has to be careful not to draw conclusions only from highly frequent events (small storms) and then transpose them to less frequent events (big storms).

Concept generalisation is dangerous and still too often applied in the model conceptualisation process.

The identification of dominating flow generating processes is a major issue, but very difficult to accomplish. Example: 'hortonian' overland flow often is treated as a dominating process, while subsurface processes might actually be as relevant, or even more important.

Another major issue lies in the fact that modellers often need information that they do not get from field observations. What measurements are most representative for one or several processes that are important in the rainfall-runoff generation? What has to be done when changing scales or changing basins?

Processes are changing very quickly in time and scale in a same area. Therefore, generalisations should be made extremely carefully.

Conclusions:

There is an urgent need for a better coordination of work between field hydrology/experiments and modellers. Model consistency should be assessed via field observations.

SESSION 5: 'PUB - PREDICTIONS IN UNGAUGED BASINS'

Objectives: Recent advances and developments in the PUB initiative.

In the context of 'reducing predictive uncertainty' (a key theme of PUB), oral presentations on new approaches or theory, new methodologies for more extensive use of remote sensing, *in situ* measurements, and conceptual modelling (water quantity and quality) of ungauged or poorly gauged basins have been presented.

ERB and Northern European FRIEND Project 5
International conference
**UNCERTAINTIES IN THE ‘MONITORING-CONCEPTUALISATION-MODELLING’
SEQUENCE OF CATCHMENT RESEARCH**
Luxembourg, September 20-22, 2006

TABLE OF CONTENTS

Organising committees	i
Previous ERB conferences and proceedings	ii
Preface	iii-iv
Conference synthesis	v-vii
Table of contents	viii-x

Session 1 : ‘Uncertainties in hydro-climatological measurements’

Dijksma, R., Torfs, P.J.J.F., Bier, G., Lanen, H.A.J. v., Bos, E.N. v.d. – *THE MARKOV CHAIN APPROACH: A USEFUL TECHNIQUE FOR THE DETERMINATION OF HETEROGENEITY IN A BROOK VALLEY FILL.*

..... p. 1-6

Doležal, F., Kulhavý, Z., Švihla, V., Čmelík, M., Fucík, P. – *UNCERTAINTY IN ESTIMATING RUNOFF AND WATER QUALITY CHARACTERISTICS IN AGRICULTURAL CATCHMENTS AND TILE DRAINAGE SYSTEMS.*

..... p. 7-13

Hoeven, P.C.T v.d., Warmerdam, P.M.M., Kole, J.W. – *EFFECT OF INACCURACY OF PRECIPITATION MEASUREMENTS ON THE WATER BALANCE OF THE CASTRICUM LYSIMETERS.*

..... p. 15-20

Krein, A., Salvia-Castellvi, M., Iffly, J.-F., Barnich, F., Matgen, P., v.d. Bos, R., Hoffmann, L., Hofmann, H., Kies, A., Pfister, L. – *UNCERTAINTY IN CHEMICAL HYDROGRAPH SEPARATION.*

..... p. 21-26

Session 2 : ‘Reduction of uncertainties in model concepts using experimental data’

Schumann, G., Hostache, R., Puech, C., Pappenberger, F., Matgen, P., Cutler, M., Black, A., Hoffmann, L., Pfister, L. – *MOVING TOWARD AN IMPROVED FLOOD-MODELLING CONCEPT USING REMOTE SENSING.*

..... p. 27-34

Somorowska, U. – *QUANTIFYING UNCERTAINTIES IN THE TERRESTRIAL WATER STORAGE – STREAMFLOW RELATION USING IN SITU SOIL MOISTURE DATA.*

..... p. 35-41

Session 3 : ‘Calibration of hydrological models : coping with concept shortcomings and data uncertainties’

Kiczko, A., Pappenberger, F., Romanowicz, R.J. – *FLOOD RISK ANALYSIS OF THE WARSAW REACH OF THE VISTULA RIVER.*

..... p. 43-49

Montanari, A., Toth, E. – *SPECTRAL MAXIMUM-LIKELIHOOD PARAMETERIZATION OF HYDROLOGICAL MODELS.*

..... p. 51-59

Session 4 : ‘New ideas, developments and experiences in small basin research’

Bača, P. – *HYDROGRAPH SEPARATION APPLIED TO THE INVESTIGATION OF THE SIGNIFICANCE OF FACTORS CONTROLLING SUSPENDED SEDIMENT DYNAMICS.*

..... p. 61-65

Chirila, G., Matreata, S. – *USE OF THE WATBAL MODEL FOR THE EVALUATION OF CLIMATE CHANGE IMPACT ON RUNOFF IN A SMALL RIVER BASIN.*

..... p. 67-73

Dijksma, R., Lanen, H.A.J. van, Hasan, S., Kroner, C., Troch, P.A. – *DISTRIBUTED WATER STORAGE AND LOCAL GRAVITY : A FIELD EXPERIMENT AT MOXA (GERMANY).*

..... p. 75-79

Gerrits, A.M.J., Savenije, H.H.G., Pfister, L. – *FOREST FLOOR INTERCEPTION MEASUREMENTS.*

..... p. 81-86

Gergov, G., Karagiozova, T. – *BED LOAD SAMPLERS FOR PRACTICAL USE.*

..... p. 87-92

Hernández-Santana, V., Martínez-Fernández, J., Morán, C., Cano-Crespo, A. – *MEASUREMENT OF SOIL AND TREE WATER CONTENT IN TWO MEDITERRANEAN FORESTED CATCHMENTS USING TIME DOMAIN REFLECTOMETRY.*

..... p. 93-99

Herrmann, A., Schumann, S., Thies, R., Duncker, D. Stichler, W. – *INVESTIGATIONS OF THE RUNOFF GENERATION PROCESS IN LANGE BRAMKE BASIN, HARZ MOUNTAINS, GERMANY USING ENVIRONMENTAL AND ARTIFICIAL TRACERS.*

..... p. 101-108

Mul, M.L., Uhlenbrook, S., Mutiibwa, R.K., Foppen, J.W., Savenije, H.H.G. – *SURFACE WATER / GROUNDWATER SYSTEMS ANALYSIS IN THE SEMI-ARID SOUTH-PARE MOUNTAINS, TANZANIA.*

..... p. 109-115

Penna, D., Borga, M., Boscolo, P., Dalla Fontana, G. – *DISTRIBUTION OF SOIL MOISTURE OVER DIFFERENT DEPTHS IN A SMALL ALPINE BASIN.*
..... p. 117-124

Šanda, M., Novák, L., Císlarová, M. – *TRACING OF THE WATER FLOWPATHS IN A MOUNTAINOUS WATERSHED.*
..... p. 125-131

Session 5 : ‘Predictions in ungauged basins’

Bormann, H., Breuer, L., Croke, B.F.W., Gräff, T., Hubrechts, L., Huisman, J.A., Kite, G.W., Lanini, J., Leavesley, G., Lindström, G., Seibert, J., Viney, N.R., Willems, P. – *REDUCTION OF PREDICTIVE UNCERTAINTY BY ENSEMBLE HYDROLOGICAL MODELLING OF DISCHARGE AND LAND USE CHANGE EFFECTS.*
..... p. 133-139

Brocca, L., Melone, F., Moramarco, T. – *STORM RUNOFF ESTIMATION BASED ON THE SOIL CONSERVATION SERVICE – CURVE NUMBER METHOD WITH SOIL MOISTURE DATA ASSIMILATION.*
..... p. 141-148

Littlewood, I.G. – *RAINFALL–STREAMFLOW MODELS FOR UNGAUGED BASINS: UNCERTAINTY DUE TO MODELLING TIME-STEP.*
..... p. 149-155

Matreata, S., Matreata, M. – *APPLICATION OF FUZZY LOGIC SYSTEMS FOR THE ELABORATION OF AN OPERATIONAL HYDROLOGICAL WARNING SYSTEM IN UNGAUGED BASINS.*
..... p. 157-162

Mita, P., Corbus, C., Matreata, S. – *FLOOD FORECAST METHOD USING DATA FROM REPRESENTATIVE BASINS.*
..... p. 163-171

Uriburu Quirno, M., Borús, J., Goniadzki, D. – *CONTINUOUS HYDROLOGIC MODELING OF MIDDLE URUGUAY TRIBUTARY FLOWS.*
..... p. 173-181

Van den Bos, R., Matgen, P., Pfister, L. – *SEARCHING FOR AN OPTIMUM LEVEL OF SPATIAL DISTRIBUTION AND COMPLEXITY IN REGIONAL MODELLING.*
..... p. 183-188

ANNEX: POSTERS PRESENTED AT THE CONFERENCE..... p. 189-192

THE MARKOV CHAIN APPROACH: A USEFUL TECHNIQUE FOR THE DETERMINATION OF HETEROGENEITY IN A BROOK VALLEY FILL

R. Dijkma¹, P.J.J.F. Torfs¹, G. Bier², H.A.J. v. Lanen¹ & E.N. v.d. Bos¹

¹Hydrology and Quantitative Water Management Group, Wageningen University, Wageningen, the Netherlands. ²Soil Physics, Ecohydrology and Groundwater Management Group, Wageningen University, the Netherlands. ³Tauw, Deventer, the Netherlands.
Corresponding author: Roel Dijkma, email: roel.dijkma@wur.nl

ABSTRACT

Holocene valley fill material in old stream beds are generally composed of weathering material from the hills. The grain size can vary from gravel to clay. The spatial distribution of the valley fill material can be simulated by using the Markov chain approach. The transition probabilities of this approach indicate the chance that one type of sediment is changing into another sediment type. The concept, which normally is used as time dependent and one-dimensional, is adapted to enable the simulation of spatial variability in more dimensions. In the Noor catchment, located in the chalk region in the south of the Netherlands, the lowermost part of the valley is filled up during Holocene with such valley fill sediments. Field experiments showed a significant small scale variation in hydraulic heads and chemical composition in this valley fill. By using the Markov chain technique 100 equally probable realizations are constructed, using well logs from drillings in the valley fill as known profiles. With these realizations 100 steady-state MODFLOW models are constructed. The influence of gravel and sand beds on the groundwater flow is determined with a statistical analysis of the modelling results. It could be concluded that the realizations of the valley fill have the same statistical properties, but the differences in the occurrence of the sediment layers are large. So the technique used here can not be used to predict the occurrence of a particular sediment type in a particular cell, but it could be used to predict the occurrence of continuous coarse grained layers in a predominantly fine grained valley fill and also the possible effect of these layers on the groundwater flow.

Keywords: Spatial distribution of sediments, groundwater flow, valley fill, Markov chains, modelling, MODFLOW, field data

Introduction

Holocene sediments are often found in catchments as valley fill in the old stream bed. Such sediments are composed of weathering material from the hills, often varying from gravel to clay. Streams normally do not mix these sediments, but create coarse gravel beds in the stream bed and fine grained layers in the back swamps. Highly heterogeneous flow patterns will be the result. An example of a brook with a heterogeneous valley fill is the Noor brook. This brook is located in the Netherlands, close to Maastricht (Fig. 1). The catchment is part of a plateau and valley landscape. The surrounding hills consist of Cretaceous siltstone and chalk formations. During Pleistocene the stream has been predominantly cutting into these formations (ice ages). During Holocene sedimentation of clays, sands and gravels in the lowermost part of the valley prevailed, forming an approximately 6m thick valley fill, with nature reserve as dominant land use (Van Lanen and Dijkma, 2004). From this geomorphological context, it can be expected that the Noor brook formed coarse gravel beds in the stream bed and fine grained layers in the back swamps. Where vertical flow prevails in the predominantly fine grained valley fill, the gravel and sand beds can trigger horizontal preferential flow lines, or even small aquifers.

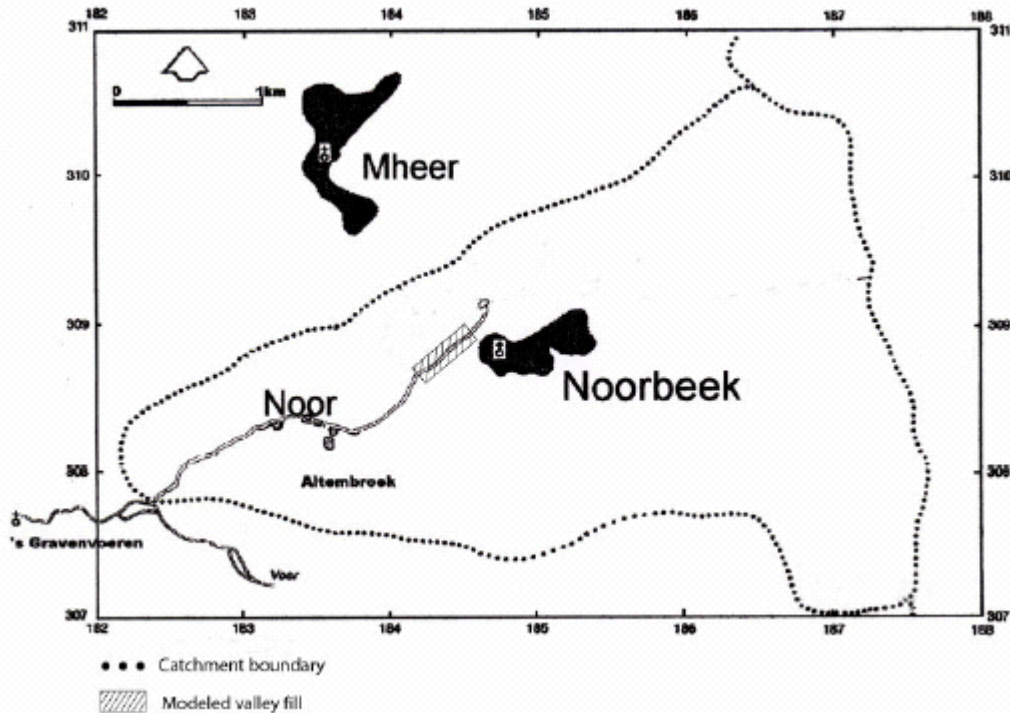


Fig. 1: The Noor catchment (Van Lanen and Dijkma, 2004).

Hydrogeological research in the valley fill showed that seepage conditions prevail, but with an irregular head distribution (Van Lanen and Dijkma, 2004; Klonowski, 1997; Klonowski et al., 2001). Also the chemical composition of the groundwater in the valley fill showed a large variation on a local scale. These variations could not be explained with the concept of a homogeneous sediment distribution. So the concept of a heterogeneous sediment distribution was tested. As is the case in most other hydrogeological research in catchments, only little information is available on the geological profile: the point information from the available drillings. In the valley fill of the Noor 39 drillings were available, with variable depth (1 – 8 m below surface). The objective of this research was to investigate the probability of more or less continuous permeable layers in the predominantly fine grained sediments, based upon these 39 drillings, by using the Markov chain approach (Carle, 1999; Carle and Fogg, 1997; Elfeki and Dekking, 2001) and MODFLOW modelling (McDonald and Harbaugh, 1988).

Methodology

One of the basic tools for the research of this paper was the simulation of the sediment distribution in the subsurface. This requires a very flexible type of stochastic modelling tool. The classical technique of Gaussian processes (as used in kriging) cannot be applied, as the observed transition between the different sediment types can possibly be modelled by correlations (or the equivalent variograms) only. In one (time) dimension, so called Markov processes are the most used alternative to Gaussian processes. Usually they are defined on a space consisting of a finite number of states. In the application envisaged by this paper, these states will be different soil types. A Markov chain is then a random sequence of these states, where the transition probability to go from one state to the other is defined by a transition matrix (see also Fig. 2). A probability on a finite number of states can be represented by a wheel of fortune: each state has a section and the fraction size of the section corresponds to the probability. Using this, a Markov transition matrix can be represented by a number of wheels: the colour in the centre of the wheel is the starting colour (the row number in the matrix), the wheel is partitioned according to the probabilities listed in that row, as illustrated by Fig. 2.

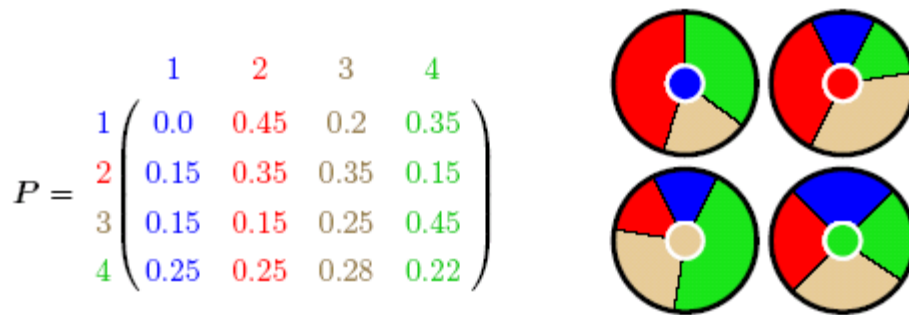


Fig. 2: An example of a transition matrix on four states and a graphical representation of the same matrix by means of ‘wheels of fortune’. Each row of the matrix is a probability on four states (each state has its own colour), and can thus be represented by a wheel of fortune. The colour in the centre of the wheel corresponds to the row.

Once the transition matrix is given, simulation is an easy programmable and fast procedure (Fig. 3). The wheel with the colour of the current cell is turned, the result is the value for the next cell.

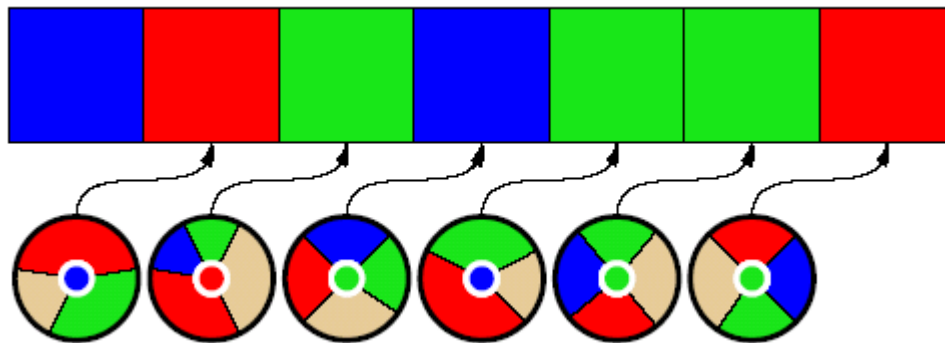


Fig. 3: Markov chain simulation.

One of the powerful properties of Markov chains is that many aspects can be calculated using just linear algebra (as is also the case for Gaussian processes). The probability for ending up in state j starting from state i in n steps e.g. is given by $P^n(i,j)$, where P^n is the n^{th} power of the matrix P . These algebraic results can also be used to make conditional simulations. This was very useful in this study, since there is information available on the geological profile at the drilling locations. Fig. 4 shows an example of the problem. The content of cell 0 and 5 is known, thus fixing start and finish conditions. One way to solve this problem would be the trial and error technique, i.e. perform all possible simulations, and only keep those that end up in the correct conditions in cell 5.

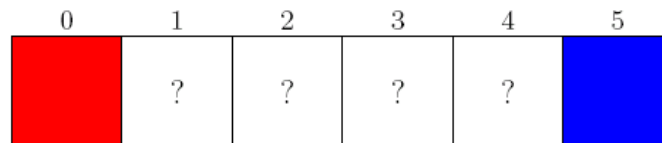


Fig. 4: Conditional simulation problem.

The simulation can however enormously be accelerated by using Eq. 1:

$$\Pr ob[X(2)=j \text{ given } X(1)=i \text{ and } X(6)=k] = \frac{P(i,j)P^4(j,k)}{P^5(i,k)} \quad \text{Eq 1}$$

Using this formula, a new wheel of fortune can easily be calculated for each step in the conditional simulation, thus avoiding tedious unsuccessful simulations, as illustrated by Fig 5.

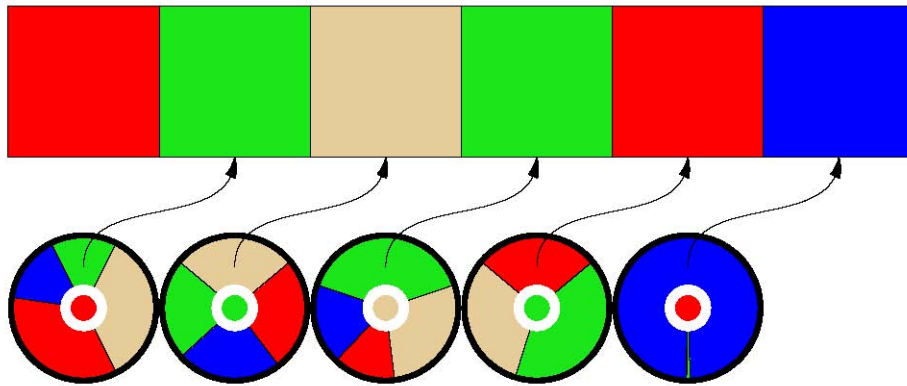


Fig. 5: Conditional simulation, the result.

Using the same calculation power, two (and more) dimensions can efficiently be simulated. Fig 6 illustrates a problem to be solved (left) and the result (right). In order to simulate a new cell, both the cells below and to the left should be taken as starting point. The brute force method: keep on simulating both vertically and horizontally until (by chance) they agree. This technique can again be replaced by using a new wheel of fortune. The equation used will be rather complex, but involves only linear algebra. Simulating a complete field, as in Fig. 6, can thus be done very efficiently.

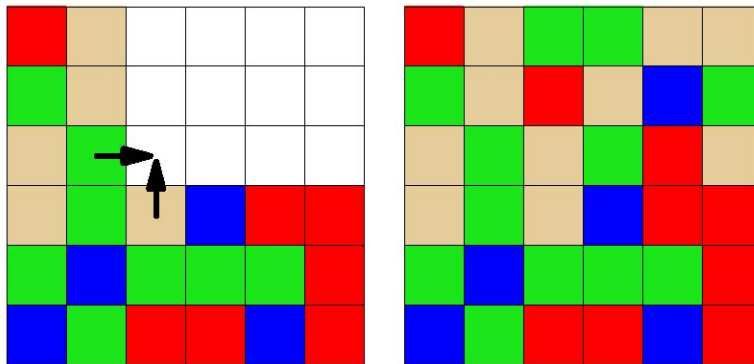


Fig. 6: Generalizing the Markov chain technique to two dimensions.

Generalizing this simulation and conditioning to three dimensions is non trivial, but can be done (Carle and Fogg, 1997; Elfeki and Dekking, 2001) and generates general fields which cannot be obtained by Kriging. Another problem to be solved is how to find such a transition probability that fits best observed transitions.

The T-PROGS program (Carle, 1999) as implemented in GMS (Groundwater Modelling System), a pre-and postprocessor for several flow codes, enables the modeller to setup a statistical large enough ensemble of equally probable MODFLOW models. The output of these models is used to analyse the effect on groundwater flow. Using T-PROGS requires however some knowledge of the technical aspects of the theory. The program also contains ways of fitting the probabilities, helped by graphics.

Results and discussion

Fig. 7 shows the top and three-dimensional views of two of the hundred realizations. The sediments (i.e. silt

(white), gravel (red), sand (pink) and clay (blue)) show a layered structure. Peat (green) is only present in small patches.

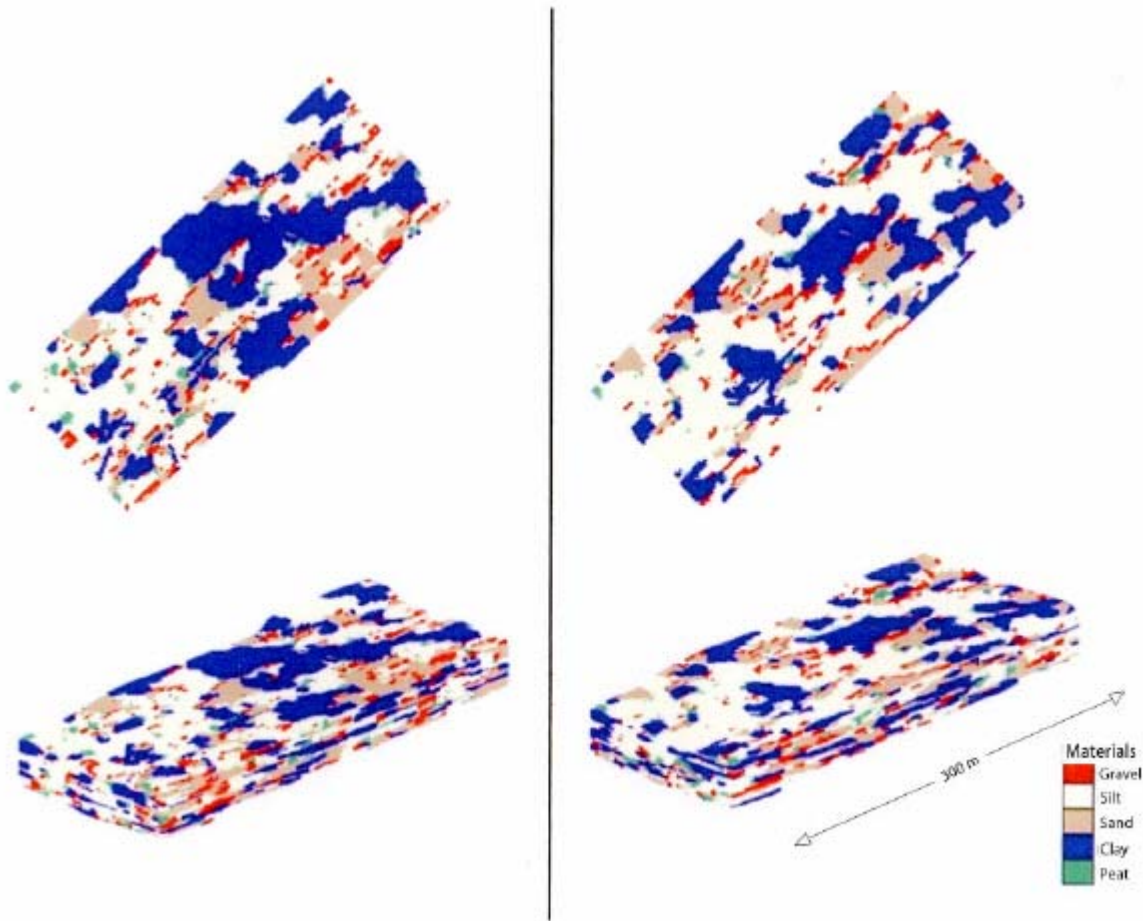


Fig. 7: Top and three-dimensional views of two realizations of the valley fill in the Noor valley (Van den Bos, 2005).

These, in this case 100, three-dimensional realisations were simulated in MODFLOW. The most important question was whether the models would predict horizontal flow through the more permeable layers. The stream was divided in a number of segments. For each of these segments it was determined whether there could be a horizontal flow component and, in the 100 realizations, which flow route these models indicate. In Fig. 8 two randomly chosen segments and the statistical distribution of the flow routes were given. A grid cell with a high percentage in Fig. 8 indicates that a high percentage of the realizations resulted in flow through this grid cell towards the specified stream segment. In both segments horizontal flow towards the stream is indicated. This implies that there is a fair chance that the predominant vertical (upward) flow through the valley fill is interrupted on a local scale by horizontal transport and redistribution of water. This might explain the irregular hydraulic head profiles and the irregular chemical composition of groundwater in the valley fill. Such irregularities in head/seepage and chemical composition have significant effects on the vegetation development.

In this study the valley fill is represented by a rectangular block. Since valley fill in reality has a predominantly irregular shape, further research is focusing on the implementation of the Markov chain approach in such an irregularly shaped volume. Then the Markov chain approach will be a very useful tool to investigate the spatial distribution of sediments in heterogeneous systems. Such information is needed for a solid understanding of water flow and transport of dissolved solids in such systems.

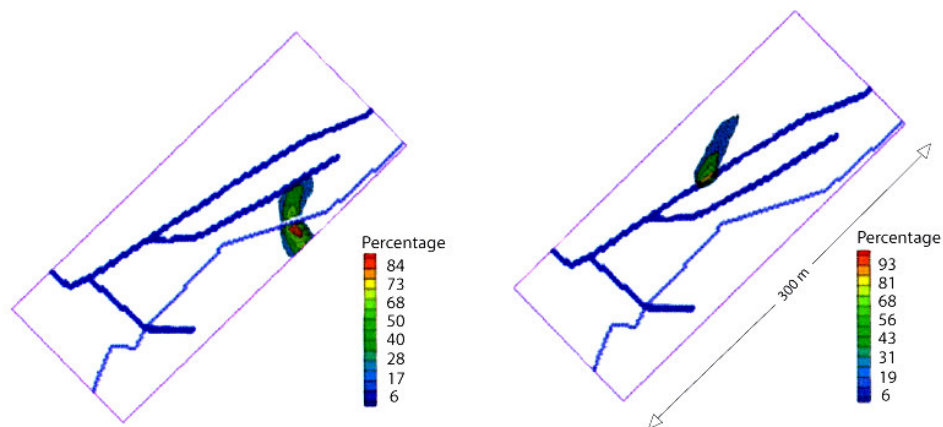


Fig. 8: Water flow through gravel beds towards the stream as an image of the statistical distribution of all realizations (Van den Bos, 2005).

References

- Bos E.N. van den (2005). *Influence of the Heterogeneity in the Valley Fill of the Noor Valley (South-Limburg) on the Groundwater Flow*. MSc thesis, Wageningen University, Wageningen, the Netherlands.
- Carle S.F. (1999). *T-PROGS; Transition Probability Geostatistical Software*, version 2.1. Hydrologic Sciences Group, University of California, Davis.
- Carle S.F., Fogg G.E. (1997). Model spatial variability with one-and multi-dimensional Markov chains. *Mathematical Geology*, 28: 891-918.
- Elfeki A., Dekking M. (2001). A Markov chain model for subsurface characterization: theory and applications. *Mathematical Geology*, 33: 569-589.
- Klonowski M. (1997). *Water Flow and Migration of Nitrate in the Chalk Catchment of the Noor Brook and Impact on the Noorbeemden Nature Reserve*. MSc thesis, sub-department Water Resources, Wageningen University, the Netherlands.
- Klonowski M., Lanen H.A.J. van, Dijksma R. (2001). Groundwater flow and nitrate migration in a Dutch-Belgian chalk catchment: observed and future concentrations. *Geological Quarterly*, 45: 53-65.
- Lanen H.A.J. van, Dijksma R. (2004). Impact of groundwater on surface water quality: role of the riparian area in nitrate transformation in a slowly responding chalk catchment (Noor, the Netherlands). *Ecology & Hydrobiology*, 4: 315-325.
- McDonald M.G., Harbaugh A.W. (1988). *A Modular Three-Dimensional Finite-Difference Ground Water Flow Model*. Techniques of Water-Resources Investigations of the United States Geological Survey, Washington, USA.

UNCERTAINTY IN ESTIMATING RUNOFF AND WATER QUALITY CHARACTERISTICS IN AGRICULTURAL CATCHMENTS AND TILE DRAINAGE SYSTEMS

F. Doležal¹, Z. Kulhavý², V. Švihla³, M. Čmelík⁴ & P. Fučík¹

¹Research Institute for Soil and Water Conservation, Žabovřeská 250, 156 27 Praha 5 - Zbraslav, Czech Republic. ²Research Institute for Soil and Water Conservation, Boženy Němcové 2625, 530 00 Pardubice, Czech Republic. ³Private consultant, Fügnerova 809, 266 01 Beroun, Czech Republic. ⁴Research Institute for Soil and Water Conservation, Sládkova 849, 539 73 Skuteč, Czech Republic.
Corresponding author: F. Doležal, email: dolezal@vumop.tel.cz

ABSTRACT

The paper presents partial results of research on runoff and water quality generation in small agricultural catchments in the Bohemian highlands, with special regard to the role of tile drainage. Flow separation and mixing analysis procedures, used and described in previous papers, are now applied not only to the period of observation as a whole but also to sub-periods (either individual hydrological years or several consecutive hydrological years). Results from three experimental catchments and two tile drainage systems located in one of these catchments are given. Two independent flow separation methods, namely, a simple conceptual model GROUND and a digital filter method, are applied to obtain daily series of three flow components: direct runoff, interflow and baseflow. GROUND was successfully validated by comparison with the manual recession limb analysis. The proportions of the three flow components vary from year to year, but individual catchments and tile-drainage systems retain their typical features, visible in the graphs and statistically identifiable. These proportions, if related to other catchments properties, can help us classify the catchments and differences between them. A simple mixing analysis, using nitrate concentration data, was applied to the same catchments and tile drainage systems. Characteristic nitrate concentrations of the three flow components, if estimated for five-year sub-periods, vary considerably from sub-period to sub-period. Neither the differences among flow components in terms of characteristic concentrations nor the patterns of temporal variations of these concentrations can be regarded as significant unless they are confirmed by a more detailed analysis.

Keywords: water quality, agricultural catchments, GROUND model

Introduction

Runoff separation, in the most general sense, corresponds to a distinction between various portions of water passing either simultaneously or at different times through the closing profile of a catchment. It is based on direct or indirect indications of where these portions come from. Each separation method is capable of distinguishing some partial runoff features, while a whole assemblage of methods is needed in order to arrive at a comprehensive picture. The separation methods used in this paper rely on the runoff information itself, without considering other data (such as precipitation, water table, chemical composition, etc.). The potential of these methods to characterise runoff patterns in small catchments and tile drainage systems was investigated by Doležal et al. (2003). A set of two complementary methods, namely, the simple conceptual model GROUND and a digital filter method, was found to give a reasonable overall picture of the catchment in terms of three runoff components, referred to as direct flow (the quickest), interflow (the intermediate) and baseflow (the slowest).

Mixing analyses, such as EMMA (end-member mixing analysis, cf. Christophersen et al., 1990), play an important role in deciphering water quality generation processes. A simple mixing analysis, based on the assumption of constant nitrate concentration in any of the three runoff components named above, was presented by Doležal and Kvítek (2004). Their conclusions were based on the data from a single catchment (Kopaninský tok) and seemed to persuasively indicate that the interflow, short-circuited by tile drainage, was

the main nitrate polluter of the stream. The same analysis was repeated later for several other catchments (Doležal et al., 2005). However, the hypothesis raised by Doležal and Kvítek (2004) was not fully confirmed. While the interflow still looked like being the “main polluter” in a slight majority of cases, baseflow or direct runoff could also be the most polluted components.

This paper, the authors hope, makes a step forward in their ongoing studies of runoff and water quality formation processes in small agricultural catchments, especially in the Bohemian and Moravian highlands, in which a considerable part of the land is tile-drained. This paper aims at:

- a) a further validation of the GROUND method of direct flow separation,
- b) an exploration of the temporal variability (and, thereby, the uncertainty) of the three-component runoff separation procedure based on the methods used hitherto,
- c) an exploration of the temporal variability (and, thereby, the uncertainty) of the simple mixing analysis used hitherto.

Methods and materials

Water flow rate was measured continuously in closing profiles of small streams and tile-drainage manholes in several small catchments of Central and East Bohemia. The catchments analysed in this paper are described in Table 1 and the tile drainage systems are characterised in Table 2. The daily flow series, rather than the instantaneous flow hydrographs, were used for the analysis because they were readily available, while the instantaneous flow data have not yet been fully digitised. The hydrological years (from November of the previous year to October of the current year) subject to the analysis are also indicated in Tables 1 and 2. No data were available for the Dolský potok and the Kotelský potok from 1994 to 1996. The contribution of tile-drainage runoff to the total stream runoff in the catchments studied is not known exactly, because not all tile drainage systems are monitored. It is estimated to vary between 10 and 30% of the annual stream runoff.

Table 1: Overview of experimental catchments

Catchment:	Černičí	Dolský potok	Kotelský potok
Latitude, longitude	49°37'N, 15°09'E	49°47'N, 15°59'E	49°47'N, 15°59'E
Altitude (m a.s.l.)	462 - 562	456 - 676	438 - 663
Area (km ²)	1.39	4.78	3.22
% arable land	75	68	76
% grassland	8	7	10
% forest	16	1	3
% tile-drained	30	30	56
Annual precipitation	724 mm (1961-90)	764 mm (1901-50)	764 mm (1901-50)
Average temperature	7.3 °C (1961-90)	6.3 °C (1901-50)	6.3 °C (1901-50)
Soil texture	sandy loam	loam	loam
Main soil type	Cambi-/Stagnosol	Cambi-/Stagnosol	Cambi-/Stagnosol
Main parent rock	paragneiss	phyllite	phyllite
Hydrological years	1992-2005	1983-93, 1997-2005	1983-93, 1997-2005

Two independent flow separation methods were applied to the daily flow series, namely the GROUND method by Doležal, described by Kulhavý et al. (2001), and the digital filter method by Chapman and Maxwell (referred to below as “Filter 1”), described by Grayson et al. (1996). GROUND is a very simple conceptual model for which the stream hydrograph is the single input. It assumes that the slow runoff component reacts

with a one time step (typically, one day) delay upon the onset of the total flow rise. The intensity of reaction is determined by a dimensionless parameter C, which denotes the initial ratio between the rate of the total flow rise and the rate of the slow flow component rise. As long as the total flow hydrograph remains convex, this ratio gradually increases, otherwise it remains unchanged. The slow flow component ceases to rise as soon as it becomes equal to total flow or, under certain conditions, one time step earlier. Hence, the slow flow pattern is derived from the total flow pattern, which itself is mainly determined by the direct runoff pattern. The method is therefore suitable for separation of the direct runoff from the rest of the flow (the sum of interflow and baseflow). In this paper, the parameter C was taken as 0.075, the same as in all previous calculations.

In order to make GROUND more trustworthy, its results were compared with those of the classical recession limb analysis (cf. Chow, 1964) for 19 selected events in the Černičí catchment. The method approximates the recession limb of a “well-developed” flood hydrograph with a broken line, consisting of three straight intercepts. The last straight intercept is then extrapolated backwards up to the time of flood peak. Its terminal point, lying just under the peak, is connected with the starting point of the rising limb of the same hydrograph. In this way, the slow component hydrograph is obtained. The selection of suitable floods, the fitting of the recession limbs to broken lines and the choice of the starting points of the rising limbs were done manually. The quick and the slow component volumes for each flood hydrograph, for either of the two methods (GROUND and the recession analysis), were obtained by numerical integration between the start of the rising limb and the end of the second intercept of the recession limb approximation.

Filter 1 was chosen mainly because of its computational simplicity. It is based on the recurrent equation:

$$Q_{total} = Q_{quick} + Q_{slow} ; \quad Q_{slow}(i) = \frac{k}{2-k} Q_{slow}(i-1) + \frac{1-k}{2-k} Q_{total}(i) \quad \text{Eq. 1}$$

$$Q_{slow}(i) \leq Q_{total}(i)$$

where Q(i) is the average daily flow on i-th day, either the total flow or the slow component or the quick component (as indicated by the subscript), and k is a dimensionless flow recession constant. In contrast to GROUND, Filter 1 is not suitable for separating direct runoff from the rest of the runoff, i.e. from the sum of interflow and baseflow. A moderately realistic separation can only be obtained if k approaches unity, in which case the resulting slow flow component is small and slowly reacting. In our case, k was taken as 0.99483 (the same as in previous calculations). This value was obtained by comparing the results of Filter 1 with those of two other baseflow separation methods (see Doležal et al., 2003, for details).

Table 2: Overview of experimental tile drainage systems.

Catchment	Drainage system	Area (ha)	Spacing/Depth of laterals (m)	Position in the landscape	Hydrological years for flow/nitrate data
Černičí	S1	0.6	13/1.0	Valley floor	1995-2005/1995-96, 2002-5
Černičí	S2	1.8	13/1.0	Lateral gully	1995-2005/1995-96, 2002-5

GROUND was used for separating the direct runoff and Filter 1 was used to separate the baseflow. The difference between the slow component left by GROUND and the one left by digital filter was regarded as an estimate of interflow. The following equations were applied:

$$Q_{slow, GROUND} = \hat{Q}_i + \hat{Q}_b ; \quad Q_{quick, GROUND} = \hat{Q}_d ; \quad Q_{slow, Filter1} = \hat{Q}_b ;$$

$$\hat{Q}_i = Q_{slow, GROUND} - Q_{slow, Filter1} \quad \text{Eq. 2}$$

where Q_{total} is the total flow, Q_d is the direct runoff, Q_i is the interflow and Q_b is the baseflow, while Q_{slow} and Q_{quick} are the slow and the quick components of the total flow, respectively, obtained either by GROUND or by Filter 1, as indicated by the second part of the subscript. The hat signs over the symbols denote estimates of true values. The procedure resulted in daily series of the three flow components (direct runoff, interflow and

baseflow). Sometimes small adjustments had to be made to avoid negative interflow values. While admitting that the methods used are empirical and not directly related to physically-based isotopic or chemical separation procedures, the authors hold that the pattern of runoff variation in time, reflecting the contributions due to various flow mechanisms, is correctly described.

Water quality was sampled in one to four week intervals in the closing profiles of the streams and the tile-drainage manholes referred to in Tables 1 and 2. No samples were taken from S1 and S2 between January 1997 and August 2001. The nitrate concentrations were determined in the laboratory by cadmium reduction in a Skalar segmented flow analyser. The data were processed to obtain characteristic nitrate concentrations of individual flow components, using a simple mixing analysis in which it was assumed that the water supplied to the stream by a particular flow component has a constant (characteristic) concentration. Then the actual concentration of nitrate in stream water can be obtained as a linear combination of these characteristic concentrations, according to the mass balance equations:

$$Q_t = \sum_j Q_j ; \quad Y_t = \sum_j Y_j = Q_t c ; \quad Y_j = Q_j c_j \quad \text{Eq. 3}$$

where Q_t is the total stream discharge (e.g., in $L \cdot s^{-1}$), Q_j is the stream discharge due to the j -th runoff component (in the same units), Y_t is the total nitrogen yield (e.g., in $mg \text{ NO}_3 \cdot s^{-1}$), Y_j is the nitrogen yield due to the j -th runoff component (in the same units), c is the average nitrate concentration in stream water (e.g., in $mg \text{ NO}_3 \cdot L^{-1}$) and c_j is the characteristic constant concentration of water brought in by the j -th runoff component (in the same units), wherein j stands for direct runoff, interflow or baseflow, respectively. The unknown component concentrations c_j were estimated by nonlinear optimisation. This analysis can be regarded as a rudimentary form of the end-member mixing analysis (EMMA, cf. Christophersen et al., 1990). It differs from the full EMMA in three aspects:

- a) a single water quality indicator (nitrate) is used instead of two or more indicators,
- b) the characteristic nitrate concentrations of flow components are constant over the entire period of observation, i.e. are not regarded as event-dependent,
- c) water quality of individual end members (flow components) is not measured directly.

In addition to what was done in previous papers (Doležal et al., 2003, 2005; Doležal and Kvítek, 2004), the uncertainty of the flow separation and mixing analysis results was tested by analysing separately data of particular hydrological years and of longer partial periods comprising five consecutive hydrological years.

Results and discussion

Fig. 1 displays relative volumes of quick runoff components (expressed as percentages of total flood wave volumes) for 19 selected flood waves in the closing profile of the Černičí catchment, as estimated by GROUND and by the manual recession analysis. These results indicate that GROUND gives considerably higher volumes of the quick component for some events and considerably lower volumes for other events. On average, however, the results of both methods coincide surprisingly well, without any *a priori* or *a posteriori* adjustment. The average quick flow volume is 48.7% according to GROUND and 50.4% according to the recession analysis. Hence, the C parameter of GROUND, presently estimated as 0.075 (for the daily time steps of flow data), may remain as it is. The differences between the two methods can be attributed, to a large extent, to their sensitivity to small irregularities in the shape of flood waves.

The flow component proportions for individual hydrological years were calculated for all units (catchments and tile drainage systems). The proportions vary from year to year but, generally speaking, individual units retain their typical features, discernible in graphs (not shown) and testable statistically, using, for example, t-tests (see Table 3). The importance of direct runoff decreases and the importance of baseflow increases along the sequence Kotelský potok – Dolský potok – Černičí – S1 – S2. Interflow is the largest part of the total runoff (except for the Kotelský potok). The catchments differ from each other in terms of direct flow proportions, but

S1 does not differ from S2 in this respect. Mutual similarity among different units is highest in terms of interflow proportions. S1 differs from S2 in terms of both interflow and baseflow, which suggests that the two sites are hydrogeologically different. The proportions can be related to other catchment properties, such as geology, geomorphology, climate, land use, tile drainage etc., helping us thereby to classify the catchments and the differences between them.

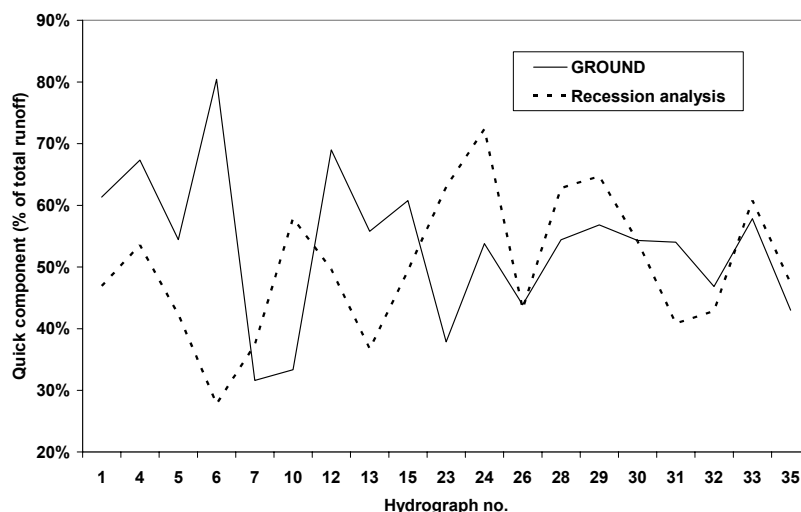


Fig. 1: Performance of two quick-flow separation algorithms: the simple model GROUND and the manual recession analysis, for 19 selected flood hydrographs in the Černičí catchment, 1993-2006.

Table 3: Runoff separation results for individual hydrological years: comparison among catchments. The differences were judged using two-sided t-tests, $P = 0.05$: 1 = significant, 0 = insignificant.

Baseflow (in % of total runoff):			Significantly different from				
Catchment	Mean	Std.dev.	Ce	Do	Ko	S1	S2
Černičí (Ce)	26.21%	5.08%	0	0	1	0	1
Dolský potok (Do)	23.39%	6.54%	0	0	1	1	1
Kotelský potok (Ko)	18.31%	3.48%	1	1	0	1	1
S1	28.99%	5.21%	0	1	1	0	1
S2	35.28%	5.08%	1	1	1	1	0
Interflow (in % of total runoff):							
Catchment	Mean	Std.dev.	Ce	Do	Ko	S1	S2
Černičí	43.53%	5.99%	0	0	1	0	0
Dolský potok	41.03%	6.87%	0	0	0	1	0
Kotelský potok	38.24%	7.04%	1	0	0	1	0
S1	46.86%	4.07%	0	1	1	0	1
S2	40.82%	4.89%	0	0	0	1	0
Direct runoff (in % of total runoff):							
Catchment	Mean	Std.dev.	Ce	Do	Ko	S1	S2
Černičí	30.26%	6.83%	0	1	1	1	1
Dolský potok	35.59%	7.93%	1	0	1	1	1
Kotelský potok	43.45%	8.24%	1	1	0	1	1
S1	24.15%	6.13%	1	1	1	0	0
S2	23.91%	3.24%	1	1	1	0	0

The confidence limits (plus minus one standard deviation) of characteristic nitrate concentrations are plotted in Fig. 2 for moving sub-periods composed of five consecutive hydrological years, for the Černíčí catchment only. While the mixing analysis of the Černíčí stream for the whole period of observation (hydrological years 1993 to 2005) indicates that the highest characteristic nitrate concentration pertains to interflow (114 mg NO₃ L⁻¹), followed by direct runoff (65 mg NO₃ L⁻¹) and baseflow (60 mg NO₃ L⁻¹), the same analysis made for moving five-year periods shows that both the characteristic concentrations and the ranking of flow components in terms of their degree of pollution vary from period to period. Hence, differences between flow components and sub-periods in terms of their characteristic nitrate concentrations cannot yet be regarded as significant (t-tests, not shown here, confirm this conclusion). The same conclusions apply to the tile drainage systems (the results are not shown).

The role of tile drainage in the processes of catchment runoff and water quality generation manifests itself in the fact that the temporal variations of nitrate concentrations in the stream and in the tile drainage are almost parallel (not shown) and in the similarity of interflow proportions.

Conclusions

The results presented above are partial and should be understood in a broader context of the present authors' work. The flow separation procedures, the same as in previous papers, have now been applied to partial sub-periods in order to explore how variable and how reliable the results of these procedures are. It was found that the inter-annual variability of runoff separation results is perceivable, but acceptable, and the results of separation are meaningful and statistically significant. This set of separation procedures can be meaningfully used for an overall characterisation of runoff patterns in small catchments and tile drainage systems. On the other hand, the simple mixing analysis proposed by Doležal and Kvítek (2004), when applied to sub-periods, suggests that the uncertainty in estimating the characteristic nitrate concentrations of flow components is probably too high and that the mixing analysis methodology will have to be refined.

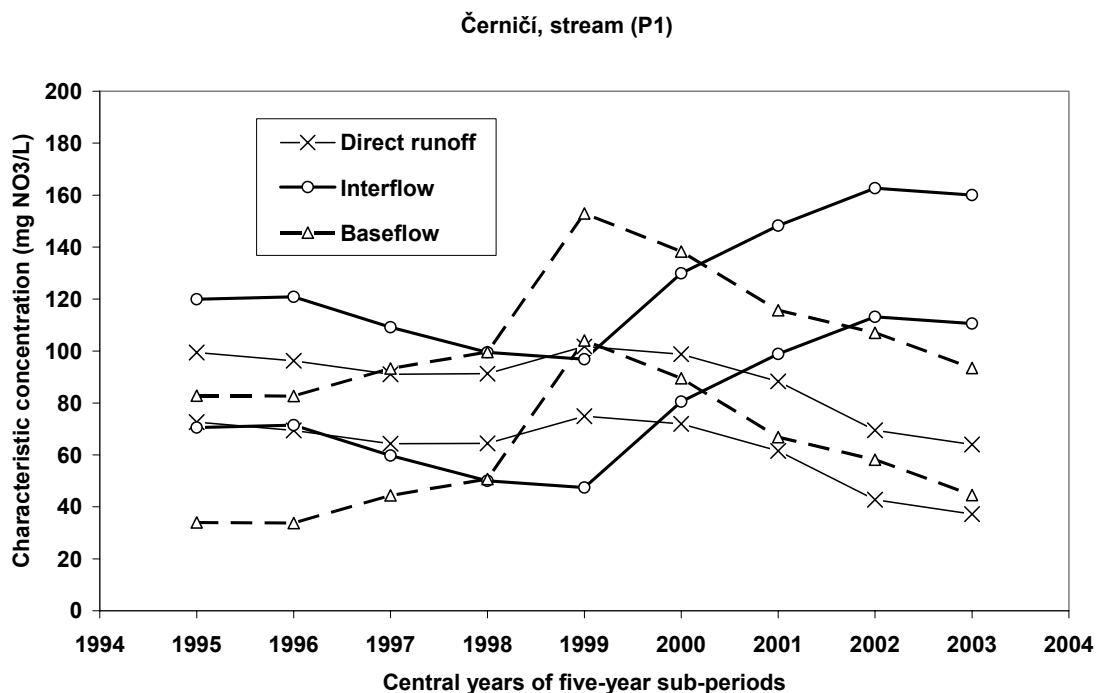


Fig. 2: Confidence limits (plus minus standard deviation) of characteristic nitrate concentrations in flow components, obtained by optimisation according to the simple mixing model (3) for moving sub-periods consisting of five consecutive hydrological years, Černíčí, 1993-2005.

Acknowledgements

The study relies on data sets collected and processed over previous years and decades. In the final stage, the work was supported by the RISWC programme MZE0002704901, financed by the Ministry of Agriculture of the Czech Republic, and the National Agency for Agricultural Research projects QF3095 and QF3301. A substantial contribution of those who measured and processed the data is gratefully acknowledged.

References

- Chow V.T. (1964). *Handbook of Applied Hydrology*. McGraw-Hill, New York.
- Christophersen N., Neal C., Hooper R.D., Voigt R.D., Andersen S. (1990). Modelling streamwater chemistry as a mixture of soilwater end-members – a step towards second-generation acidification models. *Journal of Hydrology*, 116: 307-320.
- Doležal F., Kulhavý Z., Kvítek T., Soukup M., Tipl M. (2003). Methods of runoff separation applied to small stream and tile drainage runoff. In: L. Holko, P. Miklánek (Eds.), *Interdisciplinary Approaches in Small Catchment Hydrology: Monitoring and Research. Technical Documents in Hydrology*, 67, UNESCO, Paris: 131-136.
- Doležal F., Kvítek T. (2004). The role of recharge zones, discharge zones, springs and tile drainage systems in peneplains of Central European highlands with regard to water quality generation processes. *Physics and Chemistry of the Earth*, 29: 775-785.
- Doležal F., Kvítek T., Soukup M., Kulhavý Z., Čmelík M., Tipl M., Pilná E. (2005). Runoff and water quality regime of small highland catchments in Central and East Bohemia. *Landschaftsökologie und Umweltforschung (TU Braunschweig)*, 48: 131-138.
- Grayson R.B., Argent R.M., Nathan R.J., McMahon T.A., Mein R.G. (1996). *Hydrological Recipes: Estimation Techniques in Australian Hydrology*. Cooperative Research Centre for Catchment Hydrology, Clayton, Victoria, Australia, 125 p.
- Kulhavý Z., Doležal F., Soukup M. (2001). Separation of drainage runoff components and its use for classification of existing drainage systems (In Czech). *Vědecké práce VÚMOP Praha*, 12: 29-52.

EFFECT OF INACCURACY OF PRECIPITATION MEASUREMENTS ON THE WATER BALANCE OF THE CASTRICUM LYSIMETERS

P.C.T. van der Hoeven¹, P.M.M. Warmerdam² & J.W. Kole²

¹retired from the Royal Dutch Meteorological Institute. ²Wageningen University, sub-department Water Resources, the Netherlands.

Corresponding author : Piet Warmerdam, email : Piet.Warmerdam@wur.nl

ABSTRACT

The estimation of precipitation as a water balance element is subject to considerable uncertainties. This was already a point of concern in the early 20th century when studies on the influence of vegetation on the building up of exploitable water supplies in the dunes north west of the city of Amsterdam were set up. In the years 1938-1941 four lysimeters were built to estimate water losses through a bare sand plain, natural dune vegetation, deciduous (oak) and pine forest.

Although data users generally assume the correctness of rainfall measurements this is not so for normally exposed gauges. Interaction of wind on point measurements results in an underestimation of the true amount of rainfall. To examine the wind effect, rain gauges were installed at heights of 40 and 150 cm above surface level at the lysimeter station. In this study the rainfall catches of the gauges are compared with a pit gauge as control. The elevated gauges caught 5 to 10% less rain than the pit gauge. The paper describes the lysimeter system, the comparison of rain gauges and the uncertainty of evaporation computation of the lysimeters using data of elevated rain gauges. It is concluded that the best way to reduce rainfall measurement uncertainties in hydrological investigations, is the use of data collected with pit gauges.

Keywords: Castricum lysimeter, rainfall measurement errors, wind effect

Introduction

Early in the 20th century the Provincial Water supply Company North-Holland (PWN) became responsible for the supply of drinking water to the city of Amsterdam and for the maintenance of the vulnerable landscape of the dune area. In this north-west part of the Netherlands the fresh groundwater in the dunes accomplished the main resource for drinking water. PWN set out to gather knowledge about the influence of various vegetation types on the building up of exploitable water supplies in the dunes. It finally led to the decision of PWN by the end of the 1930s to set up an ambitious lysimeter experiment in the dunes nearby the village of Castricum (Wind, 1958).

Four large lysimeters measuring 25x25x2.5 meters were built in concrete in 1938-1941. One of the lysimeters was left bare, the others were planted with natural dune scrub, oak-seedlings and seedlings of *Pinus nigra austriaca*. Figure 1 shows the experimental station and location of the lysimeters. The percolation water of the lysimeters was caught by drainage systems at the bottom and collected in tanks. These measurements continued over a period of almost sixty years up to 2001. From the start it was clear that correct measurement of precipitation was essential to accurately estimate water losses through the bare sand and three vegetation types. To examine the wind effect, rain gauges were installed at different heights at a meteorological station near to the bare sand lysimeter (Fig. 1).

For more than 25 years three observers were employed at the experimental site to collect data. Between 1941 and 1972 a tremendous amount of data was collected in a period without computers and calculators.

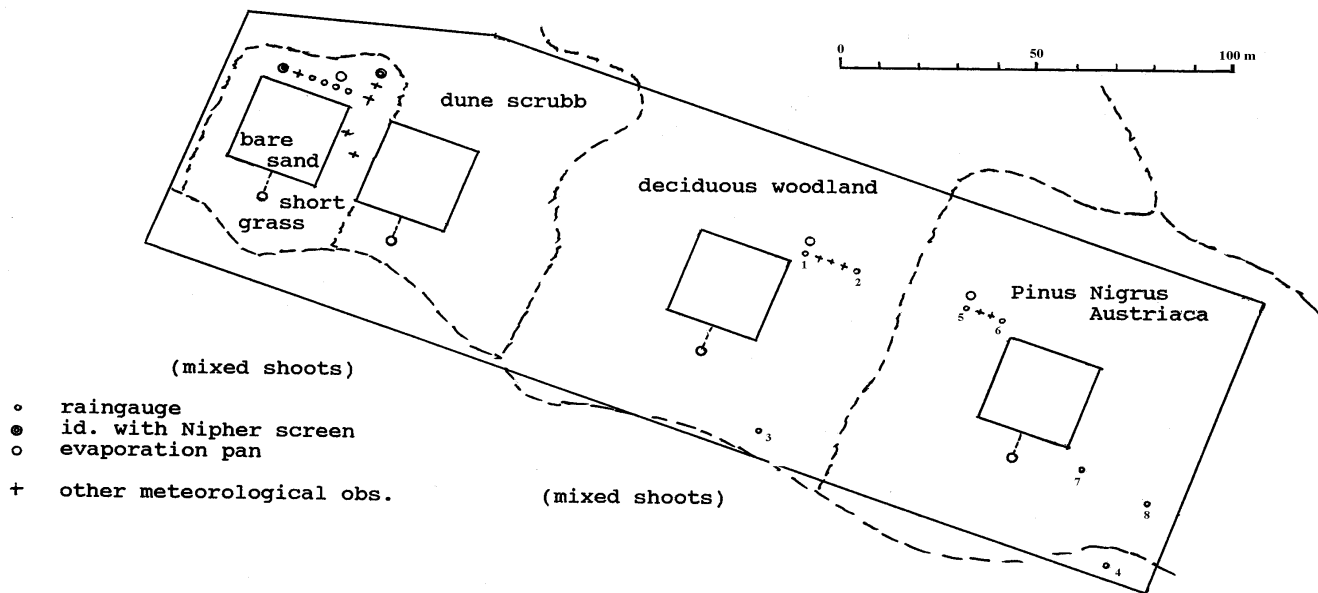


Fig. 1: The lysimeter station Castricum and location of the four lysimeters. Observation period 1941-2001.

The raw observations were written in monthly notebooks, achieving a total length of 1.50 m on the bookshelf and about 5000 monthly A3-forms, completely covered with observations or hourly abstracts of the registrations. The first author started to digitize a selection of this material during the last decade. A description of the lysimeter station and comparison of rain gauges can be found in Mulder (1983), Van der Hoeven (2005a) and Van der Hoeven et al. (2005).

This paper describes the uncertainties of loss estimation when data of elevated gauges are being used.

Uncertainties in precipitation measurements

Water balance studies, studies of interception and throughfall assume the rainfall caught in the gauge to be correct. Yet this is not so because the common type of elevated gauge systematically catches less rain due to wind than if the gauge were absent (Rodda, 1971; Sevruk, 1989). Wind is not the only error source in point measurements of rainfall.

Other uncertainties in rainfall measurement are related to changes in gauge type, exposure, elevation and movement to another site. The wetting losses which are still unknown for many types of gauges are much larger than the 0.5% as assumed in literature. Also the change of observer could affect the accuracy of measurement. Therefore, an analysis of the accuracy of rainfall measurements is important in order to reduce or eliminate uncertainties.

At the start of the project it was clear that errors in assessing how much water is available for drinking water use depends largely on the precision or accuracy of rainfall measurements.

Meanwhile it was known (Abbe, 1889) that the elevated standard gauges interfere with wind causing measurement deficits. This problem is much more accentuated when measuring snowfall. To cope with this wind effect an inverted cone surrounding the gauge was successfully introduced by Nipher to eliminate the turbulence at the rim.

Precipitation gauge comparison

In 1941 the standard height of the Dutch rain gauge was 150 cm and the gauge orifice measured 4 dm². As wind speed reduces remarkably near the ground, it was a cheap solution to have the rim of the rain gauge as low as possible. In order to prevent splashing in from the ground, it was decided not to choose a height of less than 40 cm.

To examine the wind effect of the standard gauge at the lysimeter station four 4 dm² rain gauges were installed at heights of 40 cm and 150 cm with and without Nipher Screen. Observations were done daily at 08MPT. One rain gauge at 40 cm was added which was observed three times per day (3xday gauge) from 1941-1965. The measurements with the 150 cm gauge continued over a period from 1941 to 1957 and with the 40 cm from 1941 to 1965. Fig. 2 displays the various gauges used.

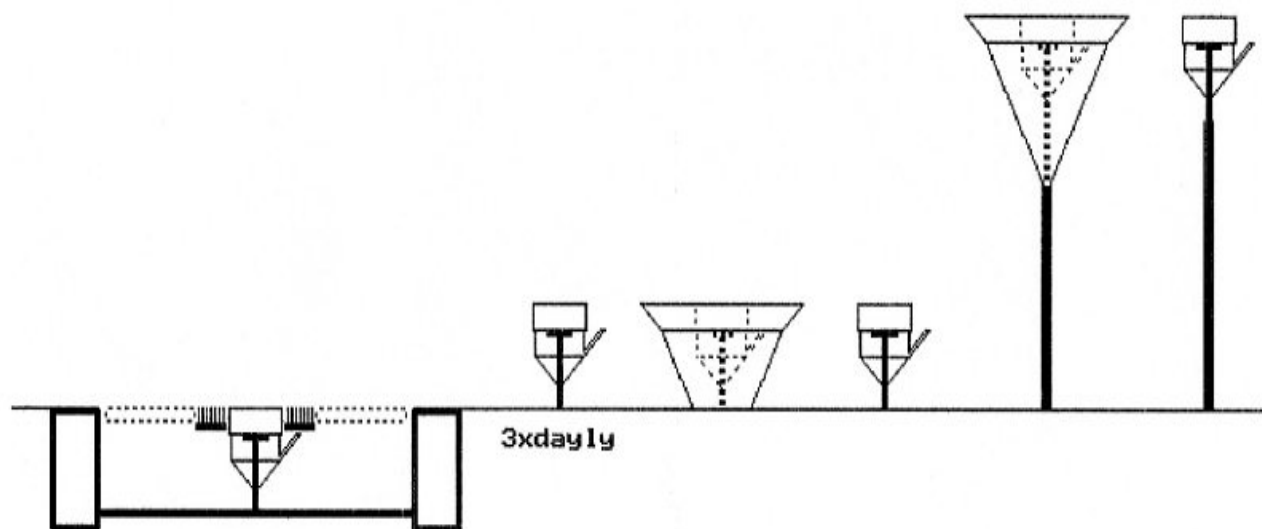


Fig. 2: Pit gauge, 40 cm sampled 3xday, 40 cm with Nipher shield, 40 cm, 150 cm gauge shielded and 150 cm (from left to right) at the lysimeter station.

To achieve precipitation measurements of a quality matching the accuracy of the lysimeter drainage measurement one rain gauge was installed in a wide pit, with the gauge rim at the surface level. To prevent from splashing the pit opening was surrounded by a brush mat and covered with a grid. Thus the largest source of errors, the wind effect, was eliminated and this pit gauge now yields the most accurate observations in all circumstances.

A serious disadvantage of pit gauges is wind blowing of fallen snow into the gauge. This problem required processing of all weather and snow cover observations and snow measurements. Since the thrice daily measurements were used in order to divide those of the pit gauge into three periods per day, also the corrected snow measurements were divided into thrice daily observations.

Results

The mean ratios of the 150 cm and 40 cm gauge with the pit gauge are found to be 91% and 94%, respectively for annual totals of precipitation. The thrice daily gauge corrected for snow shows a ratio of 96%. The ratios of the 150 cm and 40 cm gauges equipped with a Nipher screen are 94% and 95% (Van der Hoeven, 2005b). Apparently the effect of the screen is greater at the higher elevated gauge. Other studies of gauge comparison show similar results (Neff, 1977; Warmerdam, 1981).

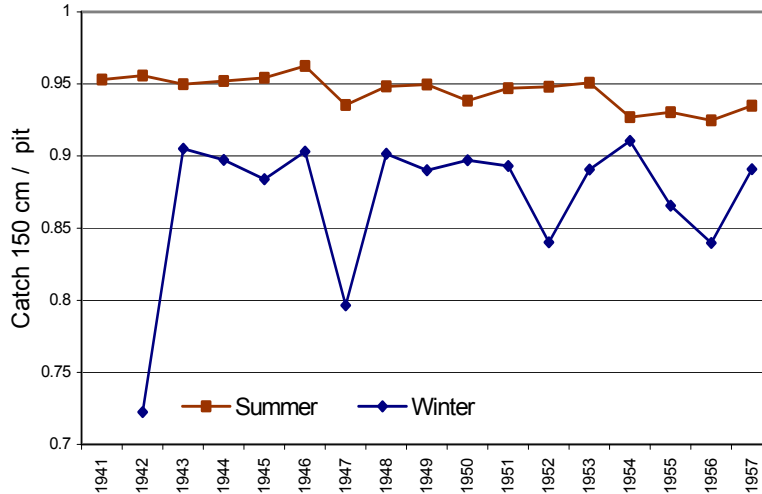


Fig. 3: Ratio of summer and winter catches of the 150 cm gauge and the pit gauge.

The monthly differences in catch of the various rain gauges are varying systematically with the season. Fig. 3 shows the ratio of catch with the 150 cm and pit gauge for summer (May-October) and winter (November-April) periods. Almost generally the summer half of the year appeared to show a rather constant pattern of catch losses as compared with the pit gauge. This does, however, not apply to the winter periods. The large deviations of 1942, 1947 and 1952 are connected to heavy snowfall. Apart from this, there are significant seasonal differences with higher deficits in winter than in summer.

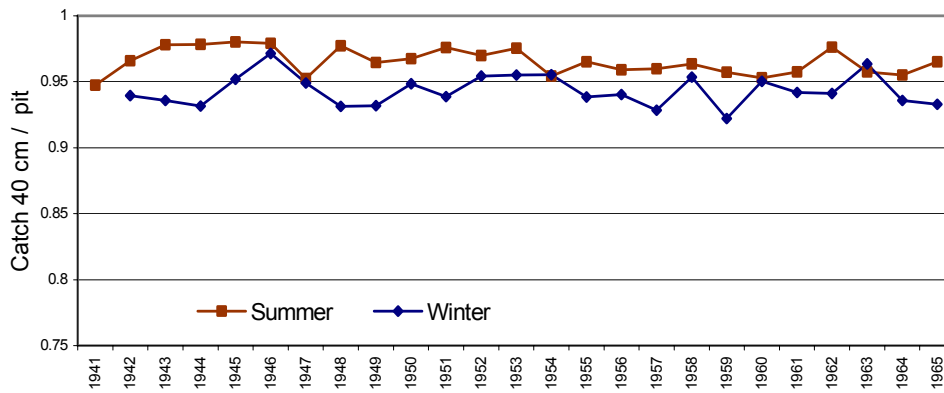


Fig. 4: Ratio of summer and winter catches of the 40 cm gauge and the pit gauge.

Fig. 4 shows the ratio of the 40 cm and pit gauges for summer and winter in the years 1941 to 1965. The summer ratio is somewhat higher than 95%, while in winter it appears slightly smaller.

In the Netherlands rainfall is distributed regularly in winter and has a rather low intensity. In summertime storms of higher intensities occur more frequently. The catch of these high intensity summer storms appears less sensitive to wind than in winter with its prevailing low intensity storms.

As shown in Fig. 3 and 4 the wind effect of the 150 cm gauge is considerably larger than at 40 cm and it is larger in winter. Although not portrayed, the ratios of both not shielded 40 cm gauges appear very similar. The only difference between these 40 cm rain gauges is that with the thrice daily observation the snow is well processed. This result was the reason for diminishing the old standard height from 150 cm to 40 cm by the end of the 1940's.

Over the period of 1941 to 1957 the mean annual precipitation of the pit gauge was 827 mm, the 150 cm 756 mm and the 40 cm 778 mm. This means an average underestimation of 71 mm and 49 mm per year as measured with the gauges at 150 cm, respectively 40 cm above ground surface. The significant differences in rainfall justify the use of the pit gauge in this study to eliminate errors due to wind. Whether the deficiency in gauge catch is important depends upon the use of the rainfall data, but it is obvious that many other intensive hydrological investigations need to use precipitation data from pit gauges instead of the normally exposed gauges to prevent the misunderstanding of hydrological processes.

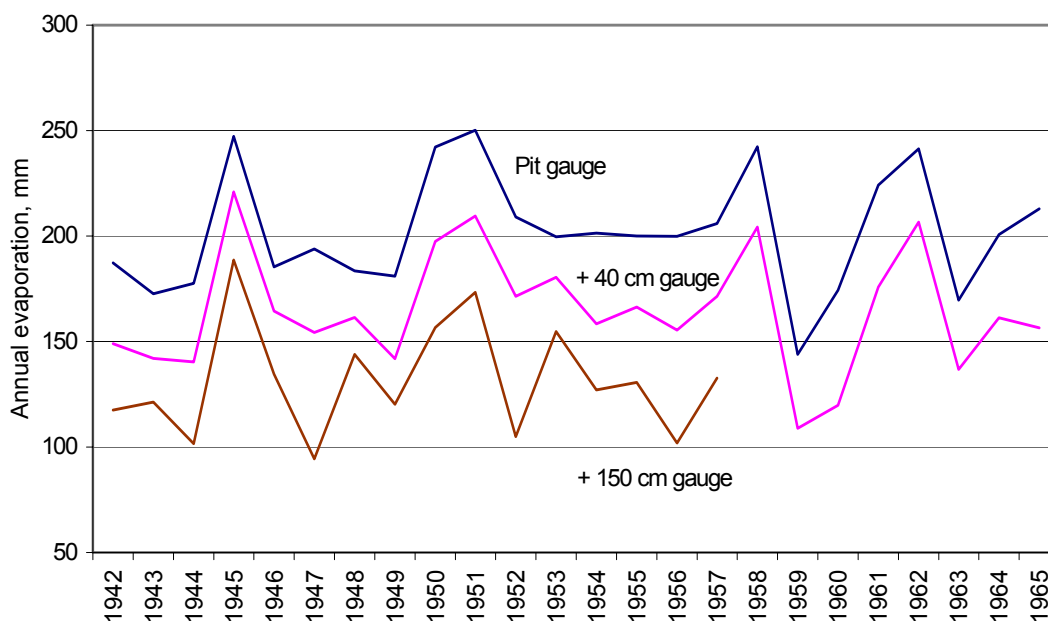


Fig. 5: Annual evaporation of lysimeter 1 (bare) derived from rainfall measurements of pit gauge, 40 cm and 150 cm elevated gauge precipitation for the period 1941 to 1965, respectively 1957.

Fig. 5 displays the annual evaporation of lysimeter 1 (bare) computed with precipitation values of the pit gauge, 40 cm and 150 cm gauges. The annual deficits of elevated gauges appear nearly systematic. As these deficits produce average annual underestimates in the order of 50 mm up to 70 mm for the 40 cm, respectively 150 cm gauges, it justifies the use of pit gauges to eliminate wind errors in accurate water balance studies.

Annual evaporation of bare sand plotted in Fig. 5 shows a very constant path around the 200 mm mark (Van der Hoeven and Warmerdam, 2005). Using precipitation of 40 cm and 150 cm produces mean evaporation values of 152 and 131 mm respectively, which is an inadmissible deviation in studying the evaporation of various vegetation types in the dunes.

Conclusions

The most serious threat for uncertainties in rainfall measurements are losses due to wind blasts. Compared with the pit gauge, the elevated gauges (measured at 40 cm and 150 cm above ground surface) have average annual catch deficits of 5% and 9%. There is a strong seasonal effect of wind on precipitation measurements.

There are several other uncertainties in point rainfall measurements inducing much larger errors. Such uncertainties can hamper progress of hydrological process understanding.

The error of the most important input variable of the water balance can have adverse effects on other components such as evapotranspiration. It is argued to use gauges for which the wind effect is eliminated.

This study proves that precipitation records should not be used without considering effects of potential measurement errors. It should be noted that not more confidence can be placed in the data than justified by the technique of measurement.

References

- Abbe C. (1889). Determination of the amount of rainfall. *American Meteorological Journal*, 6.
- Hoeven van der P.C.T. (2005a). Lysimeters Castricum. Report 1. 61 p.
- Hoeven van der P.C.T. (2005b). Regenmetervergelijking, Castricum 1941-1971. Report 2. 50 p.
- Hoeven van der P.C.T., Warmerdam P.M.M. (2005). Elaboration of the water balance of the Castricum lysimeters 1941-1997, Castricum, the Netherlands. *Proceedings of the Conference on Forest Impact on Hydrological Processes and Soil Erosion*. Yundola, Bulgaria.
- Hoeven van der P.C.T., Warmerdam P.M.M., Kole J.W. (2005). Description of the Castricum lysimeters 1941-2000, The Netherlands. Comparison of rain gauges and throughfall. *Proceedings of the Conference on Forest Impact on Hydrological Processes and Soil Erosion*. Yundola, Bulgaria.
- Mulder J.P.M. (1983). *A Simulation of Rainfall Interception in a Pine Forest*. PhD thesis, Rijksuniversiteit Groningen.
- Neff E.F. (1977). How much rain does a rain gage gage? *Journal of Hydrology*, 35: 213-220.
- Rodda J.C. (1971). *The Precipitation Measurement Paradox - the Instrument Accuracy Problem*. WMO No. 316, Geneva.
- Sevruk B. (1989). *Precipitation Measurement*. WMO/IAHS Workshop St. Moritz.
- Warmerdam P.M.M. (1981). The effect of wind on precipitation measurements; a comparative study. *H₂O*, 14.
- Wind R. (1958). The lysimeters in the Netherlands. Committee for Hydrological Research TNO. *Proceedings and Informations*, No. 3. The Netherlands Central National Council for Applied Scientific Research TNO: 165-228.

UNCERTAINTY IN CHEMICAL HYDROGRAPH SEPARATION

A. Krein¹, M. Salvia-Castellvi¹, J.-F. Iffly¹, F. Barnich¹, P. Matgen¹, R. v.d. Bos¹, L. Hoffmann¹, H. Hofmann², A. Kies² & L. Pfister¹

¹*Centre de Recherche Public - Gabriel Lippmann, Département Environnement et Agro-Biotechnologies, 41, rue du Brill, L-4422 Belvaux, Grand Duchy of Luxembourg.* ²*Université du Luxembourg, Laboratoire Physique des Radiations, 162a, avenue de la Faïencerie, L-1511 Luxembourg, Grand Duchy of Luxembourg.*

Corresponding author: Andreas Krein, email: krein@lippmann.lu

ABSTRACT

Runoff generation processes have been investigated in forested experimental catchments in the Luxembourgish Attert river basin. Possible end-members were sampled and characterised chemically. In order to separate different storm runoff components a three-component end-member analysis was applied. The hydrological behaviour of the studied basins varied as a consequence of different geology. In the Huewelerbach the main contribution to the stream discharge is a groundwater component generated from sandstone springs. The second end-member is the overland flow, which configures the shape of the storm peak. The shallow soil water is the third end-member of this system, estimated around 10 percent in the separations performed. On the contrary, overland flow was almost irrelevant in the schistose Weierbach basin. Less than 2 percent of total storm discharge is delivered by a delayed groundwater flow. With more than 90 percent of total discharge, the Weierbach presents an important throughflow rate from the weathered shales. Uncertainties in our chemical hydrograph separations were large, mainly as a result of the high spatial and temporal variations of the chemical characteristics of our end-members. To conclude, in our case study, the expected end-members are no end-members.

Keywords: EMMA, hydrochemistry, rainfall/runoff, Luxembourg

Introduction

Understanding where streamwater comes from during a rain event is one of the goals of hydrology. Water stored in various regions of a basin has different chemical characteristics. Furthermore, streamwater chemistry is dependent on pathways in which water travels to the stream. Knowing dominant flow paths and how they change during a rain event is crucial to understanding runoff generation. This study presents the results of hydrochemical observations of two temperate forest catchments in Luxembourg.

We used the EMMA approach (End Member Mixing Analysis) to quantitatively estimate the processes controlling streamwater chemistry during rainstorms. The identification of stormflow generating processes and the estimation of their volumetric contributions to runoff are based on investigations by Hooper and Shoemaker (1986), Christophersen et al. (1990) and Hooper et al. (1990).

It is our intention to quantify the uncertainty connected to the mentioned mixing approach. Especially the chemical variation of the end-members is expected to cause larger variability in our calculations.

Study sites and methods

Hydrograph separations were applied to two catchments of the Attert basin (Belgium-Luxembourg). The studied micro-basins are the Huewelerbach (2.7 km², mostly silty-sandy brunisols) and the Weierbach (0.4 km², mostly silty-cobbly soils). Both headwater catchments differ in their geological substrate. The

Huewelerbach comprises Mesozoic formations with 80% sandstone. The Weierbach is situated on Devonian schists (Fig. 1). Both catchments are forested without any urbanised zone.

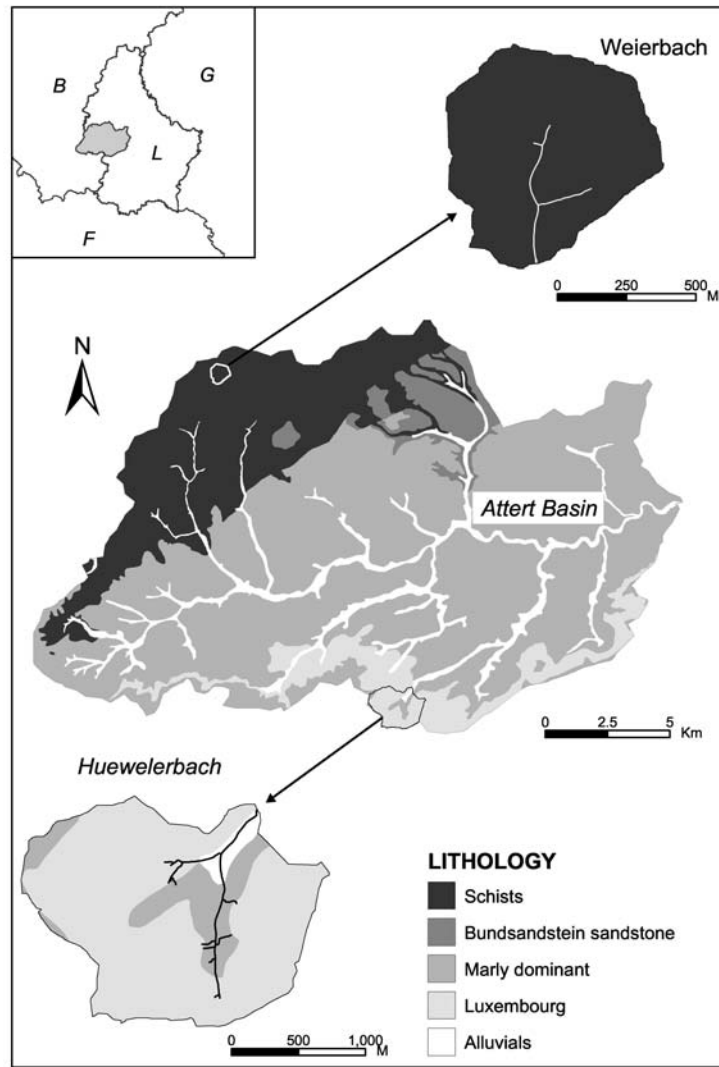


Fig. 1: Area of investigation.

The component "soil water" is characterized by analysing the water collected by groups of suction cups distributed in three plots per basin (n=254). Rainfall (n=23) and throughfall (n=22) were collected in rain gauges. Overland runoff (n=81) is irregularly collected during the flood event mainly on forest roads. Spring water is grab sampled at monthly intervals and automatically during the analysed storms (n=147). In the Mesozoic Huewelerbach micro-basin, alluvial ground water is also grab collected from a network of 21 piezometric tubes installed in the alluvial plain (n=168).

Analysed parameters comprise conductivity (WTW LF197i), SiO₂ (ammonium molybdate method with photometer) and UV-absorbance by 254 nm (Beckmann Coulter spectrophotometer).

Results

One assumption of the EMMA approach is that at any given time, the chemical composition of streamwater can be explained as the result of the linear mixing of runoff-contributing sources. In order to evaluate the

spatial and temporal variations of solute concentrations in the different source components, results from analysed parameters were grouped and statistically analysed. Electrical conductivity, SiO₂ and absorbance units at 254 nm conveniently discriminate between superficial (or shallow) and deep water in the Huewelerbach and the Weierbach basin (Fig. 2).

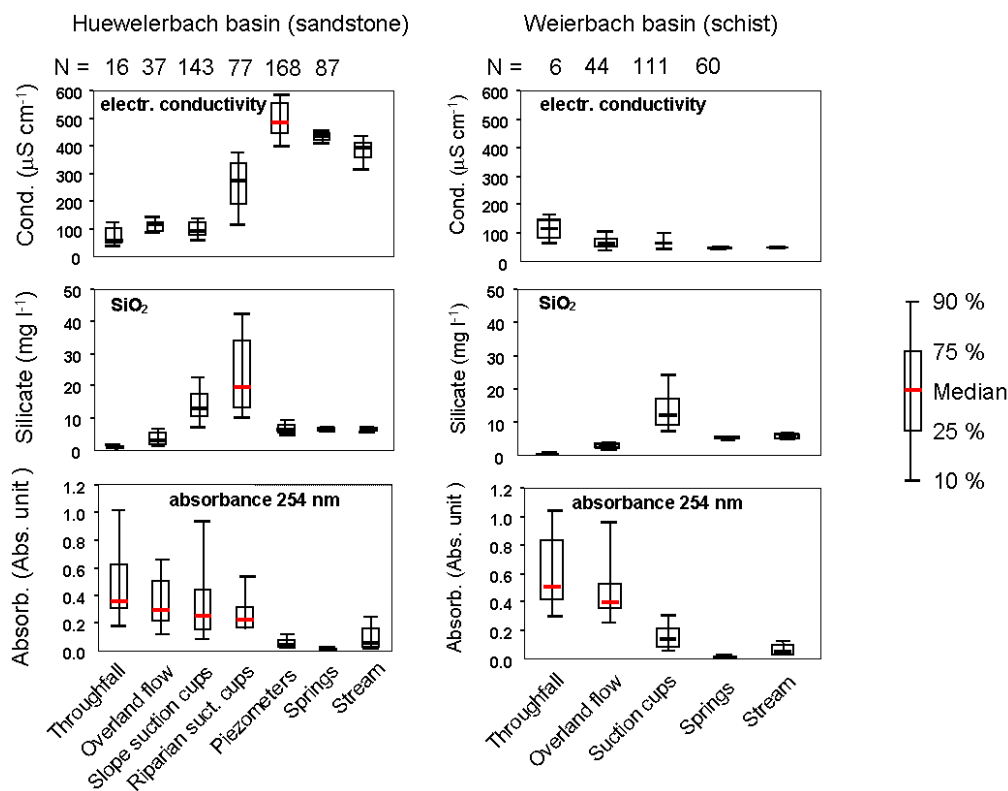


Fig. 2: End-member characteristics in the basins under investigation.

Figs. 3 and 4 highlight an example of a storm event in the Huewelerbach using different tracers. The proportion of overland flow changes depending on the tracer used. With silica and conductivity, at the peak discharge, the surface runoff component reaches 56 percent and the shallow soil water amounts to 6 percent, whereas for the pair UV-absorbance and conductivity, they are 49 percent and 13 percent respectively. The contribution of the bedrock groundwater is 38 percent in both approaches (Fig. 4).

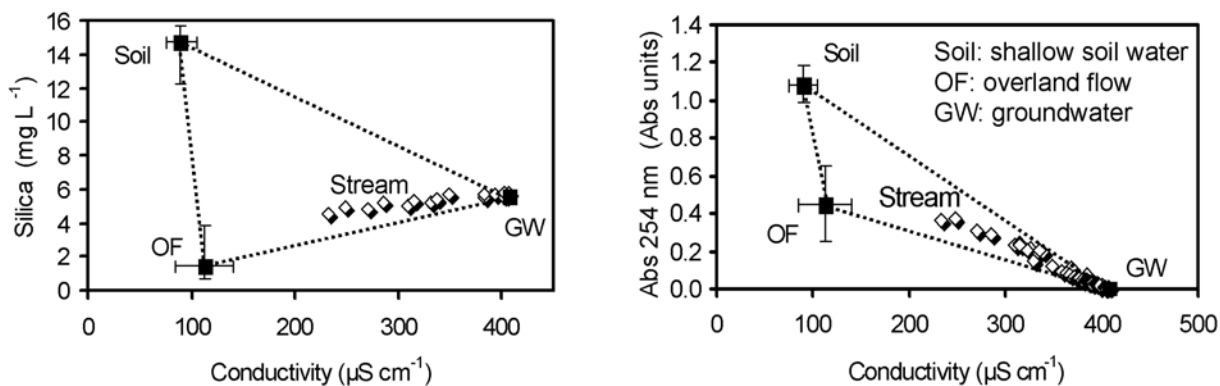


Fig. 3: Mixing diagrams of silica versus conductivity (left) and absorbance versus conductivity (right) in the Huewelerbach.

Generally speaking, in the Huewelerbach basin the main contribution to stream discharge during flood events is a groundwater component generated from sandstone springs. Depending on the antecedent hydrological conditions and the rainfall intensity, the contribution of the overland flow component varies from 7 to 70 percent at peak discharge.

In the schistose Weierbach basin, overland flow is almost irrelevant (Fig. 5). Runoff is mainly generated by a delayed groundwater flow, supplied by the weathered shale of the basin. The soil contribution to runoff is varying between 4 and 12 percent, depending on the rainfall intensity and antecedent soil moisture.

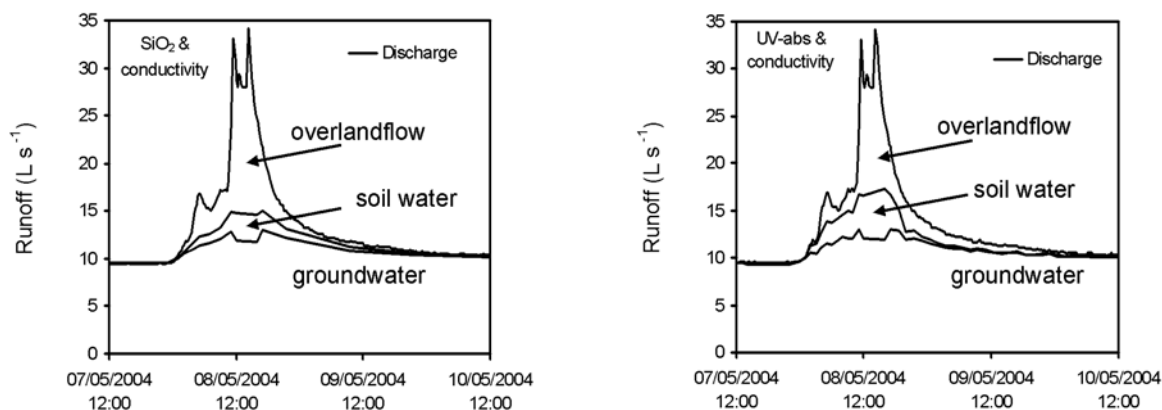


Fig. 4: Three-component separations with median concentrations of silica & conductivity (left) and median values of UV absorbance & conductivity (right) in the Huewelerbach.

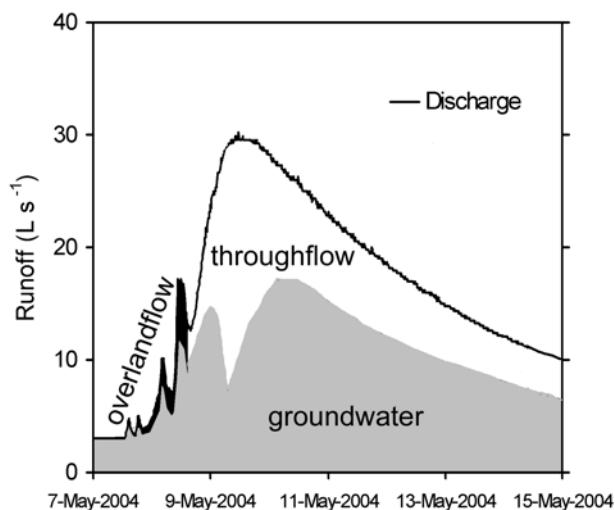


Fig. 5: Three-component separation with median concentrations of silica & conductivity in the Weierbach.

Uncertainties in the equations of the hydrograph separation turned out to be considerable. This is the result of trespassing assumptions used in deriving the separation equations (no total mixing, see Krein and De Sutter 2001) and due to a high variance in the chemical characteristics of our end-members.

Deviations associated with variations in the end-member concentrations are investigated in the following. Figure 6 highlights the variability of silica in the overlandflow end-member during the storm event of May 8th in the Huewelerbach catchment. The concentration increases from 1 and 3 mg L⁻¹ at the beginning of the event to more than 5 mg L⁻¹ at the time of the falling limb of the flood. Possibly, the overlandflow changes from a “real overlandflow” to a return flow that is higher mineralized due to its longer soil passage. Another

possibility might be that the overlandflow at the end of the rain event is delivered from farer distances. During this transport the water is showing increased solvent and silica concentrations.

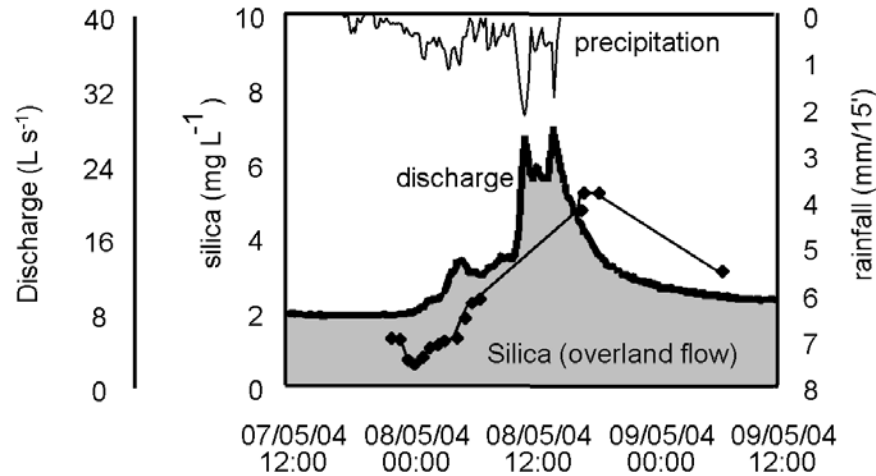


Fig. 6: Variability of silica in the overlandflow end-member during the storm of May 2004.

Figure 7 illustrates the uncertainty of hydrograph separation in the storm of May 2004. We calculated with the medium value (left) and the 75 percentile (right) of silica in the overlandflow end-member previously shown in Fig. 6. At peak discharge, overlandflow varies from 40 to 50 percent. What is even more important are the consequences for soil water runoff. Soil water disappears totally when we use the 75 percentile of silica concentrations in our calculation.

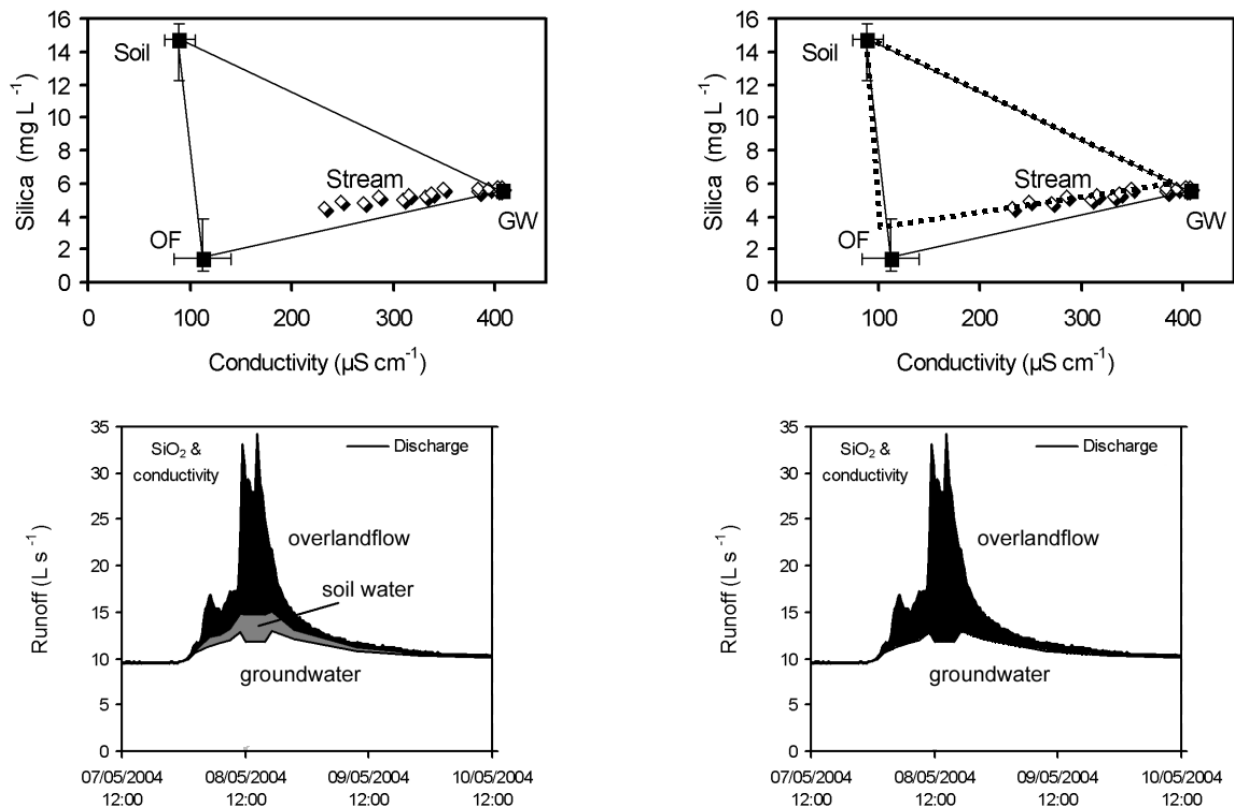


Fig. 7: Uncertainty of hydrograph separation in the storm of May 2004; calculation with the medium (left) and 75 percentile (right) of silica in the overlandflow end-member.

Conclusions

The temporal variations in rainfall, throughfall, discharge rates, groundwater levels and solute concentrations related to rainstorms were observed in two forested small catchments. A three-component end-member mixing analysis was applied using chemical tracers. In the Huewelerbach catchment the first end-member is a constant groundwater component generated from the sandstone springs. The second end-member is the saturated overland flow component. The contribution of the third end-member to the discharge is the soil water from the alluvial zone.

On the contrary, overland flow was almost irrelevant in the Weierbach basin, which presents a large rate of delayed discharge (including at the peak discharge) giving evidence of an important throughflow rate (weathered shales).

The selected end-members are not constant throughout the year and during the flood events exhibiting variances in their chemical properties. The uncertainty associated to these variations is similar to the divergence observed when using a different pair of tracers.

Uncertainties in our chemical hydrograph separations were large, mainly as a result of the high variations of the chemical characteristics of our end-members. In our case study, the expected end-members might be seen as no real end-members.

Acknowledgements

The Fonds National de la Recherche supported this research project: 'Study of the Water Cycle Components in the Attert River Basin (CYCLEAU)'.

References

- Christophersen N., Neal C., Hooper R.P., Vogt R.D., Anderson S. (1990). Modelling streamwater chemistry as a mixture of soil water end-members - a step towards second-generation acidification models. *Journal of Hydrology*, 116: 307-320.
- Hooper R.P., Christophersen N., Peters N.E. (1990). Modelling streamwater chemistry as a mixture of soil water end-members - an application to the Panola Mountain catchment, Georgia, USA. *Journal of Hydrology*, 116: 321-343.
- Hooper R.P., Shoemaker C.A. (1986). A comparison of chemical and isotopic hydrograph separation. *Water Resources Research*, 22: 1444-1454.
- Krein A., De Sutter R. (2001). Use of artificial flood events to demonstrate the invalidity of simple mixing models. *Hydrological Sciences Journal*, 46: 611-622.

MOVING TOWARD AN IMPROVED FLOOD-MODELLING CONCEPT USING REMOTE SENSING

G. Schumann^{1,2}, R. Hostache³, C. Puech³, F. Pappenberger⁴, P. Matgen¹, M. Cutler², A. Black², L. Hoffmann¹ & L. Pfister¹

¹Public Research Centre – Gabriel Lippmann, Department of Environment and Biotechnologies, rue du Brill 41, L-4422 Belvaux, Luxembourg. ²University of Dundee, Environmental Systems Research Group, DDI4HN, Nethergate, Dundee, UK. ³UMR TETIS CEMAGREF-CIRAD-ENGREF, Maison de la Télédétection en Languedoc-Roussillon, rue J.F. Breton 500, F-34093 Montpellier, Cedex 5, France. Now at 1. ⁴Hydrology and Fluid Dynamics Group, Lancaster University, Environmental Science Department, Lancaster, LA14YQ, UK. Now at the European Centre for Medium-range Weather Forecasts (ECMWF), RG29AX, Shinfield Park, Reading, UK.

Corresponding author: G. Schumann, e-mail: schumann@lippmann.lu

ABSTRACT

In hydraulic modelling there is much argument on model simplicity. A low number of model parameters are preferred, as it facilitates model calibration. An important model parameter to be calibrated is roughness. Flood inundation modelling is commonly performed with a minimum number of (channel) roughness parameters, as there is a lack of spatially distributed evaluation data to constrain parameter uncertainty and because roughness is difficult if not impossible to measure appropriately in the field. Despite the simplicity argument, it is sensible to suggest that if additional data demonstrate the need to increase the number of parameters in order to improve model performance, model complexity seems justified and should in such a case not be avoided. This study proposes a methodology that makes use of spatially distributed satellite radar-derived water level data to demonstrate that locally adapted model parameters are needed to improve flood inundation predictions at the local level. The methodology is developed on a flood event that occurred in early January 2003 on the River Alzette (G.D. of Luxembourg) and which was recorded by the Advanced Synthetic Aperture Radar (ASAR) instrument onboard the ENVISAT satellite. It is shown that reach-scale (average) performing model simulations are easy to obtain with a minimum number of parameters but locally acceptable model predictions can only be generated when model complexity is increased to allow (channel) roughness to be spatially distributed across the modelled reach. This illustrates the great potential that remote sensing, in particular SAR, holds in terms of identifying new ways to improve existing modelling concepts and to contribute to the development of improved flood inundation models.

Keywords: remote sensing, flood inundation model error, Monte Carlo-based computation, spatially distributed parameter, behavioural criteria

Introduction and objective

From a global perspective, floods account for about a third of all natural disasters by number and economic losses and are responsible for over half the recorded deaths (Knight, 2006). In the past decade, flood disasters and their mitigation have therefore attracted increasing attention. This has led national agencies to review major current issues in flood warning (e.g. ICE, 2001) and there is also an increasing seriousness with which responsibilities are taken with regard to both flood forecasting and warning. There is a pressing need to update flood risk maps and to improve their accuracy, especially in development hot spots (ICE, 2001), which tend to extend more onto natural floodplains and closer to stream channels given the current scarcity in space. With this in mind, more efforts must be made before, during and after a flood to gather information to be used in flood forecasting systems.

Water level data at appropriate scales are at the heart of a well-performing hydrodynamic model that is a crucial component of an early warning system. Accurate flood inundation prediction is technically demanding due to inadequately structured models, poor estimation of model parameters and data errors. Given that both

model results and data are highly uncertain, it is reasonable to say that no ‘perfect’ model exists which will perform well in all locations of the modelled domain. The issue of a model performing well at one location whilst constantly underperforming at another has been raised a number of times (e.g. Pappenberger et al., 2007; Pappenberger et al., 2006a; Freer et al., 2004; Beven, 2000) and is largely due to inadequate data on channel geometry and reach topography and, more often, on effective roughness coefficients that are difficult to estimate. Overcoming the limitations of inadequate (channel) roughness parameter information would certainly allow reducing flood inundation prediction uncertainties, which is essential for adequate assessment of flood risk. Model uncertainty could be constrained by using additional sources of information in the modelling process. This said, additional datasets are often neglected in the modelling process, as there is the need to keep the model as simple as possible, so as to facilitate its calibration. However, if such information could offer additional uncertainty constraints, an increased model complexity would be justified.

Additional data on how roughness or other parameters are spatially distributed within the modelled reach would presumably help constrain model uncertainty. Most work on researching roughness characteristics has been done in the laboratory or undertaken on floodplain roughness related to land use types (e.g. Werner et al., 2005; Straatsma and Middelkoop, 2006). Measuring roughness, particularly channel roughness distributions, in the field is a very difficult task (Lane, 2005). A possible solution could come from the integration of flood inundation models and the fully distributed nature of satellite remote sensing information. In particular, Synthetic Aperture Radar (SAR) image data are of value, given the instrument’s all-weather capability and sensitivity toward a smooth open water surface. The success of SAR data in flood inundation model calibration has been shown in several studies (e.g. Bates et al., 1997; Aronica et al., 2002; Matgen et al., 2004; Pappenberger et al., 2006b; Horritt, 2006).

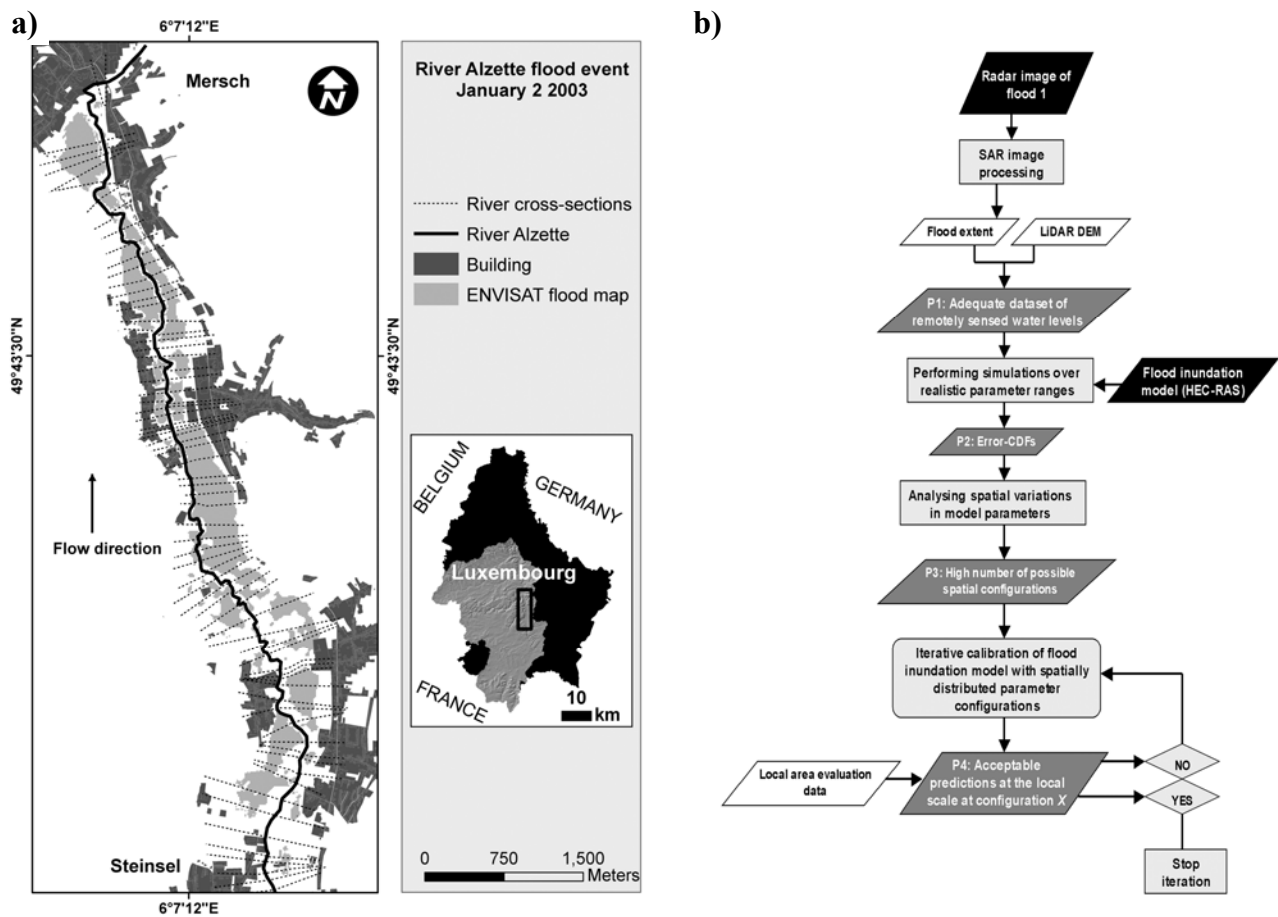


Fig. 1: (a) Map showing study site location and (b) flow chart of proposed step-based methodology.

In this context, it is the aim of this study to introduce a step-based methodology that makes use of an adequately processed SAR dataset to identify a way to allow regional clustering of distributed roughness parameters that reflect spatial variations in cross-sectional channel conveyance. It is expected that the proposed procedure allows the generation of model predictions that perform well at the local scale, which is most needed for successful flood hazard management. The methodology is developed on a flood event that occurred in early January 2003 on the River Alzette (G.D. of Luxembourg) and was recorded by the Advanced Synthetic Aperture Radar (ASAR) instrument onboard the ENVISAT satellite (Fig. 1a).

Proposed methodology

The proposed methodology to derive spatially distributed roughness values is largely motivated by the discussion and conclusion of Pappenberger et al. (2006a). In their innovative study, they analyse the influence of uncertain model structure on flood inundation predictions and observe that:

- Cumulative distribution functions (CDFs) can be computed at each river cross-section for the Manning surface roughness based on model performance.
- These CDFs, which depend on the nature of the evaluation data used, can be correlated with each other to identify cross-sections that require different roughness coefficient values.
- There is a noticeable temporal and spatial shift in behavioural surface roughnesses.
- The model is influenced by a complex interaction of parameters, which makes it difficult to pin point how parameters should be changed locally.
- Such local adjustments would suggest an improved model performance.

These findings encourage the challenge to come up with an improved model or modelling concept that generates flood inundation predictions that perform well at the local level. The modelling concept in this study includes local (cross sectional) roughness parameters derived from a detailed analysis of the interaction between local flooding characteristics and model configuration. Local flooding characteristics are reflected by varying water levels at each model cross section. At present, observing flood water levels at this scale seems only likely with the fully distributed nature of remote sensing imagery. Such data are used in this study to generate flood area representative CDFs for the channel roughness at each river cross section based on the distance (i.e. error) between SAR-observed and model-simulated water stages. Thereafter, the cross sections are classified according to their sensitivity toward roughness. By defining spatial patterns of important model parameters, it is expected that the predictive uncertainty of a flood inundation model will be reduced in such a way as to allow acceptable performances at local scales.

The proposed methodology follows the procedure illustrated in Fig. 1b. The subsections below explain the different methodology steps with their respective processing outputs (P 1-4) in detail.

SAR image processing

The dual-polarised (VV-VH) ENVISAT flood image was acquired at flood peak in C-band at 5.3 GHz and with an incidence angle of 35°. Using a 5x5 pixel Frost filter window, most of the image noise is removed without significant degradation of the flood boundary precision of 12.5 m (the raw PRI image product had been downscaled from 25 m using multi-look filtering). The VH-polarisation is selected for further processing given its superior sensitivity toward the horizontal nature of a smooth floodwater surface (Henry et al., 2006). A flood map (Fig. 1a) was extracted applying a simple but nonetheless effective image thresholding technique. A 'valley' within the image histogram helps locate an appropriate threshold value, which is confirmed using GPS marks of the maximum flood extent. The ENVISAT-derived flood boundary matches the position of the GPS marks and agrees generally well with the digital photography of the event.

P1: Following Schumann et al.'s (2007a) approach, the ENVISAT flood boundary is overlain on a high-resolution, high-precision LiDAR (± 15 cm RMS error in the vertical) to extract water height data at every river cross section for which flood detection is feasible. Assuming a horizontal water level at each cross-section, the mean between left and right riverbank data is taken to calibrate the well-known 1D hydrodynamic HEC-RAS model (USACE, 2002). It is worth noting that the linear flood waterline model for the Alzette reach as proposed by Schumann et al. (2007a) is not used here, as the non-linearity of the 'raw' radar data is preferred, so as not to force the dynamic model toward a simplified GIS model output.

Initial model runs

The HEC-RAS model (www.hec.usace.army.mil), which solves the 1D hydrodynamic St Venant equations for mass and momentum, was used in this study to perform unsteady flow calculations (USACE, 2002) for the Alzette River flood of 2003. The model requires detailed river cross section and hydraulic structure geometry as well as topographic data, which are provided by precision terrain surveying and LiDAR scanning, respectively. The only model parameters that need calibration are the channel and floodplain Manning roughness coefficients. As it has been shown in previous studies (e.g. Pappenberger et al., 2006a; Matgen et al., 2004) that floodplain roughness is not important at any cross section in the modelled reach, only channel roughness is further investigated. The model is setup in a Monte Carlo computation environment to allow a very large number of simulations to be performed over defined parameter ranges. Initially, 5000 runs are performed over a realistic range of channel roughness coefficients from 0.025 to 0.08.

Spatial variations in model parameters

P2: Thereafter each model run is evaluated with the ENVISAT-derived spatially distributed water levels. This enables CDFs to be computed at each river cross section for the Manning surface roughness based on model performance given by Eq. 1, as suggested by Pappenberger et al. (2006a).

$$LE_H = |H_M - H_R| \quad \text{Eq. 1}$$

Where LE_H stands for local error in water level, H_M is the water level simulated by the model and H_R is that derived from the radar image. Subsequently each cross section CDF is subtracted from a discrete uniform distribution for which prediction errors are the same across the sampled parameter space. This procedure seems adequate for this study, as it can be argued that the highest possible degree of uncertainty is expressed by the uniform distribution (Krykacz-Hausmann, 2001). The difference between an individual CDF curve and the uniform distribution line indicates whether or not a given cross section requires an additional channel roughness parameter. This can be used to identify the number of additional model parameters needed to obtain acceptable flood inundation predictions at the local level. Eq. 2 gives the formula that provides information on the local parameter effects, LS_M .

$$LS_M = \sum_{i=1}^n (x_{cdf} - x_{du}) \quad \text{Eq. 2}$$

Where x_{du} denotes the expected CDF value according to a uniform distribution of errors across the sampled parameter range at model run i and x_{cdf} represents the CDF value of the actual parameter distribution at model run i , with n being the number of runs performed. CDFs representing similar model error characteristics are allocated to a given class using the k-means clustering algorithm. The algorithm tries to minimize the total intra-cluster variance, or the function:

$$V = \sum_{i=1}^k \sum_{j \in S_i} |x_j - \mu_i|^2 \quad \text{Eq. 3}$$

Where there are k clusters S_i , $i = 1, 2, \dots, k$ and μ_i is the mean point of all the points $x_j \in S_i$.

Iterative model calibration with spatially distributed parameters

P3: The k-means algorithm is applied to all error-CDFs. The variable k, which assigns k number of channel roughness clusters to the reach according to the local parameter effects (LSM), is not predetermined subjectively. Instead, a number iteratively increased by 1 is attributed to the reach until the kth number of clusters, denoted nk, which satisfies the behavioural criterion set for local scale (see below), is found. In other words, first, during a high number of simulations run in a Monte Carlo environment, randomly chosen roughness values are attributed to one single cluster regrouping all cross sections in the entire reach (k = 1). Then, k is increased by one, and for each model simulation, the same randomly chosen roughness value within a predefined range is attributed to all cross sections within one cluster.

Each model simulation is evaluated with seven field-based water stages recorded at wrack lines shortly after the event, thereby applying the following local behavioural criteria: the absolute error at each location between a given model simulation and the field-based water stage mark must not be larger than the associated uncertainty of that mark (Refsgaard et al., 2006). A level of uncertainty as low as 0.1 m for the automatically registered water level at two bridges and of 0.3 m for the maximum water level recorded in the floodplain ensure that a model run performs well at every location of field data with respect to the measurement uncertainties.

P4: The model is actually run with spatially distributed roughness parameter values, the spatial arrangement of which has been conditioned on satellite radar-derived water stages. The procedure is stopped when nk clusters allow the generation of locally acceptable model simulations. It is not desirable to investigate the effects of more clusters than those really needed to obtain acceptable model predictions at the local scale, as it is reasonable to argue that any unnecessary increase in model complexity should be avoided.

Results and discussion

A detailed result analysis and an extended discussion are beyond the scope of this short paper, the focus of which is on the proposed methodology. A more complete result and discussion part is provided in a full-length paper in submission (Schumann et al., 2007b). Nevertheless, it is indispensable to briefly present the River Alzette study results for the January 2 2003 flood event and subsequently highlight the main points worth discussing.

Initial calibration results without spatial variation of the channel roughness parameter show that 19% of all simulations are performing at least as good as a reach-scale (average) model linearly interpolated between the lower- and uppermost field-based water stage mark. However, no model satisfies the behavioural criteria set at each location. This confirms the argument of some authors that it is difficult to obtain a simulation that performs acceptable at every location (Pappenberger et al., 2007; Frost and Knight, 2002).

Plotting cross section CDFs of a high number of runs over a range of possible roughness values enables the modeller to compare and investigate the behaviour of individual cross sections in relation to the roughness parameter. Indeed, when analysing the effect of the channel roughness on individual cross section behaviour (Fig. 2a), it becomes clear that there is a need for a spatial adjustment of the roughness parameter. However, doing so adds more parameters to the flood inundation model. It may be argued that any increase in model complexity has to strike the fine balance between over-parameterization and fitting the model to the data.

In fact, during the iterative model calibration with possible combinations of spatially adapted channel parameters, it is demonstrated that a model configuration with two clusters of the channel roughness parameter generates acceptable flood inundation predictions at each field-based validation point (0.1% of 10000). Fig. 2b provides a visual comparison between the best model simulation with one channel roughness parameter and the best simulation with spatially varying the channel roughness parameter. As is clearly illustrated, only by varying the roughness parameter does the model meet the behavioural criteria everywhere.

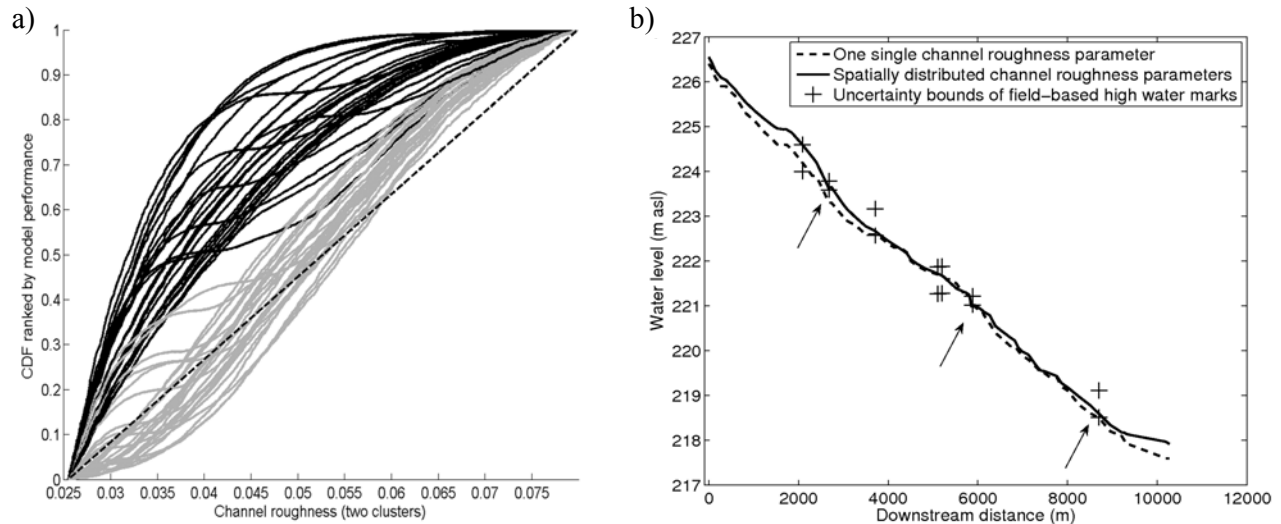


Fig. 2: Cross section CDF curves implicitly demonstrating different channel roughness behaviour for different cross sections (a); the impact of spatially varying channel roughness parameters on model performance. Arrows point to locations where a simulation with one single roughness parameter fails (b).

These findings demonstrate that there is the need to consider and analyse the spatial variations of flood inundation model parameter values and also the effects they have on local flooding. This is particularly important if a flood disaster response may be to produce flood extent and depth maps or risk maps (Pappenberger et al., 2007) with acceptable uncertainties at local scales. An innovative methodology is proposed that uses water level observations based on remote sensing data (SAR) to conduct such analyses. Acceptable model performances at the local level can be obtained when important model parameters are adequately varied over space. In this context, it is worth noting several important issues that need particular attention and thus are discussed in detail in Schumann et al. (2007b):

- Parameter uncertainty, which is spanning over the entire sampled range for reach-scale (average) behavioural model simulations, is remarkably constrained in the case of locally acceptable simulations where channel roughness parameters become identifiable.
- An investigation on the impact of a further increase in model parameter number (i.e. $n_k > 2$) shows that although more model predictions are acceptable locally (as is to be expected with an increased degree of freedom), the identifiability of the channel roughness parameter is much reduced again.
- Application to two other flood events of different magnitude recorded with remote sensing instruments indicates that the proposed model concept/configuration is robust.
- However, it is also illustrated that a limitation to the robustness is related to flood inundation process complexity that cannot be adequately replicated by a 1D or even 2D hydrodynamic model. Such process complexity, in the form of non-connectivity of the flooded plain to the channel, groundwater resurgence or Hortonian overland flow, may be present locally, but is not predominant, during events.

It is important to note that deriving spatial patterns of the channel roughness with SAR remote sensing was possible because of the simple functioning of a 1D flood inundation model. In simple terms, water stage magnitude, which is a direct result from the interaction between the amount of water conveyed by a given cross section and the roughness associated with that cross section, determines overtopping, the degree of which is reflected in the position of the flood extent. Furthermore, cross sections are regionally grouped when the CDF clusters in Fig. 2a are mapped into real space, which also reflects the physical functioning of the model. A roughness value at one cross section influences water stages at adjacent cross sections upstream and

downstream. No field-based roughness estimates were available to verify the SAR-derived roughness allocation.

Conclusion

It is now fairly recognised that all model setups, regardless of their complexity, are to some extent in error (Freer et al., 2004). Such error information has been used in this study to introduce a methodology to derive spatial patterns of the channel roughness parameter. The aim has been to find a model configuration with which to obtain acceptable simulations at the local level.

For the studied reach (Alzette River, G.D. of Luxembourg), two different clusters of channel roughness are required to find model predictions that perform well at each location of field-based measurements. At the reach scale (i.e. looking at average model performance over the reach), many flood simulations are already acceptable without spatially distributing the roughness parameter. However, when distributing channel roughness, parameters (need to) become identifiable in order to obtain locally acceptable model simulations.

This way, acceptable flood inundation predictions at the local scale can be obtained, which is particularly important for flood hazard management where crucial flood information is required locally. However, further, more detailed analysis is needed to find supporting evidence of the spatial allocation of clusters from radar imagery in the field. This could be done using correlation analysis of a classification of riverbank vegetation pictures at cross sections and the radar-derived clusters.

References

- Aronica G., Bates P.D., Horritt M.S. (2002). Assessing the uncertainty in distributed model predictions using observed binary pattern information within GLUE. *Hydrological Processes*, 16: 2001-2016.
- Beven K.J. (2000). Uniqueness of place and process representations in hydrological modelling. *Hydrology and Earth System Sciences*, 4: 203-213.
- Freer J.E., McMillan H., McDonnell J.J., Beven K.J. (2004). Constraining dynamic TOPMODEL responses for imprecise water table information using fuzzy rule based performance measures. *Journal of Hydrology*, 291: 254-277.
- Frost L., Knight D. (2002). Catchment and river basin management. In: G. Fleming (Ed), *Flood Risk Management*. ICE, Thomas Telford Publishing, London, UK: 51-89.
- Henry J.B., Chastanet P., Fellah K., Desnos Y.L. (2006). ENVISAT multi polarised ASAR data for flood mapping. *International Journal of Remote Sensing*, 27: 1921-1929.
- Horritt M.S. (2006). A methodology for the validation of uncertain flood inundation models. *Journal of Hydrology*, 326: 153-165.
- ICE (2001). *Learning to Live with Rivers*. Final report of the ICE Presidential Commission to review the technical aspects of flood risk management in England and Wales. The Institution of Civil Engineers, London, UK, pp. 87.
- Knight D.W. (2006). Introduction to flooding and river basin modelling. In: D.W. Knight, A.Y. Shamseldin (Eds), *River Basin Modelling for Flood Risk Mitigation*. Taylor and Francis Group, London, UK: 1-21.
- Krykacz-Hausmann B. (2001). Epistemic sensitivity analysis based on the concept of entropy. *Proceedings of SAMO 2001*, Madrid, Spain: 31-35.
- Lane S.N. (2005). Commentary: Roughness – time for a re-evaluation? *Earth Surface Processes and Landforms*, 30: 251-253.
- Matgen P., Henry J.B., Pappenberger F., de Fraipont P., Hoffmann L., Pfister L. (2004). Uncertainty in calibrating flood propagation models with flood boundaries observed from Synthetic Aperture Radar imagery. *Proceedings of the 20th Congress of the ISPRS*, Istanbul, Turkey, 12-23 July, CD-ROM.

- Pappenberger F., Beven K., Frodsham K., Romanowicz R., Matgen, P. (2007). Grasping the unavoidable subjectivity in calibration of flood inundation models: a vulnerability weighted approach. *Journal of Hydrology*, 333: 275-287.
- Pappenberger F., Frodsham K., Beven K., Romanowicz R., Matgen P. (2006a). Fuzzy set approach to calibrating distributed flood inundation models using remote sensing observations. *Hydrology and Earth System Sciences Discussions*, 3: 2243-2277.
- Pappenberger F., Matgen P., Beven K., Henry J.B., Pfister L., De Fraipont P. (2006b). Influence of uncertain boundary conditions and model structure on flood inundation predictions. *Advances in Water Resources*, 29: 1430-1449.
- Refsgaard J.C., Van der Sluijs J.P., Brown J., Van der Keur P. (2006). A framework for dealing with uncertainty due to model structure error. *Advances in Water Resources*, 29: 1586-1597.
- Schumann G., Hostache R., Puech C., Hoffmann L., Matgen P., Pappenberger F., Pfister L. (2007a). High-resolution 3D flood information from radar imagery for flood hazard management. *Transactions on Geoscience and Remote Sensing, Disaster Special Issue*. In press.
- Schumann G., Matgen P., Pappenberger F., Hostache R., Pfister L. (2007b). Deriving distributed roughness values from satellite radar data for flood inundation modelling. *Journal of Hydrology*. Revision submitted.
- Straatsma M.W., Middelkoop H. (2006). Airborne laser scanning as a tool for lowland floodplain vegetation monitoring. *Hydrobiologia*, 565: 87-103.
- United States Army Corps of Engineers (USACE), 2002. Theoretical basis for one-dimensional flow calculations. In: USACE (Eds.), *Hydraulic Reference Manual*. Version 3.1, USACE, Davis, CA: 2.1-2.38.
- Werner M.G.F., Hunter N.M., Bates P.D. (2005). Identifiability of distributed roughness values in flood extent estimation. *Journal of Hydrology*, 314: 139-157.

QUANTIFYING UNCERTAINTIES IN THE TERRESTRIAL WATER STORAGE - STREAMFLOW RELATION USING *IN SITU* SOIL MOISTURE DATA

U. Somorowska

The University of Warsaw, Faculty of Geography and Regional Studies, Department of Hydrology, Krakowskie Przedmieście 30, 00-927 Warsaw, Poland
Corresponding author: Urszula Somorowska, email: usomorow@uw.edu.pl

ABSTRACT

This study provides an insight into uncertainties present in the terrestrial water storage - streamflow relation. The uncertainties considered comprise both model structure uncertainty and model parameter uncertainty. The water storage - streamflow relation is approximated by a simple regression model. It provides a statistical relationship between variables. The water storage parameter is considered as an input variable into the model. Uncertainty in the water storage parameter is quantified and its effect on the streamflow behaviour of the catchment is investigated. The range of possible responses of catchment streamflow is presented as a result of incorporated uncertainty in the model input parameter. Soil water storage and effective relative soil moisture are applied as estimates of terrestrial water storage. The study is facilitated by a high-quality data set of extensive soil moisture records covering a ten-year period (1995-2004). Experimental data include volumetric soil moisture measured by the Time Domain Reflectometry (TDR) field operating meter in a small lowland catchment situated in central Poland. Soil characteristics (texture and porosity) and groundwater levels are considered as major local factors influencing terrestrial water storage. The focus is on uncertainty resulting from the variability of such soil properties. Uncertainty originating from measurements (errors in data) is assumed negligible. The range of possible streamflow values connected to the range of soil water storage is assumed to characterize the catchment response. The concept of a simple regression model is presented, in which high quality soil moisture data from *in situ* measurements are assimilated. It has been found that uncertainty in soil water storage causes uncertainty in estimates of streamflow values over a broad range.

Keywords: soil moisture data, terrestrial water storage, streamflow, regression model, uncertainty

Introduction

Terrestrial water storage in the upper soil layers plays an important role in most of the processes present at the land-atmosphere interface. It controls water fluxes appearing during infiltration, evapotranspiration and groundwater recharge. Estimates of soil water storage are necessary in the anticipation of wetness conditions controlling streamflow at catchment scale. The *in situ* data collected from reference sites can be used to quantify patterns of terrestrial water storage at a pedon scale. Then the patterns can be used to characterize the relationship between stages of terrestrial water storage and streamflow values. Due to the high spatial variability of soil properties the uncertainty of the terrestrial water storage - streamflow relation should be considered.

Detecting the terrestrial water storage – streamflow relation in this study follows an approach presented by Scipal et al. (2005) in which differences in streamflow values are, to a certain extent, explained by the soil moisture differences detected from coarse resolution data. Simultaneously, the approach applied here refers to the notion of the ‘Dominant Processes Concept’ (Blöschl, 2001), in which the need for identifying dominant processes that control hydrological response, is the main concern. Generally, merging the soil water storage at a pedon scale with streamflow at a catchment scale coincides with the conceptual framework for multiscale bridging in hydrogeology (Lin, 2003), in which bridging from mesoscopic to macroscopic level is highlighted.

As a result of this study, a simple model representing catchment response is confronted with a field data set. This supports current efforts to incorporate field data sets in hypothesis testing rather than putting too much stress on the calibration of increasingly complex models (Clifford, 2002). As the dynamics of daily streamflow of the catchment in question has strong groundwater contributions (Somorowska, 2006), it is expected that terrestrial water storage evaluated by varying seasonal patterns of subsurface soil moisture is well correlated with streamflow values. Adopting the simple definition of uncertainty provided by Brown and Heuvelink (2005) that “uncertainty is an expression of confidence about what we “know”,...”, the uncertainty in model output originating from uncertainty in input data is reviewed through special boundaries for uncertainties.

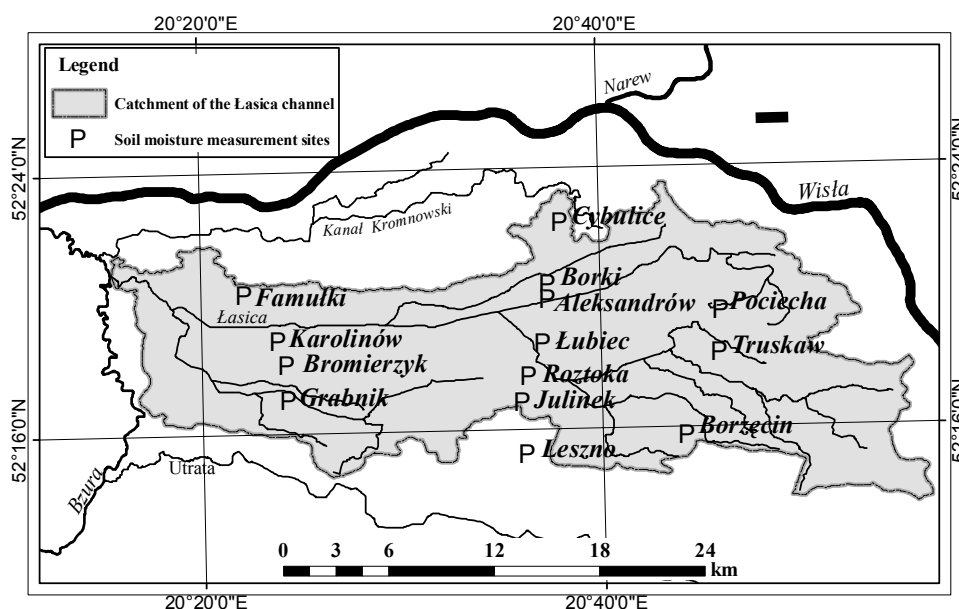


Fig. 1: Location of the soil moisture measurement sites in the Lasica catchment, central Poland.

The overall aim of this study is to link different stages of wetness conditions with streamflow using a simple regression model and to evaluate the uncertainty of this relation. The specific objectives were: (1) to evaluate the possible range in the soil water storage estimates at a pedon scale, (2) to apply a common dimensionless parameter representing soil water storage for different *in situ* conditions, for pedon scale considerations, (3) to link soil water storage evaluated at a pedon scale with streamflow recorded at catchment scale, (4) to specify the range of uncertainty of model inputs. A data set of soil moisture inferred from *in situ* measurements was used for this research (Somorowska, 2005). It covers the 10-year period (1995–2004) of TDR measurements conducted in selected experimental sites in the Lasica catchment which is located in central Poland (N 52°15' – N 52°24' and E 20°15' - E 20°57') as presented in Fig. 1.

More sophisticated analyses using rainfall-runoff models can be applied to investigate streamflow behaviour. An example of rainfall-runoff model calibration with measured soil moisture data is described e.g. by Robinson and Stam (1993). It requires, however, continuous soil moisture data to calibrate the model, preferably using the depth varying water content profile.

Data

Volumetric soil moisture data were used in this study. Measurements have been conducted in contrasting seasons of the year. Portable TDR meters were applied to track the characteristic stages of soil water storage of shallow soil layers in fourteen experimental sites. At each site, measurements of soil moisture were taken at

depths of 5, 10, 20, 30, 50, 70, 90 and 110 cm. At selected sites, measurements were taken in dry seasons to the depth of 190 cm.

In addition to the soil moisture data set, groundwater and discharge data are used in this study. Groundwater records from the monitoring system of the Kampinos National Park represent groundwater elevation as well as the depth to the groundwater measured every two weeks. Daily discharge data of the Lasica Channel at Wladyslawow gauging station used in the regression model are supplied by the Institute of Meteorology and Water Management in Warsaw.

Methodology

Interactions between patterns of terrestrial water storage and streamflow are displayed in the form of a simple regression function. Observed stages of soil water storage derived from field measurements are linked here with values of streamflow. Patterns of terrestrial water storage are considered for three different synthetic soil profiles (types I, II and III) representing different regimes of soil moisture. Type I profile comprises wet sites with a very shallow groundwater table, type II profile – wet sites with a shallow groundwater table and type III profile - dry sites with a shallow groundwater table. Drying and wetting patterns of the soil moisture profiles represent different stages of wetness conditions. Soil water storage patterns are derived from the soil moisture profiles and then linked with streamflow values.

Based on the volumetric soil moisture values measured by the TDR field operating meter, soil water storage is calculated. Water storage WS (mm) in the layer of depth $\Delta z = z_2 - z_1$ (mm) is obtained from the expression $WS = 0.01 \cdot \theta \cdot \Delta z$, where θ represents the volumetric moisture content (%). Thus water storage WS (mm) in the soil profile is expressed as a sum of water storage in particular soil layers WS_i (mm) and is calculated as follows:

$$WS = \sum_{i=1}^n WS_i = 0.01 \sum_{i=1}^n \bar{\theta}_i \cdot \Delta z_i \quad \text{Eq. 1}$$

The value of $\bar{\theta}_i$ (%) represents the mean soil water content in layer i and Δz_i (mm) is the depth of a particular soil layer. Taking into account the location of the TDR soil moisture probes installed at different depths, the soil profiles have been schematized in a number of soil layers. Thus water storage in the soil profiles of a depth of 0-100 cm is calculated according to the following expression:

$$WS_{0-100\text{cm}} = WS_{0-7.5\text{cm}} + WS_{7.5-15\text{cm}} + WS_{15-25\text{cm}} + WS_{25-40\text{cm}} + WS_{40-60\text{cm}} + WS_{60-80\text{cm}} + WS_{80-100\text{cm}} \quad \text{Eq. 2}$$

where: $WS_{0-100\text{cm}}$ – soil water storage in the layer of 0–100 cm, $WS_{0-7.5\text{cm}}$, $WS_{7.5-15\text{cm}}$, $WS_{15-25\text{cm}}$, $WS_{25-40\text{cm}}$, $WS_{40-60\text{cm}}$, $WS_{60-80\text{cm}}$ and $WS_{80-100\text{cm}}$ – soil water storage estimated accordingly in layers of 0–7.5 cm, 7.5–15 cm, 15–25 cm, 25–40 cm, 40–60 cm, 60–80 cm and 80–100 cm. Values of θ measured at depths of 5 cm, 10 cm, 20 cm, 30 cm, 50 cm, 70 cm and 90 cm are assumed to represent mean soil water content ($\bar{\theta}_i$) of subsequent layers described in equation (2). Thus equation (2) can be expressed as follows:

$$WS_{0-100\text{cm}} = 0.01(\theta_5 \cdot 75 + \theta_{10} \cdot 75 + \theta_{20} \cdot 100 + \theta_{30} \cdot 150 + \theta_{50} \cdot 200 + \theta_{70} \cdot 200 + \theta_{90} \cdot 200) \quad \text{Eq. 3}$$

$$WS_{0-100\text{cm}} = 0.75\theta_5 + 0.75\theta_{10} + \theta_{20} + 1.5\theta_{30} + 2\theta_{50} + 2\theta_{70} + 2\theta_{90} \quad \text{Eq. 4}$$

where: $WS_{0-100\text{cm}}$ – soil water storage in the layer of 0–100 cm, θ_5 , θ_{10} , θ_{20} , θ_{30} , θ_{50} , θ_{70} and θ_{90} – volumetric soil moisture (%) measured accordingly at depths of 5 cm, 10 cm, 20 cm, 30 cm, 50 cm, 70 cm and 90 cm.

The following regression model was applied to link the values of streamflow (Q) with water storage (WS):

$$Q = a \cdot \exp(b \cdot WS_{0-100\text{cm}}) \quad \text{Eq. 5}$$

where: Q – streamflow (m^3/s), $WS_{0-100\text{cm}}$ – soil water storage in the layer of 0–100 cm. In the above equation soil water storage is characterized by soil water depth expressed in mm. Additionally, to express soil water storage in a dimensionless way, the parameter of effective relative soil moisture is applied. Effective relative soil moisture is defined in this study as $x = (s - s_w)/(s_{fc} - s_w)$, where s – relative soil moisture (dimensionless), s_{fc} – relative soil moisture at field capacity (dimensionless), s_w – relative soil moisture at wilting point (dimensionless). Relative soil moisture s is defined as $s = \theta_v/n$, where: θ_v – volumetric soil moisture, n – porosity. Thus, effective relative soil moisture, which is dimensionless, can be alternatively expressed as $x = (\theta_v - \theta_{\min})/(\theta_{\max} - \theta_{\min})$, where θ_{\min} – minimum measured volumetric soil moisture, corresponding to wilting point and θ_{\max} – maximum measured volumetric soil moisture, corresponding to field capacity. Thus the regression model can be alternatively expressed in the following form:

$$Q = a \cdot \exp(b \cdot x_{0-100\text{cm}}) \quad \text{Eq. 6}$$

where: $x_{0-100\text{cm}}$ – effective relative soil moisture in the layer of 0–100 cm. The relation was established for the three types of synthetic soil moisture profiles as well as for their mean.

Input variables to the regression models expressed by equations (5) and (6) are estimates of terrestrial water storage calculated for the soil layer of 0-100 cm depth. It is assumed that the bottom part of this soil layer constitutes a source of free gravity water present in the coarse pores of the soil which contributes to streamflow generation. Although in situations with deeper groundwater level, it is just a transition zone for the water recharging the groundwater. Thus applied estimates of soil water storage reflect the wetness stages of soil layers that are interacting with shallow groundwater. Surface streamflow is of insignificant order in the studied catchment (Somorowska, 2006) and therefore the values of streamflow used in this study correspond to the groundwater contribution. The range of the soil wetness stages gives an estimate of uncertainty of soil water storage used as an input parameter to the regression model.

Results and discussion

Patterns of terrestrial water storage

Selected soil moisture profiles for the three profile types are displayed in Fig. 2. Variable soil moisture profiles correspond to the variable groundwater levels. Water storage capacity is a derivative of soil porosity which is the highest in type I profiles in the surface layer. The difference between the envelope curves of the soil moisture profiles detected in wet and dry conditions represent differences in soil water storage.

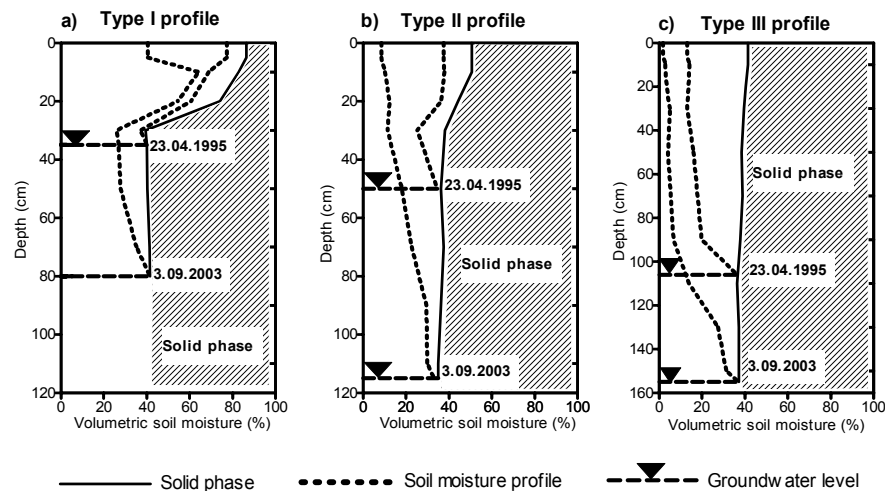


Fig. 2: Distribution of soil moisture during selected dry and wet seasons for the three profile types.

Terrestrial water storage - streamflow relation

The relation between estimates of soil water storage and streamflow expressed in the form of equation (5) is presented in Fig. 3. The soil water storage $WS_{0-100\text{cm}}$ applied as input variables is calculated as an average for the three profile types. Although most of the variance (76%) between variables is explained by the regression, the scatter plot of points around the regression line indicates that there are deviations from the established predictive relationship. Similar values of soil water storage are observed for different streamflow values, e.g. soil water storage of approximately 290 mm is present for streamflow recorded within the range 0.9-2.09 m^3/s . The possible cause is the hysteresis of soil water retention. Although the estimated relationship has broad bounds consisting of detected empirical values of soil water storage estimates, generally the changes of streamflow values follow the changes of soil water storage. Thus it can be concluded that changes of streamflow are, to a certain extent, synchronous with changes of soil water storage.

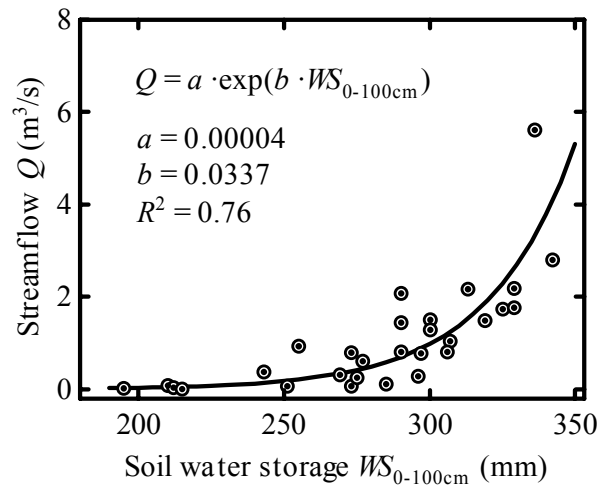


Fig. 3: Relationship between streamflow and catchment wetness stage expressed as soil water storage.

Uncertainties in the terrestrial water storage - streamflow relation

The soil water storage in the three profile types linked to the streamflow is presented in Fig. 4a. The broad range of soil water storage detected in different patterns of the soil profiles sheds light on the amount of soil water present in the upper soil layers during different catchment wetness stages. The broad range of soil water storage reflects the high uncertainty of the spatially variable soil water storage.

In order to compare the functional behaviour of different profiles the dimensionless parameter of effective relative soil moisture is applied and linked with the streamflow values. Fig. 4b presents the streamflow values simulated according to the regression models expressed by equation (6), separately for different profile types. It can be concluded that retention of the type I profile fills up fastest to the field capacity in a fastest way. On the contrary, retention of the type III profile fills much slower; during periods of relatively high values of streamflow there is still a capacity within the layer 0-100 cm to be filled to the maximum value. Thus the evaluation of the mean relation between soil water storage and streamflow at catchment scale requires a more detailed consideration of the areal contribution of particular profile types to streamflow.

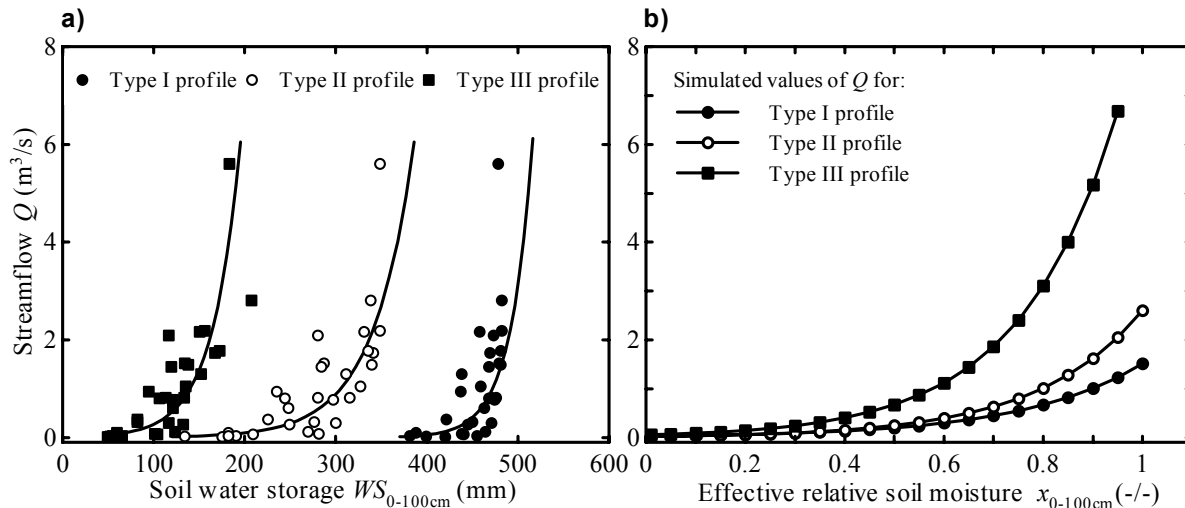


Fig. 4: Relationship between streamflow and soil water storage for different types of soil profiles. Soil water storage is expressed as water depth (a) and as effective relative soil moisture (b).

Conclusions

Enhanced understanding of quantitative relationships between terrestrial water storage and streamflow is revealed through the consideration of their uncertainties. The research provides an insight into two types of uncertainty present in the soil water storage - streamflow relation: the uncertainty of the model structure and uncertainty in model input parameters. Uncertainty of the model structure is evaluated by the range of streamflow values simulated for varying values of soil water storage expressed by a dimensionless parameter. Uncertainty in model input parameters is evaluated by the range of soil water storage described by dimensional and dimensionless parameters. Uncertainty in soil water storage causes uncertainty in estimates of streamflow values over a broad range. Application of the simple regression model is considered as a parsimonious approach in which streamflow values are dependant on the observed patterns of soil water storage. The overall conclusion is that for the reduction of uncertainty in the terrestrial water storage – streamflow relation an additional consideration of spatial organization of soils is required.

Acknowledgements

The soil moisture research has been supported by the Department of Environmental Sciences and Policy of the Central European University, Budapest by a Grant No. 92-14. Additional funds have been awarded by the Ministry of Science, Committee for Scientific Research in Poland for the Investment Grant No. 4441/IA/115/2003.

References

- Blöschl G. (2001). Scaling in hydrology. *Hydrological Processes*, 15: 709-711.
- Brown J.D., Heuvelink G.B.M. (2005). Assessing uncertainty propagation through physically based models of soil water flow and solute transport. In: M.G. Anderson (Ed.), *Encyclopedia of Hydrological Sciences*, Wiley & sons, Vol. 2, Part 6: 1181-1195.
- Clifford N. J. (2002). Hydrology: the changing paradigm. *Progress in Physical Geography*, 26: 290-301.
- Lin H. (2003). Hydrogeology: bridging disciplines, scales, and data. *Vadose Zone Journal*, 2: 1-11.

- Robinson M., Stam M.H. (1993). A study of soil moisture controls on streamflow behaviour: Results from the Ock basin, UK. *Acta Geologica Hispanica*, 28: 75-84.
- Scipal K., Scheffler C., Wagner W. (2005). Soil moisture runoff relation at the catchment scale as observed with coarse resolution microwave remote sensing. *Hydrology and Earth System Sciences*, 2: 417-448.
- Somorowska U. (2005). Temporal patterns of subsurface water storage inferred from the TDR measurements. In: F. Maraga, M. Arattano (Eds.), *Progress in Surface and Subsurface Water Studies at Plot and Small Basin Scale. Proceedings of the 10th ERB Conference*, Turin, Italy, 13-17 October 2004. *UNESCO, IHP-VI, Technical Documents in Hydrology*, 77: 27-34.
- Somorowska U. (2006). *Impact of the Subsurface Water Storage on Streamflow in Lowland Catchment* (In Polish: Wpływ stanu retencji podziemnej na proces odpływu w zlewni nizinnej). Warsaw University Press (Wydawnictwa Uniwersytetu Warszawskiego), Warsaw.

FLOOD RISK ANALYSIS OF THE WARSAW REACH OF THE VISTULA RIVER

A. Kiczko¹, F. Pappenberger² & R.J. Romanowicz³

¹*Institute of Geophysics, Polish Academy of Sciences, Warsaw, Poland.* ²*European Centre for Medium Range Weather Forecasts, Reading, UK.* ³*Lancaster Environment Centre, Lancaster University, Lancaster, UK.*

Corresponding author: Adam Kiczko, email: akiczko@igf.edu.pl

ABSTRACT

This paper presents a flood risk analysis of the Warsaw reach of the Vistula River (Poland). We argue that any model of an urban area has to be evaluated and calibrated using local performance as well as global measures. In this particular flooding estimation problem, the main challenge lies in the very limited amount of available calibration data. This was overcome by an extensive survey of the river channel and floodplains geometry and application of a model with a simplified flow dynamics description, corresponding to the scarcity of data. Calibration of the model is based on observed water levels during the flood event in July 1997. Simulations are performed for 10 different events with a specified value of probability of reoccurrence (including uncertainties) estimated by the Institute of Meteorology and Water Management in Warsaw. By combining information about model uncertainties and event occurrence probabilities, it was possible to produce a spatially distributed uncertainty of prediction of water levels along the river reach.

Keywords: GSA, GLUE, flood risk, Warsaw, Vistula

Introduction

In this paper we outline a methodology for the assessment of risk from flooding for urban areas and in particular, the estimation of the inundation probability along the Warsaw reach of the Vistula River. Risk is defined here as the probability of flooding in certain areas multiplied by the cost of the possible damage due to flooding. Urban areas are characterised by a large variability in the costs of flooding. Thus it is necessary to estimate the spatial distribution of probabilities of flooding along the river reach. For example, infrastructure or buildings will show more damage than green areas along the river banks. This indicates the necessity for assessing risk on a local rather than at global scale (Pappenberger et al., in press).

All flood protection measures should be related to an analysis of flood cost, which combines the estimated flood inundation probability field with an economic losses model. There are different possible approaches to the problem of the estimation of probability of flooding and the cost evaluation. One approach, presented by Dutta et al. (2003), consists in the application of a deterministic hydrologic basin model combined with a unit flood loss model.

We present here a stochastic methodology to the evaluation of river overflow risk, as a primary element of risk assessment, with a special focus on the significance of a local approach. In order to estimate the risk from flooding we derive a flooding which in turn requires the application of a distributed flood routing model. As the process of flooding is non-linear, the model structure should reflect this nonlinearity. In this work we have used the 1D flood model with simplified dynamics. To analyse the model parametric sensitivity and to identify sources of uncertainty the Global Sensitivity Analysis was used. Model calibration and proper uncertainty analyses were performed following the Generalised Likelihood Uncertainty Estimation (GLUE) methodology introduced by Beven and Binley (1992).

Approach and methods

The GSA methodology

Generally Sensitivity Analysis (GSA) consists in the evaluation of a relation between input and output variations. It plays a very important role in the modelling exercise. For example, in the case of over-parameterized models, it allows a reasonable reduction of the parameter space to be accomplished. This significantly improves computation properties and it helps identifying possible uncertainty sources in model parameters and their ranking.

In this assessment we have used the variance based Global Sensitivity Analysis approach introduced by Archer et al. (1997). In this method, the whole set of model parameters acquired from the Monte Carlo sampling is analysed simultaneously and there is no restriction about monotonicity or additivity of the model, therefore it is very suitable for over-parameterized spatially distributed models.

According to variance based methods, variance of an output Y which depends on the variable input set X_i , can be treated as a sum of top marginal variance and a bottom marginal variance (Ratto et al., 2001):

$$V(Y) = V[E(Y | X_i = x_i^*)] + E[V(Y | X_{-i} = x_{-i}^*)], \quad \text{Eq. 1}$$

where $V[E(Y|X_i = x_i^*)]$ is the variance of estimated Y output where x_i parameters are fully fixed and others are normally varying and $E[V(Y|X_{-i} = x_{-i}^*)]$ is the estimated variance in case all parameters are fixed, except x_i , which is varying.

The direct sensitivity of output Y to the input X_i , represents the first order sensitivity index S_i , which takes the following form:

$$S_i = \frac{V[E(Y | X_i = x_i^*)]}{V(Y)} \quad \text{Eq. 2}$$

The model sensitivity to the interactions among subsets of factors, so called higher order effects, is investigated through a total sensitivity index: S_{Ti} . It represents the average interactions that involve x_i . It is defined as:

$$S_{Ti} = \frac{E[V(Y | X_{-i} = x_{-i}^*)]}{V(Y)} \quad \text{Eq. 3}$$

The use of a total sensitivity index is advantageous, since there is no need for an evaluation of a single indicator for every possible parameter combination. On the basis of these two indicators, S_i and S_{Ti} , it is possible to efficiently trace the significance of each model parameter. In this work the estimation of the sensitivity indices S_i and S_{Ti} is made via the Sobol method.

The GLUE methodology

The basic assumption of the GLUE methodology (Beven and Binley, 1992) is that in a case of over-parameterized environmental models a unique solution of the inverse problem is not possible to achieve, because of a lack of data (an interactive discussion on this topic is promoted by Pappenberger et al., 2006). There can be many different parameter sets which provide reasonable results. Therefore, calibration should consist of the estimation of the multidimensional distribution of model parameters. For such an analysis the Bayesian formula is used:

$$f(\theta \setminus z) = \frac{f(\theta)L(z|\theta)}{L(z)} \quad \text{Eq. 4}$$

where z is the observation vector, $f(\theta|z)$ is the posterior distribution (probability density) of the parameters conditioned on the data, $f(\theta)$ is the prior probability density of the parameters, $L(z)$ is the scaling factor, $L(z|\theta)$ represents the likelihood measure based on the theoretical information on the relationship of z and θ . On the basis of information on the prior distribution of model parameters, which comes from knowledge of the physical structure of the modelled process, it is possible to estimate the posterior distribution of parameters. Assuming that the prior distribution of model parameters is related to an uncertainty introduced into the model, the posterior distribution will provide information on the uncertainty of the model results.

It is important to note that as equation 4 is defined over the specified parameter space, parameter interaction will be implicitly reflected in the calculated posterior distribution. This feature is especially important in a case of spatially distributed models, where parameters are very dependent. The marginal distributions for single parameter groups can be calculated by an integration of the posterior distribution over the rest of the parameters as necessary.

The essential element of the GLUE methodology is a practical determination of the likelihood measure $L(z|\theta)$. In this paper it was assumed that it is proportional to the Gaussian distribution function:

$$L(z|\theta) \approx e^{-(z-z_{sim}(\theta))^2 / \delta^2}, \quad \text{Eq. 5}$$

where z is the water level obtained from observations, z_{sim} is a computed water level and δ^2 , as mean error variance, determines the range of the distribution function. It is important to note that in the GLUE methodology a subjective control of the distribution width is allowed. On the basis of posterior likelihood values, the distribution of simulated water levels can be evaluated and subsequently used to derive spatial probability risk maps of flooding in the area.

The model parameter space is sampled using the Monte Carlo method. It is important to note that the prior distribution $f(\theta)$ of parameters is introduced at this stage of processing. It takes the form of the probability function used in the number generator and sampling ranges. The number of model realizations depends on the unimodality of the resulting distribution.

Application: Warsaw reach of Vistula river

Study area

The 36 km long Warsaw reach of the Vistula river (Fig. 1) starts from the Nadwilanowka river gauge and ends before the Vistula's tributary Narew. Due to its glacial history, the upper part of this reach forms the so called "Warsaw corset", where river width decreases rapidly from 7500 m at 507 km to 600 m in Warsaw (514- 516 km). The mean annual discharge at the Nadwilanowka gauge is 573 m³s⁻¹. This part of the river valley is highly urbanized and embankment systems are situated on both river banks along the entire length of the reach. The floodplains consist mainly of a diversified vegetation cover and only small parts of the left bank are protected with solid cement constructions. From the flood protection point of view, the tree rich habitats, which exist along the whole right bank possibly play an important role – it is seen especially in the variation of roughness coefficients.

Low flows are regulated by a system of replying spurs. The character of flood-endangered city areas is diversified along the river reach. Generally, upstream parts of the reach are densely populated and downstream parts consist of a dispersed development; however, each part differs significantly. On the right bank large

housing complexes exist in the direct neighbourhood of embankments and such areas are considered as especially endangered.

There were just a few works published on flood modelling of the Warsaw reach of Vistula. Kuźniar (1997) estimated water surface levels for a 500-year flood event and compared it with historical observations (Kuźniar, 1997). Hydroprojekt Warszawa developed a complex program of flood prevention for the middle Vistula, in which a 1D steady-state flow model was used to assess flood inundation zones (Hydroprojekt, (1999). Nowadays this assessment is used in the majority of administration proceedings. Both approaches are deterministic, so the estimated flood risk zones do not reflect the uncertainty of the model parameters and its boundary conditions (Romanowicz et al., 1996; Romanowicz and Beven, 2003).

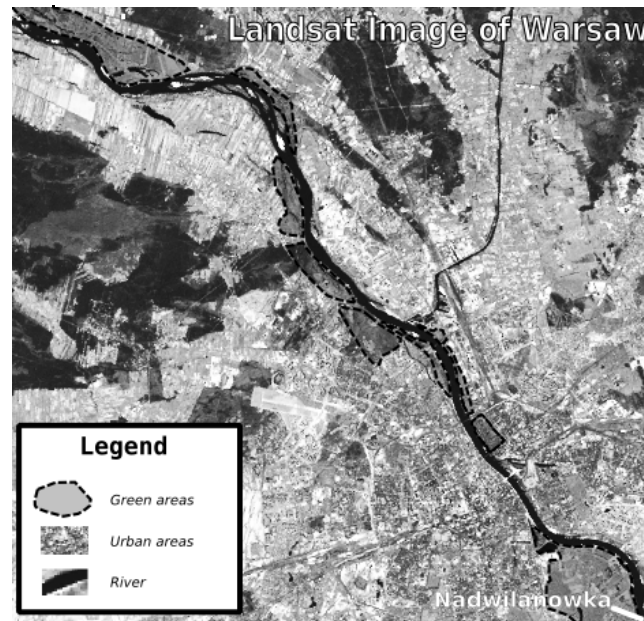


Fig. 1: Landsat image of Warsaw with marked urban and green areas (landsat.usgs.gov).

Flood routing methods

The coarse element flood inundation model developed by Romanowicz et al. (1996) was chosen for the purpose of this research. Its formulation is similar to the quasi-two-dimensional model of Cunge (1975). According to this concept, a river valley can be seen as a system of interconnected storage cells and it is assumed that there is a unique relationship between the storage of each cell and the water surface level, as well as the cross section/water level and hydraulic radius/water level relations at the boundaries of each cell. These functions can be derived from river and floodplain geometric data in the form of look-up tables. Assuming that the flow builds up slowly on the floodplains and hence storage and resistance terms are more important than inertial and acceleration terms in a flow equation, it is possible to describe water exchange between neighbouring cells on the basis of these geometric functions applying Manning-Strickler resistance laws. Whilst in more common flood routing models a geometric representation of the channel and the floodplain is restricted to the cross sections, this model may incorporate more accurate spatial information about the river and floodplain geometry in the form of the storage water level functions.

In its original version, this model gives a quasi-2D description of the flow routing process. The river is usually divided into three types of storage cells, representing different active zones: main channel, left and right floodplain. In the present research only the flow between embankments was considered and there was no need to use such a detailed description. Therefore a 1D version of the model based only on the cells responsible for the main channel was applied. As a result of this simplification an increased model computational performance was achieved. In this form the model was implemented in the Matlab Simulink iconographic language.

Data

Triangulated Irregular Network Digital Terrain Model (TIN DTM) from aerial imaging and about 78 channel cross-sections constitute the basis for the representation of the river valley topography. Measurements of the channel were carried out by Wierzbicki (1999). They provide very useful information for this research. The DTM on a regular grid of 20x20 m resolution was prepared in order to integrate the elevation data. The evaluation of model functions from this type of elevation data gives similar advantages to using a finite element model, since it is possible to include spatial diversification not only at a cross-section, but also between them.

Model cells were assigned according to the location of the 78 cross-sections, which gave 77 sub-reaches. For each model cell it was necessary to evaluate the relationship between a hydraulic radius/water level and area/water level values at the closing cross-section and cell storage functions in the form of water level/volume relation. All geometric functions were written in the form of look-up tables.

The upstream end of the river reach was placed at the Nadwilanowka river gauge. It enabled the use of water level observations from this station as the upper boundary condition. It was important because it was the only cross-section in the whole reach where a discharge rating curve was available. Additionally, estimates of the probability of occurrence of flood discharges are available for this river gauge. In this study the discharge values of probability of exceedence of 0.001 - 9960 m³s⁻¹, estimated by the Institute of Meteorology and Water Management (2001, 40 years observation period 1921-1960), and 0.01 - 6786 m³s⁻¹ estimated by Wierzbicki (2001, 50 years observation period 1948- 1997), were used.

The water surface elevation profile of the flood event of July 1997 was used for model calibration. These data itself provide a very good representation of the river system during flood events. The only important problem was that there was no unique estimate of the maximum discharge available. In 1997 IMGW estimated it as 5150 m³s⁻¹ but this value seemed to be exaggerated. Later, in 2001 Wierzbicki estimated it at just 4300 m³s⁻¹. In this work inflow discharges (the upper boundary condition) were considered as one source of the model uncertainty. The water surface elevation profile of the flood event of July 1934, corresponding to an estimated discharge of 5348 m³s⁻¹, was also available. This profile refers to the 10 km river reach, from the Nadwilanowka gauge (cross-section at 504 km) to the Poniatowski Bridge. These data were used for model verification. A map of the area is shown in Fig. 1.

Results

Model calibration is the most important stage of flood risk assessment. It was assumed that uncertainty introduced to the model by elevation data was much less important than uncertainty related to the estimation of roughness parameters and boundary conditions. Therefore Monte Carlo simulations were made for two kinds of parameters. The first one were roughness parameters at storage cells and the second one was the downstream boundary condition in the form of the water slope at the end of the river reach.

Because there was no *a priori* information on the parameter distribution, a uniform prior distribution was assumed (Beven, 2001). After the Global Sensitivity Analysis (GSA) of the model performance using different parameter sets, the following parameter ranges were chosen for the MC simulations using uniform priors: Manning roughness coefficients 0.02 – 0.16 and water slope: 1.3192×10^{-4} – 8.7950×10^{-4} . The wide range of roughness coefficients, which exceed values normally observed in the river, is justified by the need of including uncertainty in other inputs like channel geometry.

The GSA allowed to identify major uncertainty sources introduced into the model. The most important is the downstream boundary condition. It seems to be in accordance with Kuźniar's (1997) suggestions that backwaters from the Narew tributary may play a significant role in the formation of flood effects in the downstream part of the considered reach. Other important sources of model uncertainty are connected with the

area of the Warsaw corset, where relatively small changes in roughness coefficients result in big water level variations.

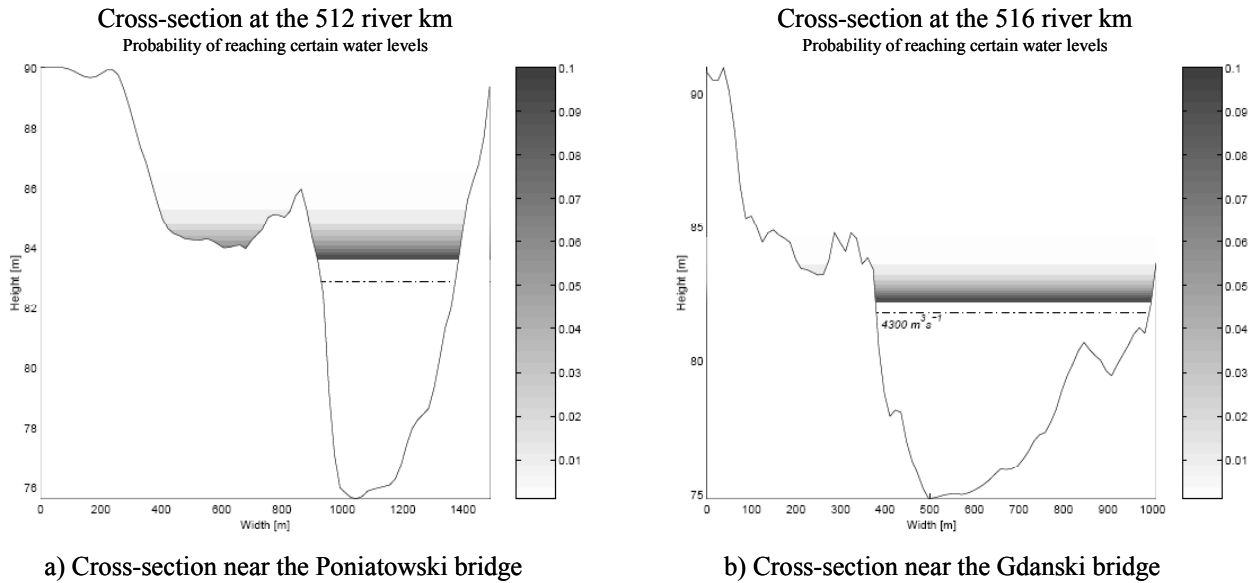


Fig. 2: Probability of reaching certain water levels.

Initial Monte Carlo runs were performed for flow conditions corresponding to observations from 1997. Following the GLUE methodology, posterior likelihood values for each model run were evaluated based on the errors between the observed and simulated water levels at each cross-section. These likelihood values were used to estimate the posterior distribution of parameters used in further simulations. Main model runs were made for 10 hypothetical flow events of a known probability of occurrence.

Computational results for selected cross sections (at 505, 512, 519, 533 km) are shown in Figs 2a-b. The combination with the DTM allowed to produce a map of the spatial distribution of the inundation probability, with an assumption that embankments do not exist. This information was combined with a site plan of Gocław, one of Warsaw’s districts, and a simplified losses model, based on the losses report from the flood that occurred in Wrocław in 1997. The losses model was conditioned only by the inundation water level. A resulting risk map is shown on Fig. 3. It can be noticed that the probability of losses (as a product of probability and costs) is the highest in densely populated, low-lying areas.

Conclusions

This paper describes the derivation of flood inundation maps for the estimation of the flooding risk in the Warsaw reach of the Vistula River, Poland. A Generalised Likelihood Uncertainty Estimation (GLUE) approach is applied together with the SIMULINK based nonlinear flow routing model to derive the probability of a flooding of areas along the river floodplains. The model was run for two sets of inflows, with the probability of occurrence being equal to 0.001 and 0.01, respectively. The resulting longitudinal profiles depicting the different probability of flooding along the river reach (Fig. 2) were used together with the map of cost of infrastructure in the area to build flood risk maps for a district of the city of Warsaw. This can also be combined either with the structural risk analysis to identify the embankment areas under the highest risk of breaching, or the urban area flood inundation model to develop detailed urban risk maps.

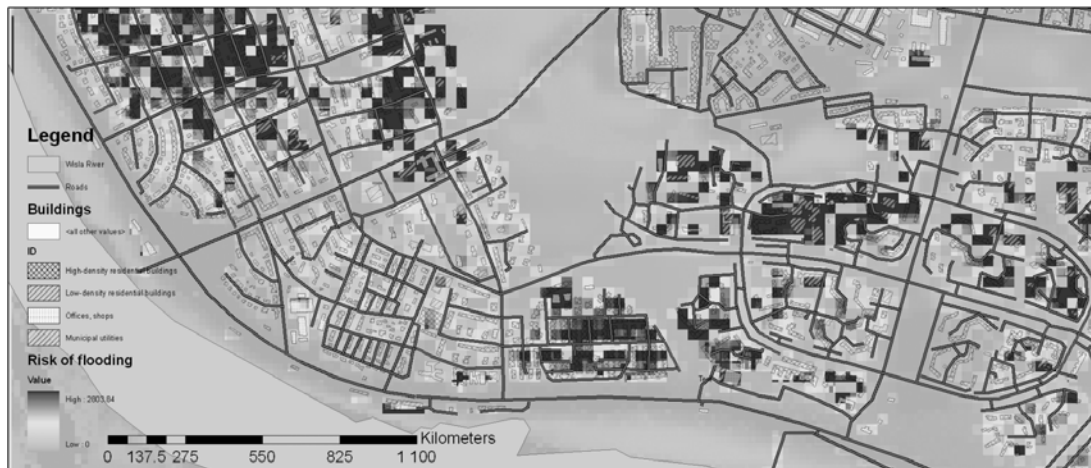


Fig. 3: Risk map for the Gocław district, see the legend on the left side of the picture.

Acknowledgments

This work was supported in part by grant 2 P04D 009 29 from the Ministry of Higher Education and Science and the UK Flood Risk Management Research Consortium Research.

References

- Archer G., Saltelli A., Sobol I.M. (1997). Sensitivity measures, anova-like techniques and the use of bootstrap. *Journal of Statistical Computation and Simulation*, 58: 99–120.
- Beven K. (2001). How far can we go in distributed hydrological modelling? *Hydrological and Earth System Sciences*, 5: 1-12.
- Beven K., Binley A. (1992). The future of distributed models: model calibration and uncertainty prediction. *Hydrological Processes*, 6: 279–298.
- Cunge J.A. (1975). Two-dimensional modelling of flood plains. In: K. Mahmood, V. Yevjevich (Eds). *Unsteady Flow in Open Channels*. Water Resources Publications, Fort Collins, Colorado: 705–762.
- Dutta D., Herath S., Musiak K. (2003). A mathematical model for flood loss estimation. *Journal of Hydrology*, 277: 24–49.
- Hydroprojekt (1999) *Kompleksowy, regionalny program ochrony przeciwpowodziowej dorzecza Środkowej Wisły na terenie RZGW w Warszawie*. Technical report.
- Kuźniar P. (1997). *Woda 500 letnia w Warszawie w świetle materiałów historycznych i symulacji komputerowych*. Forum Naukowo-techniczne.
- Pappenberger F., Beven K., Frodsham K., Romanowicz R., Matgen P. (2006). Grasping the unavoidable subjectivity in calibration of flood inundation models: A vulnerability weighted approach. *Journal of Hydrology*, 333: 275-287.
- Pappenberger F., Harvey H., Beven K., Hall J. (2006). Decision tree for choosing an uncertainty analysis methodology: a wiki experiment (www.floodrisk.net). *Hydrological Processes*, 20: 3793-3798.
- Ratto M., Tarantola S., Saltelli A. (2001). Sensitivity analysis in model calibration: Gsa-glue approach. *Computer Physics Communications*, 136: 212–224.
- Romanowicz R., Beven K. (2003). Estimation of flood inundation probabilities as conditioned on event inundation maps. *Water Resources Research*, 39: 1073, doi:10.1029/2001WR001056.
- Romanowicz R., Beven K.J. Tawn K.B.J. (1996). Bayesian calibration of flood inundation models. In: M.G. Anderson, D.E. Walling, P.D. Bates (Eds). *Floodplain Processes*. Wiley, Chichester : 336–360.
- Wierzbicki J. (1999). *Stalność pionowego układu i morfologii koryta oraz zwierciadła wód Wisły warszawskiej na odcinku położonym pomiędzy ujściem rz. Pilicy a ujściem rz. Narwi -stan 1998*. Technical report, Politechnika Warszawska, Warszawa.

SPECTRAL MAXIMUM-LIKELIHOOD PARAMETERIZATION OF HYDROLOGICAL MODELS

A. Montanari & E. Toth

Faculty of Engineering, University of Bologna, Via del Risorgimento 2, I-40136 Bologna, Italy.

Corresponding author: E. Toth, e-mail: elena.toth@mail.ing.unibo.it

ABSTRACT

This study considers the use of the maximum likelihood estimator proposed by Whittle for calibrating the parameters of hydrological models. Whittle's likelihood provides asymptotically consistent estimates for Gaussian and non Gaussian data, even in the presence of long range dependence. This method may represent a valuable opportunity in the context of ungauged or scarcely gauged catchments. In fact, the only information required for model parameterization is the spectral density function of the actual process simulated by the model. When long series of calibration data are not available, the spectral density can be inferred by using old and sparse records, regionalization methods or information on the correlation properties of the process itself. The proposed procedure is applied to a case study referring to an Italian river basin, for which a lumped rainfall-runoff model is calibrated by emulating scarcely gauged situations. It is shown that the Whittle estimator can be applied in such a context with satisfactory results.

Keywords: parameterization, rainfall-runoff, Whittle's likelihood, maximum likelihood, spectral density function

Introduction

Parameter calibration of hydrological models involves the processing of input data through the model and the adjustment of parameter values in order to produce a reliable simulation. The goodness of the fit is usually evaluated by comparing the data simulated by the model with the corresponding observed variables. This direct comparison can be performed only when referring to catchments where sufficiently long and simultaneous records of input and output variables are available. When the catchment or the location of interest is poorly gauged or ungauged, that is, when hydrological data are limited or unavailable, alternative methods for identifying model parameters are needed.

The purpose of this paper is to propose the use of the maximum likelihood estimator introduced in the context of time series analysis by Whittle (1953) for calibrating hydrological model parameters. The estimator has good statistical properties, as it is asymptotically consistent. It was successfully used in other hydrological applications (e.g. Montanari et al., 2000; Montanari, 2003). In the context of scarcely gauged/ungauged basins it has significant advantages with respect to traditional calibration procedures, as in principle the calibration can be carried out even when observed output data are not available. In fact, the parameter estimation, rather than attempting to fit observed and simulated output time series, is carried out essentially by matching the spectral densities of the model simulation and the actual process. In absence of observed data, it is argued here that the spectral density of the process can be derived from different types of information that could be available in poorly gauged situations.

Two applications of the proposed estimator for calibrating a lumped rainfall-runoff model to the Reno river basin (Italy) are shown herein. In the first case the model is parameterized by using input and output data referring to different observation periods and measured at a different time step. In the second case, the parameterization is carried out by exploiting some basic statistical properties of the output river flows that could be, for example, inferred at regional scale. The results show that the Whittle's likelihood can allow the user to profit from information that could not be used with traditional calibration methods.

The approximation proposed by Whittle to the Gaussian maximum likelihood function

The likelihood measure proposed by Whittle (1953) for the parameters of a generic model will be denoted in the following as $L(\theta)$, where θ is the model parameter vector. Note that the likelihood of a parameter set θ is proportional to the probability of obtaining a correct model simulation when the model parameter set is θ . Therefore maximizing the likelihood for varying θ allows one to identify the optimal parameter set.

For a stationary time series $L(\theta)$ is computed on the spectral density (see, for instance, Beran (1994), Montanari et al. (2000) and Chouduri et al. (2004)). In practice, the model calibration is carried out essentially by matching the spectral densities of model output and river flow process. Given that any time series can be decomposed in a sum of periodic components through a harmonic analysis, the spectral density describes the variability of the time series that is explained by each component. It is essential to note that the spectral density can be derived from the autocovariance function of the data. Therefore one may say that Whittle's likelihood performs model calibration essentially by matching the autocovariance functions of model output and observed river flow record.

Whittle's likelihood has been widely used in the time series literature for constructing estimators. Referring to the case of rainfall-runoff (R-R) models, for the purpose of introducing $L(\theta)$ let us first focus on the gauged basin case, for which N river flow observations are available to calibrate the model (the scarcely gauged basin case will be introduced in the following). In this case, the approximation of the observed streamflow, $Q_{obs}(t)$, performed by the rainfall-runoff transformation can be written as:

$$Q_{obs}(t) = M[\theta, I(t)] + e(t) \quad , \quad t = 1, \dots, N \quad \text{Eq. 1}$$

where $M[\theta, I(t)]$ is the transformation operated by the hydrological model, that is assumed to be stationary, and $I(t)$ is the input vector (for instance rainfall and temperature or evapotranspiration at time t).

The R-R model residuals $e(t)$ can be modeled by an autoregressive stochastic process (Brockwell and Davis, 1987). In general, the autoregressive process is conditional on the hydrological model output $M[\theta, I(t)]$. An extensive study carried out by the World Meteorological Organisation (1992) proved that a first order autoregressive process is sufficient to account for correlation in the residual series of many practical applications of rainfall-runoff models. A first order autoregressive model, denoted as AR(1), may be represented in the form:

$$e(t) = \phi_1 e(t-1) + \varepsilon(t) \quad , \quad \text{Eq. 2}$$

or, in the backshift notation:

$$(1 - \phi_1 B)e(t) = \Phi(B)e(t) = \varepsilon(t) \quad \text{Eq. 3}$$

where B is the backshift operator, such that $Be(t) = e(t-1)$, $\Phi(B)$ is the autoregressive operator, which is in charge of taking into account the correlation in $e(t)$, and $\varepsilon(t)$ represents a zero mean, independent and identically distributed (i.i.d.) random variable. The assumption of zero mean for $\varepsilon(t)$ is essential and will be thoroughly discussed below.

Under this assumption, equation (1) becomes:

$$Q_{obs}(t) = M[\theta, I(t)] + \Phi^{-1}(B)\varepsilon(t) \quad , \quad t = 1, \dots, N \quad \text{Eq. 4}$$

where $\Phi(B)$ may be an autoregressive operator of any order.

The Whittle's likelihood $L(\theta)$ for the model given by equation 4 can be computed through the relationship:

$$L(\theta) = \exp \left[- \sum_{j=1}^{N/2} \left\{ \log [f_M(\lambda_j, \theta) + f_e(\lambda_j, \Phi)] + \frac{J(\lambda_j)}{f_M(\lambda_j, \theta) + f_e(\lambda_j, \Phi)} \right\} \right] \quad \text{Eq. 5}$$

where $\lambda_j = 2\pi j/N$ are the Fourier frequencies; J is the periodogram (which is an estimate for the spectral density) of the series of the N observed river flows; f_M is the spectral density of the hydrological model output that depends on the parameter vector θ and f_e is the spectral density of the autoregressive operator Φ , that is,

$$f_e(\lambda_j, \Phi) = \frac{\sigma_\varepsilon^2}{2\pi \left| \Phi(e^{-i\lambda_j}) \right|^2} \quad \text{Eq. 6}$$

where σ_ε is the standard deviation of $\varepsilon(t)$.

The periodogram $J(\lambda_j)$ of an observed time series at the frequency λ_j can be computed as (Brockwell and Davis, 1987):

$$J(\lambda_j) = \sum_{|k| < N} \gamma(k) e^{-ik\lambda_j} \quad \text{Eq. 7}$$

where $\gamma(k)$ is the sample autocovariance coefficient at lag k and i is the imaginary unit. For more details about the derivation of the approximation proposed by Whittle (1953) to the Gaussian maximum likelihood function the interested reader is referred to the book by Beran (1994) which provides a detailed explanation.

To derive analytically the spectral density $f_M(\lambda_j, \theta)$ of a hydrological model might be not possible in many cases. To solve this problem the spectral density can be approximated numerically, by computing the periodogram, $J_M(\lambda_j, \theta)$, of a sufficiently long model simulation.

Given that maximizing $L(\theta)$ as given by (5) is equivalent to minimizing the absolute value of the quantity between square brackets in the right-hand side of (5), model calibration can be carried out by minimizing

$$W(\theta) = \sum_{j=1}^{N/2} \left\{ \log [J_M(\lambda_j, \theta) + f_e(\lambda_j, \Phi)] + \frac{J(\lambda_j)}{J_M(\lambda_j, \theta) + f_e(\lambda_j, \Phi)} \right\} \quad \text{Eq. 8}$$

In the present study the minimization of (Eq. 8) was performed numerically (see Section 3.2). Whittle's likelihood provides asymptotically consistent and normally distributed estimates for the hydrological model parameters in the case of Gaussian and linear models even in the presence of long range dependence (which induces the Hurst Effect) (Fox and Taqqu, 1986; Montanari, 2003). This means that for Gaussian and linear models the estimator is capable of providing the probability distribution of the parameters, which allows one to derive their confidence limits. Asymptotic normality and consistency is assured under mild conditions also in the non Gaussian case (Giraitis and Surgailis, 1990), while asymptotic normality is no more guaranteed for non linear models, as it is the case in many practical applications in hydrology. Nonetheless, the absence of asymptotic normality does not affect the consistency of the estimator but only the computation of the confidence limits of the parameters. Therefore, when applying the Whittle's estimator to non-linear models alternative methods for computing the confidence limits are to be sought (Giraitis and Taqqu, 1999).

When contemporaneous input records and river flow data are available over a time period $[0, T]$, the estimator given by (Eq. 8) can be used to perform a classical model calibration based on the analysis of the goodness of the fit of observed data. In this case the fit is evaluated by comparing the frequency behaviors of simulated and actual records. We will refer to this procedure with the term “Whittle direct calibration”. Once a trial value for the parameter vector θ is selected, the periodogram $J_M(\lambda_j, \theta)$ of the simulation run over $[0, T]$ can be computed. Subsequently, the model residuals over $[0, T]$ can be calculated depending on θ so that the autoregressive model $\Phi(B)$ can be identified and its parameters estimated. Therefore it is possible to compute $f_e(\lambda_j, \Phi)$ and, finally, $W(\theta)$ accordingly to (Eq. 8), that can be minimized in order to identify the best θ .

Some relevant properties of the estimator and their effect in practical applications

One of the hypotheses of the Whittle’s likelihood is the stationarity of the process. Note that this is not in contrast with the seasonal structure of many hydrological records. In fact, seasonality is reflected in the spectral density and is fully compatible with a stationary process.

Attention should also be focused on the i.i.d. assumption for $\varepsilon(t)$. In fact, in real world applications the $\varepsilon(t)$ are often heteroscedastic and therefore are not identically distributed. In fact, during peak flow periods the errors $e(t)$ of the hydrological model are usually higher, therefore implying an amplification (and a corresponding heteroscedasticity) of the $\varepsilon(t)$. Consequently, a bias can be induced in the parameter estimates. Note that if the quantities $Q_{obs}(t)$ and $M[\theta, I(t)]$ were taken to be log transformed observations and hydrological model output, then the effect of a residual variance that changes with the magnitude of the observations would be accounted for. Transformations, such as the normal quantile transform, may also be used to stabilize the variances (Montanari and Brath, 2004). In this study these transformations were not applied because the analysis is focused on ungauged basins: given the high uncertainty of the parameter estimates in this case, the approximation induced by residual heteroscedasticity can be considered negligible.

The spectral density of a process (like river flows at an assigned location) does not convey any information about the mean value and phase of the process itself. In practice, the periodogram of a time series does not change after a shift in the mean or a shift of the whole time series in time (this latter shift is equivalent to a change in phase). The estimator provided by equation (8) preserves the mean of the process through the assumption of zero mean for $\varepsilon(t)$. This condition implies that the hydrological model error $e(t)$ has zero mean as well, which corresponds to imposing equality for the mean values of observed and simulated data.

Preservation of the process phase, therefore avoiding possible shifts of the model output in time, is attained through the term f_e , i.e., the spectral density of the hydrological model error $e(t)$. In fact, f_e and the phase of the hydrological model are strictly connected. A change in phase of the hydrological model simulation (or in other words a shift in time of its simulation) implies a change in the variance (and therefore the spectral density) of $e(t)$. The result is that minimizing equation 8 implies an optimization of the phase of the simulated record.

The considerations above imply two important consequences for the use of the Whittle’s likelihood. First, those parameter sets that lead to significant differences $\Delta\mu_{obs,sim}$ in the mean values of observed and simulated river flows should be rejected, as in this case the assumption of zero mean for $\varepsilon(t)$ would be violated. Strictly speaking one should exclude the parameter sets that do not allow one not to reject the hypothesis of null value of $|\Delta\mu_{obs,sim}|$ at an assigned confidence level. Second, one should note that neglecting the term f_e in the estimation procedure may imply an imprecision in fitting the phase of the signal.

Application to ungauged or scarcely gauged catchments

When contemporaneous input and output records are not available, the direct calibration is not applicable and indirect estimation methods for ungauged basins need to be worked out. In this case, the Whittle’s likelihood

can be an interesting opportunity, because the streamflow periodogram might also be obtained in an indirect way. We will refer to this procedure with the term “Whittle indirect calibration”. For example, since the periodogram of a time series can be computed from its autocovariance function (see equation (7)), the model estimation may be based on information on the autocorrelation structure of streamflow values, that may be derived also from regionalization procedures, under assumptions that will be discussed here below.

In the remainder of the paper we will consider some examples of indirect calibrations. The first situation refers to a river basin whose data set consists of input observations, that is precipitation and temperature data, and streamflow measures that are not simultaneous. In this case, the availability of an old, and possibly sparse, streamflow series may allow a successful application of the Whittle method. In fact, once a trial value for the parameter vector θ is selected, the spectral density function of the model, f_M , can be estimated by computing the periodogram J_M of a simulation run obtained by using the available input data. If the process is assumed to be stationary, the periodogram J of the actual river flow process can be estimated by using old records or sparse measurements. Assuming that the role of the spectral density of the hydrological model residuals, f_e , is negligible, the estimator given by equation (8) may be applied without the availability of contemporaneous input and output data.

The second situation refers to a river basin for which observed river discharges are not available but information is at disposal about the mean value, the variability and the autocorrelation structure of the river flows. This type of knowledge could be derived by using regionalization procedures and allows one to infer the periodogram J of the river flow record. In this case also, f_e is assumed to play a negligible role.

As mentioned earlier, neglecting f_e implies that the estimator is no more able to fit the mean and phase of the signal, as only the correct fitting of the spectral density of the model is assured. Therefore, when referring to scarcely gauged catchments the user is required to specify a value for the mean, μ_{obs} , of the river flows, in order to be able to reject the parameter sets that lead to a difference $|\Delta\mu_{obs,sim}|$ exceeding a given threshold. Such mean value may be problematic to identify. However, given the high uncertainty involved in the analysis of ungauged catchments, the approximation due to the choice of a perceptual value for μ_{obs} may be considered scarcely influent.

The lack of fitting of the phase of the signal is a minor problem in the case of many modern hydrological models, whose spectral density significantly depends on the values of parameters describing hydrographs characteristics that are related to the phase of the signal, like the base time or time to peak. This evidence is confirmed by the applications presented here below, where a satisfactory fit is reached after neglecting f_e . However, the user should be aware that neglecting f_e may induce rough approximations for those models whose spectral density is not related to the displacement in time of the hydrograph, like for instance the Nash model (Nash, 1958).

Description of the applications to a scarcely gauged catchment

The performances of the Whittle estimator were tested by developing two applications, for which a situation of data scarcity was emulated. In detail, in the first application we tested the possibility to use the Whittle’s likelihood in order to calibrate a lumped R-R model when the hydrological information consists of (a) recent records of rainfall and temperature and (b) old records of river flows, possibly observed at a different time step. The possibility to calibrate a R-R model by using non contemporary records of input and output variables constitutes an interesting opportunity. In fact, the rainfall and temperature monitoring network is generally quite dense in many countries, while the information about the river flows is much more sparse, fragmentary and sometimes obsolete. The second application considers the use of the Whittle’s likelihood in order to calibrate a lumped R-R model on the basis of (a) recent records of rainfall and temperature and (b) mean value, standard deviation and lag one autocorrelation coefficient of the river flow process.

The test site herein considered refers to a medium sized watershed located in the Apennines Mountains in North-Central Italy, the Reno River. The Reno River at the closure section of Casalecchio, just upstream the city of Bologna, has a drainage area of the watershed of 1050 km². The main stream is around 76 km long. The average elevation is 635 m above sea level, the highest peak and the outlet being at an altitude of 1900 and 63 m above sea level, respectively. The majority of precipitation events occur from October to April, November being the wettest month and the runoff regime follows closely the precipitation trend. The 10-year return period discharge is estimated as around 1100 m³/s, from the sample cumulative distribution function of 70 observed annual maxima.

The observed data set is formed by eight years of hydrometeorological hourly data, from the 1st of January 1993 to the 31st of December 2000, and fifty years of daily streamflows at Casalecchio, from the 1st of January 1930 to the 31st of December 1979. The hourly data set consists of streamflow measures at Casalecchio, the temperatures recorded in 7 gauges and the precipitation depths measured in 13 raingauges, even if not all contemporarily operative for the whole observation period.

Conceptual rainfall-runoff model

The ADM rainfall-runoff model (Franchini, 1996) is formed by two main blocks: the first represents the water balance at soil and subsoil level, while the second represents the transfer of runoff production at the basin outlet. The basin, in turn, is divided into two zones: the upper zone produces surface and subsurface runoff, having as inputs precipitation and potential evapotranspiration, while the lower zone (whose input from the first one is the percolation flow) produces base runoff. The transfer of these components to the outlet section takes place in two distinct stages, the first representing the flow along the hillslopes towards the channel network and the second the flow along the channel network towards the basin outlet. The surface runoff generation is based on the concept of probability distributed soil moisture storage capacity of the Xinanjiang model (Zhao, 1980), where the total surface runoff is the spatial integral of the infinitesimal contribution deriving from the saturated elementary areas. The model has a total of 11 parameters to be estimated: 2 for the computation of surface runoff, 4 for interflow and percolation, 1 for the base flow and four parameters for the transfer components. The estimates of potential evapotranspiration, the second meteorological variable provided as input, is obtained from temperature data through a simplified form of the radiation method (Doorenbos et al., 1984).

Numerical maximization of the Whittle's likelihood function and reference baselines

In this study we used a genetic algorithm in order to perform numerical optimization, namely, the GENOUD method (GENetic Optimization Using Derivatives; see Sekhon and Mebane (1998)). GENOUD combines evolutionary algorithm methods with a derivative based, quasi Newton method to solve optimization problems. A relevant feature of GENOUD is its computing time, which is sustainable even when working with high dimensional parameter sets.

As a reference baseline, the performances of the Whittle direct estimations were compared with those obtained by maximizing the traditional Nash-Sutcliffe efficiency (Nash and Sutcliffe, 1970) of the simulated river flows. To obtain a term of comparison for appraising the performances of the indirect calibration we performed an extensive test of models characterized by random parameters. In detail, for each calibration exercise we computed the Nash-Sutcliffe efficiency obtained by running the model with 100000 random parameter sets. These were generated according to a uniform distribution within the same parameter range that was utilized when running the GENOUD optimization algorithm for indirect calibration. The resulting median value of the efficiency obtained with random parameters (median efficiency with random parameters) was assumed as a reference performance for a calibration that is carried out without using any type of optimization information but the predefined parameter range.

Results of model calibration

Calibration by using past river flows

A real data case study was implemented referring to the Reno river basin by emulating a situation with scarcity of observed river flow data. In this case the direct calibrations, making use of simultaneous input and output data, were performed on the eighth years of hourly data, both with the Whittle estimator and the Nash-Sutcliffe efficiency maximization.

The indirect calibration was carried out by exploiting the daily streamflow measured in the 1930-1979 period for estimating the periodogram J in equation (8), along with the hourly precipitation and temperature data relative to the years 1993-2000 for estimating the periodogram of the hydrological model J_M . The 1993-2000 hourly streamflow measures were not used in the indirect calibration.

Table 1. Reno River basin. Nash-Sutcliffe efficiency coefficients obtained for the 8 years of hourly data (1993-2000) with the Nash-Sutcliffe direct calibration, Whittle direct and indirect calibrations. The median efficiency with random parameters is also shown.

Nash-Sutcliffe direct calibration	Whittle direct calibration	Whittle indirect calibration (past river flows)	Whittle indirect calibration (river flow statistics)	Median efficiency with random parameters
0.77	0.73	0.48	0.51	-0.63

Table 1 compares the values of the efficiency of the simulation of the 8-year hourly flow data obtained with the Whittle indirect calibration, Whittle direct calibration and Nash-Sutcliffe direct calibration. The median efficiency with random parameters is also shown.

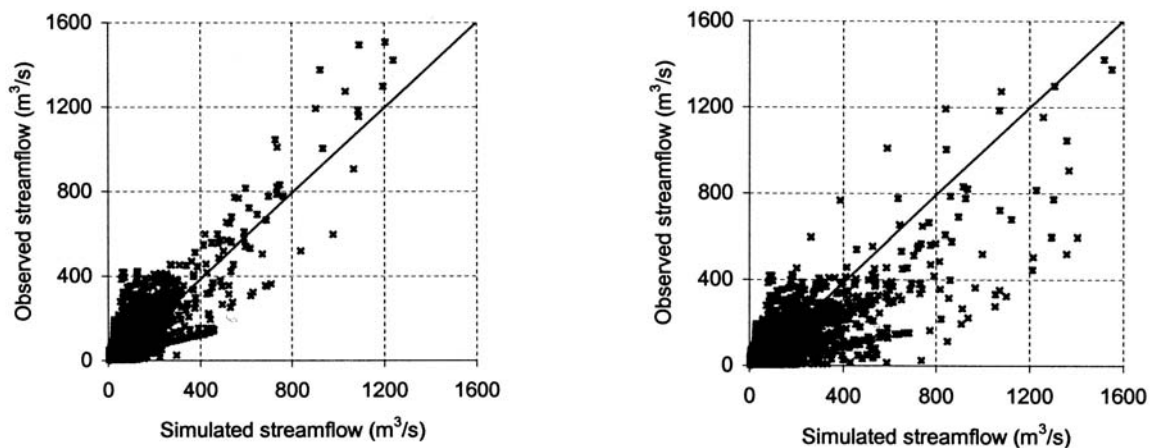


Fig. 1: Reno River basin (1993-2000). Scatterplot of simulated versus observed hourly streamflow data for the Nash-Sutcliffe direct calibration (left) and indirect Whittle calibration (right).

Figure 1 shows the scatterplot of simulated versus observed hourly streamflows for the Nash-Sutcliffe direct calibration and the Whittle indirect calibration. Table 1 suggests that the two direct calibrations perform similarly, thus confirming the efficiency of the Whittle estimator. The simulation obtained with the Whittle indirect calibration, even if obviously less accurate than those allowed by the direct procedures, is satisfactory (see Fig. 1), especially when compared with the performances obtained with random parameters (Table 1). In addition, one should consider also in this case that the simulation is carried out in validation mode and that the calibration was based on a kind of information that is not exploitable with a traditional calibration procedure.

Calibration by using river flow statistics

A second implementation was developed for the Reno River, by applying again the ADM model. In detail, in this case it is assumed that the river flow process can be described by utilizing a first order autoregressive process. Obviously, assuming that the dynamics of the river flow can be approximated by a linear model provides a crude approximation of reality, that can be accepted for the purpose of calibrating the model in condition of data scarcity, by exploiting basic statistical information of the actual process. Under this assumption, the autocovariance function (and therefore the periodogram J in equation (8)) of the process can be derived depending on the mean, variance and lag one autocorrelation coefficient of the river flows (see also equation (6), which refers to a zero mean, autoregressive process of generic order). In the present application the above statistics were inferred by computing their value in the river flow record of the year 1993 alone. The periodogram of the hydrological model J_M was derived by using the same precipitation and temperature data used in the application presented in the section dealing about the calibration based on past river flows.

Table 1 shows the value of the efficiency of the simulation obtained over the 8-year hourly data using this indirect calibration based on river flow statistics. In this case also, the efficiency of the Whittle indirect calibration is much better than the median efficiency with random parameters, that is obtained without any calibration, and shows another way for taking into account, in a statistical framework under given assumptions, a type of information that could be derived on a regional basis and is not exploitable with a traditional calibration procedure.

Concluding remarks

The proposed calibration procedure, that uses the approximation proposed by Whittle (1953) to the Gaussian likelihood function, can be an interesting approach for estimating the parameters of hydrological models in the context of ungauged or scarcely gauged catchments. As an example, two implementations are presented in the paper that could be representative of application in scarcely gauged situations.

The main feature of the proposed method, which is based on the comparison between the spectral density of the simulated and actual process, lies in the possibility to perform the model calibration also in absence of the output measurements, since the spectral density may be inferred also from an alternative information. The applications illustrated in the present work are only possible examples of the practical use of the Whittle estimator, which may be applied also by inferring the spectral density of the process from perceptual knowledge.

Of course, when applying an indirect calibration procedure the uncertainty may be relevant, whatever technique is chosen; nonetheless, the Whittle method may be useful to reduce the feasible parameter space in order to identify a set of behavioural models in the framework of equifinality (Beven and Binley, 1992; Gupta et al., 1998; Beven and Freer, 2001). This operation can be carried out by exploiting a type of knowledge that could not be used within traditional parameterization procedures. For instance, when a direct calibration provides more than one parameter set equally acceptable, the proposed technique may help to identify the parameterisation that better represents old or sparse measurements or information of different type that may be available for inferring the spectral density of the simulated process.

It is worth noting that in the case of sufficient data availability the proposed method may have advantages in preserving statistical characteristics of the river flow records such as variance, autocovariance structure and spectral properties across selected Fourier frequencies. Moreover, the focus on signatures of observed streamflow variability, such as the spectral signature, rather than on the raw time series may help the hydrologist to understand the signal behaviour beyond what can be learned from curve-fitting.

A software for the application of the Whittle estimator, in direct mode, which runs under the R package is available at the web page: <http://www.costruzioni-idrauliche.ing.unibo.it/people/alberto/indexeng.html>.

References

- Beran J. (1994). *Statistics for Long-Memory Processes*. Chapman & Hall. 315 pp.
- Beven K.J., Binley A. (1992). The future of distributed models: model calibration and uncertainty prediction. *Hydrological Processes*, 6: 279–298.
- Beven K.J., Freer J. (2001). Equifinality, data assimilation, and uncertainty estimation in mechanistic modelling of complex environmental systems using the GLUE methodology. *Journal of Hydrology*, 249: 11–29.
- Brockwell P.J., Davis R.A. (1987). *Time Series: Theory and Methods*. Springer, New York. 577 pp.
- Chouduri N., Ghosal S., Roy A. (2004). Contiguity of the Whittle measure for a Gaussian time series. *Biometrika*, 91: 211–218.
- Doorenbos J., Pruitt W.O., Aboukhaled A., Damagnez J., Dastane N.G., van der Berg C., Rijtema P.E., Ashford O.M., Frere M. (1984). *Guidelines for Predicting Crop Water Requirements*, FAO Irrig. Drainage Paper.
- Fox R., Taqqu M.S. (1986). Large sample properties of parameter estimates for strongly dependent stationary Gaussian time series. *The Annals of Statistics*, 14: 517–532.
- Franchini M. (1996). Use of a genetic algorithm combined with a local search method for the automatic calibration of conceptual rainfall runoff models. *Hydrological Sciences. Journal*, 41: 21–39.
- Giraitis L., Surgailis D. (1990). A central limit theorem for quadratic forms in strongly dependent linear variables and application to asymptotical normality of Whittle's estimate. *Prob. Th. Rel. Fields*, 86: 87–104.
- Giraitis L., Taqqu M.S. (1999). Whittle estimator for finite-variance non-gaussian time series with long memory. *The Annals of Statistics*, 27: 178–203.
- Gupta H.V., Sorooshian S., Yapo P. (1998). Toward improved calibration of hydrologic models: Multiple and noncommensurable measures of information. *Water Resources Research*, 34: 751–763.
- Montanari A. (2003). Long range dependence in hydrology. In : P. Doukhan, G. Oppenheim, M.S. Taqqu (Eds), *Theory and Applications of Long-Range Dependence*. Birkhauser, Boston: 461–472.
- Montanari A., Brath A. (2004). A stochastic approach for assessing the uncertainty of rainfall-runoff simulations. *Water Resources Research*, 40, doi:10.1029/2003WR002540.
- Montanari A., Rosso R., Taqqu M.S. (2000). A seasonal fractional ARIMA model applied to the Nile River monthly flows at Aswan. *Water Resources Research*, 36: 1249–1259.
- Nash J.E. (1958). The form of the instantaneous unit hydrograph. *IAHS Publication*, 42: 114–118.
- Nash J.E., Sutcliffe J.V. (1970). River flow forecasting through conceptual models 1: a discussion of principles. *Journal of Hydrology*, 10: 282–290.
- Sekhon J.S., Mebane W.R. (1998). Genetic optimization using derivatives. *Political Analysis*, 7: 187–210.
- Whittle P. (1953). Estimation and information in stationary time series. *Ark. Mat.*, 2: 423–434.
- World Meteorological Organisation (1992). *Simulated Real-Time Intercomparison of Hydrological Models*, WMO Publication.
- Zhao R.J., Zhuang Y.L., Fang L.R., Liu X.R., Zhang Q.S. (1980). The Xinanjiang model. *IAHS Publication*, 129: 351–356.

HYDROGRAPH SEPARATION APPLIED TO THE INVESTIGATION OF THE SIGNIFICANCE OF FACTORS CONTROLLING SUSPENDED SEDIMENT DYNAMICS

P. Bača

*Institute of Hydrology Slovak Academy of Sciences, Račianska 75, Bratislava 831 02, Slovakia
Corresponding author: P. Bača, e-mail: baca@uh.savba.sk*

ABSTRACT

The shape of the hysteresis loop in the relationship between water discharge and suspended sediment concentration results from, among others, sediment availability and dilution of suspended sediment concentrations by the baseflow. The aim of the paper is to improve the understanding of single factors that may control suspended sediment concentrations and dynamics. Hydrograph separation using dissolved silica was done to determine the portion of event water (rainfall) and pre-event water (soil and ground water) in the stream hydrograph. Since the baseflow contribution during the recession limb did not increase, sediment availability related to soil aggregate stability in different soil moisture and temperature conditions emerges as the major factor controlling suspended sediment dynamics.

Keywords: dissolved silica, hydrograph separation, hysteresis loop, sediment availability, suspended sediment dynamics

Introduction

Most studies on suspended sediment dynamics describe clockwise or positive hysteresis loops. Suspended sediment concentrations on the rising limb of a storm hydrograph are higher than those measured at equivalent flows on the falling limb. Hence, sediment concentrations typically reach their maximum prior to the hydrograph peak. This effect is caused by, among others, sediment depletion in the channel system (Church and Gilbert, 1975; Walling and Webb, 1981; Van Sickle and Beschta, 1983; Zăvoianu, 1996; Bhutiyani, 2000; Bronsdon and Naden, 2000; Bača and Koniček, 2006; Picouet et al., 2001) or the increased baseflow contribution during the recession limb (Walling, 1974, 1978; Wood, 1977; Becht, 1989).

However, anti- or counter-clockwise hysteresis can occur (Benkhalel and Remini, 2003). This is probably due to bank collapse (Sarma, 1986; Ashbridge, 1995; Russel et al., 2001) or sediment originating from distant sources (Klein, 1984).

As mentioned above, the shape of the hysteresis loop results from sediment availability and dilution of suspended sediment concentrations by the baseflow. From the point of view of a precise prediction of erosion rates, it is necessary to improve the understanding of the significance of the factors controlling suspended sediment dynamics. In this study the influence of the dilution of suspended sediment concentrations by baseflow and subsurface flow on the shape of the hysteresis loop and suspended sediment dynamics was investigated.

Surface flow is the part of total runoff that causes transport of soil particles from a slope into watercourses, where fine soil particles are defined as suspended sediment. Thus, hydrograph separation using silica based on a two-component mixing model was done to determine the portion of event water (rainfall water) and pre-event water (soil and ground water) in the stream hydrograph.

Study area, Rybárik basin

The study focuses on the agricultural micro-basin Rybárik (Fig. 1), near Považská Bystrica (Western Slovakia, Central Europe). The Rybárik basin is a part of the experimental Mošteník brook and is limited by latitudes 49°06'N, 49°07'N and longitudes 18°24'E, 18°25'E. The Mošteník basin is a part of the Váh River catchment, which is the main tributary of the Danube River from the territory of Slovakia. The area of the Rybárik basin is 0.12 km². The mean elevation of the basin is about 400 m a. s. l. (min-375 m a. s. l., max-434 m a.m.s.l.) with slope angles of 8-25%. Length of the Jelšové stream from the spring, which is found in the Rybárik basin, to the outlet section is 255 m and average gradient is 9.1%. The geological conditions in this micro-basin are characterised by flysch substrates (alternating layers of clay and sandstones). Soils are clay loams and are classified as Cambisols. The Rybárik basin is mainly arable, only 10.4% of the area is covered by forest. Mean annual temperature is 8.09°C, mean annual precipitation is 738 mm and average runoff reaches 231 mm year⁻¹.

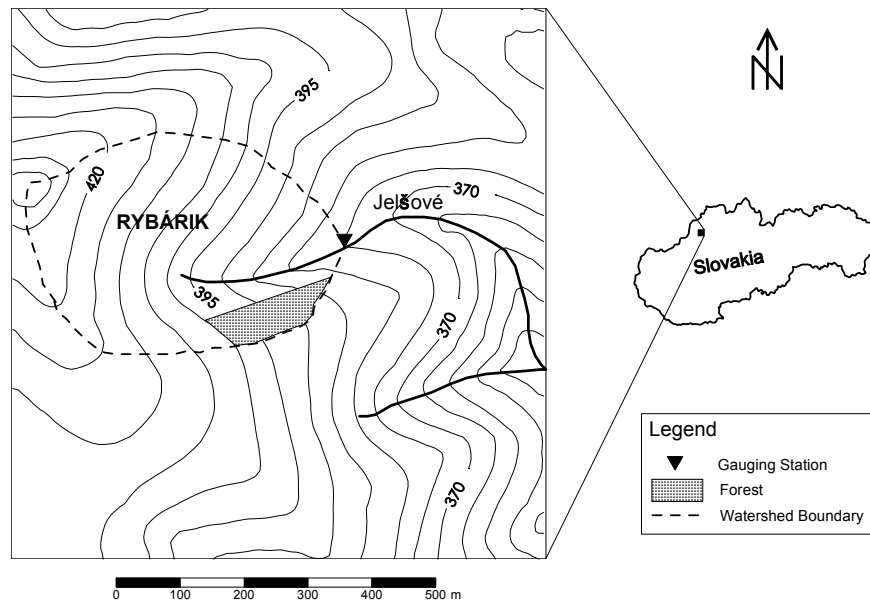


Fig. 1: The experimental Rybárik basin.

Discharge is measured continuously by a weir equipped with a recording gauge. The water levels of the Jelšové stream is stable most of the year. Discharge values are low and range between 0.04-0.5 l s⁻¹. However, water level increases were recorded as a response to snow melt (in winter and spring months) and rainfall (mainly in summer months). Annual peak discharges range between 10.9-364.2 l s⁻¹ (over the period of 40 years 1965-2004) (Pekárová et al., 2005).

Field and laboratory methods

In order to distinguish between event and pre-event water, dissolved silica was chosen for hydrograph separation. The values of silica concentrations are significantly higher in ground water than in surface flow that represents rainfall water. It results from the fact that silica is the most abundant solute in all subsurface solutions and it dominates the chemistry of low flows (Atteia, 1992). Storm water silica concentration is equal to zero (Kennedy, 1971). Monitoring of suspended sediment concentrations (SSC) and dissolved silica concentrations were carried out during rainfall-runoff events that occurred in August 2005. In order to record suspended sediment data, 1000-ml plastic sampling bottles were used to collect water samples manually from the Jelšové stream at the Rybárik basin outlet. The water samples were filtered through pre-weighed filter

papers of pore size less than 3 μm . Filter papers were oven dried, weighed, and suspended sediment concentrations determined gravimetrically.

Stream water samples for silica analysis were collected manually at the basin outlet in 125-ml polyethylene bottles, which were filled as full as possible. The samples were immediately filtered after collection on 0.45 μm paper filters and stored in a dark location, close to 0°C, until analysis. All the samples for SSC and silica analysis were collected at the same time with a frequency of 5 min to 2 h during the event of August 24, 2005.

Hydrograph separation

Contribution of event (new, rainfall) and pre-event (old, ground and soil) water was calculated using the equation (3) which is derived from equations (1) and (2):

$$Q_t = Q_p + Q_s \quad \text{Eq. 1}$$

$$C_t Q_t = C_p Q_p + C_s Q_s \quad \text{Eq. 2}$$

$$X_s = 1 - \left[(C_t - C_s) / (C_p - C_s) \right] \quad \text{Eq. 3}$$

where C is the tracer concentration, Q is discharge, X_s ($1 - Q_p/Q_t$) is the contribution of event (storm) water to total flow and the subscripts t , s , and p refer to total, storm and pre-storm (baseflow) components, respectively.

Results and Discussion

Hydrograph separation was applied to the rainfall-runoff event of August 24, 2005, during which a positive hysteresis loop between SSC and discharge occurred (Fig. 2). It must be noted that the method of hydrograph separation based on a two-component mixing model has the following uncertainty: event-water does not represent surface runoff and surface runoff is a portion of event-water; the portion of soil water may be neglected if tracer concentrations are different in soil and ground water. If the concentration of a tracer in soil water is lower than in ground water the contribution of event water may be overestimated and vice versa (De Walle et al., 1988). The underestimation of event water may occur as the result of a substantial dissolved load obtained by the storm component during its brief contact with the soil surface (Pilgrim et al., 1979; Laudon and Slaymaker, 1997).

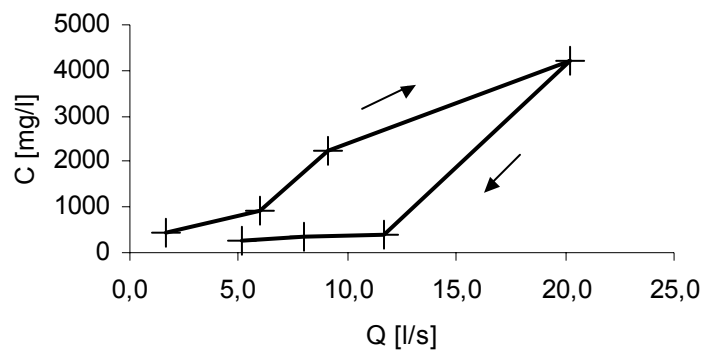


Fig. 2: Positive hysteresis loop between suspended sediment concentration (C) and water discharge (Q) for the discharge wave of August 24, 2005 in the Rybárik basin.

Even though the hydrograph separation contains uncertainties, an increased contribution by pre-event water during the recession limb was not identified (Fig. 3) and the shape of the hysteresis loop did not change

significantly. Thus, the dilution of the suspended sediment concentrations by the baseflow is not such an important factor controlling sediment dynamics as initially expected. This factor only influences suspended sediment concentrations and masks a realistic view on sediment dynamics. Although in other cases the dilution of suspended sediment concentrations by the baseflow may affect the shape of a hysteresis loop, the event of August 24, 2005 indicates that temporal and spatial variability in sediment availability related to soil aggregate stability still remains significant factor controlling sediment dynamics.

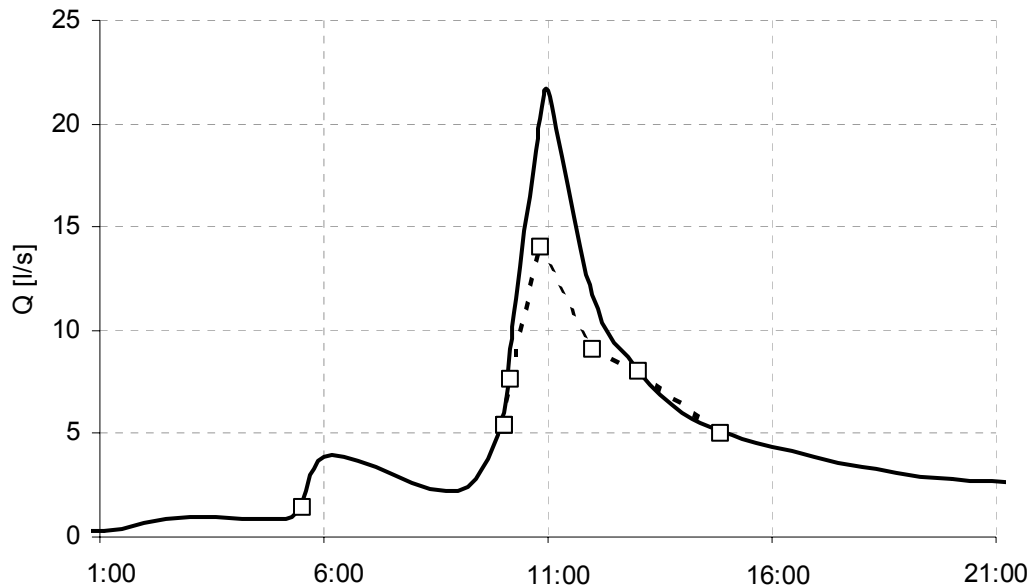


Fig. 3: Hydrograph separation using dissolved silica for event of August 24, 2005 at Rybárik basin. The dashed line with squares (collected water samples) indicates the pre-event water contribution.

Soil aggregation is the result of aggregate formation and stabilization. The aggregates are primarily formed by physical processes (wetting and drying) and biological and chemical processes are mainly responsible for their stabilisation. As shown in Fig. 2, the beginning of the discharge wave of August 24, 2005 is characterised by a supply of easily available sediment. It is obvious that lower soil moisture before and at the beginning of this event resulted in lower soil aggregate stability. Soil water content controls not only infiltration intensity and thus the formation of overland flow but also soil aggregate stability and thus soil erosion intensity.

Acknowledgements

This research was supported by the Science and Technology Assistance Agency (Slovakia) under contract no. APVT-7804 and by the Science Granting Agency (Slovakia) under contract no. VEGA-5055.

References

- Ashbridge D. (1995). Processes of river bank erosion and their contribution to the suspended sediment load of the River Culm, Devon. In: *Sediment and Water Quality in River Catchments*. Wiley, Chichester: 229-245.
- Atteia O. (1992). *Rôle du Sol dans le Transfert des Eléments Traces en Solution – Application à l’Etude de Quelques Ecosystèmes d’Altitude*. Thèse présentée au département du génie rural pour l’obtention du grade de docteur es sciences, Ecole Polytechnique Fédérale de Lausanne, 253 pp.
- Bača P., Koníček A. (2006). Factors controlling suspended sediment dynamics during rainfall-runoff events in a small basin. *Journal of Hydrology and Hydromechanics*, 54: 43-57.

- Becht M. (1989). Suspended load yield of a small alpine drainage basin in upper Bavaria. Landforms and landform evolution in West Germany. *Catena* (supplement), 15: 329-342.
- Benkhald A., Remini B. (2003). Variabilité temporelle de la concentration en sédiments et phénomène d'hystérésis dans le bassin de l'Oued Wahrane (Algérie). *Hydrological Sciences Journal*, 48: 243-255.
- Bhutiyan M.R. (2000). Sediment load characteristics of a proglacial stream Siachen Glacier and the erosion rate in Nubra valley in Karakoram Himalayas, India. *Journal of Hydrology*, 227: 84-92.
- Bronsdon R.K., Naden P.S. (2000). Suspended sediment in the Rivers Tweed and Tevoit. *The Science of the Total Environment*, 251/252: 95-113.
- Church M., Gilbert R. (1975). Proglacial fluvial and lacustrine environments, glaciofluvial and glaciolacustrine sedimentation. In: A.V. Jopling, B.C. McDonald (Eds), *Society of Economic Paleontologist and Mineralogists. (Spec. Publ.)*, 23: 40-100.
- De Walle D.R., Swistock B.R., Sharpe W.E. (1988). Three component tracer model for stormflow from a small Appalachian forested catchment. *Journal of Hydrology*, 104: 301-310.
- Kennedy V.C. (1971). Silica variation in stream water with time and discharge. *Advances in Chemistry*, 106: 94-103.
- Klein M. (1984). Anti clockwise hysteresis in suspended sediment concentration during individual storms. *Catena*, 11: 251-257.
- Laudon H., Slaymaker O. (1997). Hydrograph separation using stable isotopes, silica and electrical conductivity: an alpine example. *Journal of Hydrology*, 201: 82-101.
- Pekárová P., Koníček A., Miklánek P. (2005). *Landuse Impact on Runoff Regime in Experimental Microbasins of IH SAS*. VEDA SAS, Bratislava, 216 pp. (in Slovak with English summary).
- Picouet C., Hingray B., Olivry J.C. (2001). Empirical and conceptual modelling of the suspended sediment dynamics in a large tropical African river: the Upper Niger river basin. *Journal of Hydrology*, 250: 19-39.
- Pilgrim D.H., Huff D.D., Steele T.D. (1979). Use of specific conductance and contact time relations for separating flow components. *Water Resources Research*, 15: 329-339.
- Russell M.A., Walling D.E., Hodgkinson R.A. (2001). Suspended sediment sources in two small lowland agricultural catchments in the UK. *Journal of Hydrology*, 252: 1-24.
- Sarma J. N. (1986). Sediment transport in the Burhi Dihing River, India. In: Hadley R.F. (Ed.), *Drainage Basin Sediment Delivery. IAHS Publication*, 159: 199-215.
- Van Sickle J., Beschta R.L. (1983). Supply-based models of suspended sediment transport in streams. *Water Resources Research*, 19: 768-778.
- Walling D.E. (1974). Suspended sediment and solute yields from a small catchment prior to urbanisation. In: K.J. Gregory, D.E. Walling (Eds.), *Fluvial Processes in Instrumented Watersheds. Institute of British Geographers (Spec. Publ.)*, 6: 169-192.
- Walling D.E. (1978). Suspended sediment and solute response characteristics of the river Exe, Devon, England. In: R. Davidson-Arnott, W. Nickling (Eds.), *Research in Fluvial Systems, Geoabstracts*: 169-197.
- Walling D.E., Webb B.W. (1981). The reliability of suspended load data. In: *Erosion and Sediment Transport Measurement. IAHS Publication*, 133: 177-194.
- Wood P.A. (1977). Controls of variation in suspended sediment concentration in the River Rother, West Sussex, England. *Sedimentology*, 24: 437-445.
- Zăvoianu I. (1996). Relationship between rainfall, slope runoff and erosion in the Valea Muscel Basin. *Geographical Journal*, 48: 113-120.

USE OF THE WATBAL MODEL FOR THE EVALUATION OF CLIMATE CHANGE IMPACT ON RUNOFF IN A SMALL RIVER BASIN

G. Chirila & S. Matreata

National Institute of Hydrology and Water Management, Sos. Bucuresti – Ploiesti 97, 013686, Bucharest, Romania

Corresponding author: G. Chirila

ABSTRACT

This paper presents some results regarding the climate change impact on the water resources, in a small river basin. For the evaluation of the climate change impact more hypothetical scenarios were used; scenarios which take into consideration uniform changes for temperature and precipitation. The impact of those possible climatic changes on the catchment runoff was analysed using an integrated water balance model – the WATbal model. The analysis was done on the Representative Basin Tinoasa Ciurea, which is a small catchment situated in the north-eastern part of Romania. The simulation results show a significant vulnerability of the water resources to climate change. For example, the impact estimated using the WATbal model, shows that an increase of air temperature by 1° C should reduce runoff by 3.5%, and an increase or a decrease of precipitation by 20% leads to an increase or a decrease of runoff by more than 30%.

Keywords: WATbal model, small basin, climate change impact

Introduction

This paper aims at estimating through the use of the WATbal model the vulnerability of water resources in a small river basin, as a response to climate change. Another objective of this paper is the estimation of differences resulting from the application of the model in the same representative basin, but using as input meteorological data that were recorded at meteorological stations situated outside of the studied basin.

For the evaluation of climate change impacts in the analyzed basin, several hypothetical scenarios were used, representing a series of future possible climates. The chosen scenarios take into consideration uniform annual changes for temperature and precipitation, considering that they will cover the future possible range of climate change.

The WATbal Model (WATER BALANCE Model) – relies on concentrated parameters and was developed by Kazmarek (1993). It uses simple hypotheses linked to the water balance and robust physical estimation approaches of potential evapotranspiration. Due to the capacity of the WATbal model to allow different approaches, variable time steps can be used depending on available data and river basin characteristics.

Methodology

The components of the Watbal model

The uniqueness of this global conceptual model for representing the water balance consists in using continuous functions for the relative storing (accumulation) in order to determine the surface, subsurface runoff and evapotranspiration. In this approach the mass balance is written as a differential equation and the accumulation is presented as a unique reservoir, conceptualized with discharge and infiltration components depending on the state, relative storage variable.

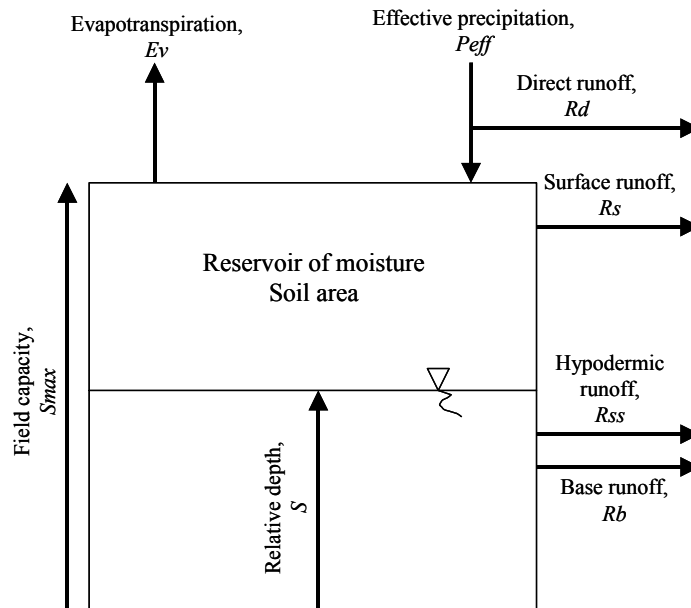


Fig. 1: Conceptualization of the water balance for the WATbal model (after Yates and Strezepek, 1994b).

The model has two components:

- The water balance component (using continuous functions in order to describe water movements in a conceptualized basin);
- Potential evapotranspiration, based on the Priestley-Taylor method (Yates 1994a).

The water balance component (Fig. 1) contains 5 parameters which refer to:

- Direct runoff, β
- Surface runoff, ε
- Subsurface runoff, γ
- Maximum capacity of the water retention basin (field capacity, S_{\max})
- Base runoff, R_b .

The direct runoff coefficient β and the strength factor of hypodermic runoff γ are not part of the automated optimization procedure (they are defined by the author).

The potential evapotranspiration is calculated with the Priestley-Taylor method which contains 3 parameters:

- C_f = has a value of 1.26 for a humid climate (relative humidity > 60%) and 1.74 for an arid humid climate (relative humidity < 60%);
- Priestley-Taylor coefficient PT
- terrain coverage coefficient GC

For the calibration and validation of the model the data on precipitation, potential evapotranspiration, and runoff (discharge) are needed. Potential evapotranspiration can be provided as mean monthly values (calculated with different methods). Alternatively, it can be calculated by the model with the Priestley – Taylor method. In such a case, temporal series of air temperature, duration of sunshine, relative sunshine and wind speed are needed as input data.

The evaluation of the model is based on the use of two data series: one used for calibration and another for validation. If the statistical values, namely the correlation coefficient (ρ) and the mean monthly error between the measured discharges and the simulated ones ($E_{P,O}$), resulting from the calibration and validation procedures are similar, the model can be considered acceptable.

The variation coefficient is given by:

$$\rho_{Q_O, Q_P} = \frac{Cov(Q_O, Q_P)}{\sigma_{Q_O} \sigma_{Q_P}} \quad \text{Eq. 1}$$

where: $Cov(Q_O, Q_P)$ is the covariation of the observed and simulated discharges $\sigma_{Q_O} \sigma_{Q_P}$ are the standard deviations of the observed and simulated series.

The mean monthly error between the simulated and the observed discharges is given by:

$$E_{P,O} = \frac{\sum abs(Q_P - Q_O)}{n} \quad \text{Eq. 2}$$

where: Q_O is the observed mean monthly discharge,

Q_P is the mean monthly discharge simulated with the model.

The elaboration of scenarios for the evaluation of an impact of climate change

The elaboration of the scenario for the evaluation of the impact of a climatic change was made through the hypothetical scenario method. The hypothetical scenarios are a set of future possible climates. These chosen scenarios consider uniform changes for air temperature (ΔT) and precipitation (%P), in the following combinations, considering that they will cover the possible future climate domain (Table 1).

Table 1: Used uniform climatic scenarios (0*- basic scenario) T [°C], P[%].

T+0, P+0*	T+0, P+10	T+0, P+20	T+0, P-10	T+0, P-20
T+2, P+0	T+2, P+10	T+2, P+20	T+2, P-10	T+2, P-20
T+4, P+0	T+4, P+10	T+4, P+20	T+4, P-10	T+4, P-20

Case study

Physical – geographical description of the analyzed river basin – R. B Tinoasa – Ciurea

The representative basin Tinoasa Ciurea has a catchment area of 4.17 km² and its elevation ranges between 119 and 410 m. a.s.l. The average slope is 15.9% with a predominantly northern orientation.

It has an excessive continental climate which is characterized by an annual precipitation of 600-650 mm. The seasonal distribution of precipitation is uneven during the year: minimum monthly precipitation of 30 mm is recorded between August and October. Almost half of the annual precipitation falls between May and August with a maximum in July, often having torrential character. The mean annual temperature is around 9 °C (the hottest month is July with 21.3 °C and the coldest month is January with a mean temperature of minus 3.6 °C; the temperature drops below 0°C starting with the second decade of December). This type of climate generates a large amplitude in runoff.

Forests cover the largest part of the catchment (63%) and contribute to the diminishing of surface runoff quantity.

Calibration and validation the WATbal model

For the Ciurea Basin 16 years of data were available (1979-1994), from which 10 were used for calibration (1979-1988) and the last 6 years for validation. The results are presented in figures 2-3.

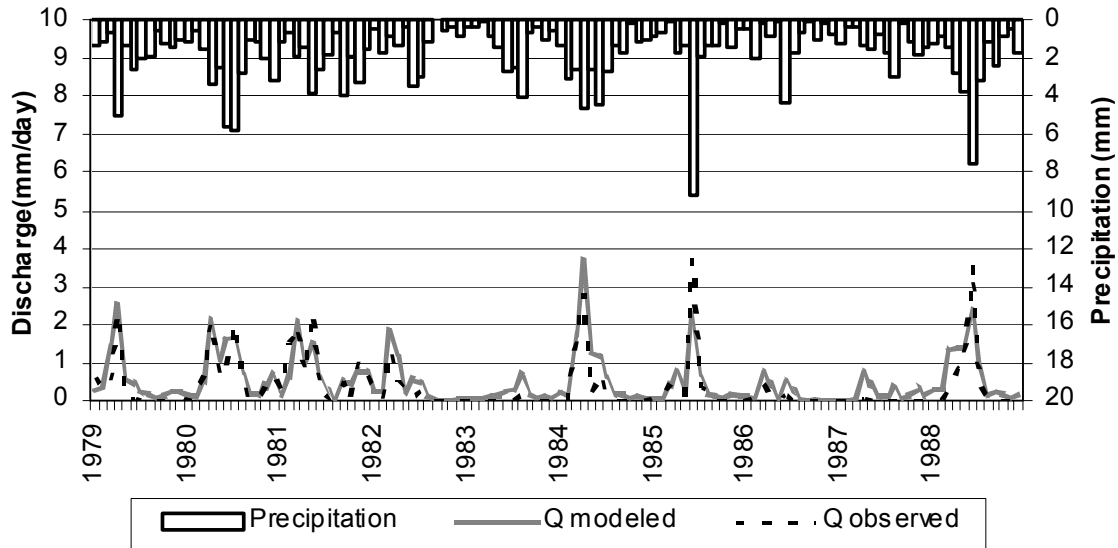


Fig. 2: Precipitation and mean monthly observed and modeled hydrographs in the calibration period – R.B. Tinoasa Ciurea.

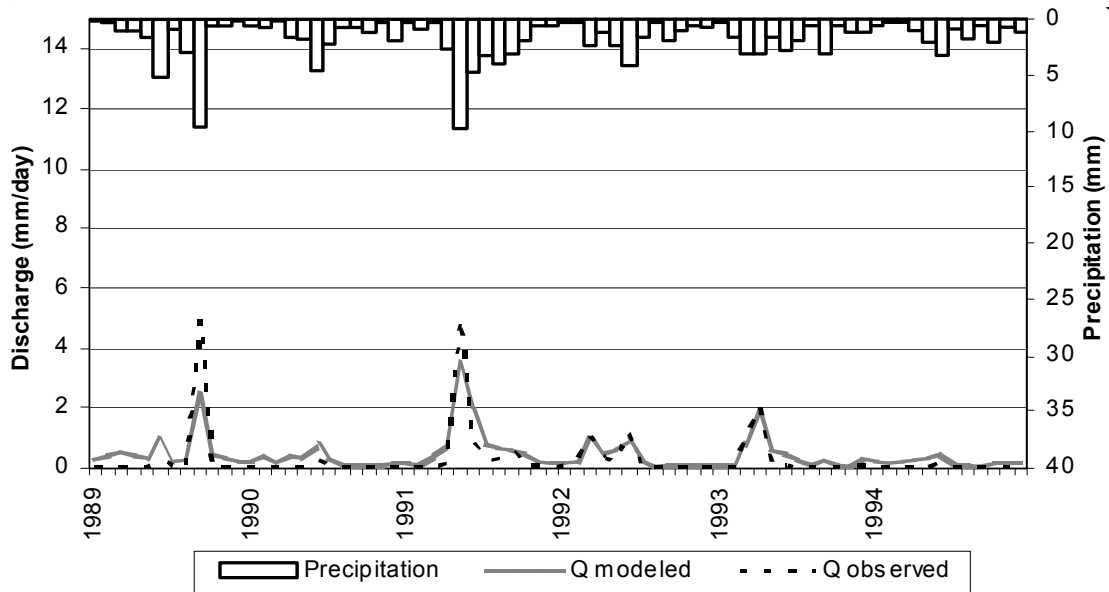


Fig. 3: Precipitation and mean monthly observed and modeled hydrographs in the validation period – R.B. Tinoasa Ciurea.

Calibrated and validated coefficients used in the WATbal model for the Tinoasa-Ciurea basin are:

- subsurface flow coefficient $\gamma = 2.0$
- subsurface flow coefficient $\alpha = 1.0$

- surface runoff coefficient $\varepsilon = 1.34$
- maximum accumulation capacity coefficient $S_{\max} = 313$
- initial accumulation $z_i = 0.5$
- direct runoff coefficients $\beta := 0.0$
- latitude 47° N ;
- Priestley –Taylor coefficient $PT = 1.74$
- terrain coverage coefficient $GC = 0.65$
- base runoff $R_b = 0.0$

In Table 2 are presented the values of the correlation coefficients and the mean monthly errors between the measured and the simulated results for the calibration and validation periods.

Table 2: Calibration and validation values for R.B. Tinoasa – Ciurea.

	Correlation Coefficient	Mean Error
Calibration	0.88	0.24
Validation	0.90	0.27

Impacts of climate change scenarios on runoff, for R.B. Tinoasa-Ciurea:

The hypothetic impacts of climate change scenarios on runoff, estimated using the WATbal, model are presented in Table 3 and Fig. 4. Table 3 shows sensitivity of catchment runoff to the change in climatic variables. For example, an increase of air temperature by 1° C is likely to reduce runoff by 3.5%. An increase or a decrease of precipitation by 20% leads to an increase or a decrease of runoff by more than 30%.

Table 3: Change in runoff [%] in the studied catchment related to changes in air temperature and precipitation.

	P 0	P 10%	P 20%	P-10%	P- 20%
T0	0%	19%	39%	- 17%	- 34%
T2	- 7%	10%	29%	- 24%	- 39%
T4	- 15%	1%	18%	- 30%	- 44%

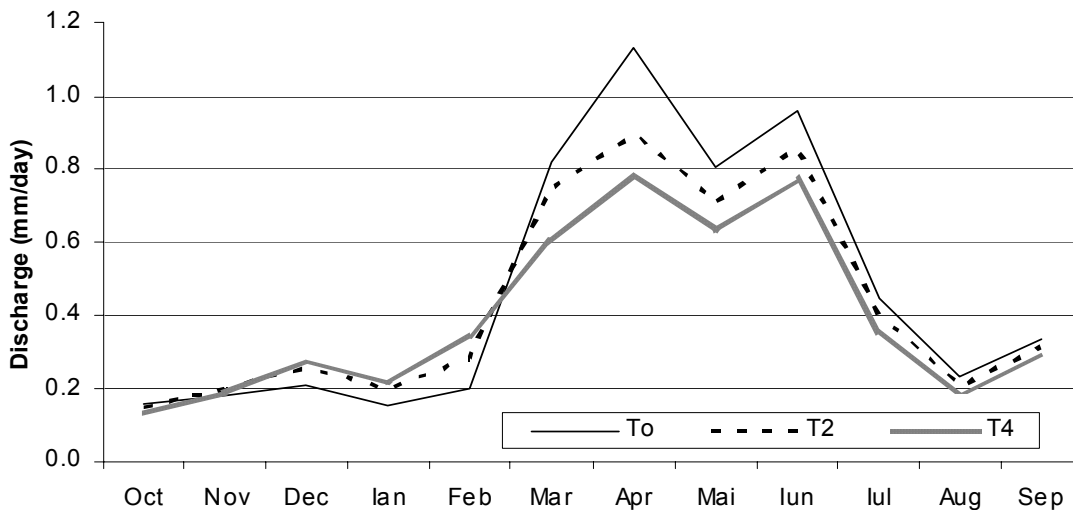


Fig. 4: Observed (To) and simulated mean monthly discharges (T2, T4), corresponding to temperature increases of 2° C and 4° C, respectively.

Another objective of the paper was the application of the model in the same representative basin, but with input meteorological data, taken from a meteorological station situated outside of the basin (Solesti Meteorological Station situated at an altitude of 118 m.a.s.l.) (Figs. 5-6). Catchment precipitation was calculated from several nearby stations using the elevation gradient method. Statistical parameters for calibration and validation periods (Table 4) emphasize weaker results that are caused by the extrapolation of the input data.

Table 4. Calibration and validation values using data from M.S. Solesti.

	Correlation coefficient	Average error
Calibration	0.75	0.28
Validation	0.68	0.30

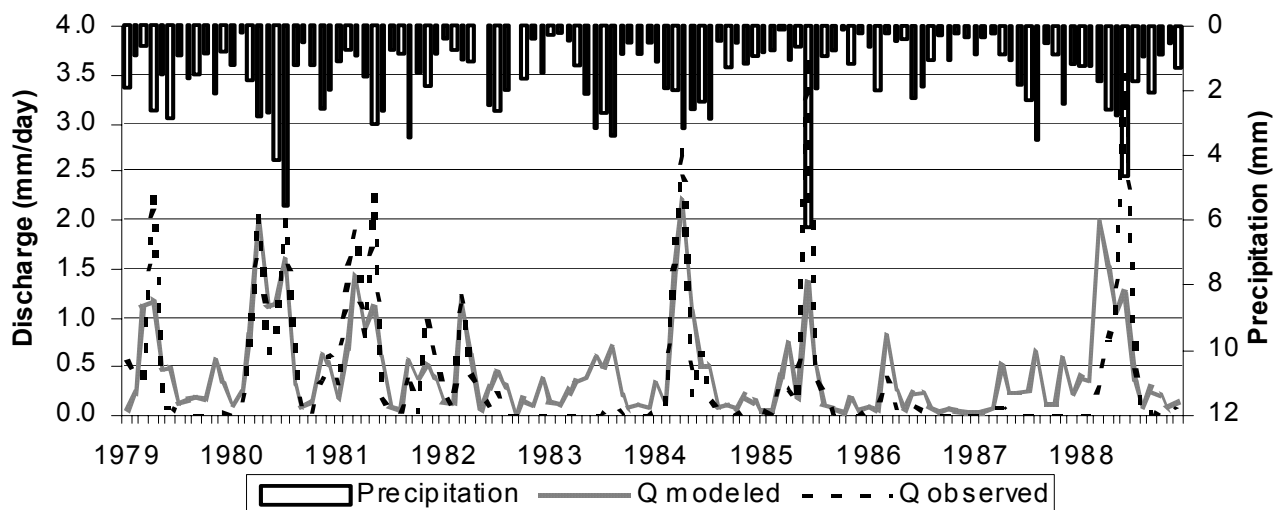


Fig. 5: Precipitation and the observed and modeled mean monthly hydrographs in the calibration period – R.B. Tinoasa Ciurea, M.S. Solesti.

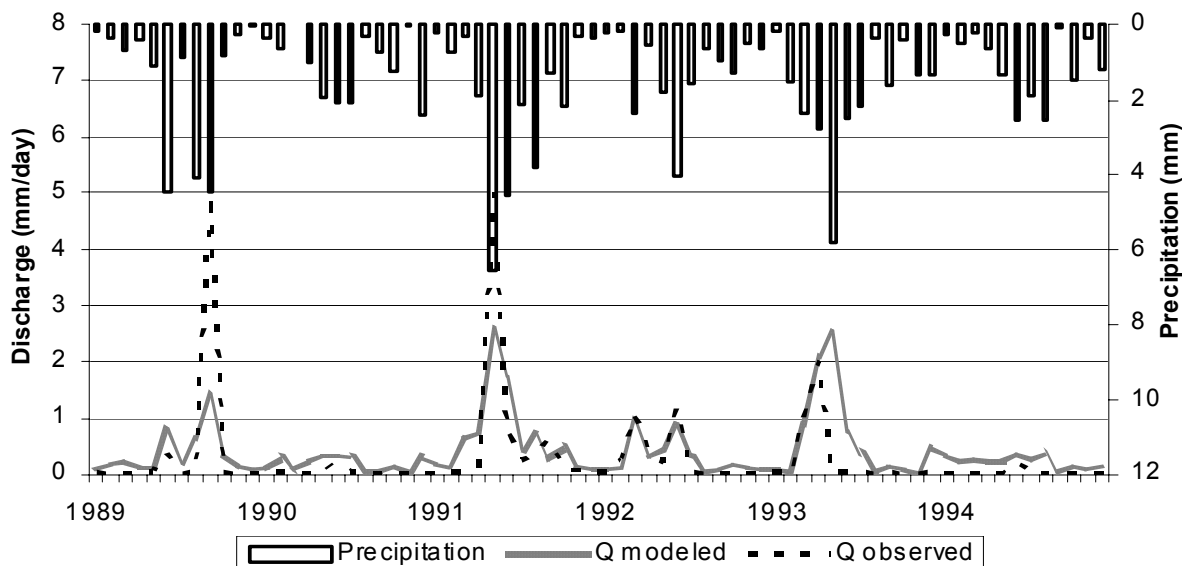


Fig. 6: Precipitation and mean monthly hydrographs in the validation period – R.B. Tinoasa Ciurea, M.S. Solesti.

Conclusions

The WATbal model chosen in the present study is a water balance model for the evaluation of climate change impacts in a river basin. The model uses a simple hypothesis regarding the water balance and a strong physical approach for the estimation of potential evapotranspiration. The model was applied to the representative basin Tinoasa-Ciurea. Even though the WATbal model has a quite simple conceptual structure, the good results confirm the possibility of using it in the case of a little hydrographic basin, too.

After calibration and validation of the model on this representative basin Tinoasa – Ciurea, it was possible to evaluate the impact of different climate changes using more hypothetical scripts. Thus, for a uniform increase of temperature with 1°C resulted a decrease in discharge of 3.5%. An increase or a decrease of precipitation by 20% would lead to an increase or a decrease of catchment runoff of more than 30%.

To point out the model's sensitivity to the accurate estimation of the input data, a comparative analysis of the model's performances using input data from a station situated outside of the basin was done. A significant decrease of the calibration and validation performance was noted as a result.

References

- Kaczmarek Z. (1993). Water balance model for climate impact analysis. *Acta Geophysica Polonica*, 41: 1-16.
- Yates D.N., Strzepek K.M. (1994a). *The Impact of Potential Evapotranspiration Methodology on the Determination of River Runoff*. IIASA Working Paper, WP-94-46, Laxenburg, Austria.
- Yates D.N., Strzepek K.M. (1994b). *Comparison of Models for Climate Change Assessment of River Basin Runoff*. IIASA Working Paper, WP-94-45, Laxenburg, Austria.

DISTRIBUTED WATER STORAGE AND LOCAL GRAVITY: A FIELD EXPERIMENT AT MOXA (GERMANY)

R. Dijkma¹, H.A.J. van Lanen¹, S. Hasan¹, C. Kroner² & P.A. Troch³

¹Hydrology and Quantitative Water Management Group, Wageningen University, Wageningen, the Netherlands. ²Institute of Geosciences, Friedrich-Schiller University, Jena, Germany. ³Department of Hydrology and Water Resources, University of Arizona, Tucson, USA.
Corresponding author: Roel Dijkma, email: roel.dijkma@wur.nl.

ABSTRACT

Water storage at and below the land surface has effect on the gravity field. A thorough understanding of this relation will help to filter the hydrological signal from the gravity signal, and can also enable the use of the gravity signal for hydrological purposes. The implementation of a number of superconducting gravimeters in the framework of the Global Geodynamics Project offers the opportunity to investigate the relation between catchments-scale processes and gravity. When this relation is known, then gravity data could be used for a better understanding water storage change (e.g. interception, snow, subsurface water).

Keywords: Hydrological processes, gravity, distributed water storage, streamflow generation, MODFLOW modeling, field campaign

Introduction

Traditionally, the gravity field has been treated as essentially steady-state because 99% of the field is more or less static in historic time (Troch et al., 2007). The remaining 1% is caused by processes that vary on time scales varying from hours to thousands of years. The hydrosphere is a source of irregular variations in the mass distribution. Research is focusing at understanding this relation between variations in the gravity field and basin scale water storage changes. *In situ* observations, with super-conducting gravimeters are then assumed to provide explicit information about local hydrology, where satellite (GRACE) data could provide very useful information about temporal changes in water storage changes in large areas.

This paper shows the first indicative result of a joint research of Wageningen University (the Netherlands) and Friedrich-Schiller University (Jena, Germany) in the Silberleite catchment.

Experimental area

The Silberleite catchment, located near Moxa, Germany is approximately 3.4 km² in size (Fig. 1). In this catchment the Geodynamic Observatory of the Friedrich-Schiller University Jena is located (Kroner et al., 2004). The catchment's subsurface consists predominantly of slates, which are fractured at the top and intersected by faults. These slates are covered by a permeable weathering layer and a clayey soil with a variable depth. The catchment has an undulating landscape and is predominantly covered with coniferous forest. The hill slope just east of the gravimeter is rather steep (~20°), while the hill slope west of the gravimeter is relatively gentle (~10°). In the downstream part of the valley, where the observatory is located at the foothill of a steep slope, a natural valley fill consisting of predominantly fine grained sediments is covered with a mainly coarse artificial valley fill with an increasing thickness in southward direction (max. 3 m thick). Observed streamflow at different locations shows that the catchment quickly responds to rainfall after filling up the subsurface stores.

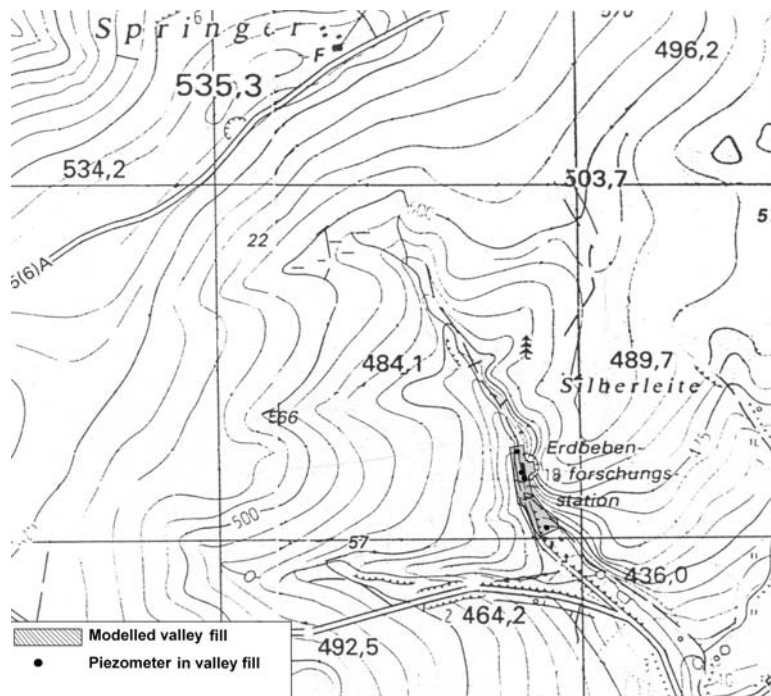


Fig. 1: The Silberleite area.

Methods

During several intensive field campaigns in the period 2004 – 2006 the geological profile and its hydrogeological properties were studied by constructing soil pits, by drilling and by performing hydraulic conductivity tests. The upper part of the geological profile at the steep slope east of the Geodynamic Observatory is shown in Fig. 2. Within the catchment area the precipitation, the piezometric heads and the discharge of the Silberleite and its tributaries are measured continuously.



Fig. 2: Geological profile at the steep slope, 50 m east of the observatory.

An explorative saturated groundwater flow model was constructed using MODFLOW. This model did not cover the entire catchment, but was concentrated on the area with artificial valley fill, i.e. the area where the gravimeter is located and where the largest effects of water storage changes on the gravimetrical signal are expected. The model boundaries were considered as flux-boundaries, to enable groundwater inflow from the hills into the modeling area.

Results and discussion

Initial research results show that short-term gravity variation, which is corrected for a number of effects (e.g. polar motion, earth tides) is highly correlated with substantial rainfall. Any substantial rainfall causes an increase in groundwater and stream levels, but in first a drop in the gravity signal. This drop in the gravity signal is due to water mass changes above the gravimeter during and just after the rain event. The downward movement of these water masses then causes a decrease in water mass above the gravimeter level and an increase in water mass below the gravimeter level. As a consequence the gravity signal is then increasing.

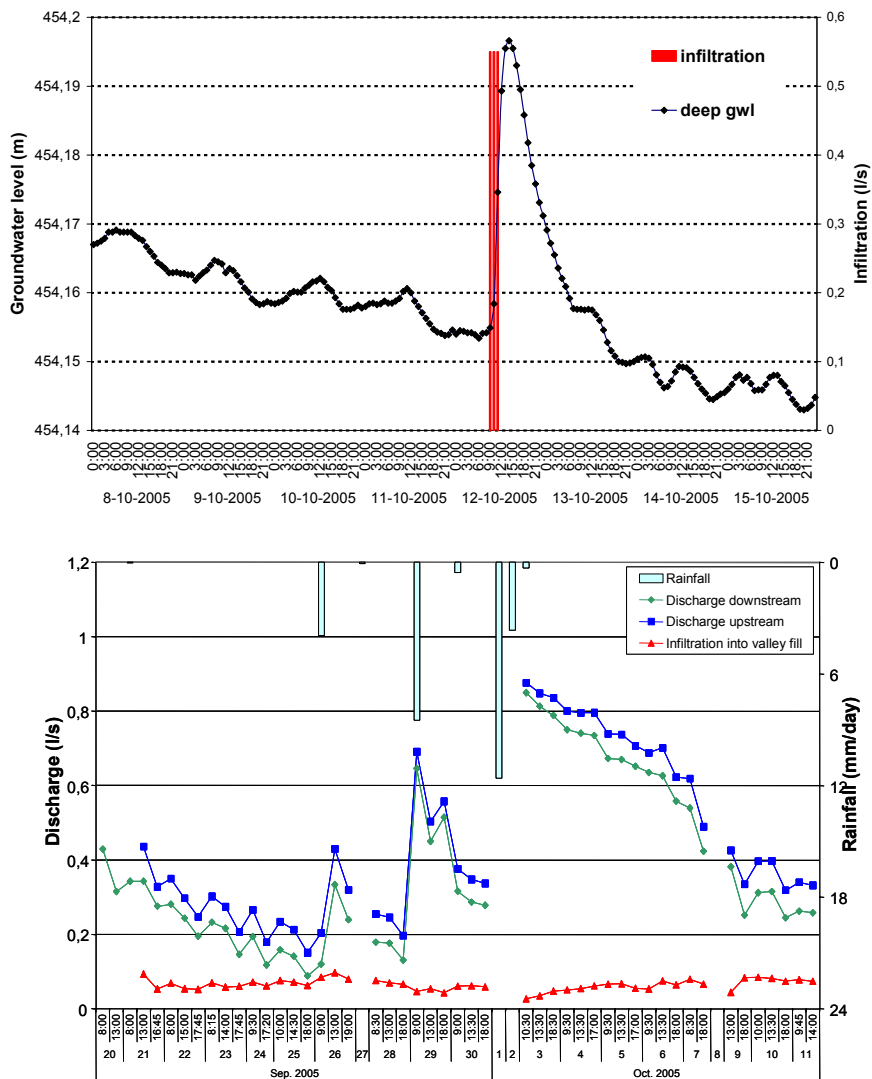


Fig. 3: Response of groundwater level in the valley fill on infiltration at the steep slope (upper) and infiltration of water from the stream into the valley fill (lower) (Niessen and Wesselius, 2006).

Simulated gravity variation (integrated over the influence sphere) with a rainfall-runoff model, in which the spatial and temporal distributed water storage is converted to gravity, agrees well with observed gravity variation except for periods that groundwater storage change affects gravity (e.g. 3 – 8 May 2004 in Fig. 2).

Infiltration experiments at the steep slope above the gravimeter and at the gentle slope opposite of the gravimeter illustrate that piezometers in the valley fill respond rather quickly to groundwater flow mainly through the weathering layer and fractured slates (shallow subsurface flow).

Explorative saturated groundwater flow modeling using MODFLOW confirms that groundwater storage is affected by infiltration from the stream and that groundwater inflow from the steep slope does not flow directly into the Silberleite stream, but it flows parallel to the stream through the highly-permeable valley fill. The modeling also shows that near the gravimeter small injection cones will develop after a rain event because of the outflow from the rain pipes draining the roof of the observatory.

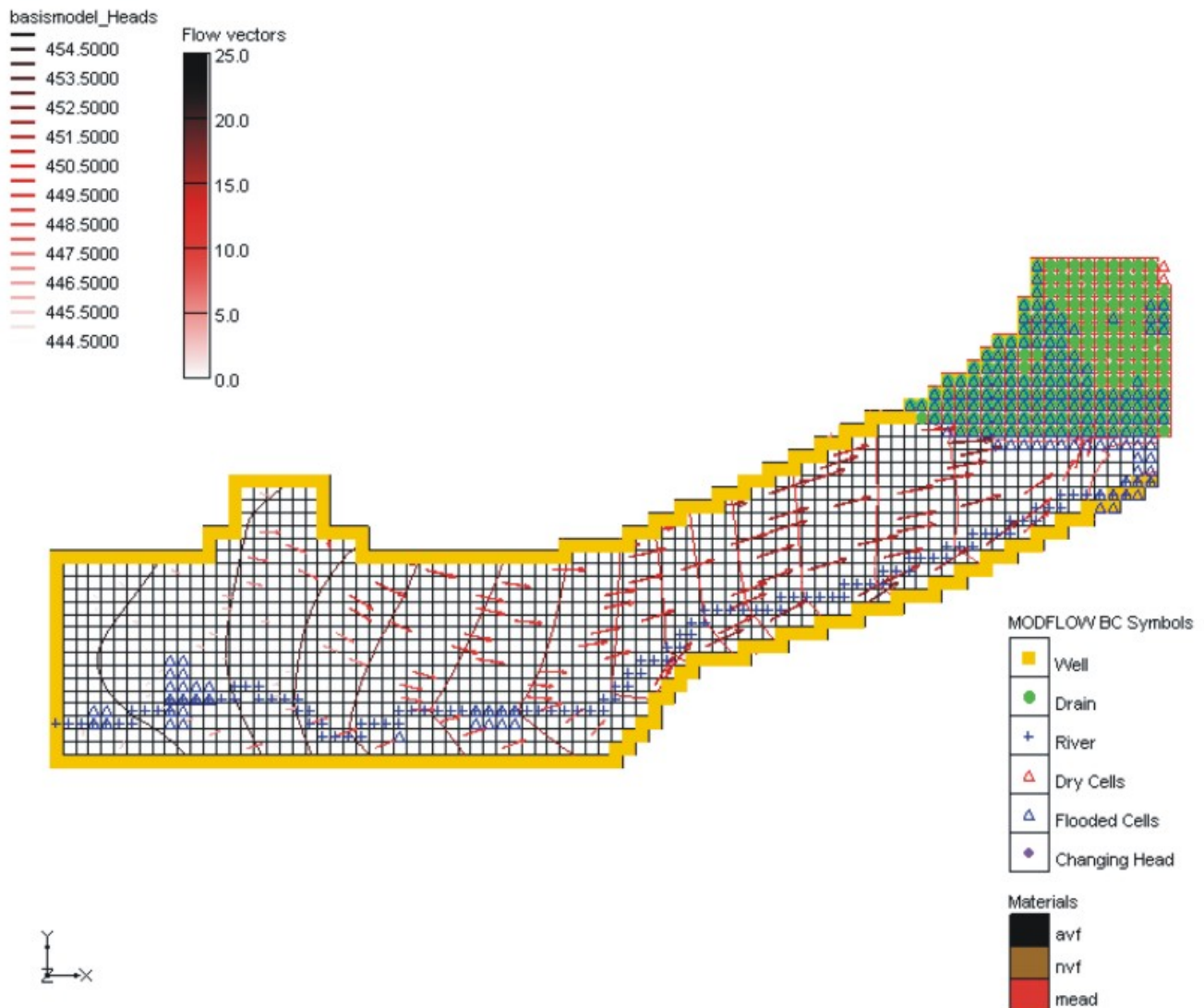


Fig. 4: Simulated saturated groundwater flow in the valley fill by using MODFLOW (Niessen and Wesseliuss, 2006).

Significant rainfall events cause quick gravity variation. The effect of mass changes on the gravimetric signal is a function of the distance to the gravimeter (Dijkma et al., 2007). As a result, quick variations are caused by water storage changes in the direct vicinity of the gravimeter. Mass increase above gravimeter level (i.e. canopy storage, uphill increase in soil moisture content) will induce a gravity reduction, mass increase below gravimeter level (i.e. groundwater level) a gravity increase. Gravity variation at longer time scales is determined by water flow and storage in the shallow subsurface. Water flow on the steep slope east of the gravimeter causes a rather quick response. Because of the steep groundwater gradient and the distance to the gravimeter significant quantities of water can move rather quick within measuring range of the gravimeter. The gentle slope, opposite of the gravimeter, will cause a somewhat slower (intermediate) and less pronounced response because of the relatively gentle groundwater gradient and the larger distance to the gravimeter. Groundwater storage changes in the valley fill contribute to the short term as well as to the long-term variation. This mechanism is controlled by groundwater inflow from the steep slope and gentle slope. The quick response is dominated by fracture flow, where the relatively slow response is due to the flow in the weathered cover and infiltration from the Silberleite stream.

Terrestrial gravity measurements offer a new way of investigating catchment-scale hydrological processes. In areas with numerous water storage reservoirs, varying in size, elevation and response time, it is difficult to fully understand the relation between water storage and gravity. More research is needed.

References

- Dijkma R., Ros G., de Jong B., Troch P.A. (2007). Local water storage changes affect in-situ gravity observations at Westerbork, the Netherlands. *Journal of Geodesy*, submitted.
- Kroner C., Jahr T., Jentzsch G. (2004). 44 months of observations with a dual sensor superconducting gravimeter at Moxa observatory. *Journal of Geodynamics*, 38: 263–280.
- Niessen S., Wesselius C. (2006). *Groundwater Distribution at the Geodynamic Observatory Moxa; Fieldwork and Hydrological Modeling*. Doctoral thesis Wageningen University, Wageningen, the Netherlands.
- Troch P.A., Dijkma R., van Lanen H.A.J., van Loon E.E. (2007). Towards improved observations and modeling of catchment-scale hydrological processes: bridging the gap between local knowledge and the global problem of ungauged basins. *IAHS Publication*, 309: 173–185.

FOREST FLOOR INTERCEPTION MEASUREMENTS

A.M.J. Gerrits^{1,2}, H.H.G. Savenije¹ & L. Pfister²

¹Water Resources Section, Faculty of Civil Engineering and Geosciences, Delft University of Technology, PO Box 5048, 2600 GA Delft, the Netherlands. ²Department Environment and Agrobiotechnologies, Centre de Recherche Public - Gabriel Lippmann, 41 rue du Brill, L-4422 Belvaux, Luxembourg.

Corresponding author: A.M.J. Gerrits, email: a.m.j.gerrits@tudelft.nl

ABSTRACT

Since the process of interception is generally considered a minor flux, it is frequently disregarded in hydrological models. If considered at all, it is often combined with transpiration, or taken as a fixed percentage of rainfall. However, previous research shows that interception can (on average) amount up to 10-50% of the precipitation. And if not only canopy interception is taken into account, but also forest floor interception, this percentage can even be twice as high as will be shown in this paper. Forest floor interception is an even more disregarded process, although it is an important mechanism that precedes infiltration. To measure forest floor interception a special device has been developed. It consists of two aluminium basins, which are mounted above each other and continuously weighed with strain gauges. The upper basin has a permeable bottom and is filled with forest floor. Water balance calculations in the Huewelerbach show that 35% of the throughfall was intercepted by the litter in November 2004. In Westerbork this amount was 85% of the rainfall and if compensated for transpiration 52% for September to October 2005.

Keywords: forest floor, litter interception, grass/moss interception

Introduction

Rainfall interception and its successive evaporation is not always considered as a significant process in the hydrological cycle. This is, besides the widely spread consideration that it is a minor flux, also due to the technical difficulties that are inherent to interception measurements (Lundberg et al., 1997; Llorens and Gallart, 2000). Hence in hydrological models interception is regularly disregarded or taken as a fixed percentage of the precipitation (Savenije, 2004). However, previous research shows that interception can amount to 10-50% of the precipitation (Klaassen et al., 1998). In these studies often only canopy interception is considered. The percentage of interception is even higher if also forest floor interception is taken into account as shown in this paper. Interception is thus a significant flux in the hydrological cycle and not only during dry and moderate weather conditions. Although the amount of interception is relatively small during floods it is very important for the generation of floods because it directly acts on antecedent soil moisture conditions. Therefore, it is important that the process of interception (i.e., interception storage and interception evaporation) is well understood and can be incorporated adequately in hydrological models.

Generally, two types of interception are distinguished: canopy and forest floor interception. Traditional research mainly focuses on canopy interception whereas this paper concentrates on forest floor interception. Forest floor interception can be interception by dry soil, interception by short vegetation (grasses, mosses, etc.) or interception by litter. The latter two are measured in an experimental plot in Westerbork (the Netherlands) and in the Huewelerbach catchment located in the centre of Luxembourg (Fig. 1), with a special developed instrument.

Site descriptions

The Huewelerbach catchment (49°42'N 5°53'E) is a hill slope area in the Grand-Duchy of Luxembourg and consists mainly of sandstone. The catchment area of the Huewelerbach is about 2.7 km² and the climate is characterized by mild winters and temperate summers. The yearly rainfall sum is about 740 mm/year and the average annual temperature is circa 9°C. The interception device is installed in an experimental plot in a 120 years old beech forest with a density of 168 trees/ha. In the experimental plot throughfall is measured intensively with a dense network of manual pluviometers and a tipping bucket. The pluviometers are close to the interception device, but are only read out every one or two weeks. To obtain data with a higher temporal resolution, the throughfall data of the pluviometers is multiplied by the intensity distribution of the tipping bucket.

The device in Westerbork (52°54'N, 6°36'E) is installed on top of a small sandy hillock, under which a concrete bunker has been built. The interception device is installed in the open field so the net precipitation is equal to the gross precipitation. The rainfall is measured with a tipping bucket. The climate in Westerbork is temperate, marine with cool summers and mild winters. Westerbork has an average yearly rainfall sum of 774 mm/year and an average temperature of circa 9°C.



Fig. 1: Location of the two measuring locations: Westerbork (mosses and grass interception) and Huewelerbach (litter interception).

Research method

A special device has been developed for the measurement of forest floor interception (see Fig. 2). The device consists of two aluminium basins mounted above each other, which are dug into the ground to reduce evaporation from the lower basin (E_l [L/T]) as much as possible. The upper basin is filled with mosses and grass vegetation in Westerbork (Fig. 3A) and filled with litter in the Huewelerbach (Fig. 3B). The bottom of the upper basin is permeable, so rainfall can infiltrate (Q_{infil} [L/T]) into the lower basin. A valve is installed in

the lower basin, which opens at a regular time step (Q_{valve} [L/T]) to avoid overtopping and evaporation from the lower basin. The weight of the two basins (S_u and S_l [L]) is measured accurately with strain gauges.

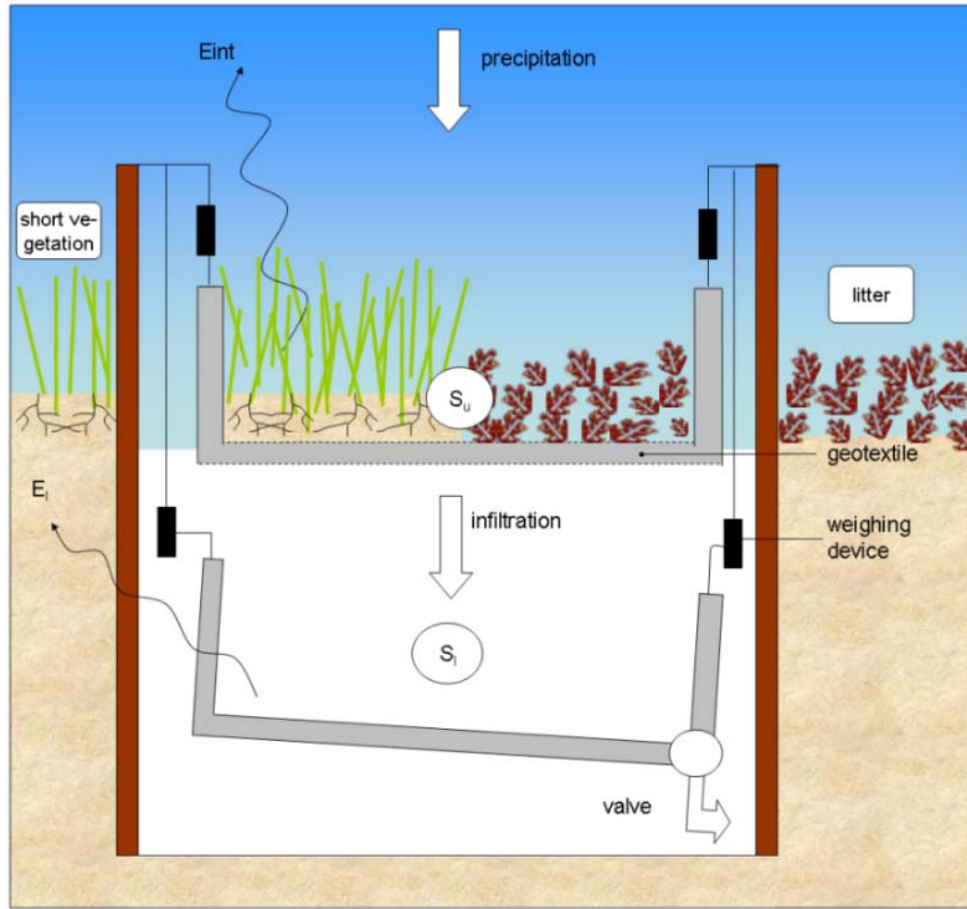


Fig. 2: Schematic drawing of the forest floor interception device with E_{int} the evaporation from interception, E_l the evaporation from the lower basin and S_u and S_l the storage in the upper and the lower basin, respectively. On the left hand side the ‘short vegetation situation’ as in Westerbork and on the right hand side the setup for litter interception as measured in the Huewelerbach.

Evaporation from the forest floor, E_{int} [L/T], can be determined by calculating the water balance of the upper and the lower basin (Equation 1), assuming that no water evaporates from the lower basin. From this water balance follows that evaporation from interception is equal to the amount of net precipitation, P_{net} [L/T], minus the discharged water from the valve, minus the change in weight of the two basins.

$$\left. \begin{aligned} P_{net} - E_{int} - Q_{perc} &= \frac{dS_u}{dt} \\ Q_{infil} - Q_{valve} - E_l &= \frac{dS_l}{dt} \end{aligned} \right\} E_{int} = P_{net} - Q_{valve} - \left(\frac{dS_u}{dt} + \frac{dS_l}{dt} \right) \quad \text{Eq. 1}$$

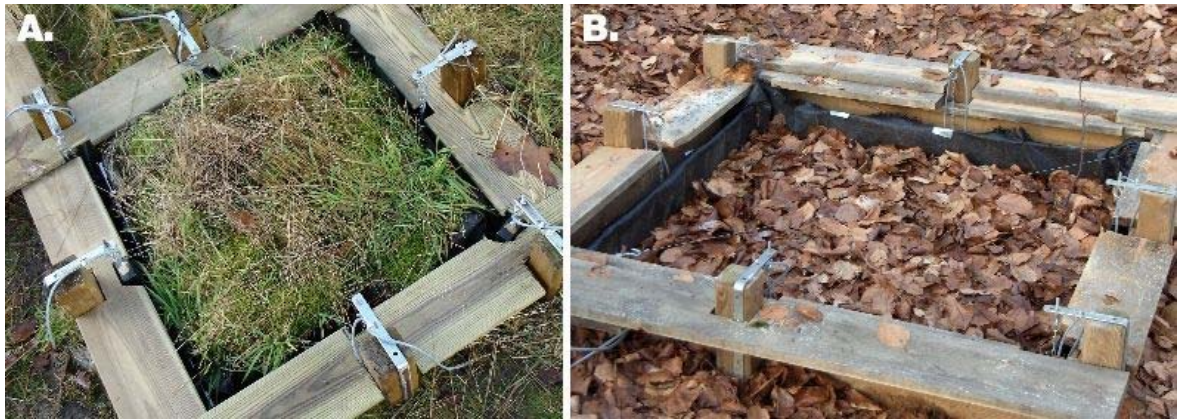


Fig. 3: A) Mosses and grass interception measuring device in Westerbork (the Netherlands); B) Litter interception measuring device in the Huewelerbach catchment (Luxembourg).

Results

The preliminary results for Westerbork and the Huewelerbach catchment are promising as can be seen for the Huewelerbach in Fig. 4. Both basins react on rainfall events by showing a weight increase and successively the depletion of the weight of the upper basin due to evaporation from interception (Fig. 4A, B). It appears that for November 2004, about 35% of the net precipitation is intercepted by the forest floor (Fig. 4C). If a simple daily threshold model is applied we find a storage capacity of 1.5 mm, which is comparable with the results from Putuhena and Cordery (1996). They found for an eucalypt floor a storage capacity of 1.7 mm. Compared to the studies of Helvey (1964) and Pathak et al. (1985) our results are much higher. Helvey (1964) measured with drainage experiments interception rates of 3% of the annual precipitation and Pathak et al. (1985) found that 11-12% of the rainfall was intercepted by the litter. However, both studies did not take evaporation during the rainfall event into account and both studies were lab experiments, which often result in disturbed samples. Additionally, Helvey (1964) only examined events which were large enough to saturate the litter and Pathak et al. (1985) did his experiments during the monsoon season, what resulted in a low ratio between intercepted water and precipitation.

The results for Westerbork are presented in Fig. 5. In the period September 2005 until mid-November 2005 85% of the rainfall has been intercepted by the moss and grass and successively evaporated or transpired. If assumed that the overall downwards slope of the upper basin (Fig. 5A) is caused by transpiration, it can be calculated that circa 42 mm in two months are transpired. This assumption can be justified by the fact that interception is a process on an hourly to daily time scale, while transpiration is a monthly time scale process. If the measurements are corrected for transpiration 52% of the (net) precipitation (Fig. 5B) is intercepted by the moss and grass. In literature similar results are found. In Thurow et al. (1987) it is stated that Clark (1940) found for big bluestem interception estimates between 57-84% and for buffalo grass estimates between 17-74% of the simulated rainfall. Haynes (1940) estimated evaporation from interception by Kentucky bluegrass to be 56% of the annual precipitation. Lower estimates are found by Beard (1956) and Kittredge (1948). They found interception estimates of respectively 13% of annual rainfall for grassland in South Africa and 26% of annual rainfall for California grassland.

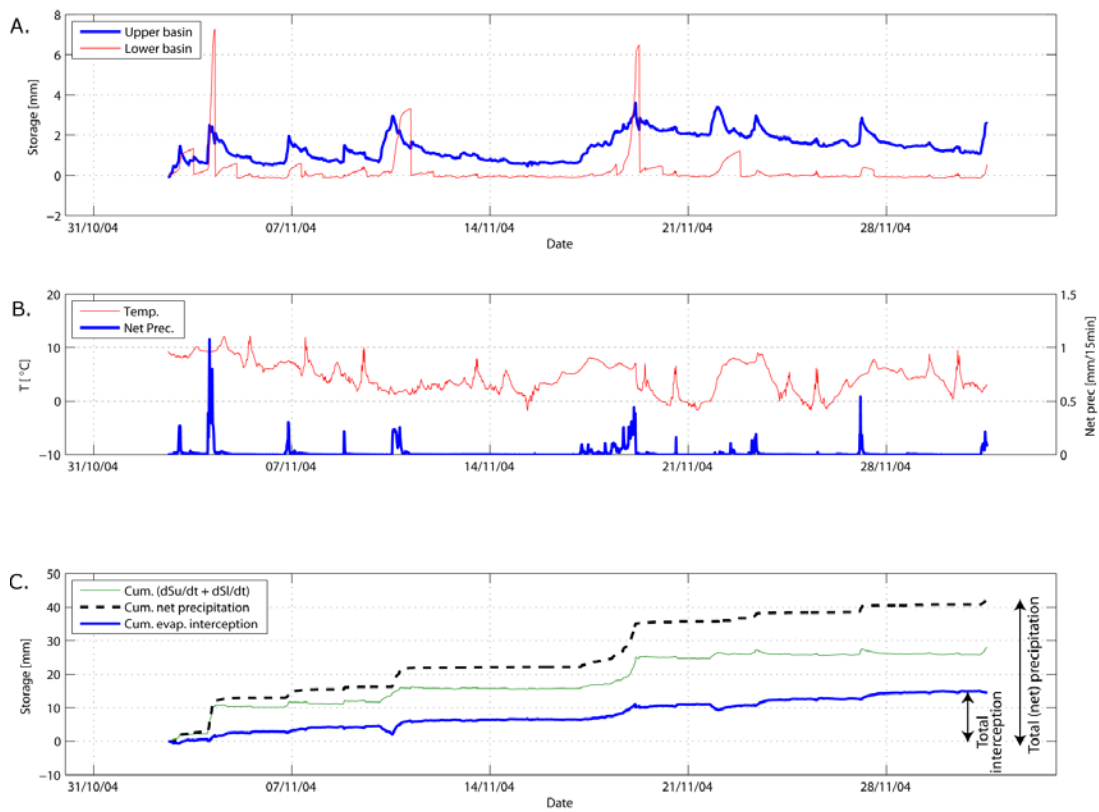


Fig. 4: Measuring results of the Huewelerbach for November 2004.

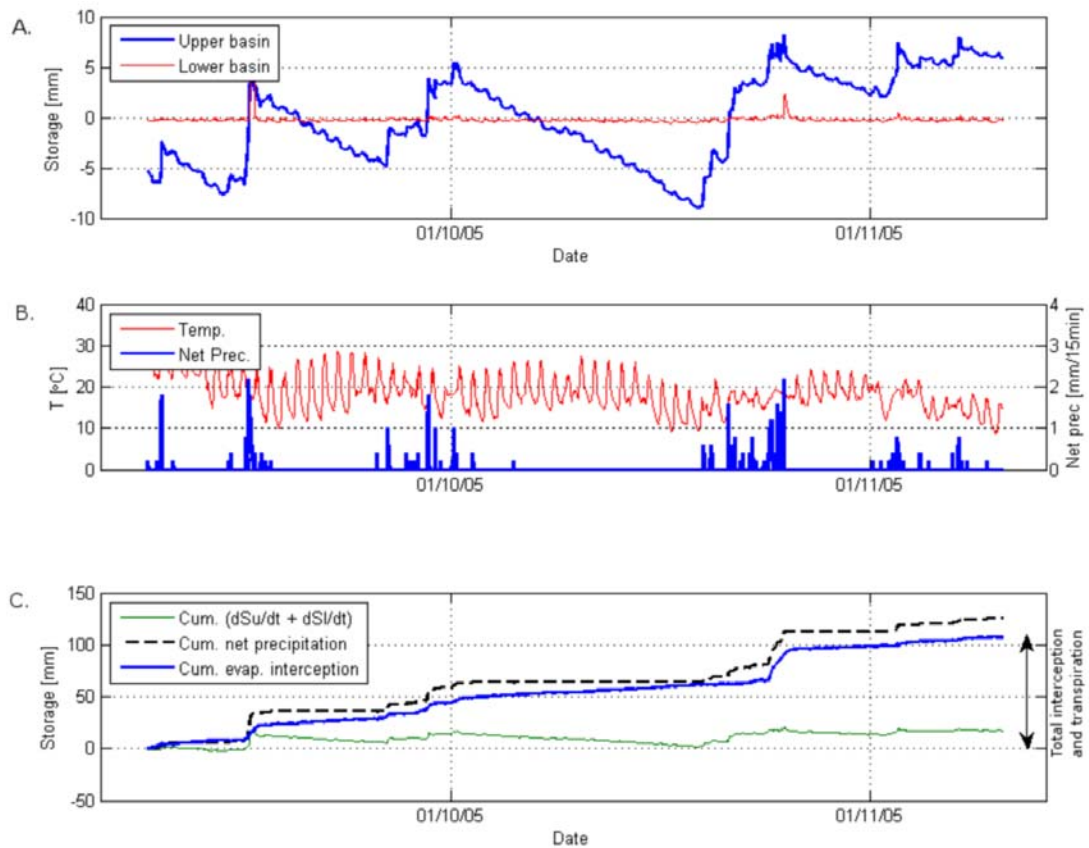


Fig. 5: Measuring results for Westerbork for September until mid-November 2005.

Although the device is generally working fine, there are some improvements possible. As can be seen clearly in Fig. 5A, B the observations are influenced by temperature. Especially, in summer when the variation in temperature during day and night is large, the strain gauges react strongly. Correcting the measured data for temperature, by using the measuring data during a dry period, is not yet fully satisfactory. Therefore a new - less temperature sensitive - sensor configuration is developed and an extra strain gauge is now installed as a dummy. On this strain gauge a known weight is mounted, so the relation between temperature variation and observed weight is known. Subsequently, the measured data can be corrected for temperature influences.

Conclusions

The preliminary results of the forest floor interception meter are very promising. Especially with the installation of a dummy and the new sensor configuration most temperature problems will be solved in the future. The first results also show that forest floor interception is a significant process. In the Huewelerbach catchment 35% of the throughfall was intercepted in November 2004. In Westerbork this amount was 85% of the rainfall for September, mid-November 2005. If compensated for transpiration circa 52% of the rainfall was evaporated from interception. Hence forest floor interception is important and should therefore be well understood to obtain better calibrated hydrological models.

Acknowledgements

The authors would like to thank the Ministry of Culture, Higher Education and Research of Luxembourg and Delft Cluster, the Netherlands, for their support for this research.

References

- Beard J.S. (1956). Results of the mountain home rainfall interception and infiltration project on black wattle. 1953-1954. *Journal of South African Forestry*, 27: 72–85.
- Clark O.R. (1940). Interception of rainfall by prairie grasses, weeds and certain crop plants. *Ecological Monographs*, 10: 243–277.
- Haynes J.L. (1940). Ground rainfall under vegetation canopy of crops. *Journal of the American Society of Agronomy*, 32: 176–184.
- Helvey J.D. (1964). Rainfall interception by hardwood forest litter in the southern Appalachians. *U.S. Forest Service Research Paper*, SE 8: 1–8.
- Kittredge, J. (1948). *Forest Influences*. McGraw-Hill Book Co, New York.
- Klaassen W., Bosveld F., deWater E. (1998). Water storage and evaporation as constituents of rainfall interception. *Journal of Hydrology*, 212-213: 36–50.
- Llorens P., Gallart F. (2000). A simplified method for forest water storage capacity measurement. *Journal of Hydrology*, 240: 131–144.
- Lundberg A., Eriksson M., Halldin S., Kellner E., Seibert J. (1997). New approach to the measurement of interception evaporation. *Journal of Atmospheric and Oceanic Technology*, 14: 1023–1035.
- Pathak P.C., Pandey A.N., Singh, J.S. (1985). Apportionment of rainfall in central Himalayan forests (India). *Journal of Hydrology*, 76: 319–332.
- Putuhena W., Cordery I. (1996). Estimation of interception capacity of the forest floor. *Journal of Hydrology*, 180: 283–299.
- Savenije H.H.G. (2004). The importance of interception and why we should delete the term evapotranspiration from our vocabulary. *Hydrological Processes*, 18: 1507–1511.
- Thurrow T.L., Blackburn W.H., Warren S.D., Taylor jr C.A. (1987). Rainfall interception by midgrass, shortgrass, and live oak mottes. *Journal of Range Management*, 40: 455–460.

BED LOAD SAMPLERS FOR PRACTICAL USE

G. Gergov & T. Karagiozova

*National Institute of Meteorology and Hydrology, Sofia, Bulgaria.
Corresponding author: T. Karagiozova*

ABSTRACT

Bulgarian water law requires total sediment load measurements in river reaches, where sand and gravel abstractions are made on a regular basis. The correct measurement of sediment fluxes is a prerequisite for a better management, ecological sustainability and mathematical modelling of their formation and movement.

The paper presents new equipments for bed sediment samplings, which were experienced on several Bulgarian rivers throughout the year 2005. The results turned out to be positive and adapted for even larger applications.

The authors have developed a device, which consists of two mashed bags, embedded one into the other. They are fixed on a flexible frame and thus they may assure a full toned contact with the bottom without any disturbance on it. Due to this, the meshes catch the moving particles and keep them inside.

Keywords: riverbed sediments

Introduction

Bulgarian water law requires total sediment load measurements in river reaches, where sand and gravel abstractions are regularly taking place. Correct measurements of sediment fluxes are thus a prerequisite for:

- their better sustainable management and use,
- their ecological sustainability and control,
- the application of the data in sediment load modeling.

The river sediment load consists of suspended and bed grain material, moving downstream. The interest of engineers and ecologists in them is increasing because:

- of their wide-spread use in building industry,
- they form a biotope for aquatic organisms,
- they participate in the fluvial processes by the formation of deep and plan forms, thus changing the geomorphological features of the rivers,
- they might be used in the assessment of soil erosion processes within the limits of a river basin.

Bed sediments are an important part of sediment load of rivers and they have a very particular form of existence and movement as a primary component. Because of this, they have been the subject of long term studies since the 1930's and especially since the 1970's. Today, scientists are convinced about their role in:

- the silting up of water reservoirs and lakes,
- the development of the building industry, once they are extracted from the riverbeds and transformed into a commercial good,
- the degradation of riverbeds downstream and around hydro-engineering facilities,
- the building of riverbed habitats for the water fauna,
- it is the media for long distance transfer and accumulation of contaminants of water, microorganisms and food cells,
- the investigation of the processes of decomposition of the primary geological structures under the influence of exogenic or endogenic factors.

The arguments stated here above illustrate that the increasing interest towards bed sediments is already a requirement for daily work on the rivers, as stated in the Bulgarian water law. Riverbed sediment studies might also become a requirement in a new Framework Directive of the European Union. Unfortunately, until now neither the scientific knowledge is sufficient, nor do long data series exist for a good start in modelling and management of bed sediment loads. One of the basic problems in that concern is the proper equipment for easy and reliable measurements on the rivers, since the techniques applied in laboratories are not suited for measurements in rivers. It is partially for that reason that numerous formulas for practical calculations have been worked out and that numerous comparisons and assessments on the reliability of the obtained results have been done, without ever achieving a strong correlation with the estimated outputs. Such a study was conducted by Znamenska (1976) and whose results are presented in Fig. 1. The complete inconsistency of the different formulas as compared with the field measurements is clearly evident.

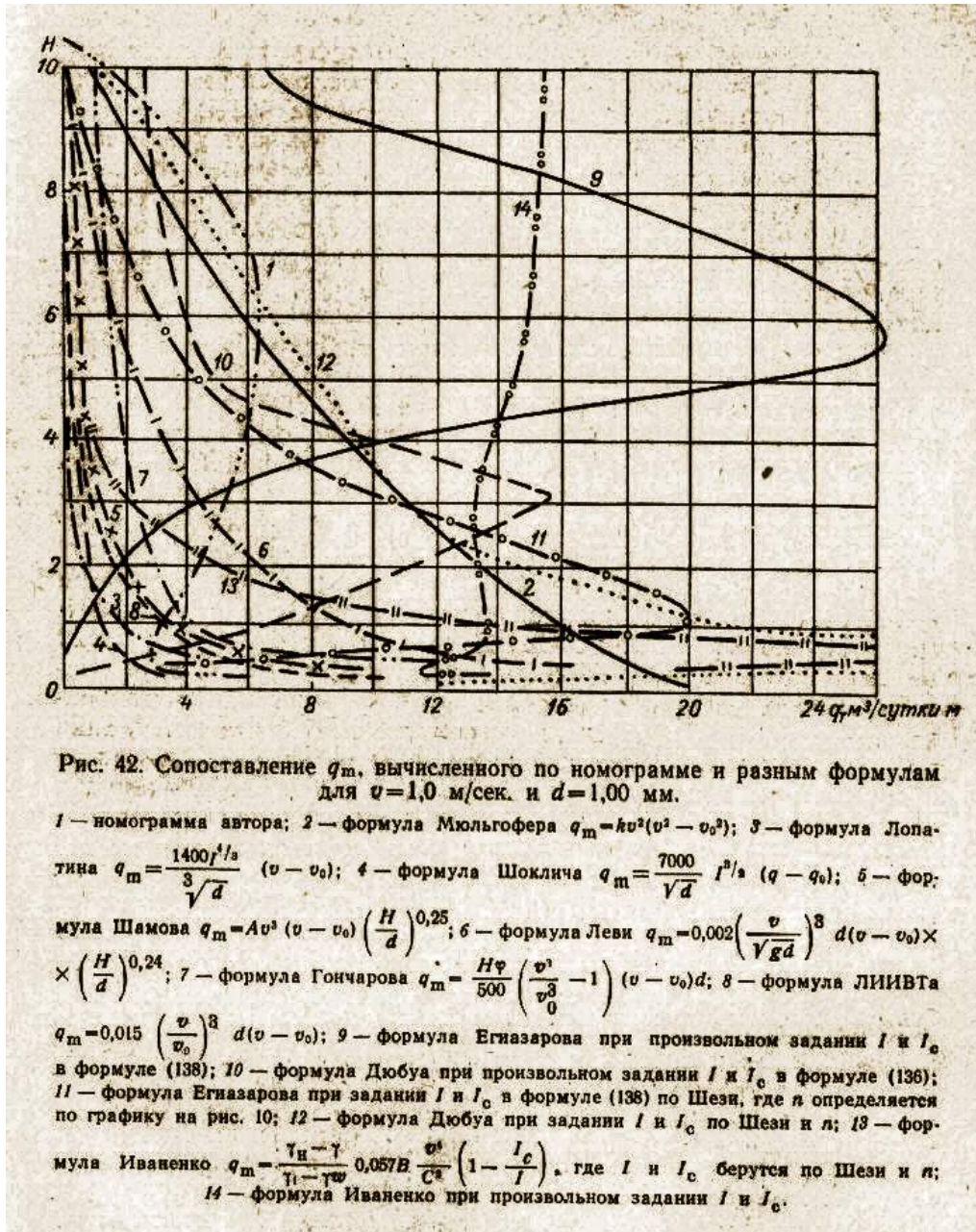


Fig. 1: Comparative analysis of riverbed sediment load, calculated by different formulas (Znamenska, 1976).

Bed load measurement devices

The majority of the existing instruments, such as “Don”, “Polyakov”, “Goncharov” in Russia (Fig. 2), ‘Holle’ in the USA and many others being in use in Hungary, Spain, Italy, Great Britain or Serbia, are not well suited for either semi-mountainous or large plain rivers.

Attempts to measure the bed sediment loads have been conducted in Bulgaria for many years as well. In the search for a solution to these difficulties, several types of sediment samplers have already been tested in variable natural conditions across the country.

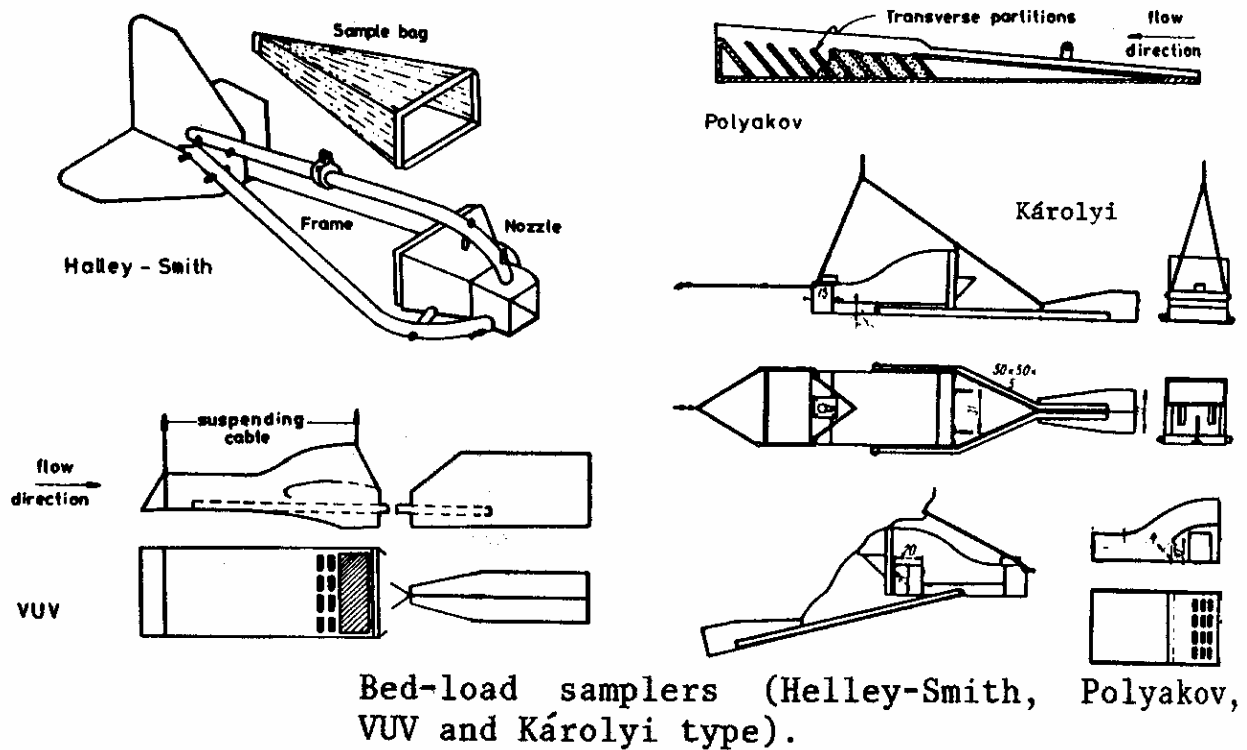


Fig. 2: Bed load samplers.

The Bulgarian case study

In the course of the past decades multiple attempts have been made to measure bed sediment load using Polyakov samplers as well as a US 48 sampler. Their large size and empty weight, as well as their great resistance to flow, proved their usefulness in practice. In sandy riverbeds, which are frequently encountered along the river stretches in plains and lowland areas, the heavy weight of the samplers leads to their sinking into the river bottom, while in semi-mountainous sections the instruments are not able to establish tight contacts with the river bottom because of the gravel particles and stones in the bed.

Papazov (1981) conducted independent attempts to measure riverbed sediments at the river bottom (Fig. 3). He assessed the sediment load from the deposited sediments in the box. The attempts to transfer this methodology to several other larger rivers gradually revealed its inapplicability.

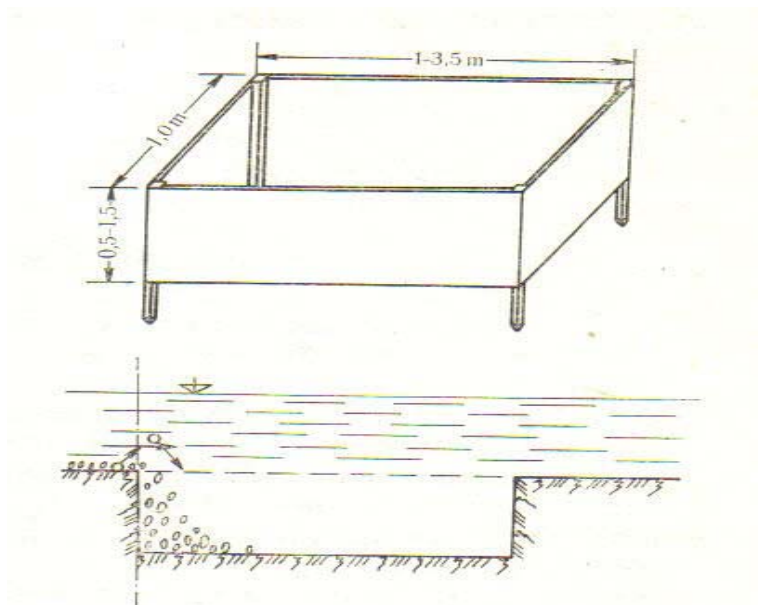


Fig. 3: Box to measure riverbed sediment load (Papazov, 1981).

Much better results on the total bed sediment load have been achieved in an experimental basin near the locality of Yundola in the Rhodopes Mountains, run by the University of Forestry in Sofia (e.g. Fig. 4) (Gergov and Rafailova, 2004). It consisted of 10 field plots, each equipped with a large accumulation tank at the outlet of the experimental basin. A huge amount of information has been collected, which allowed the determination of empirical relationships between the sediment load, the precipitation and the discharge rates of the rivers (Rafailova, 2005).



Fig. 4: Accumulation tank for bed sediments at the Yundola experimental site in Bulgaria.

Another set of experimental gauge stations for measuring the products of soil erosion and the resulting sediment load has been set up by the Forest Research Institute at the Igralishte Locality in the Ossogovo Mountains (Mandev, 1995; Marinov, 1984).

Attempts to accurately track the pathways of bottom sediments by coloring stones and gravel, during low water periods, produced no conclusive results. This is due to the fact that the traced particles were dispersed over a very long distance during a flood.

New experiments

The next attempt to invent a suitable and reasonable method for bed sediment load measurements was done in 2003 on a spillway at the Orizare instream mining site. The measuring device is a heavy iron frame, which carries a synthetic mesh with 1 mm holes (Fig. 5). The presumption is that the mesh might be taken away from time to time to weigh the total amount of sand and gravel, collected during the time elapsed between two successive measurements.

The experiments showed that it is not possible to conduct current control on the filling of the sampler. The design of the equipment makes it heavy, difficult and risky for daily use.

The latest measurement method of the bottom-level sediment load that was tested, consisted in a sampler–separator of mobile sediment particles, as illustrated in Fig. 6.



Fig. 5: Steel frame and nylon mesh to catch bed sediment load on the crest of the spillway at the Orizare open stage pit for abstraction of sand and gravel in Bulgaria.



Fig. 6: A sampler–separator of mobile sediment particles.

It consists of a rigid H-shaped frame with a big opening (40-50 cm), made of welded concrete iron. One, two or more sacks of nylon gauze with successively diminishing size of the opening might be suspended in the lower

part of the “H”. The instrument is knocked down on the riverbed until the lower end of the flexible frame hits the bottom and fits tightly on it. In the case that the water is deep or that the measurement is performed from a bridge, extensions might be used of appropriate length, which should permit performing of the operation in proper safety conditions for the operator. Tests, conducted on rivers near Sofia have shown that 10-15 minutes are sufficient for the collection of sediment load samples of different fractions, which were then separated in consecutive sampler sacks.

Conclusion

The positive results obtained so far from the conducted measurements, the analysis of the procedures and the comments of the experts who have used the instrument, have confirmed its high suitability for collecting reliable data for the modeling of the processes of formation and movement of riverbed sediments.

References

- Gergov G., Rafailova E. (2004). Hydrological investigations of experimental watershed basins. In: Hermann, Schröder (Eds.) Studies in mountain hydrology. Koblenz: 73-91.
- Marinov I.C. (1984). Soil erosion and its control in the catchment area of the Melnishka river. Ph-D thesis (in Bulgarian).
- Mandev A. (1995). Relationships in the changes of the intensity of the surface soil erosion at different methods of land use in mountain areas. In: Proceedings of the national conference ‘90 years of erosion control on the soils in Bulgaria’, Sofia: 37-42 (in Bulgarian).
- Papazov R. (1981). Sediment transport of open channel flows. In: Bulgarian Academy of Sciences, Sofia, 174 pp. (in Bulgarian).
- Rafailova E. (2005). Impact of forestry activities on hydrological processes. In: Proceedings of the workshop on ‘Forest Impact on Hydrological Processes and Soil Erosion’, Yundola: 83-89. (in Russian).
- Znamenska N. (1976). Bed load and river-bed processes. In: Gidrometeoizdat, Leningrad, 190 p. (in Russian).

MEASUREMENT OF SOIL AND TREE WATER CONTENT IN TWO MEDITERRANEAN FORESTED CATCHMENTS USING TIME DOMAIN REFLECTOMETRY

V. Hernández-Santana, J. Martínez-Fernández, C. Morán & A. Cano-Crespo

*Department of Geography, University of Salamanca, Cervantes, 3, E-37002 Salamanca, Spain.
Corresponding author : V. Hernández-Santana, email : virhs@usal.es*

ABSTRACT

In the present work, the water relationships between trees and soils are studied. Two tree species and soil moisture are monitored using the TDR technology. The tree species, *Quercus pyrenaica* and *Quercus rotundifolia*, are studied in two experimental forested catchments, Rinconada E.C. and Morille E.C., in Spain. The TDR technology is widely used to determine soil moisture but is not so common to calculate stem water content. The results of monitoring both variables are presented, concluding that TDR seems to be a valid technique to determine stem water content, and therefore to identify soil-tree water relationships. Comparing the soil moisture measured in the two forested catchments, it was also concluded that both, the Mediterranean conditions and the land use, had a greater effect on the soil moisture evolution than the differences in rainfall efficiency in the two catchments.

Keywords: stem water content, soil moisture, *Quercus pyrenaica*, *Quercus rotundifolia*

Introduction

Soil and plants are connected by several hydrological processes that are related to other types of processes as well (geomorphological, climatic, ecological, etc.). Therefore, it is of great interest to study water relationships between soils and plants. There are several methodologies for studying soil and plant water relationships (transpiration, interception, infiltration). One option to assess some basic components of these relations is to track both plant and soil water status.

Over more than 25 years, TDR (Time Domain Reflectometry) has been used to measure soil water content. The same principle applied to measure soil moisture can be applied to estimate stem water content as the dielectric constant (K_a) of water is far higher than that of the woody matrix in plant stems. Therefore any change in the dielectric constant of the tissue predominantly reflects a change in its water content. However, it is thought that equations as the one proposed by Topp et al. (1980) and others for soils are not valid for woody tissues. Constantz and Murphy (1990) developed the first equation for trees. Since then a few authors have developed new equations for different species and have applied this technology to monitor temporal variations in the stem water contents of different species. In this work, we analyze the results of trees and soils water content measurements in two Mediterranean forested catchments. Both variables are determined at the same time with TDR methodology in two small experimental catchments (Rinconada E.C. and Morille E.C.) located in the SW part of the Duero Basin (Spain) (Fig. 1).

The aim of this work is to analyze simultaneously the evolution of soil and tree water content of a deciduous oak forest (DOF) of *Quercus pyrenaica* Willd., and of a perennial oak forest (POF) formed by *Quercus rotundifolia* Lam. Both field sites are representative of two different types of Mediterranean forest. Thus, we will be able to identify the periods of soil water deficit (measured by soil water content) and therefore, the periods when trees can suffer from water stress (estimated by stem water content).

Field sites and methodology

The Rinconada experimental catchment (DOF) covers an area of 62 ha and is located 70 km south of the city of Salamanca (Fig. 1), forming part of the western sector of the *Sistema Central* mountain range. Its altitude ranges between 1140 and 1450 m and it rests on a varied geological substrate (sandstones, limestones and quartzites). Almost 70% of the surface of the catchment is occupied by melojo oak forest (*Q. pyrenaica*) and the area is used for extensive livestock-forestry activities. The climate is sub-humid Mediterranean. Mean annual temperature is 10 °C. Mean annual rainfall ranges around 1000 mm, showing considerable interannual variability, with a coefficient of variation (CV) of 26%. November is the wettest month, with 129 mm, and August is the driest, with 15 mm. Annual mean potential evapotranspiration (PET) is about 850 mm (Martínez-Fernández et al., 2004). To monitor soil moisture, we used a TDR stations network. Thus, 12 TDR stations of the 18 distributed along the catchment were used in this work. Each of them was located in the forest, measuring the soil water content from 0 to 100 cm with 5 (at 5, 15, 25, 50 and 100 cm depth) horizontally placed two-wire probes of 20 cm in length. We have also selected four plots representative of the different states of the forest to perform a specific monitoring of the water status of the soil and trees. On each plot, we selected four trees and installed 2 TDR probes in their trunks (at 20 and 120 cm above the ground) to monitor the stem water content. The two-wire probes inserted in the trunks were of 10-12 cm in length, depending on individual diameters. The two probes were inserted perpendicularly to each other and were similarly oriented in all samples. Two probes were placed under these trees to measure the soil moisture of the root zone down to a depth of 50 cm.

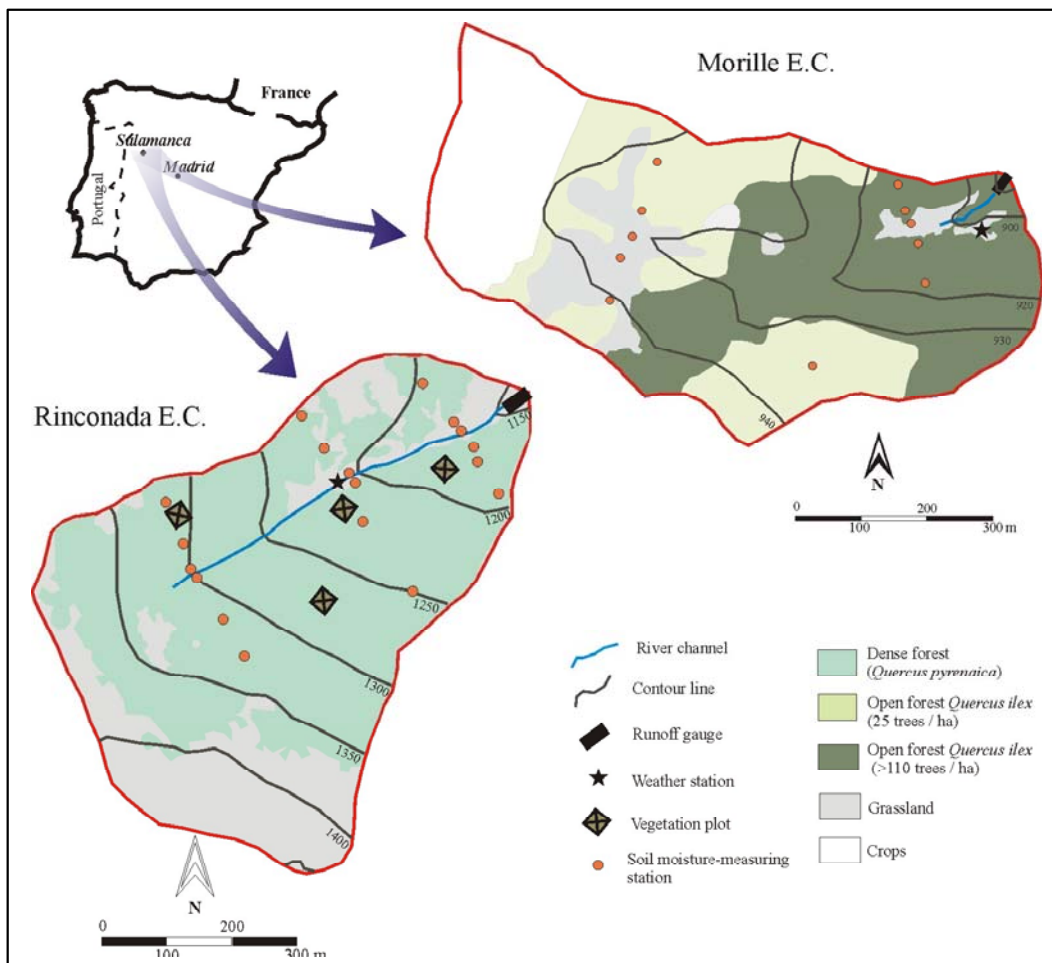


Fig. 1: Location map of the study areas: Morille (POF) and Rinconada (DOF) experimental catchments.

The second forested catchment, Morille E.C. (POF) (Fig. 1), is located 14 km south of the city of Salamanca (Spain). It has a surface of 35 ha and its altitude ranges between 945 and 900 m. The main substrate is quartzite and slates. Seventy percent of the surface is occupied by an open forest (14% surface tree cover) called *dehesa* and formed by holm oak (*Q. rotundifolia*). The main use of the land is for livestock and forestry. The climate is continental dry Mediterranean. Mean annual temperature is 11°C. Annual mean rainfall is about 500 mm, with a CV of 21%, the annual maximum being recorded in December, with 60 mm, and the minimum in July, with 13 mm. Mean annual PET is about 1040 mm (Martínez-Fernández et al., 2004). Soil moisture is measured by using 4 TDR soil moisture stations. Each one is located near the trees and measures soil moisture to a depth of 100 cm, as it was previously described in Rinconada E.C.. To measure stem water content in this catchment, 6 representative trees were selected. Two 10 cm-probes were installed at 20 and 120 cm in the trunk of these trees into predrilled holes.

Soil and stem water content have been measured at least two times per month with a Tektronix 1502C (Tektronix, Beaverton, OR). We estimated soil water content with the Topp et al. (1980) equation and stem water content was derived with the calibration equations specifically developed for these species (Hernández-Santana, 2005), which were obtained as follows. A melojo oak was felled down and six samples were cut from the tree (Fig. 2). Four of them were used for the calibration phase, and two to validate the accuracy of the calibration function (validation phase). All the bark was removed and a two-rod stainless steel probe 12 cm long was inserted into 2 parallel pre-drilled holes. The wood blocks were placed on a laboratory bench for saturation for nearly one week. Then, they were air-dried in the laboratory. Periodically, the samples were weighted on a balance and the apparent dielectric constant was measured with TDR. To eliminate all the water from the wood tissues, the samples were oven-dried at 85 °C for four days. With these data and those obtained by measuring K_a , a calibration function was obtained. The accuracy of this equation was verified with two extra samples not used in the calibration phase. The repeatability of the procedure and the measurements were tested with another individual tree after the calibration experiment. Another calibration function for holm oak was calculated with the same methodology described previously.

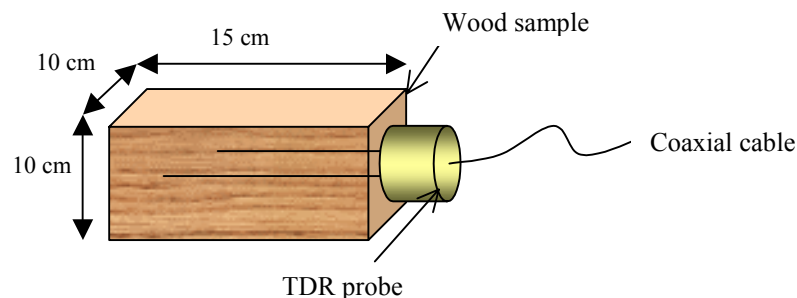


Fig. 2: Schematic drawing of the blocks and TDR probes used in the calibration and validation processes.

Results and discussion

The results obtained during the calibration processes for the melojo and holm oak revealed strong positive relationships between water contents measured gravimetrically and the K_a determined with TDR. The validation processes also revealed satisfactory results, with a very low mean error and no significant bias detected. Two different third-order polynomial regression equations were fitted to the pooled data (Fig. 3).

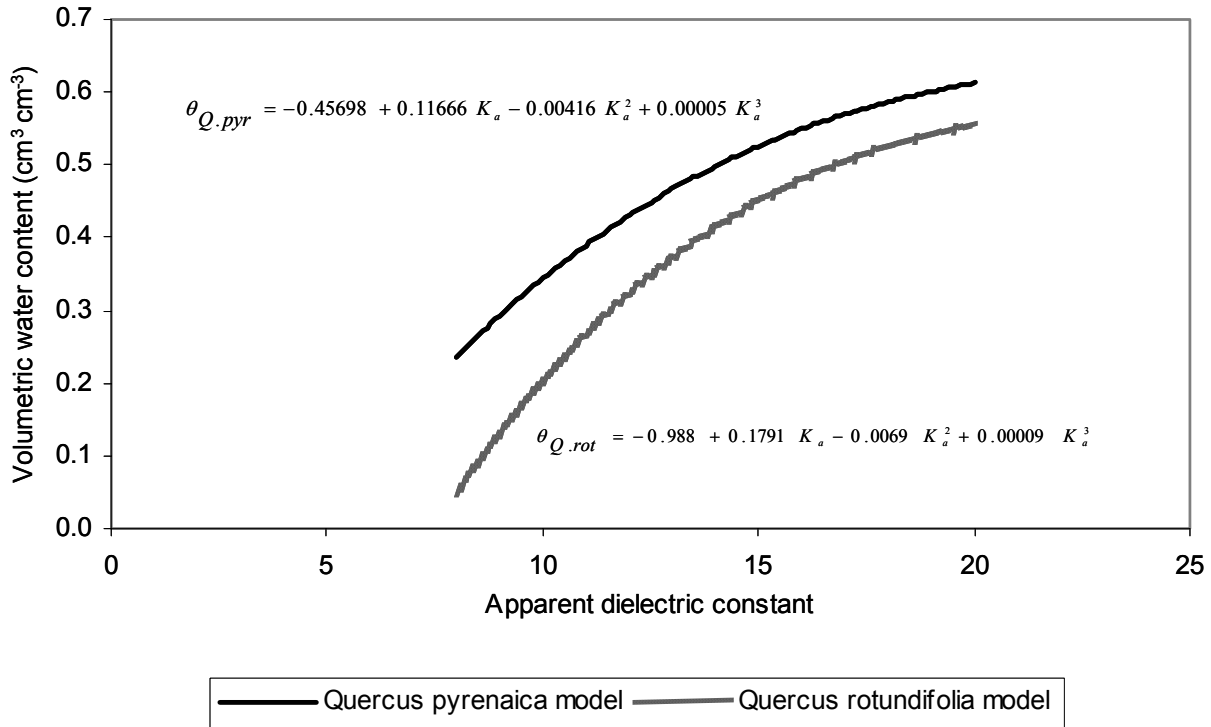


Fig. 3: Comparison between the equations calculated for *Quercus pyrenaica* and *Quercus rotundifolia* (θ is the volumetric water content and K_a refers to the apparent dielectric constant).

A strong parallelism between stem and soil water content evolution was found. As shown in Fig. 4a, the average stem water contents of 16 oaks of Rinconada E.C. reflect soil water contents for the measurements, except for the winter months, when the correlation between the two variables is not so clear. This weak relationship may be explained in terms of the strong effect of winter freezing on TDR measurements (Constantz and Murphy, 1990; Sparks et al., 2001). Stem water measurements in living *Quercus pyrenaica* exhibited a maximum variation of 20%. A similar variation was found in other oak species (Wullschleger et al., 1996). The average stem water content for the 16 trees increased from March to May-June. The maximum value was reached in May, associated with new leaf growth and no soil moisture deficit. Then, the stem water volume decreases gradually throughout the summer in parallel with the soil moisture content. The reduction in stem water suggests a net movement of the water out of the stem storage pool, presumably to offset some portion of the seasonal water requirements of a transpiring plant canopy (Wullschleger et al., 1996), because it is in the summer months that this species develops its activity, coinciding with less soil moisture, high temperatures and a high transpiration rate. Accordingly, transpiration is not covered only by water uptake from the soil but also by the water stored in plant tissues (Waring and Running, 1978). The minimum value was reached at the beginning of October, i.e. at the end of the dry and hot season. Once the soil had been rewatered through autumn precipitation, the stem was partially recharged. Fewer measurements were taken for the holm oak (May-December 2005) than for the melojo oak, but a parallelism between the stem water content of the measured trees and the soil moisture can be observed as well (Fig. 4b). As can be seen from the results, the stem water contents detected by TDR depend on both species and environmental conditions. The parameters obtained may be species-specific and the differences found in the stem water contents in the two stands can be partially explained by differences in wood structure (Wullschleger et al., 1996) (*Q. pyrenaica* is a ring-porous species whereas *Q. rotundifolia* is a diffuse/semiring-porous one). The species differ also in leaf longevity and habit. The melojo oak tends to have a nonconservative pattern of water use whereas *Q. rotundifolia* species shows a more conservative water use.

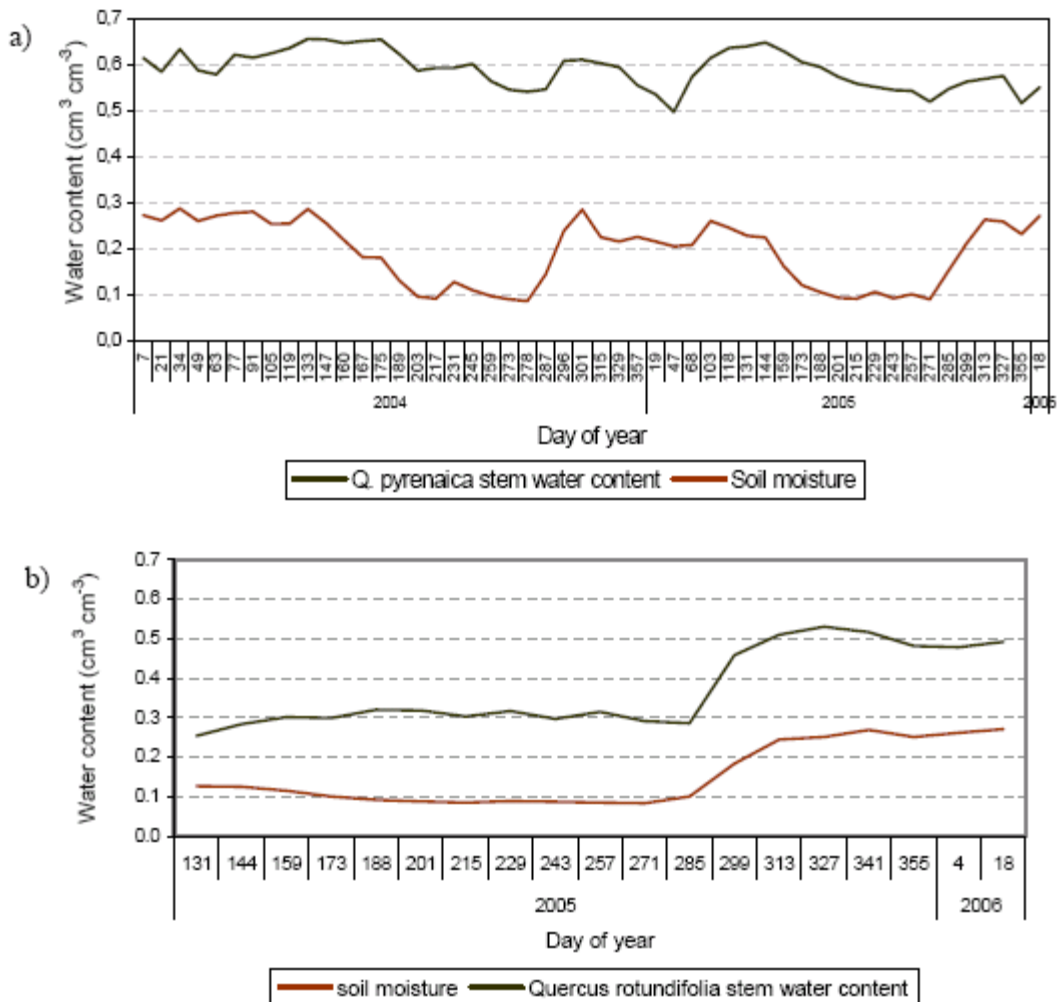


Fig. 4: Mean stem and soil water content variation of the two forest types: deciduous oak forest (a) and perennial oak forest (b).

Over a study period of more than 6 years in DOF (the soil moisture has been measured since 1999 whereas stem water content has been estimated since 2003), the soil was observed to suffer from a water deficit over 4 or 5 consecutive months, coinciding with the vegetative cycle of the forest. Over at least one or two months the water deficit was very strong. In POF the soil moisture stations network has been operating since July 2001, but stem water content measurements started in May 2005. As it happens in DOF, the soil was in a situation of deficit for 4 months (June-September). However, the level of the deficit was different in the two catchments (Fig. 5), with a less pronounced soil water deficit level in POF, than in DOF, although the precipitation was much higher in the latter catchment. This means that in DOF, where rainfall is more abundant, the soil water deficit during the dry season, which coincides with the period of maximum biological activity, is more intense than in POF with less rainfall. This can be not explained by the soil properties, as in DOF the soil water retention capacity is higher than in POF because the finer texture (average clay plus silt, 70.4%) and organic matter content are much higher (mean 3.34%) in DOF than in POF (45.7 and 1.85%, respectively). As during the dry season, the climatic characteristics of the two catchments are fairly similar in many aspects (Ceballos et al., 2004), this apparently contradictory behaviour is a result of the different kinds of forest and also of the different water use patterns of each species (Valladares et al., 2004). The dense forest of melojo oak at DOF extracts all the water from the soil in the period of maximum evapotranspiration, while in the open forest formed by holm oak, water extraction is much more limited. The much less sandy texture in DOF, (where soil water is retained with higher energy) does not prevent a higher tree consumption than in POF. The stem water content measurements in this last species are fewer than in the melojo oak, but a similar parallelism is also

observed between stem and soil water content. However, a different behaviour was found. Holm oak showed very low variation and much lower stem water content in summer months. When the soil was recharged in autumn, the water content of holm oak experienced a maximum increase (47%), much higher than in melojo oak (20%). Both species belong to genus *Quercus* but their response to drought, as it is observed with stem and soil water content measured with TDR, is different.

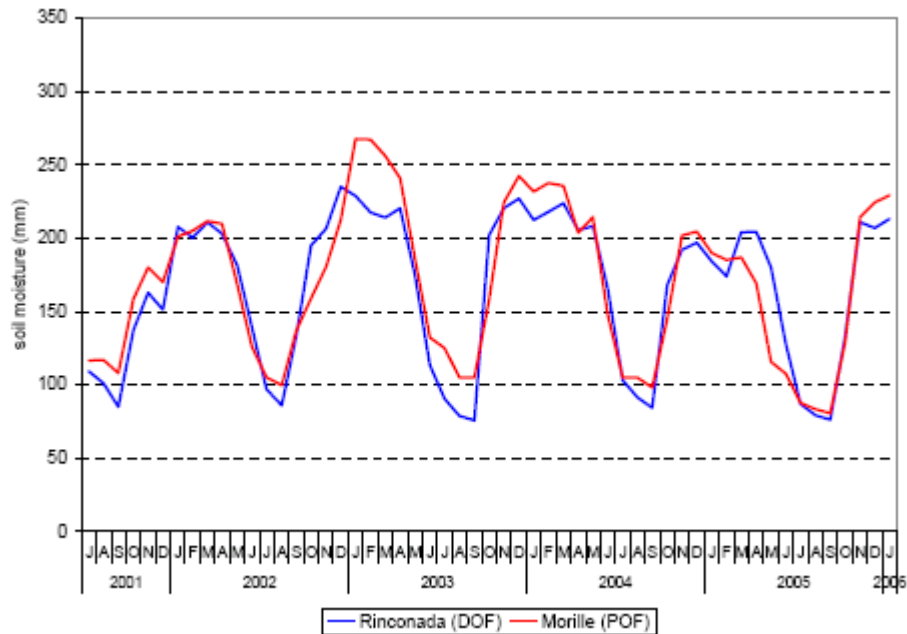


Fig. 5: Comparison of soil water content evolution of the two experimental catchments.

Conclusions

With these results stem water content measurements seem to be a valid technique to identify soil-tree water relationships. Moreover, the measurement of stem water content and soil moisture allows us to gain some knowledge of the water relationships established between trees and soils. A period of water deficit - of similar duration at the two sites - occurs and can be identified by analysing the soil water content. The summer drought means that the trees of both species are subject to water stress every year. Both, the Mediterranean conditions, essentially defined by the climate characteristics of the summer period, and the land use, have a greater effect than the differences in rainfall efficiency in the two catchments.

Acknowledgements

This study was fully supported by the Spanish Ministry of Science and Technology (REN2003-00381 Project) and the Spanish Ministry of Environment (RESEL Project).

References

Ceballos A., Martínez-Fernández J., Luengo-Ugidos M.A. (2004). Analysis of rainfall trends and dry periods on a pluviometric gradient representative of Mediterranean climate in the Duero Basin, Spain. *Journal of Arid Environment*, 58: 214-232.

- Constantz J., Murphy F. (1990). Monitoring storage moisture in tree using Time Domain Reflectometry. *Journal of Hydrology*, 119: 31-42.
- Hernández-Santana V. (2005). *Estimación del Contenido de Agua en Arboles Mediante TDR para el Estudio del Estrés Hídrico: Aplicación a Quercus pyrenaica Willd.* Tesina de Licenciatura. Universidad de Salamanca. 86 pp.
- Martínez-Fernández J., Ceballos A., Morán C., Hernández V., Casado S. (2004). Hydrological processes along a Mediterranean rainfall gradient. In: D. Tropeano, M. Arattano, F. Maraga, C. Pelissero (Eds.), *Progress in Surface and Subsurface Water Studies at the Plot and Small Basin Scale*. IRPI-CNR: 163-166.
- Sparks J.P., Campbell G.S., Black R.A. (2001). Water content, hydraulic conductivity, and ice formation in winter status of *Pinus contorta*: a TDR case study. *Oecologia*, 127: 468-475.
- Topp G.C., Davis J.L., Anan A.P. (1980). Electromagnetic determination of soil water content: measurements in coaxial transmission lines. *Water Resources Research*, 16: 574-582.
- Valladares F., Vilagrosa A., Peñuelas J., Ogaya R., Camarero J.J., Corcuera L., Sisó S., Gil-Pelegrín E. (2004). Estrés hídrico: ecofisiología y escalas de la sequía. In: F. Valladares (Ed), *Ecología del Bosque Mediterráneo en un Mundo Cambiante*. Ministerio de Medio Ambiente, EGRAF: 163-190.
- Waring R.H., Running S.W. (1978). Sapwood water storage: its contribution to transpiration and effect upon water conductance through the stems of old-growth Douglas-fir. *Plant, Cell and Environment*, 1: 131-140.
- Wullschleger S.D., Hanson P.J., Todd D.E. (1996). Measuring stem water content in four deciduous hardwood with a time domain reflectometry. *Tree Physiology*, 16: 809-815.

INVESTIGATIONS OF THE RUNOFF GENERATION PROCESS IN LANGE BRAMKE BASIN, HARZ MOUNTAINS, GERMANY USING ENVIRONMENTAL AND ARTIFICIAL TRACERS

A. Herrmann¹, S. Schumann¹, R. Thies¹, D. Duncker¹ & W. Stichler²

¹Institute of Geoecology, Department of Hydrology and Landscape Ecology, Technical University Braunschweig, Langer Kamp 19c, D-38106 Braunschweig, Germany. ²GSF-Institute of Groundwater Ecology, Ingolstädter Landstr. 1, D-85764 Neuherberg, Germany.
Corresponding author: A. Herrmann, email: a.herrmann@tu-bs.de

ABSTRACT

Selected results drawn from experiments with environmental isotopes and artificial tracers during the snow cover season 2005/06 from the Lange Bramke study basin in the Harz Mountains, Germany are presented. The aim of the experiments was to verify earlier findings and expand the hydraulic knowledge on flood runoff generation during snowmelt events on a small basin scale. It results that the fractured rock aquifer was confirmed to be by far the dominant supplier and control storage of the hydrograph generating water fluxes, whereas direct flow from event water is negligible. Therefore the water volume replacement in the aquifer must be considerably fast which is confirmed by a mean transit time of 2 years.

Keywords: environmental isotopes, flood runoff generation, Lange Bramke basin

Introduction

Runoff generation is an ecohydrological key process. Environmental tracer studies on a small basin scale as compiled by Herrmann (1997) have shown that during storm and snowmelt events groundwater is a dominant runoff component in many regions under different climatic conditions and land use. Lange Bramke is one of the experimental pilot basins in this respect.

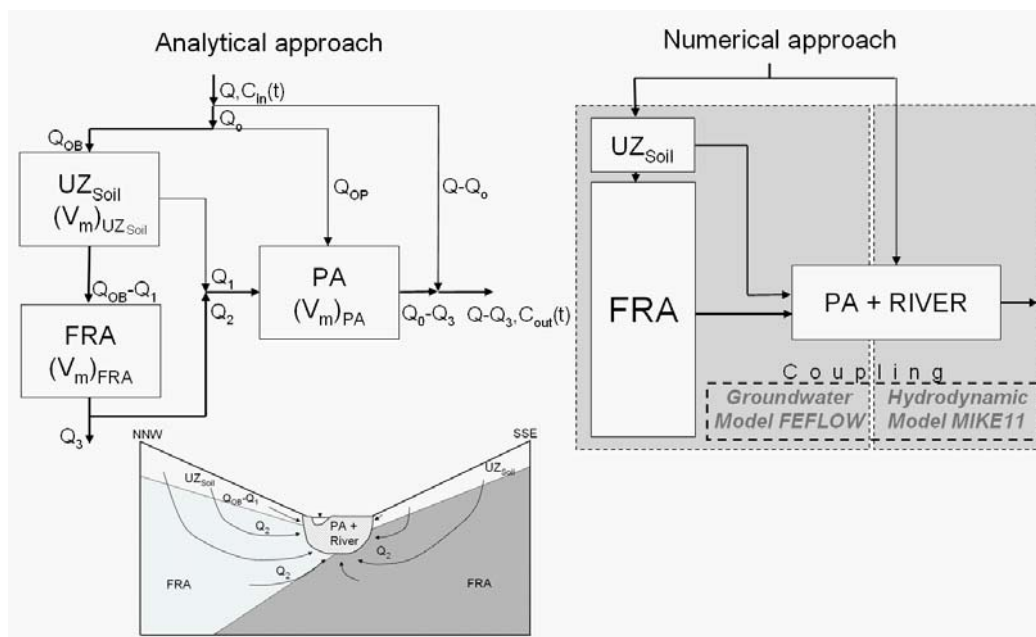


Fig. 1: The integrated runoff formation concept with analytical solution of relevant water fluxes and subsurface storages (left) and numerical approach with spatial discretisation (right).

Here a new tool for the study of runoff formation that considers the holistic Integrated Catchment Approach (ICA; Herrmann et al., 2001) was developed. ICA makes use of combined field experiments and numerical modelling as the focal methodical concept (Herrmann et al., 2006). The new tool shall allow for a suitable integrated management of drinking water reservoirs and for environmental protection in mountainous central European hard rock regions of Paleozoic age. It is an approach for process understanding, integration and modelling in the framework of research activities focusing on predictions of hydrological variables in ungauged basins (Franks et al., 2005).

The proposed tool system is presented in Fig. 1. It is based on the commercial software packages FEFLOW and MIKE11. In the conceptual hydraulic basin model that is numerically backed, the **unsaturated zone UZ** is treated as transitory zone and is described by a specific transfer function. The **saturated zone SZ** equals a **fissured rock aquifer (FRA)** which is portrayed with GIS-based FEFLOW. FRA serves hydraulically the **porous aquifer PA** of the valley filling with the main channel. To quantify and verify the simulated groundwater exfiltration volumes along the channel, FEFLOW will be coupled with the surface water software MIKE11 channel and wave propagation model in the near future by means of a special interface manager.

Lange Bramke study basin: Summary of former results and actual experiments

Experimental hydrological, tracer hydrological and hydraulic data were taken in the Lange Bramke research basin (0.76 km², 540-700 m a.m.s.l.), that is located in the Harz Mountains, Germany, and that is monitored since 1948. The basin is forested by 90% Norwegian spruce. In these areas surface runoff has never been observed. The wet valley floor, fire aisles situated perpendicular to slopes, and forestry roads represent open areas. The basin is provided with a fissured Lower Devonian rock aquifer of sandstones, quartzite, slates (FRA), and with a minor porous aquifer (PA) in the valley bottom.

Until recently the main findings were: Interflow is negligible, 90% of the discharge originate on average from groundwater. During flood events hydrographs are generated by event water by only up to 1/3 of total discharge and during peak flow only (Herrmann et al., 1989) with the groundwater-discharge relationships being significantly hysteretic (Herrmann, 2004). Special experiments with artificial tracers have shown that UZ and SZ are interconnected through preferential flow paths which indicate that SZ is just a transient storage with respect to runoff generation, and that major cross faults having conductivities in the order of $1 \cdot 10^{-4}$ m/s function as natural drain lines that favour quick and efficient groundwater exfiltration (Maloszewski et al., 1999). FEFLOW portrays latter situation quite well. In the less fissured and fractured parts of the basin however, groundwater flow and transfer are by several orders of magnitude less efficient (Herrmann et al., 2006).

From these results and the first FEFLOW modelling approaches it was concluded that additional experiments with artificial tracers in FRA are needed to improve model calibration (Herrmann et al., 2006). Furthermore, the use of environmental isotopes for hydrograph separation and discrimination of groundwater dynamics have to be considered in more detail. Hence a main goal of further studies needed to aim on a synchronous monitoring of all hydrological components that control the runoff generation process.

The topography and instrumentation for the hence set up experiments are shown in Fig. 2. Several 4" and 2" piezometers in FRA and 1" observations wells in PA are available. The deepest ones are HKLU (55 m) and HKLT (25 m), followed by HKLA, -D, -G, -K, -N, -Q and -W (each 15 m). Six piezometric multilevel triple-sets of 5 m, 10 m and 15 m depth were installed for hydraulic and artificial tracer experiments. Several 1" groundwater pipes in the shallow PA are up to 4 m deep. HKLQ, -U and -W have automatic pressure transducers for water table recording. The other groundwater tables are manually measured. HKLB, -L, -T, and HGLL are equipped with automatic water samplers, the other piezometers with electric pumps for manual sampling only. Discharge is automatically sampled at gauging station HALB. The measurement and sampling of snow cover outflows in the centre of the basin is done with two recording snow lysimeters of 1 m² surface area. One is situated in a 50 years old spruce stand and disposes of an automatic sampling device, the other,

with manual sampling, is situated in an adjacent open area. Profiles and samples of the snow covers are regularly realised aside the lysimeter areas.

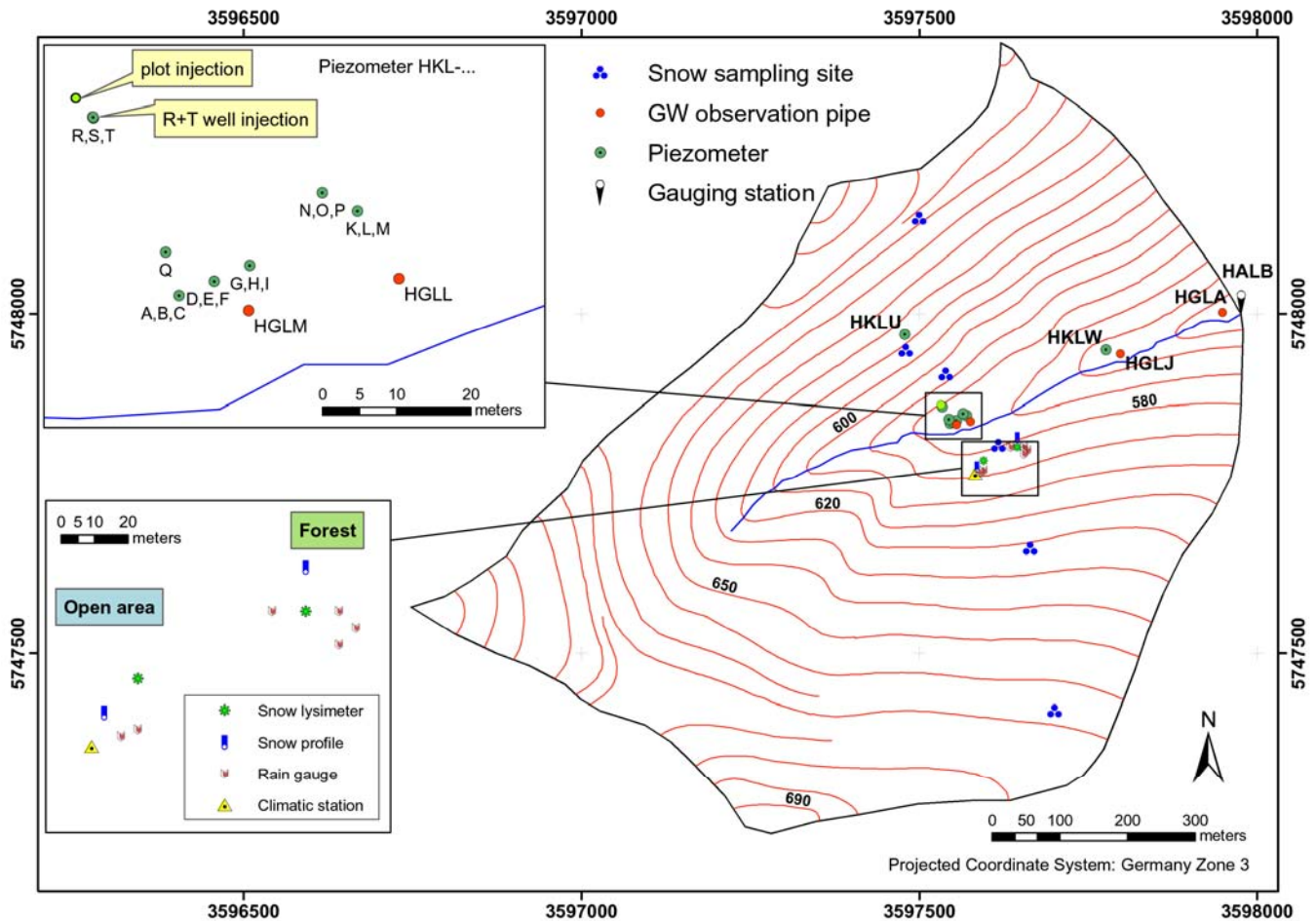


Fig. 2: Topography and instrumentation of the Lange Bramke research basin.

During the winter season 2005/06 water samples from all above mentioned sites were analysed for deuterium (H-2) and oxygen-18 (O-18). From the wells and gauging station also water was taken for tritium (H-3) analyses. On February 16, 2006 400 g of eosin and 2 kg of naphthionate were injected in 25 m depth into HKLR and in 11 m depth in HKLT respectively. Furthermore, at the onset of the final melting period, on March 27 a cocktail of 500 g of uranine and 500 g of potassium bromide (dissolved in 4 l of water) was applied to a surface area of 1.5 m² of the snow cover, situated at 3 m from the two wells. Respective sampling for the artificial tracers was done at all available wells and the gauging station. The groundwater injections were considered to inform about groundwater transport towards the main channel, and the dye application to the snow surface about meltwater percolation through the unsaturated zone to the aquifer.

Selected results

The combined effect of the snow melt event topped by rains on the melting snow cover caused end of March 2006 a distinct isotopic signal in the runoff of Lange Bramke river (Fig. 3). This allowed to separate event water (=direct flow) from (pre-event) groundwater (=indirect flow). It results that the flood hydrograph is dominantly generated by a groundwater contribution of more than 95% of total discharge. The hydrograph

separation results are hydraulically confirmed by the observation of spontaneous groundwater table rises of different magnitudes. In the fissured rock aquifer FRA HKLU rises up to 3 m (Fig. 4) starting off with the infiltration process. The physical process behind this hydraulic effect is supposed to be an initial pressure transmission in FRA. The increase in groundwater potentials is then immediately followed by mass (water) transfer into and through the complex system of fissure, fractures and faults, however during the ongoing event only into the upper portion of the fractured bedrock aquifer.

The steep rises in groundwater levels as portrayed in Fig. 4 are accompanied by decreasing 2-H ratios and in succession by deflecting artificial tracer concentrations in FRA (see Fig. 6 for selected piezometers). The naphtionate concentrations vary strongly (see Fig. 5 and 6) due to the rock fissure bound preferential transport from well to well that itself depends on the actual activation of rock fissures with changing water levels. The groundwater and discharge maxima are followed by exponentially falling limbs provided that hydrograph recession is not interrupted by new rain input impulse. In the observation pipes of the porous aquifer PA (cf. HGL in Fig. 1), i.e. HGLM in Fig. 5, little artificial tracer was traced.

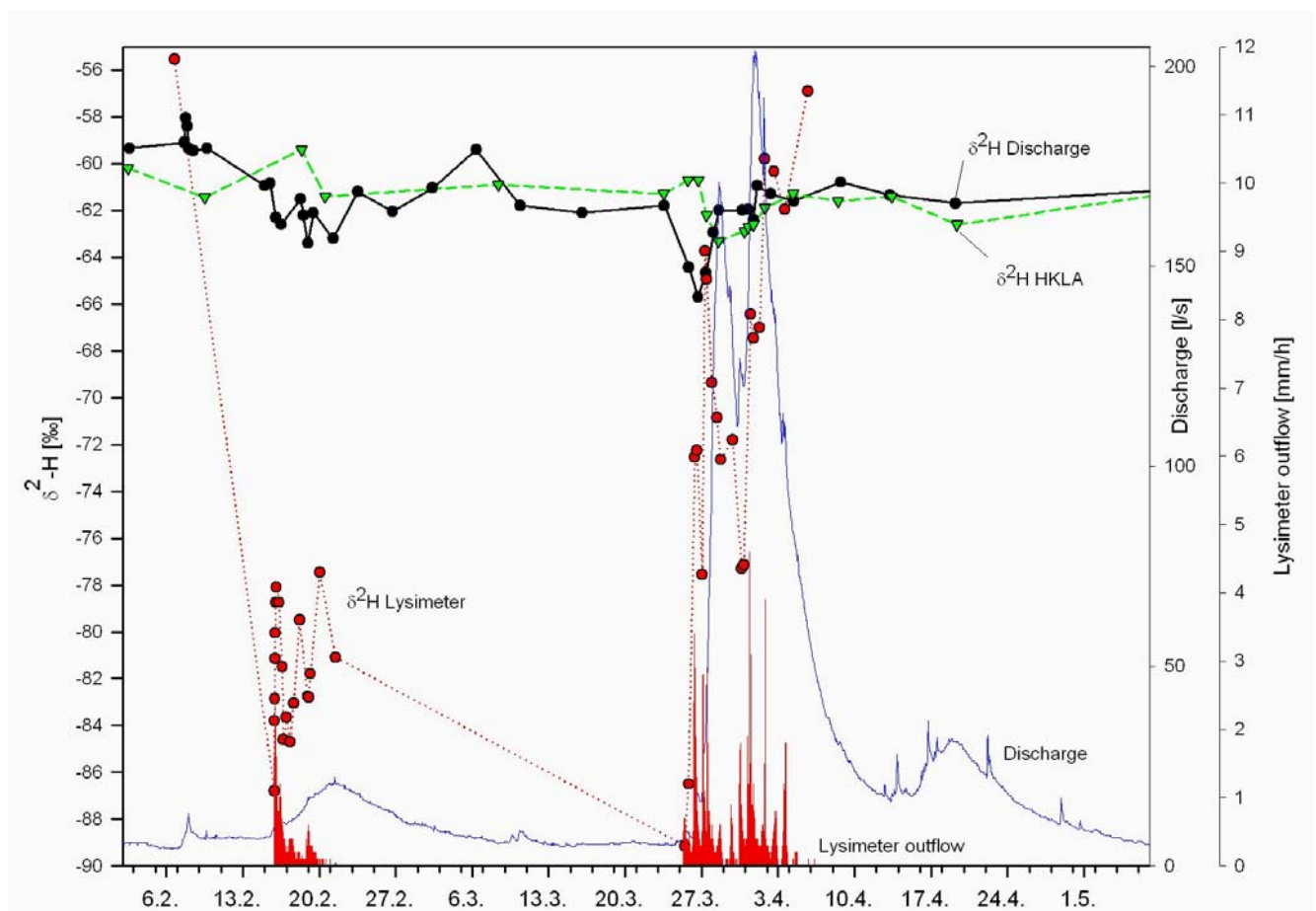


Fig. 3: Spring 2006 rain-on-melting snow cover. Hydrograph of Lange Bramke river and forest lysimeter outflows with deuterium contents of lysimeter outflows, discharge and groundwater at HKLA.

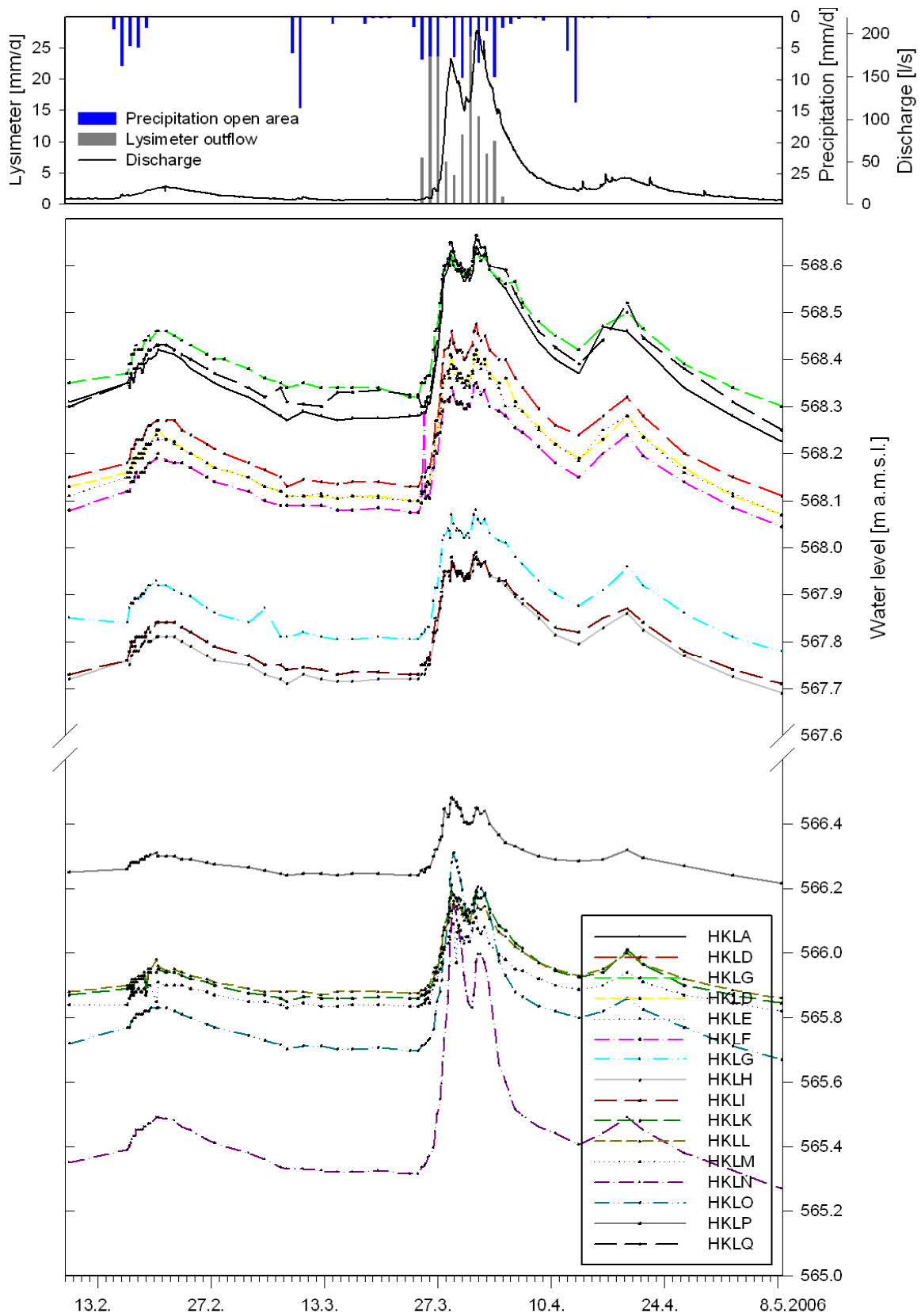


Fig. 4: Spring 2006 hydrograph of Lange Bramke river with daily open area rain amounts and forest snow lysimeter outflows (top) and reactions of selected piezometer levels on basin inputs.

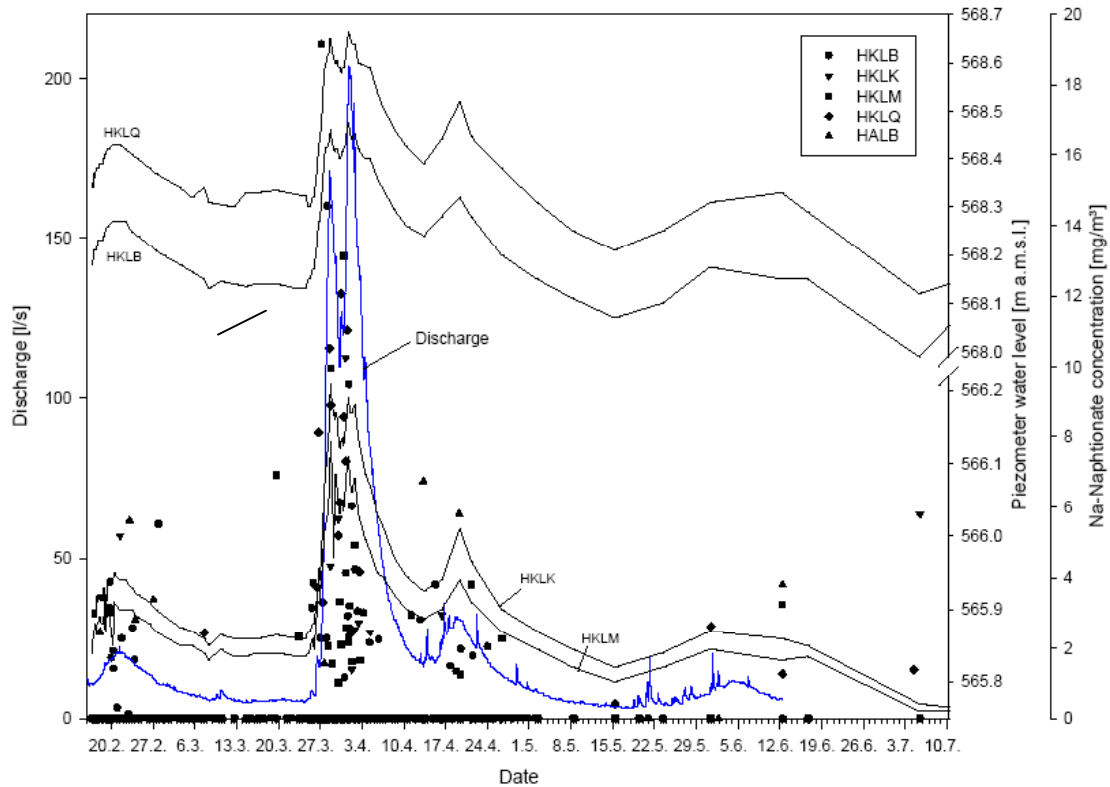


Fig. 5: Spring 2006 hydrograph of Lange Bramke river with selected piezometric levels and naphthionate concentrations of discharge and fissured rock groundwater.

Simultaneous concentration changes of natural isotopes and artificial dye tracers in the groundwater as a response on rain/meltwater basin input (cf. Fig. 4 top) are clear signals indicating a mobilisation of groundwater towards the Lange Bramke river. These observations are in-line with the rising pressure heads (as observed in the wells) that indicate an increasing hydraulic gradient towards the river channel.

The tritium contents of the fractured rock and porous groundwater of the valley filling vary in samples from June 2006 from 5 to 10 TU. The TU contents at mean low water of Lange Bramke discharge lie since 1980 at around 10 TU. This represents the mean groundwater flow. With the low discharge tritium contents measurements, the mean transit time of the tracer (t_i) through the groundwater system can be calculated with the Dispersive Model DM according to Maloszewski and Zuber (1982) that corresponds to the Ordinary Dispersive Model (ODM). The double porosity of the Bramke aquifer results in $t_i=2.9$ a (Thies, 2007). From the hydrological point of view the mean transit time of water is more interesting ($t_o= t_i/R$, with R as the retardation factor). With $R=1.45$ (cf. Herrmann et al., 1989) t_o equals to 2.0 a, which confirms the findings of Herrmann et al. (1989) who used in 1989 a much shorter tritium data series of 7 years. However, they inform more detailed about model assumptions and corresponding storage dimensions, porosities and water volumes of FRA.

A more detailed documentation and discussion of the tracer experimental results is found in Thies (2007).

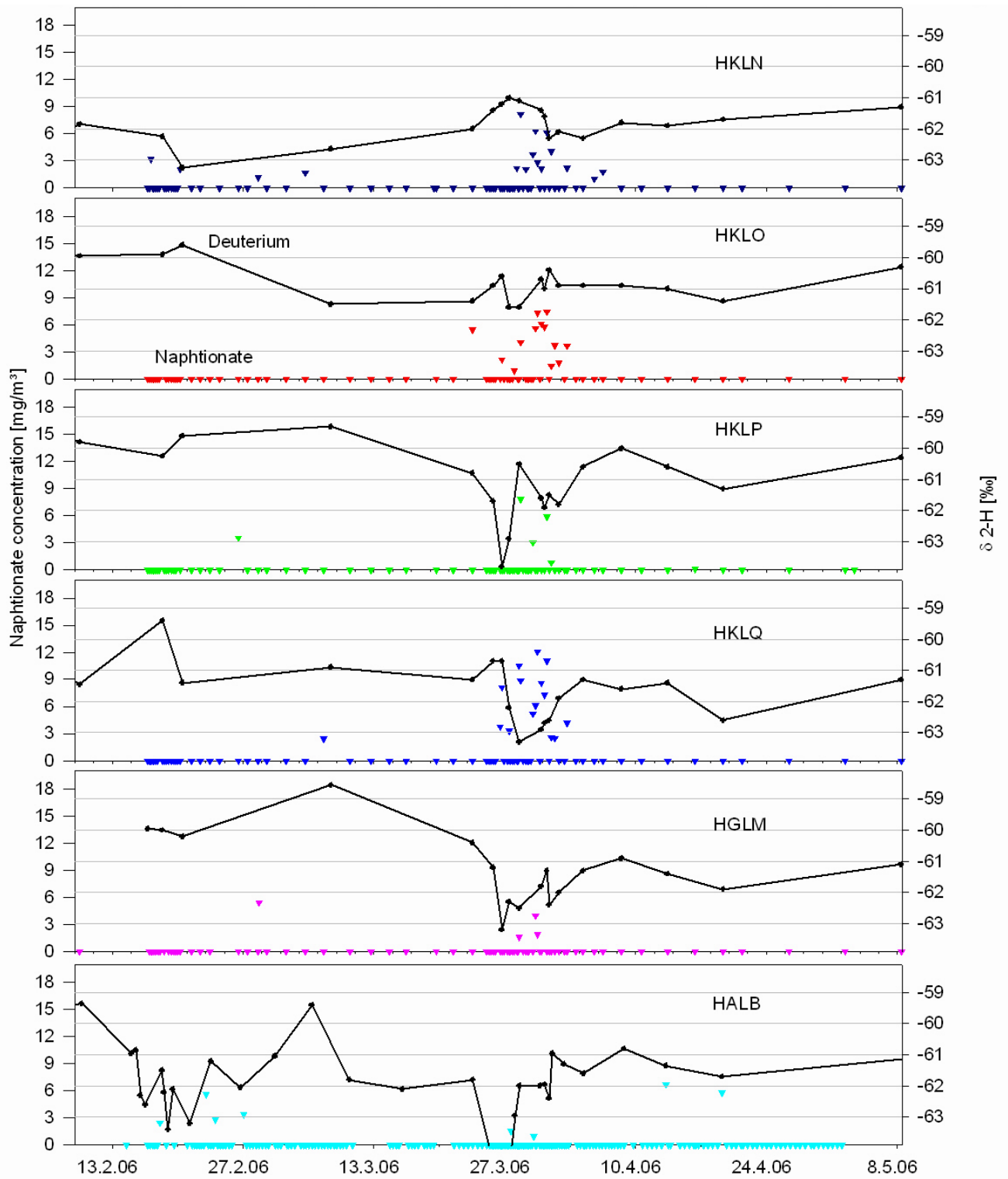


Fig. 6: H-2 and naphthionate concentrations in selected piezometers (HKL.), in porous groundwater of the valley filling (HGLM) and in Lange Bramke discharge (HALB) during the snow cover season in early 2006.

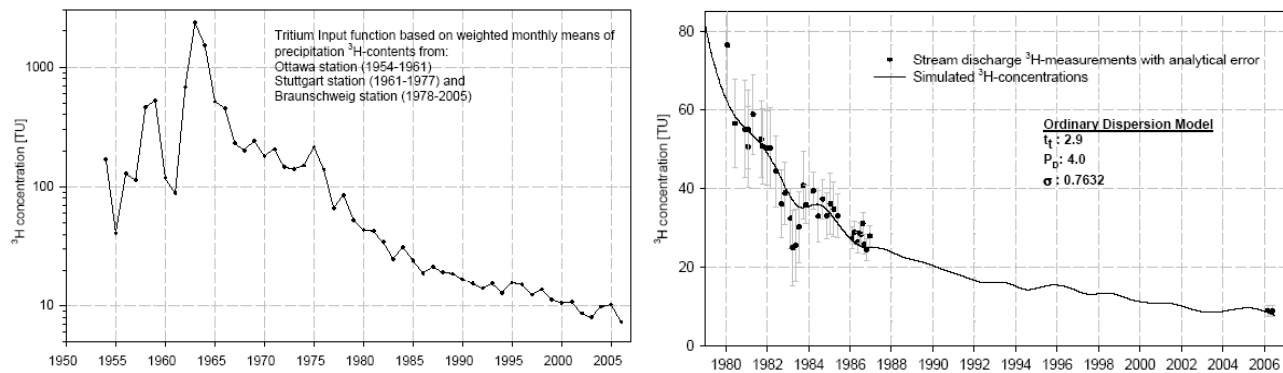


Fig. 7: Tritium input (left) and output functions (right) for Lange Bramke basin at low discharge

Conclusion

The results confirm former findings made in Lange Bramke and in other small study basins in the Harz Mountains that only very minor fractions of actual input leave the basin immediately as direct flow. The major portions, i.e. in this case of >95% of the actual input quantities, recharge the aquifers to maintain the quantitative input-output balance of the subsurface basin reserve. The mean transit time of groundwater nevertheless is short with 2.0 years. Tracer experiments are necessary to interpret hydraulic findings from traditional hydrogeological techniques in a more complete and refined form. Especially in respect to a short-term turnover of the groundwater portion during single precipitation-runoff events. The use of artificial tracers is also indispensable for the calibration of numerical groundwater models as recently carried out with FEFLOW for the same basin (Herrmann et al., 2006). It is marked that in the central European highlands where the runoff behaviour is considerably controlled by fractured Paleozoic rock aquifers runoff generation is a very complex process in source area (headwater) systems.

References

- Franks S., Sivapalan M., Takeuchi K., Tachikawa Y. (Eds) (2005). *Prediction in Ungauged Basins: International Perspectives on the State of the Art and Pathways Forward*. IAHS Publication, 301, IAHS Press, Wallingford, UK.
- Herrmann A. (1997). Global review of isotope hydrological investigations. In: G. Oberlin (Ed.), *FRIEND 3rd Report 1994-1997*. Cemagref Editions, France: 307-316.
- Herrmann A. (2004). Runoff formation in mountainous environments and possible effects of global warming. In: A. Herrmann, U. Schröder (Eds), *Studies in Mountain Hydrology. IHP/HWRP Berichte 2*, Koblenz : 1-12.
- Herrmann A., Schöniger M., Schumann S. (2001). Integrated approach of investigating and modelling runoff formation considering information from environmental and artificial tracers. *Freiburger Schriften zur Hydrologie*, 13: 90-97
- Herrmann A., Schöniger M., Schumann S. (2006). A new, physically-based, numerical runoff formation model system for the study of surface-close groundwater relationships and system reactions upon environmental changes. *Proceedings of the 4th FRIEND Conference. Havana 2006*, IAHS Publication, 308: 623-628.
- Maloszewski P., Zuber A. (1982). Determining the turnover time of groundwater systems with the aid of environmental tracers. 1. Models and their applicability. *Journal of Hydrology*, 57: 207-231.
- Maloszewski P., Herrmann A., Zuber A. (1999). Interpretation of tracer tests performed in fractured rock of the Lange Bramke basin, Germany. *Hydrogeology Journal*, 7: 209-218.
- Thies R. (2007). *Determination of Runoff Generation Processes in a Fissured Rock Aquifer (Lange Bramke Catchment, Harz Mountains)*. Institute of Geoecology, Technische Universität Braunschweig, 79 pp.

SURFACE WATER / GROUNDWATER SYSTEMS ANALYSIS IN THE SEMI-ARID SOUTH-PARE MOUNTAINS, TANZANIA

M.L. Mul^{1,2}, S. Uhlenbrook¹, R.K. Mutiibwa¹, J.W. Foppen¹ & H.H.G. Savenije^{1,3}

¹UNESCO-IHE, Institute for Water Education, PO Box 3015 DA, Delft, the Netherlands. ²University of Zimbabwe, Department of Civil Engineering, PO Box MP167, Mount Pleasant, Harare, Zimbabwe. ³Delft University of Technology, Department of Water Resources, PO Box 5048, 2600 GA Delft, the Netherlands.

Corresponding author: S. Uhlenbrook, e-mail: S.Uhlenbrook@unesco-ihe.org

ABSTRACT

Experimental investigations were carried out in the semi-arid, mountainous Makanya catchment in the Pangani Basin (approximately 300 km²). Heterogeneous rainfall patterns for the long term and during single events were observed. Some small events and one big event were investigated. The latter affected the stream gauges significantly, and two gauges were destroyed completely. Using hydrochemical mapping, hydrograph separation and electrical resistivity tomography (ERT), the main surface water and groundwater flow systems were identified. We found that the catchment was losing significant amounts of groundwater to neighbouring catchments. This paper gives an overview of the different experimental methods and reports preliminary findings.

Keywords: Semi arid hydrology, groundwater runoff, tracers, electrical resistivity tomography (ERT)

Introduction

In many parts of the world catchments are not or poorly gauged in respect to hydrological parameters, such as rainfall and runoff measurements. The IAHS has initiated the decade on “Predictions in Ungauged Basins” (PUB) (Sivapalan et al., 2003) that supports research focused on increasing our capability to predict hydrological responses in ungauged basins. Improving the understanding of the underlying hydrological processes governing the rainfall-runoff responses in a catchment is one of the main issues addressed in the PUB initiative. In particular in developing countries, catchments are predominantly ungauged, as a result of lack of adequate resources (Mazvimavi, 2003). But in particular in the developing countries that are often located in tropical regions as in sub-Saharan Africa better predictions of hydrological variables are needed, to manage the often scarce water resources in a sustainable way. Therefore, improving the process understanding to subsequently develop models that are better based on process knowledge and less model calibration is a key element of PUB.

Hydrological processes within a catchment define how precipitation reaches the catchment outlet, how long water is stored in surface water, soil water and groundwater systems, and what hydrochemical composition these sources have. To investigate these processes, different types of field studies have been conducted (e.g. McDonnell, 1990; Hornberger et al., 1991; Ladouche et al., 2001; Wenninger et al., 2004): (i) Comparisons of the hydrological responses of headwater basins were carried out (‘paired basin approach’); (ii) soil physical and hydrometrical studies, using tensiometers and piezometers, were executed at the plot scale; (iii) sprinkling experiments at hillslopes, often in combination with tracer tests, were conducted; (iv) geophysical measurements proved useful to explore subsurface soil properties; (v) finally, the use of isotopic tracers in combination with hydrochemical tracers helped to gain further insights into processes, in particular into the flowpaths, residence times of water and the mixing of different runoff components.

Each experimental method has its own strengths and shortcomings concerning costs and the temporal and spatial scale at which they can be used. The methods were mainly developed and applied in humid temperate

climates. In arid and semi-arid areas two additional factors make the process investigation additionally difficult: First, the climatic spatio-temporal variability is very high and, second, human influence often due to increasing population densities results in rapid land use and stream channel changes that affect hydrological responses.

The objective of this paper is to give a brief overview about recent experimental investigations of runoff generation processes in the semi-arid Makanya catchment. The results of the experimental studies will form the basis for process-oriented modeling of water quantities and water quality in the future.

Study area

The mountainous Makanya catchment (300 km²) is located in the South Pare Mountains, northern Tanzania (Fig. 1). Metamorphic and meta-igneous rocks are the predominant crystalline country rocks while unconsolidated formations consisting of “debris-flow” material and superficial deposits form the shallow aquifer systems. The catchment is a poorly gauged catchment with two rainfall stations with a more than 10-year record, and without any long records of discharge measurements. Rainfall in the catchment ranges from 550 mm a⁻¹ in the lowlands (~700 m) to 800 mm a⁻¹ in the highlands (up to 2000 m) and is distributed over two rainy seasons. The short rainy season is from October to December, locally known as “Vuli”, whereas the long rainy season is from March to May, locally known as “Masika”. In 2004 the SSI Programme (Rockström et al., 2004) has installed a hydrological monitoring network in the catchment, and is researching the hydrological implications of changing farmer management practices.

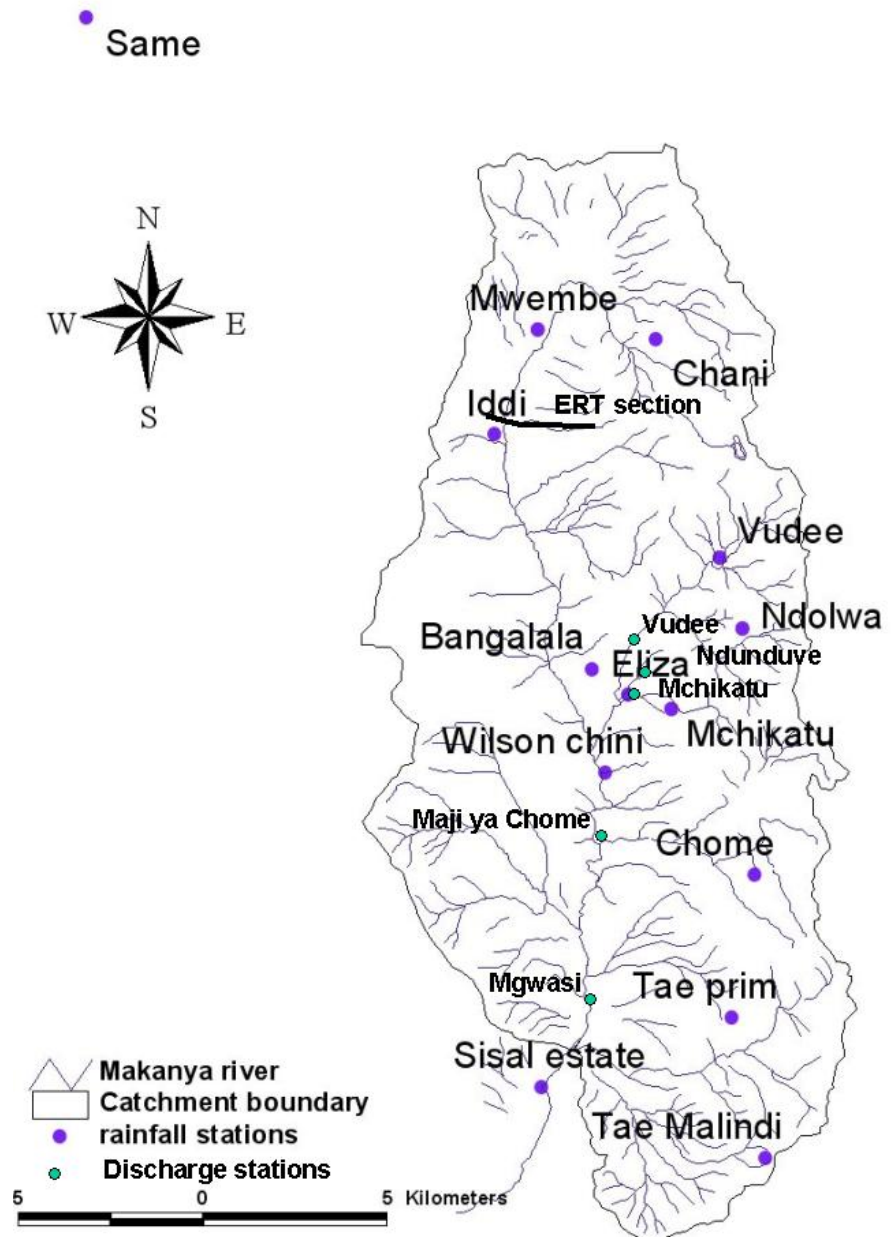


Fig. 1: Map of the Makanya catchment, South Pare Mountains, Tanzania, with instrumentation network.

Experimental investigations

Rainfall runoff measurements

Five gauging stations were built and 14 rain gauges (daily measurements) were set up to investigate the rainfall-runoff relationship (Fig. 1). A couple of events were observed during the rainy seasons 2005/06 in the sub-catchment Vudee (25 km²). These had generally low runoff coefficients (less or equal 10%) (Mul et al., 2007a&b). On the 1st March 2006 an extreme rainfall was recorded with up to 100 mm rainfall in the village Bangalala in only 3 hours. Runoff was devastating, inundating large parts of the flood plain and destroying completely the two small gauging stations. The two other gauging stations at Vudee and the main outlet were over-flown and needed repair after the event. However, flood marks and the information of local observers helped to reconstruct the discharge data (further details in Mul et al., 2007b).

The extreme event had a significant spatial variability of the rainfall over the catchment, even in areas with the same altitude. The Vudee sub-catchment was in the centre of the rainfall event, receiving about 78 mm during 3 hrs in the two upstream tributaries: the Upper-Vudee and Ndolwa, respectively. The discharge increased and subsided quickly, with the peak flow occurring just one hour after the peak of the rainfall. The subsequent base flow in the river remained at a relatively high level for the rest of the season, which is substantially higher than the normal base flow observed during the previous rainy seasons. This gives a hint that substantial groundwater recharge has happened during this event and explains also the relatively low runoff coefficient of 10%.

Hydrochemical mapping

During the short rainy season October-December 2005, which turned out to be exceptionally dry, groundwater and surface water sites were sampled and the concentrations of the major anions and cations as well as dissolved silica and fluoride were determined. Then the sites were classified into main water types and a hydrochemical map (Fig. 2) of the Makanya basin was made. Although the map could have been easily achieved by means of classical interpolation techniques, the map was rather drawn based on existing data (incl. geological data), observed trends and field observations. Zones of similar chemical characteristics (main water types) were demarcated according to Stuyfzand (1998).

The hydrochemical map demonstrates the decrease of concentrations of almost all major cations and anions as a function of altitude: in the elevated areas total ion concentrations were low, while ion concentrations were higher in the valleys. We think this was caused by the continuous dissolution of minerals, driven by the continuous addition of carbon dioxide to the system as a result of decay of organic matter in the shallow subsoil. Consequently, this type of water was mapped as shallow groundwater, sometimes resurfacing and then infiltrating again. The map also demonstrates the occurrence of isolated water points, located in the valley, that have water quality associated with deep groundwater systems, indicated through high ion concentrations and also high fluoride concentrations. The latter gives a hint to the connection with a regional groundwater system that is linked to recent volcanic activities. Interesting is also the fact that the catchments Mbaga and Kisiwani located in the east have many springs and substantially higher base flows. Because of the geology (i.e. layers dipping to the east), we had to conclude that the deep groundwater system of the Makanya catchment is losing water to these catchments.

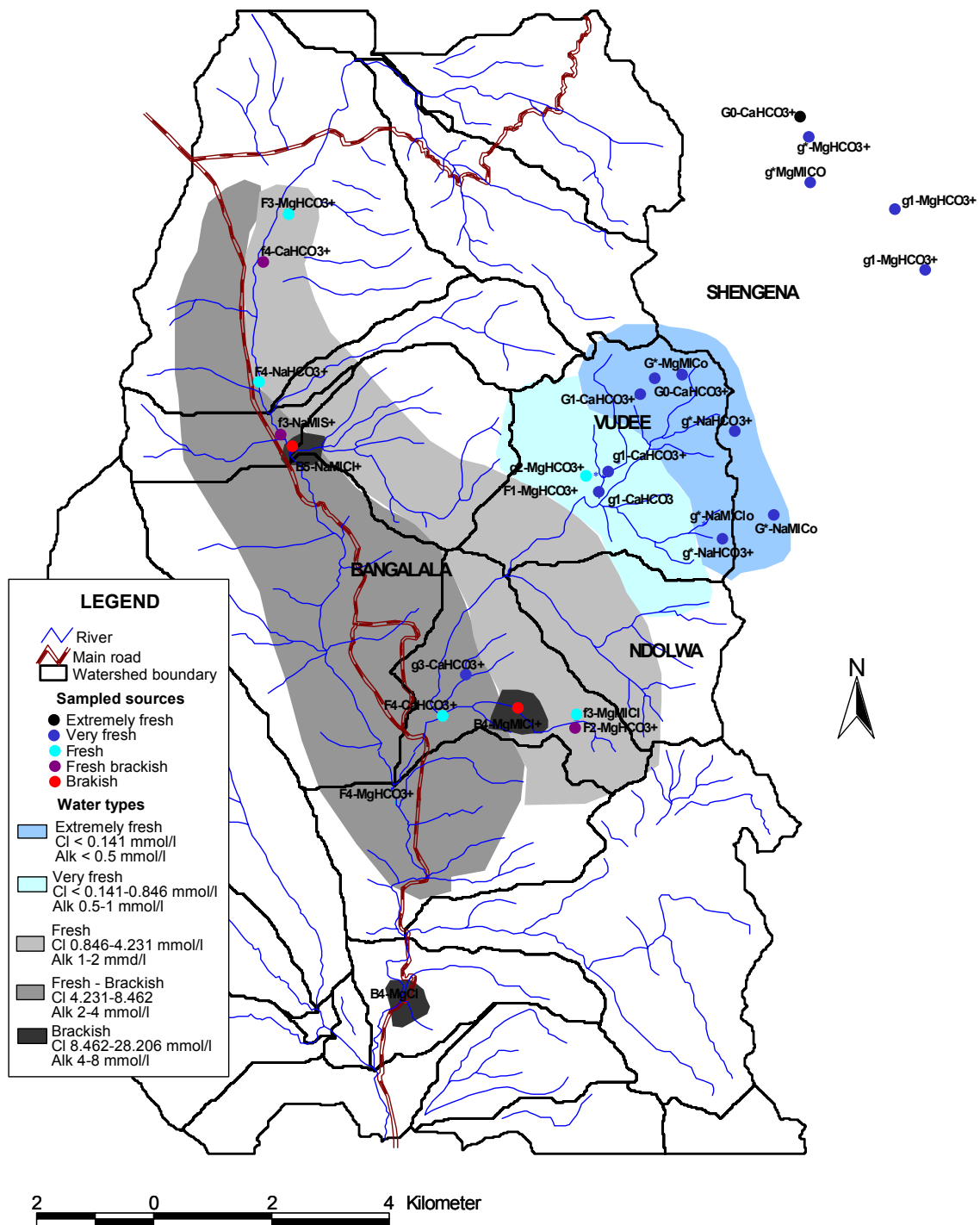


Fig. 2: Hydrochemical map of the Makanya catchment, South Pare Mountains, Tanzania.

Hydrograph separation

Chemical hydrograph separations for two relatively small flood events were carried out using hydrochemical tracers including electrical conductivity (EC), dissolved silica (SiO₂) and major anions (Cl⁻, F⁻, SO₄²⁻ and HCO₃⁻) and cations (Na⁺, K⁺, Ca²⁺ and Mg²⁺). The first event occurred on 9 November 2005 and the second event on 5 December 2005; thus, both occurred during the short rainy season in the Vudee sub-catchment (for further details see Mul et al., 2007a). This catchment has two main sub-catchments: Ndolwa, draining an area

of 8.4 km², and upper-Vudee draining 14.2 km². Separate samples were obtained from the two sub-catchments, just before the confluence during low flow, for the first event. During the second event also samples were obtained from the two sub-catchments.

During the 9 November event, the rain gauges in upper-Vudee and Ndolwa recorded 13.5 mm day⁻¹ and 7.9 mm day⁻¹, respectively. At the outlet in the valley (station Bangalala) hardly any rainfall was recorded, 3.2 mm day⁻¹. During the second event, the spatial distribution of the rainfall in the two sub-catchments was the opposite: the upper-Vudee and Ndolwa rain gauges received 7 mm day⁻¹ and 17.6 mm day⁻¹, respectively.

The water samples that were collected during these small events did not contain suspended sediments, what gives a hint to negligible amounts of Hortonian overland flow generation. All tracer concentrations decreased only to a limited extent, indicating mainly sub-surface runoff components (> 90%). Separating the total discharge into the contributions from the two sub-catchments (Fig. 3) using dissolved silica as a tracer, reflects nicely the uneven rainfall distributions during the two events.

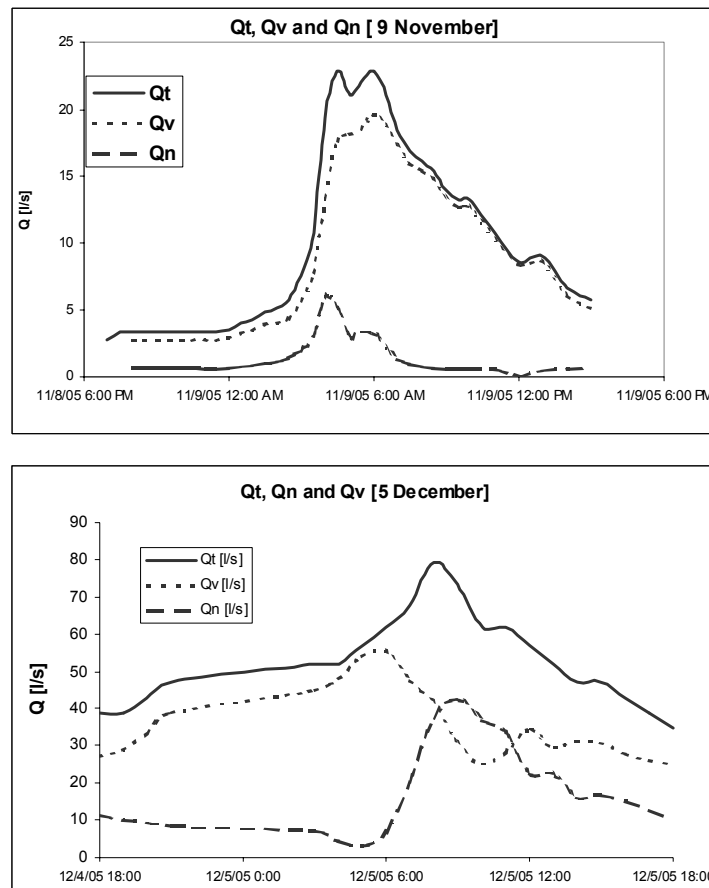


Fig. 3: Results of hydrograph separations for the two investigated storm events; Qt, Qv and Qn are total discharge (measured at gauging station Vudee), the discharge from the sub-catchment Upper-Vudee and the discharge from the sub-catchment Ndola, respectively.

Geophysical investigations

2-D electrical resistivity tomography (ERT) using the device Syscal Kid Junior with 24 electrodes was done at selected locations to gain further insights into the structure of the subsurface and the aquifers. A suitable electrode configuration (array: dipol-dipol; different spacing distances between the electrodes) was chosen and results were interpreted using the RES2DINV software (Loke, 2003). ERT measurements were done at large

scale with the maximum electrode spacing of 5 m (Fig. 4) and at a plot scale with electrode spacing of 1 m. Surface characteristics (surface slope, vegetation, outcrops and changes in soil characteristics of the top soil) and few hand-auger holes were used additionally to interpret the data.

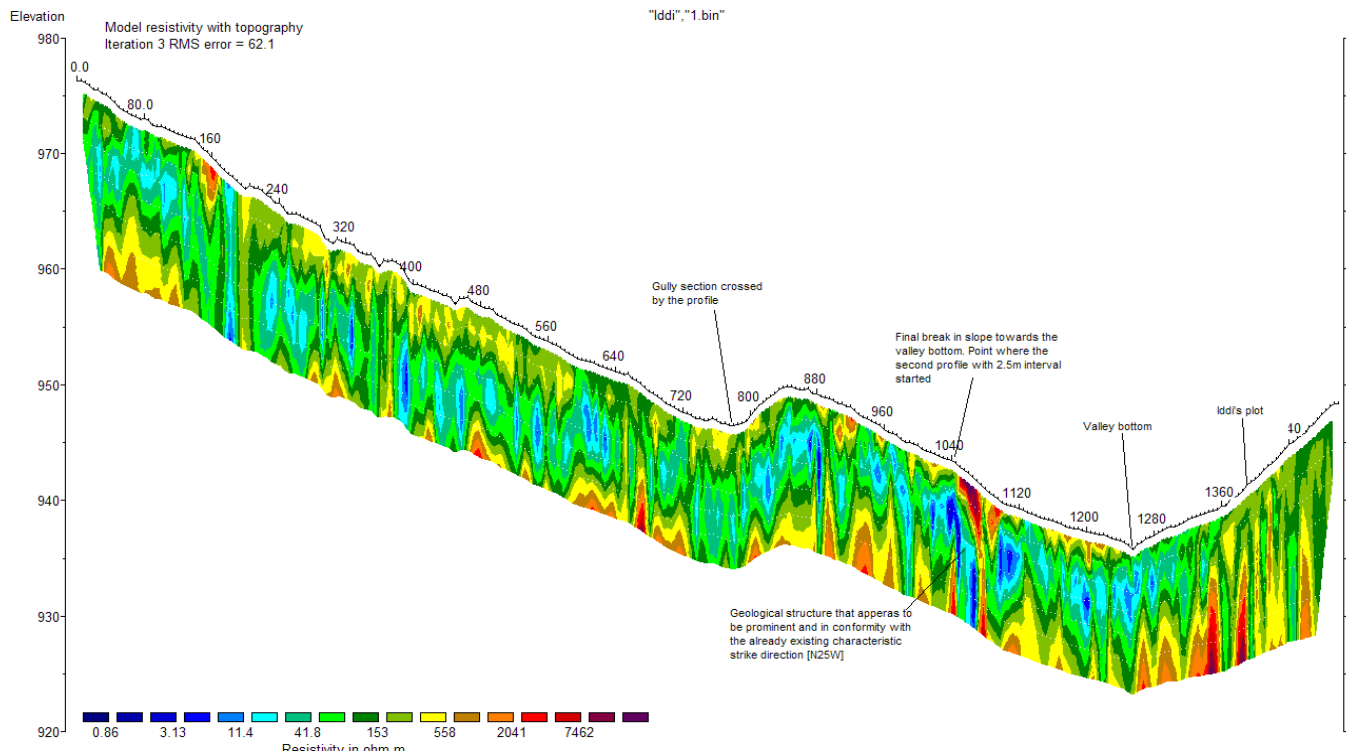


Fig. 4: Results of ERT measurements along a long cross-section of about 1500 m (see figure 1 for location).

Conclusions

The experimental investigations show that highlands receive generally more rainfall than the lowlands, but that the space-time pattern during specific events can be very heterogeneous. The differences in precipitation are reflected in the degree of weathering exhibited by the water in each sub-catchment. The rainfall-runoff relationships showed differences for the two sub-catchments of Vudee and Ndolwa. However, flood generation is dominated by sub-surface processes during small events in both catchments. During the large event, significant amounts of surface runoff were generated, and the gauging stations were destroyed. Irrespective of the occurrences of isolated water points that have water quality associated with deep groundwater systems, it was demonstrated that only local flow systems with the main aquifer/storage being the unconsolidated “debris-flow” material exist in the study area. The geology has a big influence on the groundwater flow systems, the study area is losing water to the neighbouring catchments of Mbaga and Kisiwani.

Acknowledgements

The work reported here was undertaken as part of the Smallholder System Innovations in Integrated Watershed Management (SSI) Programme funded by the Netherlands Foundation for the Advancement of Tropical Research (WOTRO), the Swedish International Development Cooperation Agency (Sida), the Netherlands Directorate-General of Development Cooperation (DGIS), the International Water Management Institute (IWMI) and UNESCO-IHE Institute for Water Education. Thanks to the WaterMill (DGIS, The Netherlands) project that supported the activities of Mr. Mutibwa (MSc fellowship). Implementation on site was assisted by the Soil-Water Management Research Group (SWMRG), Sokoine University of Agriculture, Tanzania.

References

- Hornberger G.M., Germann P.F., Beven K.J. (1991). Throughflow and solute transport in an isolated sloping block in a forested catchment. *Journal of Hydrology*, 124: 81-99.
- Ladouche B., Probst A., Viville D., Idir S., Baque D., Loubet M., Probst J.-L., Bariac T. (2001). Hydrograph separation using isotopic chemical and hydrological approaches (Strengbach catchment, France). *Journal of Hydrology*, 242: 255-274.
- Loke H.M. (2003). *Tutorial: 2-D and 3-D Electrical Imaging Surveys*. 134 pages, www.geoelectrical.com.
- Mazvimavi D. (2003). *Estimation of Flow Characteristic of Ungauged Catchments, Case Study in Zimbabwe*. PhD dissertation, Wageningen University, The Netherlands.
- McDonnell J.J. (1990). A rationale for old water discharge through macropores in a steep, humid catchment. *Water Resources Research*, 26: 2821-2832.
- Mul M.L., Mutibwa R.K., Uhlenbrook S., Savenije H.H.G. (2007a). Hydrograph separation in the South Pare Mountains. *Submitted to Physics and Chemistry of the Earth*, in review.
- Mul M.L., Savenije H.H.G., Uhlenbrook S. (2007b). Spatial rainfall variability and runoff response during an extreme event in a semi-arid meso-scale catchment in the South Pare Mountains, Tanzania. *Submitted to Physics and Chemistry of the Earth*, in review.
- Rockström J., Folke C., Gordon L., Hatibu N., Jewitt G., de Vries F.P., Rwehumbiza F., Sally H., Savenije H., Schulze R. (2004). A watershed approach to upgrade rainfed agriculture in water scarce regions through Water System Innovations: an integrated research initiative on water for food and rural livelihoods in balance with ecosystem functions. *Physics and Chemistry of the Earth*, 29: 1109-1118.
- Sivapalan M., Takeuchi K., Franks S.W., Gupta V.K., Karambiri H., Lakshmi V., Liang X., McDonnell J.J., Mendiondo E.M., O'Connell P.E., Oki T., Pomeroy J.W., Schertzer D., Uhlenbrook S., Zehe E. (2003). IAHS Decade on predictions in ungauged basins (PUB), 2003-2012: Shaping an exciting future for the hydrological sciences. *Hydrological Sciences Journal*, 48: 857-880.
- Stuyfzand J.P. (1998). Patterns in groundwater chemistry resulting from groundwater flow. *Hydrogeology Journal*, 7: 15 - 26.
- Wenninger J., Uhlenbrook S., Tilch J., Leibundgut Ch. (2004). Experimental evidences of fast groundwater responses in a hillslope/floodplain area. *Hydrological Processes*, 18: 3305-3322.

DISTRIBUTION OF SOIL MOISTURE OVER DIFFERENT DEPTHS IN A SMALL ALPINE BASIN

D. Penna, M. Borga, P. Boscolo & G. Dalla Fontana

Department of Land and Agroforest Environments, University of Padua – Italy.

Corresponding author: Daniele Penna, email: daniele.penna@unipd.it

ABSTRACT

In this study we compare measurements of soil moisture at 0-6, 0-12 and 0-20 cm depth in order to examine how representative the surface measure is with regard to the deeper layers. Detailed soil moisture data were collected over three hillslopes in the 1.9 km² wide Rio Vauz mountainous catchment, located in the central-eastern Italian Alps. The field work was carried out during summer 2005; water content values were collected at several points over the three hillslopes at 0-6 cm, 0-12 and 0-20 cm depth by means of two portable instruments being able to provide spot values: an impedance probe was used to collect surface soil moisture data while water content up to 20 cm depth was measured by a TDR probe. The comparison between soil moisture patterns at different depths is evaluated by examining: (i) summary statistical properties of the data set; (ii) scatter plots; (iii) spatial distributions via maps; (iv) evaluation of Pearson and Spearman correlation coefficients. Results show that the soil moisture generally decreases with depth. The degree of correlation between the data collected at the three depths is relatively high. The visual comparison of maps suggests a reasonable consistency of patterns; wet and dry areas on each hillslope are fairly the same at every sampled depth. Overall, spatial organization and spatial consistency are controlled by soil effects, reflecting high organization in the distribution of soils. This is consistent with the pedological characteristics of these soils, which exhibit a relatively homogeneous vertical structure.

Keywords: hillslope, soil moisture, TDR

Introduction

Soil moisture is one of the most important hydrological variables. It has a critical influence on several hydrological processes, such as floods, erosion of hillslopes, landslide triggering, on pedogenetic processes, migration of chemicals to aquifers, separation of net radiation between sensible and latent heat and also on land use, water and natural resources management (Cosh et al., 2004; Martinez-Fernandez and Ceballos, 2005; Svetlitchnyi et al., 2003; Western et al., 1999; Western et al., 2004); moreover, in hydrological modelling and flood forecasting, a correct definition of antecedent moisture conditions is a key factor for accurate predictions (Grayson and Western, 1998; Martinez-Fernandez and Ceballos, 2005). Soil moisture also represents one of the main factors in infiltration of water, surface and subsurface runoff generation and it plays an important role in the evaporation processes determining the amount of water available for plants (Grayson and Western, 1998; Martinez-Fernandez and Ceballos, 2005). In this study we compare measurements of soil moisture in 0-20 cm of soil with those in 0-6 cm and in 0-12 cm, collected by means of different instruments; we aim to examine how representative the surface measure is with regard to the root zone and to gain further information about changes in soil wetness and its variability through space and time at different depths.

Study area

Soil moisture data were collected in a small Alpine basin (Rio Vauz catchment, 1.9 km²) in the central-eastern Italian Alps, with altitudes ranging from 1835 m a.s.l. to 3152 m a.s.l. and a mean slope of 27.4°. The mean annual precipitation is 1160 mm/year, 40% of which falls as snow. Its monthly distribution shows a peak in early summer and a second one during fall (Fig. 2).

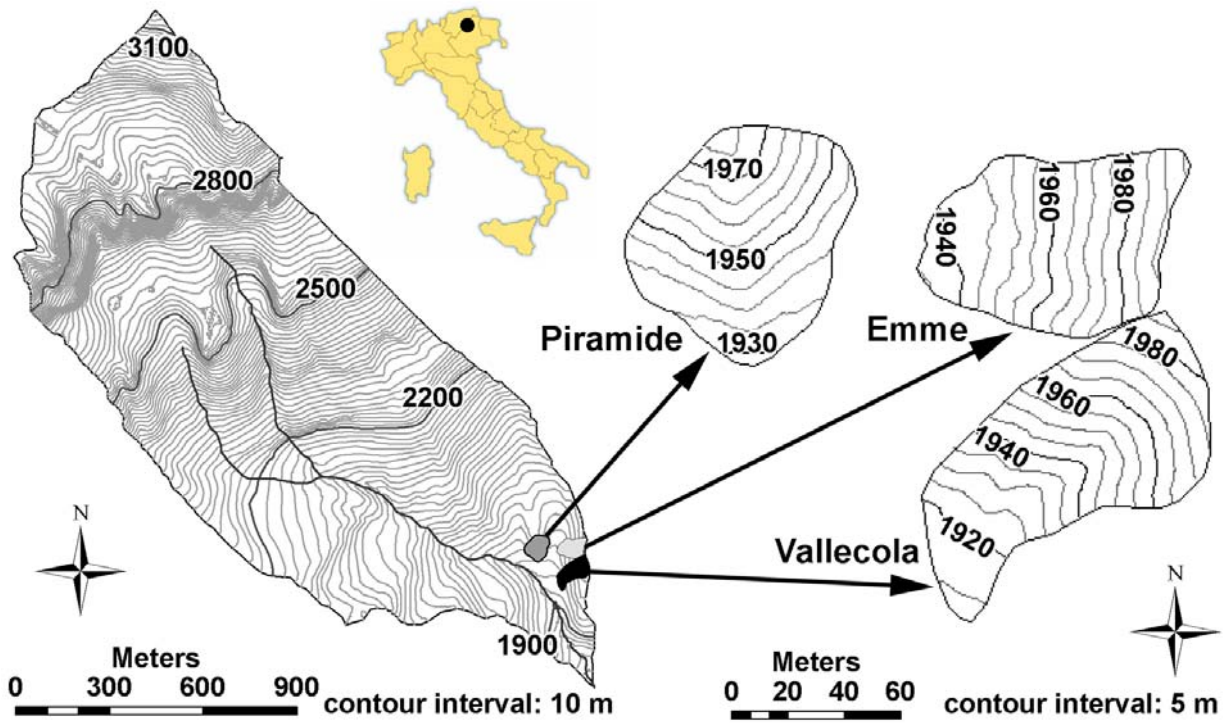


Fig. 1: Rio Vauz catchment and localization of the three hillslopes.

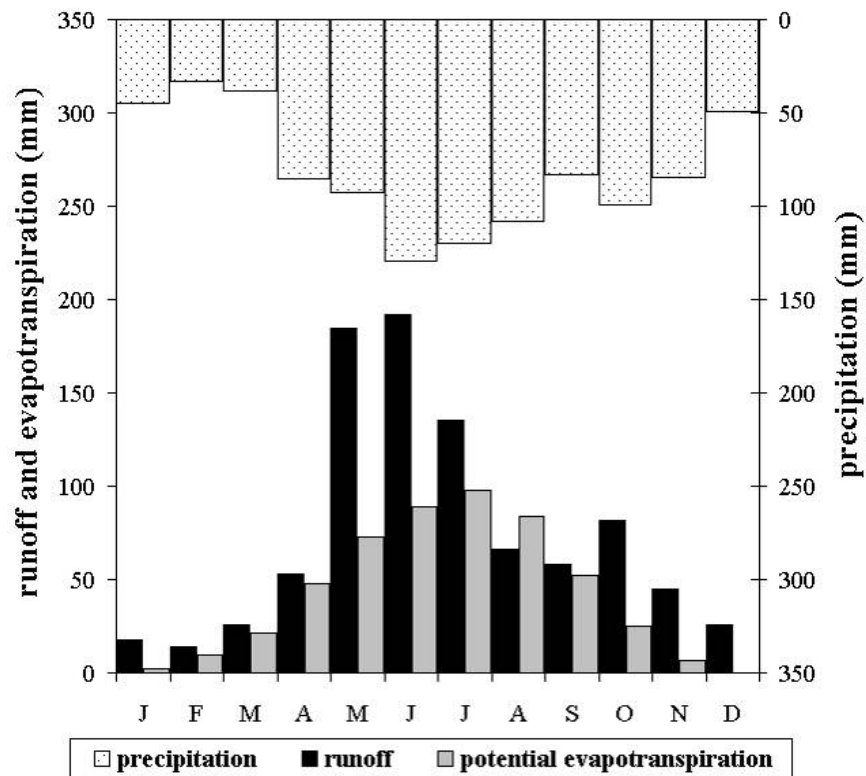


Fig. 2: Climatic conditions in the lower Vauz catchment.

In the lower parts of the catchment the snow cover period typically lasts from November to April while the upper parts of the basin are bare only for the three months from July to September. Runoff is usually dominated by snowmelt in May and June but summer and early autumn floods represent an important contribution to the flow regime. The average monthly temperature varies from -5.7°C in January to 14.1°C in July. Three hillslopes were selected in the lower part of the basin (Fig. 1) to provide detailed soil moisture data. The experimental sites have been named “Piramide”, “Emme” and “Vallecola”, with areas of 0.46, 0.47 and 0.57 ha, respectively. Topography is mainly convex (Piramide), planar (Emme) and concave (Vallecola). Gradients range between around 1:5 to 1:1.1. The soil profile consists of an organic-rich horizon (in the first ten centimetres), overlying mineral subsoil, which in turn is underlain by weathered till and bedrock. Depth of soil above compact till and bedrock ranges from 60 cm on the ridge to more than 100 cm at the base of the hillslope. No permanent watercourse exists on this hillslope.

Methodology

Soil moisture data were collected at 0-6, 0-12 and 0-20 cm depth over the three hillslopes between 30 June and 20 July 2005. During this period a cumulated rainfall amount of 130 mm was recorded, which represents almost twice the climatological average over the period. Soil moisture values at 0-6 cm depth were sampled by means of a Theta Probe, a hand-held impedance probe manufactured by Delta-T Devices Ltd. (www.deltat.co.uk). Soil moisture at 0-12 and 0-20 cm depth was evaluated by means of a TDR300, a portable probe manufactured by Spectrum Technologies Inc. (www.specmeters.com) and operating on the basis of Time Domain Reflectometry technology. The TDR probe is provided with two pairs of interchangeable rods of 12 cm and 20 cm length, which allow to sample soil moisture over these different depths. Both the Theta Probe and the TDR probes were calibrated against gravimetric samples for the specific local soil conditions (Cosh et al., 2005; Stenger et al., 2005; Walker et al., 2004). Soil moisture was measured at 26 sites over Piramide and Emme, and at 16 sites over Vallecola. At the sampling points, the first few centimetres of grass cover were removed in order to reduce the influence of roots on the measure, otherwise strongly affected by the presence of pores and discontinuity zones (Cosh et al., 2005; Tromp van Meerveld and McDonnell, 2006; Walker et al., 2004). Soil moisture data at 0-6 and 0-12 cm depth were collected over the three hillslopes, while 0-20 cm values were measured only over Piramide and Emme, due to difficulties of deeper sampling on Vallecola. At each measurement point, five measures were collected in order to ascertain the repeatability of the results and instrument errors; the trimmed mean was computed over the five values. During the field work, moisture measurements were made on several occasions (up to 25), capturing wetting and drying situations. The measures at the three depths were taken concurrently at each site to reduce the effect of temporal variability on the comparison of results. Points were sampled in the same order on each occasion. Totally, 1658 values were collected at Piramide and Emme site, 624 at Vallecola. The comparison between soil moisture patterns at different depths was evaluated by examining: (i) summary statistical properties of the data set; (ii) scatter plots; (iii) spatial distributions via maps; (iv) evaluation of Pearson and Spearman correlation coefficients.

Results

Summary statistics of soil moisture data (Table 1) show that mean soil moisture computed over each hillslope for the three depths decreases with increasing the depth. 0-6 cm soil moisture is 8.6% to 10.8% higher than 0-12 cm soil moisture and it is 13.7% to 16.1% higher than 0-20 cm soil moisture. This is due to the relatively intense storm activity during the field work. Emme is on average slightly wetter than Piramide and Vallecola, probably due to its westward main aspect.

Scatter plots drawn for pairs of soil moisture data at different depths show a reasonably high correlation between the different patterns (Fig. 3). The highest correlation (Table 2) is observed between pairs 0-6 – 0-12 cm and 0-12 – 0-20 cm depth, due to the proximity of the two layers; in particular, the higher degree of correlation between data collected at 0-12 and 0-20 cm is speculatively attributed to the use of the same measurement instrument at these two depths.

Table 1: Summary statistics of soil moisture data at the three hillslopes.

Statistics	Piramide			Emme			Vallecola	
	0-6cm	0-12cm	0-20cm	0-6cm	0-12cm	0-20cm	0-6cm	0-12cm
Total n° of measures	624	624	208	650	650	416	384	384
Mean	43.5	39.4	36.5	44.6	39.8	38.5	43.0	39.3
Standard deviation	3.9	6.6	5.5	3.8	6.2	4.9	3.0	6.5

Table 2: Pearson's correlation coefficient for pairs of soil moisture patterns.

Correlation r	Piramide	Emme	Vallecola
0-6 & 0-12 cm	0.74	0.68	0.64
0-12 & 0-20 cm	0.78	0.79	-
0-6 & 0-20 cm	0.58	0.58	-

Following previous works (Western et al., 1999, 2004; Wilson et al., 2003, 2004), resemblance of soil moisture patterns was also analyzed by comparing maps of mean water content over the whole field work period for each experimental site. Maps were drawn by Inverse Distance Weighted (IDW) interpolation for each slope and patterns obtained at different depths were visually compared (Figs. 4-6). Examination shows that surface soil layers are wetter than the deeper ones over each hillslope, as previously mentioned. Visual comparison indicates a good consistency between patterns: generally, wettest and driest points are the same at the three depths (for the wettest locations, see points E, P, X on Piramide site, and A, C, V on Emme site; for the driest locations, see points V, Q and the central area in Piramide, L, K, J forming the middle part in Emme site, G, O, K, J in Vallecola site). It is interesting to note that these spatial patterns are in general non consistent with topography (gullies are not wetter than hillslopes), with the notable exception of Piramide. For this site, drier points are located over the main ridge, reflecting higher exposure to winds and more active transpiration processes. Overall, spatial organization and spatial consistency are controlled by soil effects, reflecting high organization in the distribution of soils. This is consistent with the pedological characteristics of these soils, which exhibit a relatively homogeneous vertical structure. It has been noted that soil moisture spatial variability is partially controlled by borrows due to borrowing mammals.

To quantify the visual comparison presented above and to analyse the consistency of mean soil moisture patterns, in accordance with previous works (Cosh et al., 2003; Grayson and Western, 1998; Starks et al., 2006), Spearman rank correlation coefficients were calculated. Results (Table 3) show a positive correlation and suggest a good consistency of soil water content along the soil profile over the monitoring period; the best correlation exists between pairs 0-12 and 0-20 cm depth, as previously observed for the whole data set.

Table 3: Values of Spearman coefficient for mean soil moisture data at different depths.

Spearman rank correlation coefficient	Piramide	Emme	Vallecola
0-6 & 0-12 cm	0.74	0.79	0.76
0-12 & 0-20 cm	0.92	0.85	-
0-6 & 0-20 cm	0.69	0.69	-

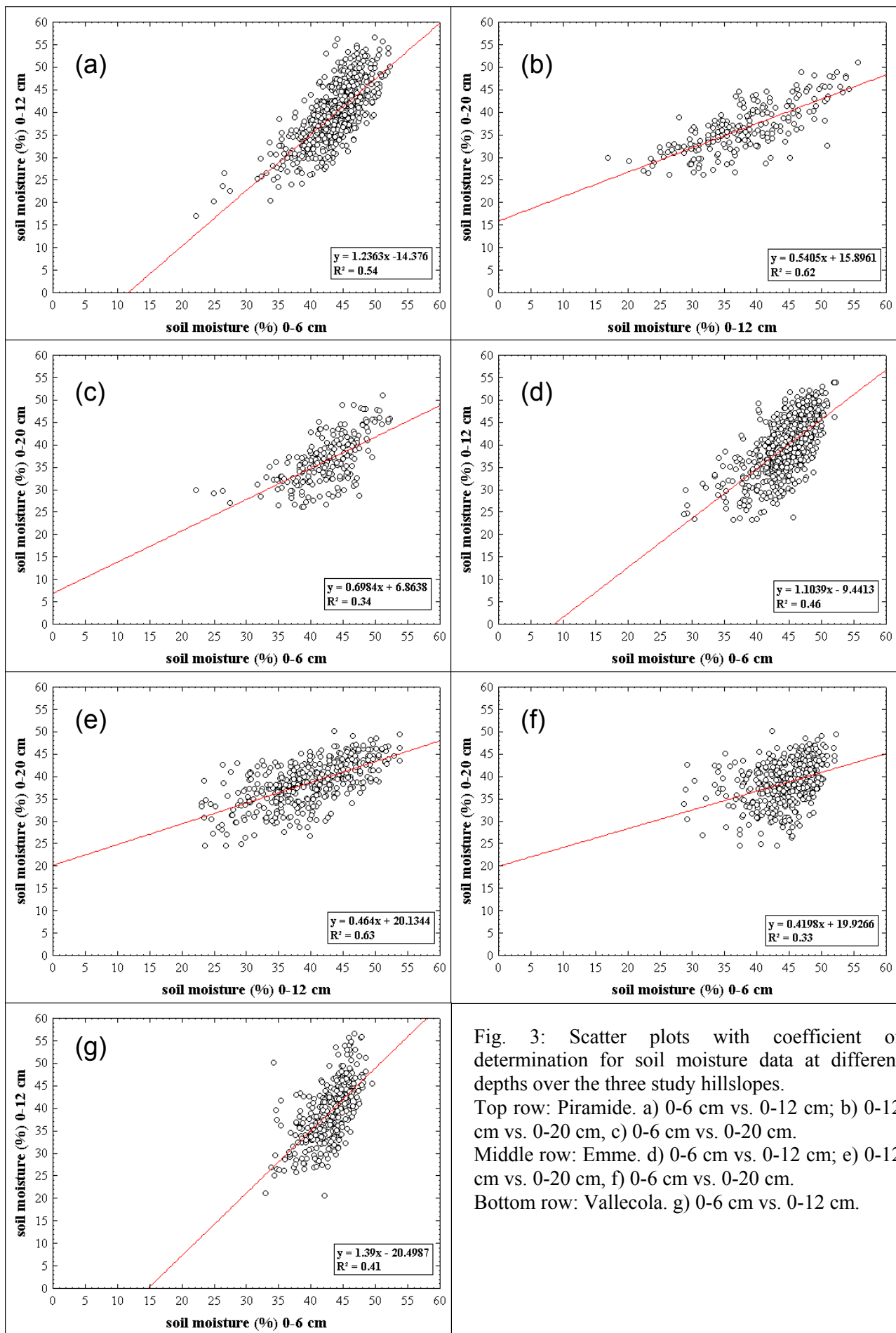


Fig. 3: Scatter plots with coefficient of determination for soil moisture data at different depths over the three study hillslopes.

Top row: Piramide. a) 0-6 cm vs. 0-12 cm; b) 0-12 cm vs. 0-20 cm, c) 0-6 cm vs. 0-20 cm.

Middle row: Emme. d) 0-6 cm vs. 0-12 cm; e) 0-12 cm vs. 0-20 cm, f) 0-6 cm vs. 0-20 cm.

Bottom row: Vallecola. g) 0-6 cm vs. 0-12 cm.

Conclusions

A comparison of soil moisture data measured over 0-6, 0-12 and 0-20 cm depth is presented for three experimental hillslopes in a small Alpine catchment. Results show that the soil moisture generally decreases with depth. The degree of correlation between the data collected at the three depths is relatively high. The highest correlation is observed between data collected at 0-12 and 0-20 cm. Consistency of soil moisture patterns was also analyzed by comparing maps of mean water content. The visual comparison of maps suggests a reasonable consistency of patterns; wet and dry areas on each hillslope are fairly the same at every sampled depth. To quantify the spatial consistency of mean soil moisture patterns, the Spearman rank correlation was also calculated. Relatively high correlation values were obtained. Overall, spatial organization and spatial consistency are controlled by soil effects, reflecting high organization in the distribution of soils. This is consistent with the pedological characteristics of these soils, which exhibit a relatively homogeneous vertical structure.

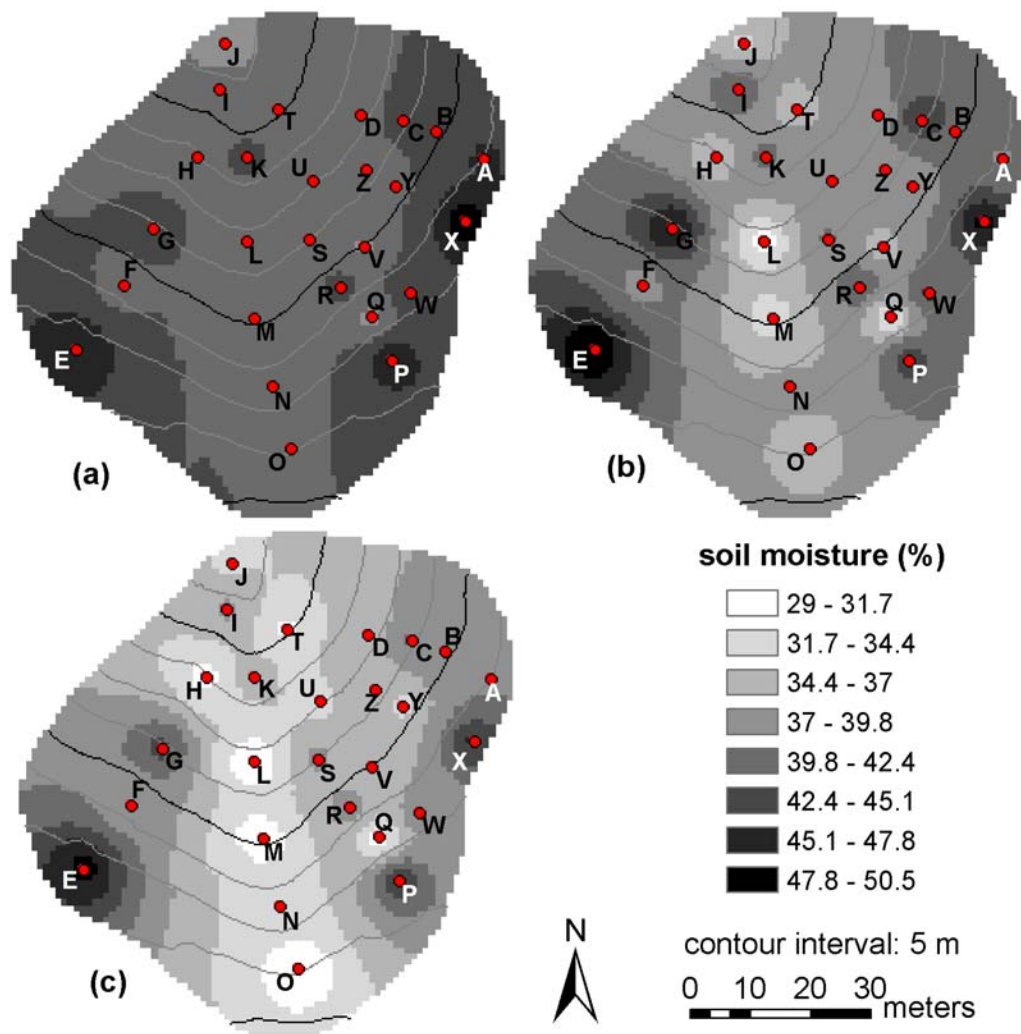


Fig. 4: Maps of mean soil moisture at Piramide site at different depths. a) 0-6 cm, b) 0-12 cm, c) 0-20 cm.

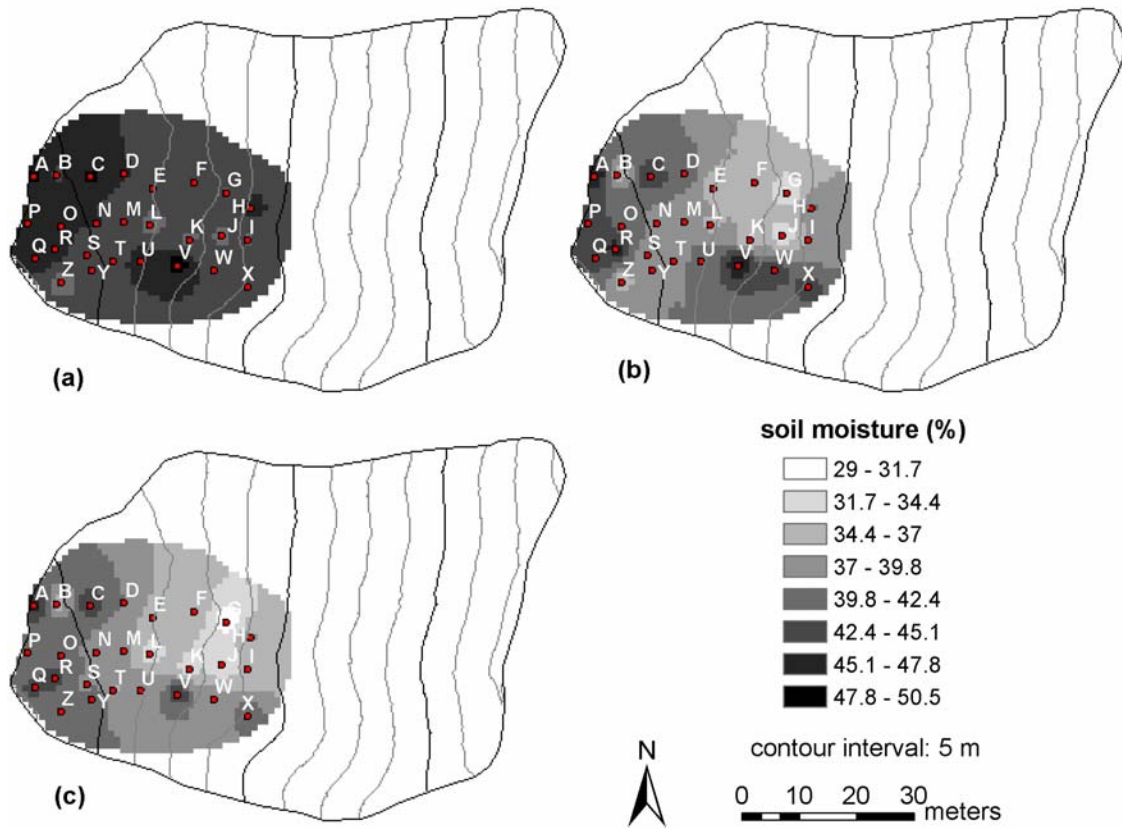


Fig. 5: Maps of mean soil moisture at Emme site at different depths. a) 0-6 cm, b) 0-12 cm, c) 0-20 cm.

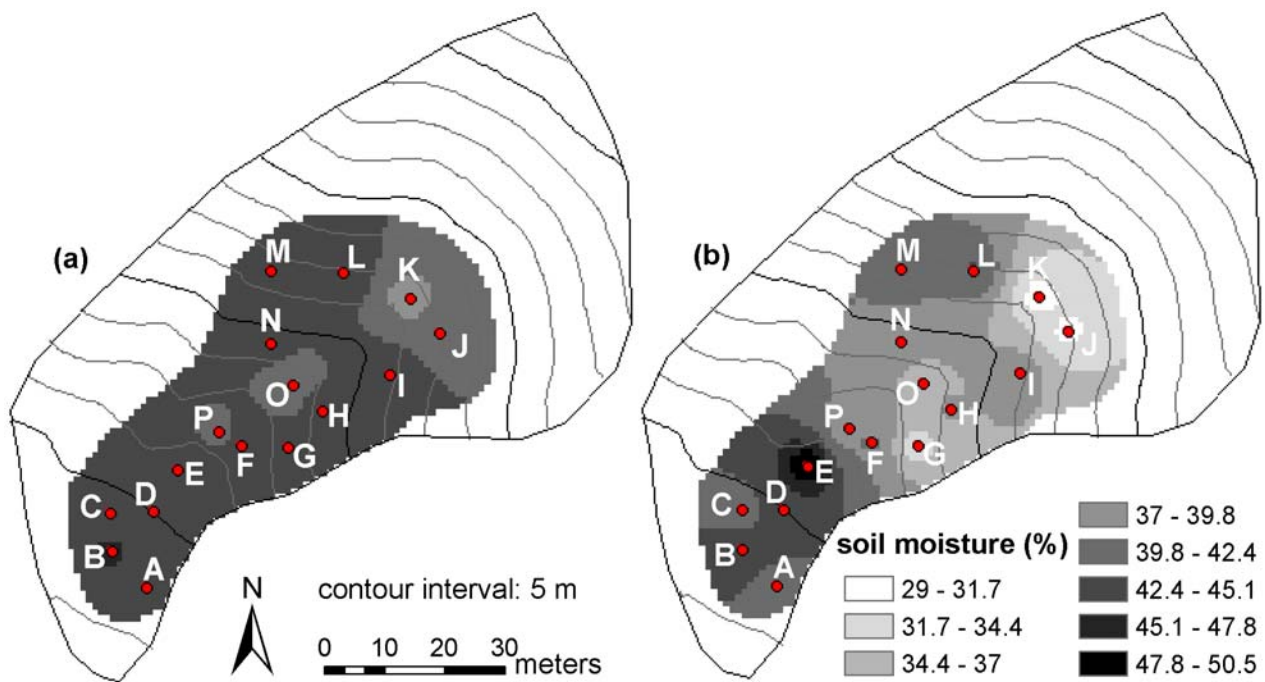


Fig. 6: Maps of mean soil moisture at Vallecola site at different depths. a) 0-6 cm, b) 0-12 cm.

References

- Cosh M.H., Jackson T.J., Bindlish R., Famiglietti J.S., Ryu D. (2005). Calibration of an impedance probe for estimation of surface soil water content over large regions. *Journal of Hydrology*, 311: 49-58.
- Cosh M.H., Jackson T.J., Bindlish R., Prueger J.H. (2003). Estimation of watershed scale soil moisture from point measurements during SMEX02. *First Interagency Conference on Research in the Watersheds*, October 27-30, 2003, Benson, Arizona.
- Cosh M.H., Stedinger J.R., Brutsaert W. (2004). Variability of surface soil moisture at the watershed scale. *Water Resources Research*, 40: W12513.
- Grayson R.B., Western A.W. (1998). Towards areal estimation of soil water content from point measurements: time and space stability. *Journal of Hydrology*, 207: 68-82.
- Martinez-Fernandez J., Ceballos A. (2005). Mean soil moisture estimation using temporal stability analysis. *Journal of Hydrology*, 312: 1-11.
- Starks J.P., Heathman G.C., Jackson T.J., Cosh M.H. (2006). Temporal stability of soil moisture profile. *Journal of Hydrology*, 324: 400-411.
- Stenger R., Barkle G., Burgess C. (2005). Laboratory calibrations of water content reflectometers and their in-situ verification. *Australian Journal of Soil Research*, 43: 607-615.
- Svetlitchnyi A.A., Plotnitskiy S.V., Stepovaya O.Y. (2003). Spatial distribution of soil moisture content within catchments and its modelling on the basis of topographic data. *Journal of Hydrology*, 277: 50-60.
- Tromp van Meerveld H.J., McDonnell J.J. (2006). On the interrelations between topography, soil depth, soil moisture, transpiration rates and species distribution at the hillslope scale. *Advances in Water Resources*, 29: 293-310.
- Walker J.P., Willgoose G.R., Kalma J.D. (2004). *In situ* measurement of soil moisture: a comparison of techniques. *Journal of Hydrology*, 29: 85-99.
- Western A.W., Grayson R.B., Blöschl G., Willgoose G.R., McMahon A. (1999). Observed spatial organization of soil moisture and its relation to terrain indices. *Water Resources Research*, 35: 797-810.
- Western A.W., Zhou S., Grayson R.B., McMahon T.A., Blöschl G., Wilson D.J. (2004). Spatial correlation of soil moisture in small catchments and its relationship to dominant spatial hydrological processes. *Journal of Hydrology*, 286: 113-134.
- Wilson J.D., Western A.W., Grayson R.B. (2004). Identifying and quantifying sources of variability in temporal and spatial soil moisture observations. *Water Resources Research*, 40: W02507.
- Wilson J.D., Western A.W., Grayson R.B., Berg A.A., Lear M.S., Rodell M., Famiglietti J.S., Wood R.A., McMahon A.T. (2003). Spatial distribution of soil moisture over 6 and 30 cm depth, Mahurangi river catchment, New Zealand. *Journal of Hydrology*, 276: 254-274.

TRACING OF THE WATER FLOWPATHS IN A MOUNTAINOUS WATERSHED

M. Šanda, L. Novák & M. Císlarová

CTU, FCE Prague, Thákurova 7, 166 29 Praha 6, Czech Republic.

Corresponding author: Martin Šanda, email: sanda@fsv.cvut.cz

ABSTRACT

Uhlířská (1.78 km²) is a typical watershed with crystalline bedrock forming Cambisols over 60% of the area of the Czech Basin. It is situated in a humid mountainous region where soils are typically shallow and highly permeable with preferential pathways. As a result of these facts, outflow caused by storms can be of a quick response and high magnitude. Monitoring of the outflow from the soil profile during the presented study showed instabilities that are typical for preferential flow. The observations clearly show that the soil profile plays a dominant role in the rainfall-runoff transformation. Data collection of the water regime in the soil profile and the subsurface flow is performed since 1998. To record also other factors of the hydrological cycle, the site is accompanied with a standard climatic station recording air temperature, net radiation, wind speed and humidity on a continuous basis. Quantitative measurements however lack the information about the nature of the transformation in space and time. Therefore additional techniques are used. As a supplement to geophysical measurements performed earlier, showing that bedrock is decayed and highly fractured, in July 2006 a new multi electrode geophysical method was employed in the watershed to provide a more detailed image of the examined subsurface.

Due to the fact that the behavior of water flows in the heterogeneous porous media and highly heterogeneous hydrogeological structure is not fully understood, a targeted study of these phenomena on the field scale has been launched in 2006. The tracing by means of the natural substances, as the only noninvasive tool available, to study the mechanisms of the outflow is in progress. For the study, stable oxygen isotope ¹⁸O and silica ions as SiO₂ were monitored in the rainfall (not applied to SiO₂), watershed outflow, subsurface stormflow, soil pore water and groundwater. Samples of the outflow from the watershed were taken on a regular daily basis, rainfall is taken daily according to its occurrence, groundwater and soil pore water have been sampled monthly. Subsurface stormflow was collected on the episode daily basis.

Keywords: flowpaths, natural tracer, soil profile, crystalline bedrock, mountainous watershed

Objectives

Focusing on the subsurface flow process, the aim of this research is to reveal the flow mechanism transforming rainfall into runoff in both variably saturated soil profiles on the instrumented hillslope and within the entire watershed. In order to get a better qualitative knowledge of the hydrological processes, natural elements tracing, together with state-of-the-art geophysical methods were employed.

Introduction

The experimental watershed Uhlířská (Fig. 1) is located in the northern part of the Czech Republic at a high elevation site within the Jizera Mountains. The watershed area is 1.87 km², of which 50% was

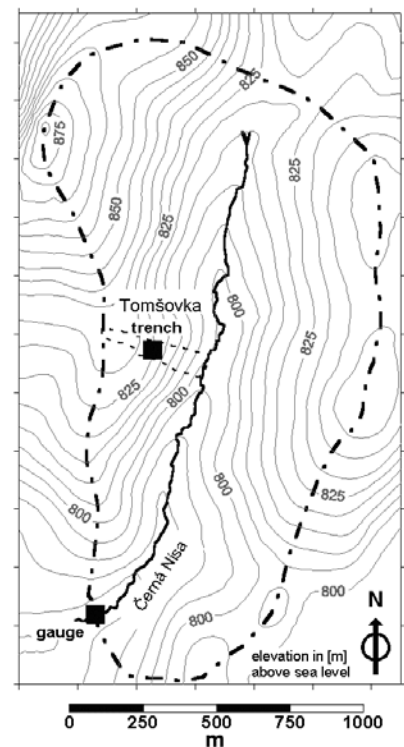


Fig. 1: Map of Uhlířská watershed

deforested in the early 80's. The average altitude is 822 m above sea-level. The average slope is 2.3% and the average length of the hillslope is 450 m. The watershed is located in a humid region, where the annual precipitation exceeds 1300 mm. At the hillslope site of interest, the soil profile is shallow and highly heterogeneous. It consists of about 80 cm of dystric cambisol, formed on the decayed fractured granite bedrock. On the hillslopes, topsoil (about 15 cm deep) is generally of a peaty character, covered by bush grass vegetation. The profile below the organic layer consists of 10 cm of the grey-black clayey loam, 25 cm of the brown sandy loam and 30 cm of the light brown loam with a high content of bedrock particles (Sanda et al., 2005).

To evaluate the subsurface flow mechanism, data monitoring of hydrological and climatic processes has been set with the focus on the processes in the soil profile. One typical hillslope location at Tomšovka has been outlined. The studied location is a transect, defined as a vertical plane of the soil profile running perpendicular to the surface contour lines. To obtain the information about the inner geometry of the subsurface flow region and its boundaries, several investigative measurements were performed.

Electrical resistivity tomography

The geophysical spatial measurement performed by means of the vertical electrical survey (Fig. 2) was chosen in 1997 to identify the bedrock surface geometry and the geological fracture system of the flow region.

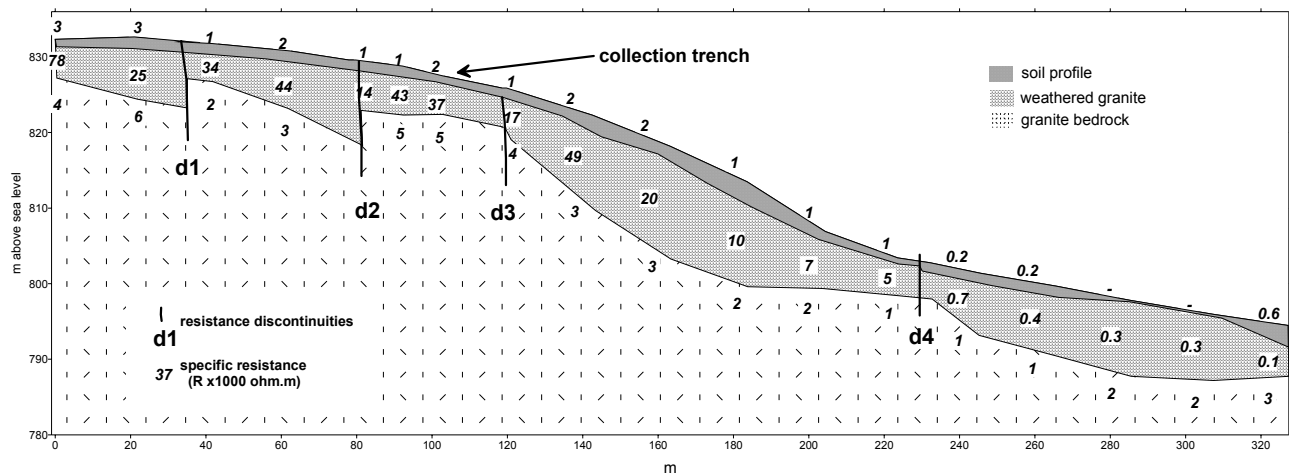


Fig. 2: Specification of the geological formation by vertical electrical survey.

In 2006, an additional geophysical survey was performed aiming at the identification of geological and hydrogeological structures by the determination of resistivity of the rock environment within the watershed. Resistivity is directly related to geological parameters, such as rock material, porosity and degree of saturation. Therefore by measuring it, the geological structure or water bodies such as aquifers, fissures and fractures can be revealed. The electrical resistivity tomography (ERT) is however a complementary method, interpretable in combination with hydrogeological knowledge and/or other geophysical measurements. ERT is based on the well known principle of a vertical electrical survey, applied in various combinations on a multicable with electrodes (Loke, 2000). The combinations of the span and operating of the electrodes is controlled by the central unit. As a response a 2D array of the apparent resistivity values is obtained.

Measurements at Uhlířská were performed in the period of July 18th to 27th 2006. For the measurements, ARES G4 by GF Instruments Brno as a control unit was used. A vertical 2D array of the electrical resistivity was measured by the Wenner-Schlumberger method. Six transects were surveyed within the watershed, mainly in the forestry management sector areas, to be able to keep straight lines. The geophysical profile/each transect is

located in a perpendicular direction to the watershed main axis formed by the stream of Černá Nisa. The layout is shown on Fig. 3.

Each profile is composed of several subprofiles. One subprofile is determined by a set of 5 multicables, each comprising 8 electrodes, installed into the soil profile in a 5 m span. Thus the total length of the combined cable with 40 electrodes makes a subprofile of 195 m. The next subprofile with an identical setup of the measurement is shifted by 120 m relative to the existing one. Therefore, the consequent subprofiles overlap by 75 m. This approach was chosen due to the limits of the measurement employing the general technique of a multicable. Here, with increasing depth, less resistivity values can be obtained. As an exception, the setup of the subprofiles in profile E comprised only 32 electrodes in the 5 m span, totalising a profile length of 155 m only. For the profiles A, B, C, D and F electrical resistivity was estimated down to the depth of 40 meters. In profile E, measurements were only made to the 30 m depth limit.

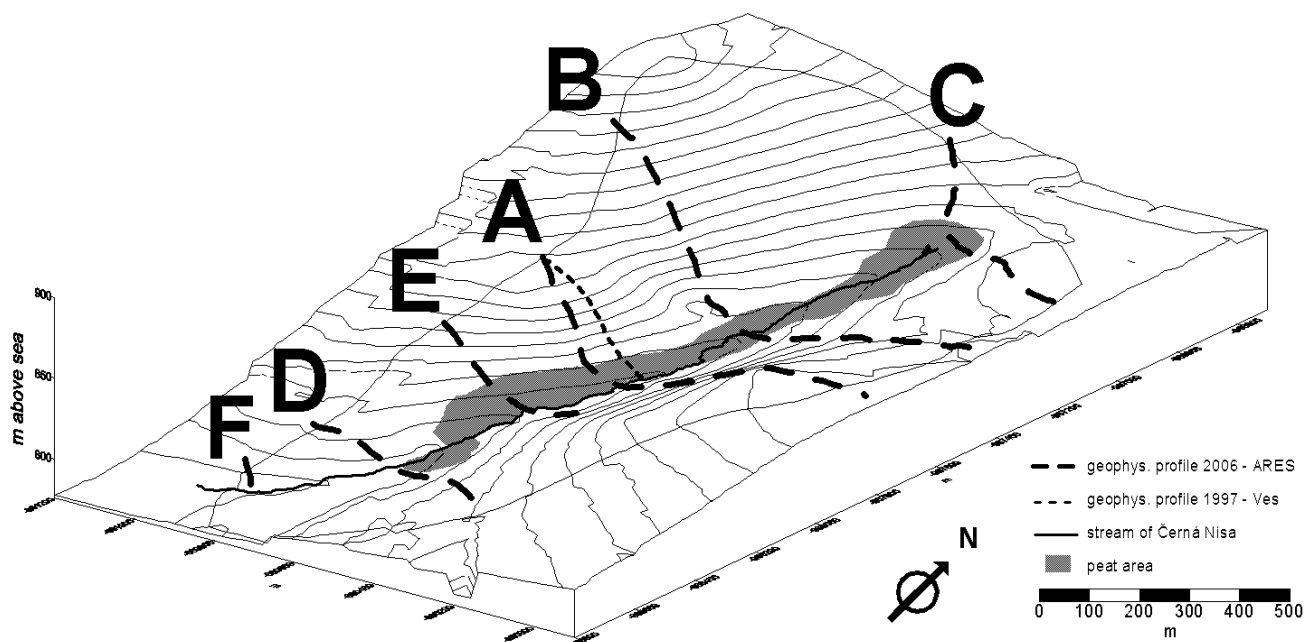


Fig. 3: Profiles of the electrical resistivity tomography.

Inverse mathematical modeling was used for the evaluation of the measurements. The Res2DInv software (Loke, 2000) was employed on this purpose. The inverse model seeks for the minimum difference of the apparent and calculated resistivity values. Due to the nature of the measurements and its analysis, there is a vast spectrum of equally good solutions, meeting the criteria of the minimal deviation of the measured and the modeled data. Therefore the iterative procedure with the condition of continuity of adjacent values is used. It tremendously reduces the set of possible solutions and makes the calculation stable. Resulting values of the electrical resistivity evaluated by Res2DInv for the profiles on the watershed Uhlířská range from 10^0 - 10^5 Ohm.m. Areas with significantly low values were detected. These regions are located in the bottom of the valley and are composed of glacial alluvial sediments, which are permanently saturated by groundwater (Fig. 4). Low resistivity values were also found in the upper parts of the watershed, where the saturation of the soil surface is not observed. Analyses most likely reflect deeper open saturated fractures in the bedrock. Their vertical extent often exceeds 25 meters. Another interpretation of measurements on the hillslopes takes into account the secondary rewetting of the soil and rock profile by the drainage of the surface forestry ditches towards the deeper zones. However, hillslope areas show mostly very high values of resistivity, which represents relatively drier or less porous weathered and solid igneous rock. To sum up, the results of the electrical imaging survey imply that water does not have to be necessarily drained directly towards the surface

stream in the valley, but in many cases is likely to be drained out of the boundaries of the hydrological watershed. Similarly, there are good reasons to believe that part of the total infiltrated water does not drain by the surface watershed outlet, but is drained in the sedimentary layers of the hydrogeological structure underneath. Neglecting these facts may impact the precision of the Uhlířská watershed water balance.

Geophysical measurements brought also particular information about the dimensions of the water body in the valley. Width of the detected aquifer is larger than it is apparent on the surface, where peat layers are present. It reaches usually 150-200 m in width. An aquifer is also present under surrounding hillslopes of the Cambisol profile, sometimes to a relatively significant depth of 40 m. Assuming the porosity of 30%, which is the estimate based on the values of the saturated moisture content obtained by means of the neutron probe for alluvial layers (Tachecí, 2002) and the length of the valley of approximately 2 km, there is about 2-4 mil. m³ of water always present in the valley aquifer. This amount relates to 1300-2600 mm of water when expressed as a rainfall depth. Such an amount equals the long term average rainfall of 1-2 years. Due to the fact that rainfall at Uhlířská is mostly transformed into a quick subsurface shallow runoff (Šanda et al., 2005) and the evapotranspiration also plays a significant role, deeper drainage towards the groundwater is only partial. This simple calculation indicates, that the water residence time in the aquifer is of at least several years. However, more precise estimates might be biased with the error comprising heterogeneity of the aquifer in terms of porosity and complicated geometry. The geophysical measurements performed serve as an indicator of the structure of the subsurface. Results showing the heterogeneity of the subsurface on Fig. 4 give a clear picture, indicating that a simple interpolation in between adjacent cross-sections could be misleading in terms of a precise depiction of the aquifer body. Despite the uncertainties, outcomes of the geophysical measurements build an important database, which is to be used for the water pathway evaluation by means of mathematical modeling.

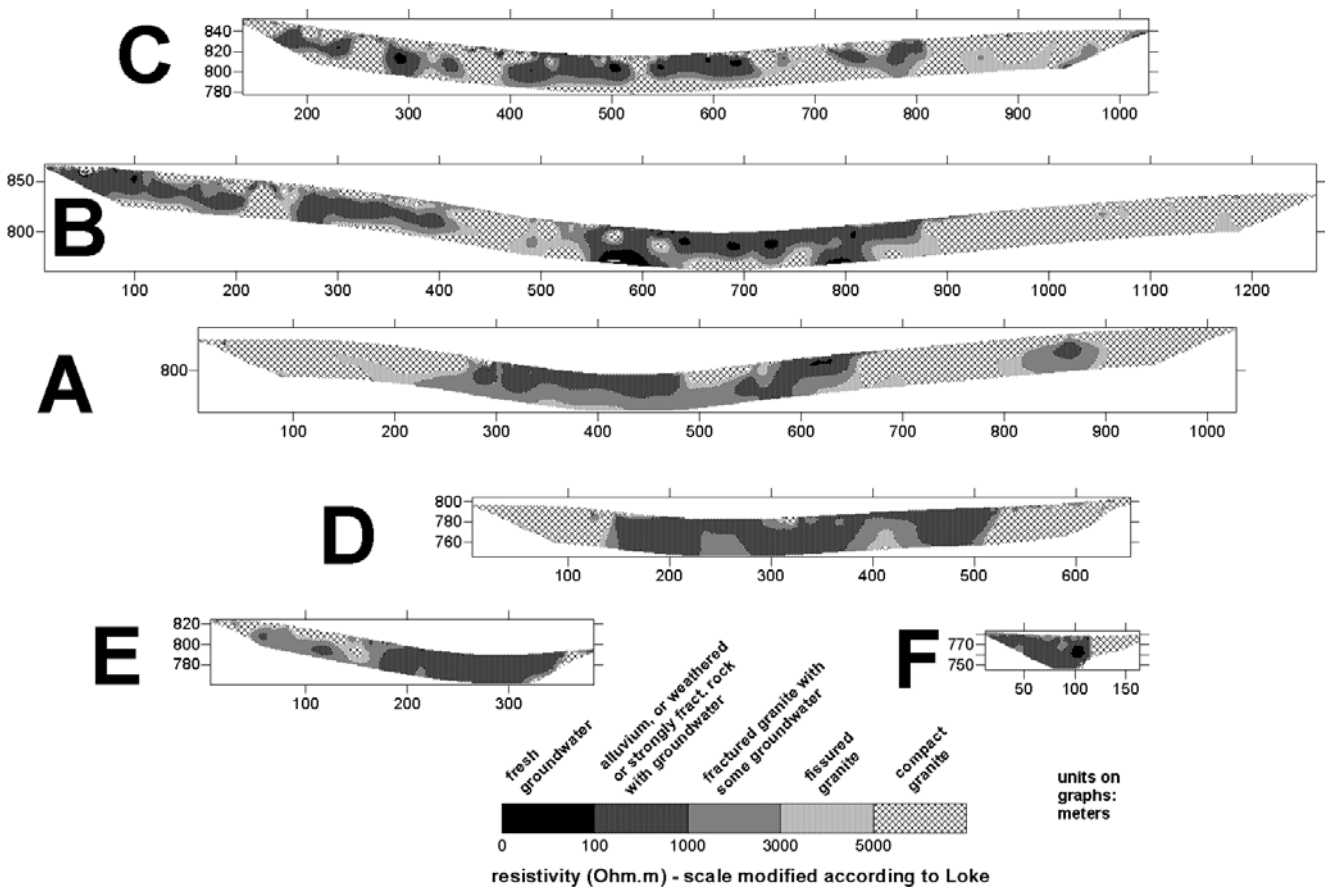


Fig. 4: Vertical cross-sections of the electrical resistivity determined by means of inverse modeling.

Observation of the rainfall-runoff episodes

Water flows in a heterogeneous porous environment, including the soil profile and hydrogeological saturated structure, cannot be satisfactorily described by using quantitative hydrological variables only. Therefore, alternative and more precise approaches must be applied. Tracing natural elements is a non-invasive procedure to better understand the flow mechanism, employing qualities permanently present in the watershed. The most common tools are the isotopic methods. The most frequent method is the tracing of ^{18}O (Kendall and McDonnell, 1998). From the geochemical point of view the best tracer to be used is silica in the form of SiO_2 (Kennedy, 1971).

Both of these elements are sampled at selected spots in the watershed since spring 2006 (Fig. 5). These activities cover the sample collection of rainfall, snowmelt, snow cover, subsurface stormflow, groundwater, soil water from suction lysimeters and the stream discharge at two gauging stations. Silica is not sampled in meteoric water (snowmelt and rainfall), since it is assumed not to be present.

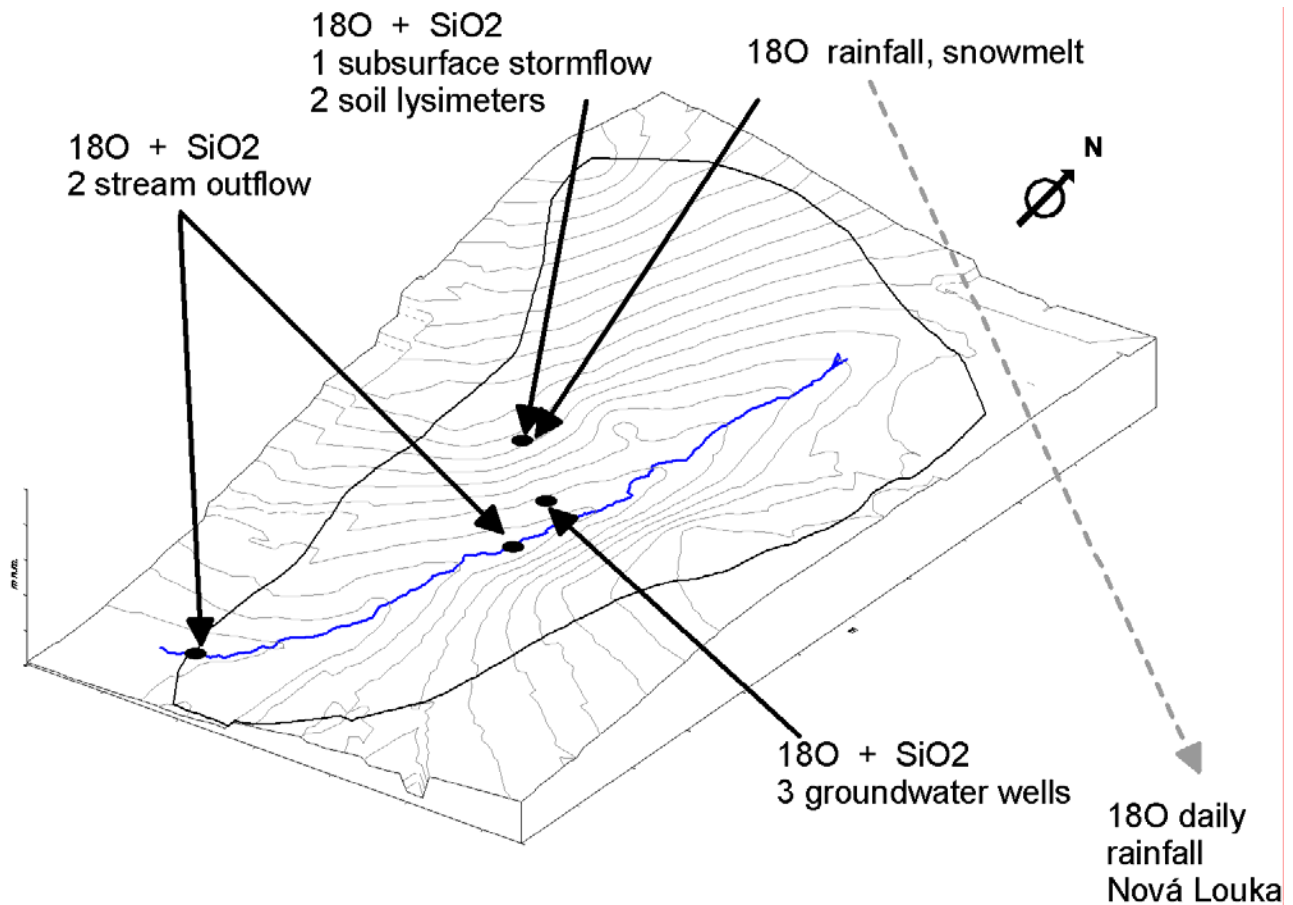


Fig. 5: Sampling scheme of ^{18}O and SiO_2 in water.

During 2006, two significant episodes were observed – the snowmelt in March-May and a frontal extreme storm in August. Snowmelt extended from 25.3.to18.5.06. Total amount of snow at the watershed was estimated in the range of 500-600 mm of the water equivalent. In addition, 81 mm of rain contributed since 12.4.06. Values of $\delta^{18}\text{O}$ and SiO_2 are presented in Fig. 6. There is a clearly visible impact of the melting water at the beginning of the episode. In the last phase, the subsurface trench outflow was also sampled. A complex picture indicates the replacement of pre-melt water in the subsurface outflow and the stream outflow as well.

Outflow is transformed by the variably saturated soil profile and then in the saturated aquifer. Variation of SiO_2 prior to the snowmelt shows the range of low concentration values, however since the commencement of the snowmelt, a rapid rise is observed.

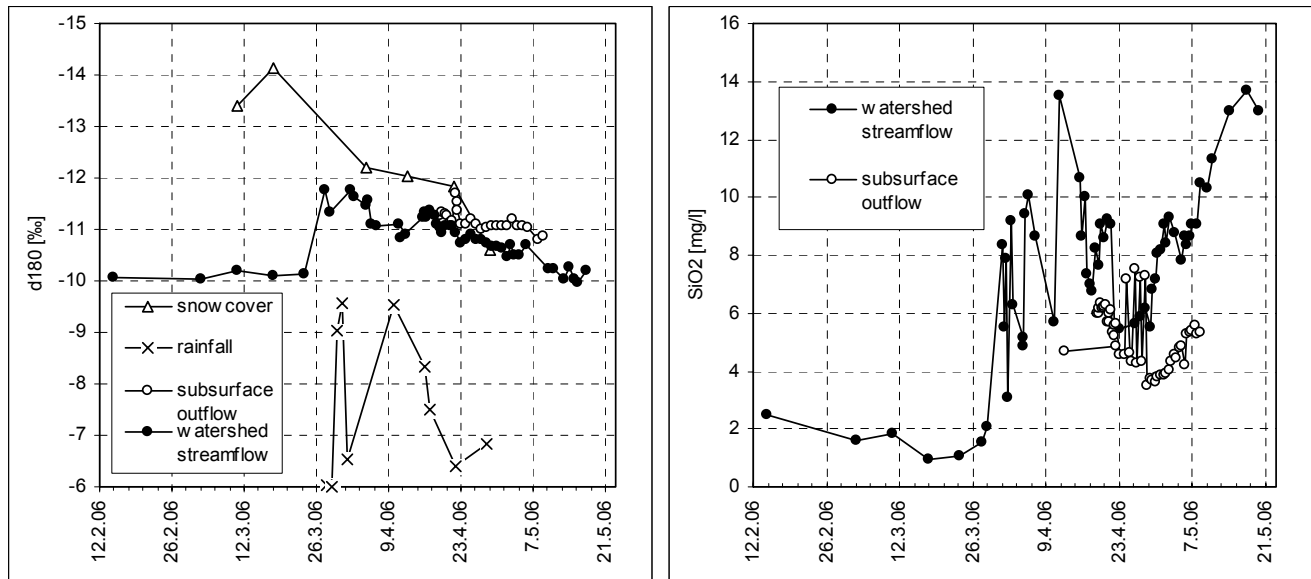


Fig. 6: Signature of $\delta^{18}\text{O}$ and SiO_2 concentration in water during snowmelt.

Possibly, the pre-event baseflow drains the aquifer via pathways, which are washed permanently, where silica can not be dissolved into the water at higher concentrations. The snowmelt water however replaces the soil water stagnant during the winter season in the soil profile. Given a sufficient time to dissolve silica in soil water, this contributes to its rapid rise in the streamflow. The silica concentration is depending on the antecedent water regime (length and intensity of previous events, thus forming conditions in the topsoil for an efficient silica dissolution. Water temperature plays an important role in silica dissolution, making the general picture even more complex.

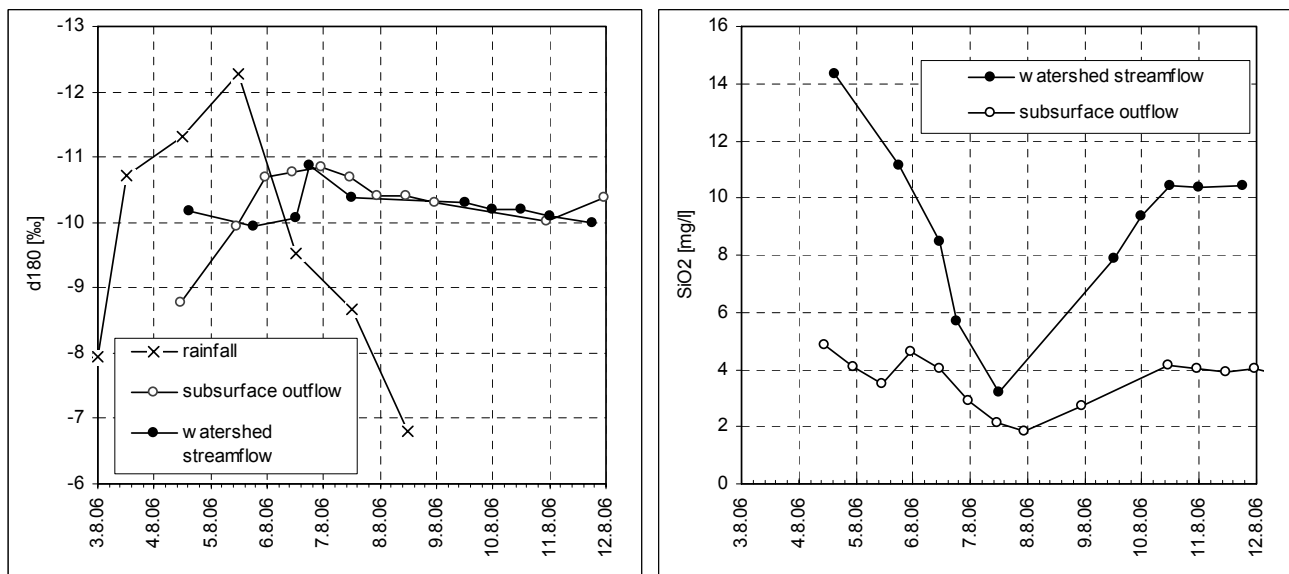


Fig. 7: Signature of $\delta^{18}\text{O}$ and concentration of SiO_2 in water during storm.

Significant storm rainfall occurred from 4.8. to 8.8.06, with 247 mm of rain, resulting in one of the two highest discharge values (estimated as 3.2-3.8 m³/s), since the start of the observations in 1981. The evolutions of $\delta^{18}\text{O}$ and SiO_2 are shown in Fig. 7. Here, the quicker response of the soil profile to the change of $\delta^{18}\text{O}$ is evident. It supports the hypothesis of a partial transformation of rainfall into runoff within the soil profile, employing preferential pathways. Later, the differences of the oxygen isotope signatures found in the subsurface stormflow and the watershed streamflow are diminishing, probably due to the extreme nature of the event, where most of the pre-event water is already displaced with the causal rainwater. The course of the concentrations of SiO_2 at the same checkpoints is similar. The fall of SiO_2 concentrations during the culmination of the flow is observed, due to the extreme amount of the outflow from the watershed and from the soil profile, lacking enough time for silica to dissolve in the shallow subsurface stormflow.

At the selected locations, soil water and shallow groundwater are sampled for the discussed elements during 2006. In the future, analyses of the samples are expected to help to determine the basic signature of the pre-event water.

Preliminary conclusions

1. The valley aquifer contains a large amount of water. It possibly serves as a buffer for mixing water of the varying signature of the oxygen isotope during a season.
2. Through the analysis of geochemical and isotope data, the hypothesis of the dominant impact of the subsurface flow on the watershed streamflow has been supported.
3. Quick subsurface flow from the soil profile and the total stream discharge exhibit similar dynamics.

Acknowledgements

This research is supported by the grant 205-06-0375 of the Czech Grant Agency.

References

- Kendall C., McDonnell J.J. (Eds.) (1998). *Isotope Tracers in Catchment Hydrology*. Elsevier Science B.V., Amsterdam.
- Kennedy V.C. (1971). Silica variation in stream water with time and discharge, in nonequilibrium systems in natural water chemistry. *Advances in Chemistry Series*, 106: 94–130.
- Loke M.H. (2000). *Electrical Imaging Surveys for Environmental and Engineering Studies. A Practical Guide to 2-D and 3-D Surveys*. GEOTOMO software guide, pp 59.
- Šanda M., Vogel T., Císlarová M. (2005). Hydrograph formation in a hillslope transect. Progress in surface and subsurface water studies at plot and small basin scale. *Proceedings of 10th ERB Conference*. Turin, Italy, 13-17 October 2004. *UNESCO IHP-VI, Technical documents in Hydrology*, 77: 21-26.
- Tachecí P., 2002. *Hydrologický režim malého horského povodí a posouzení vlivu odlesnění*. Dissertation thesis (in Czech) FCE, CTU, Praha.

REDUCTION OF PREDICTIVE UNCERTAINTY BY ENSEMBLE HYDROLOGICAL MODELLING OF DISCHARGE AND LAND USE CHANGE EFFECTS

H. Bormann¹, L. Breuer², B. Croke³, T. Gräff⁴, L. Hubrechts⁵, J.A. Huisman⁶, G.W. Kite⁷, J. Lanini⁸, G. Leavesley⁹, G. Lindström¹⁰, J. Seibert¹¹, N.R. Viney¹² & P. Willems¹³

¹University of Oldenburg, Department of Biology and Environmental Sciences, Germany. ²University of Gießen, Institute for Landscape Ecology and Resources Management, Germany. ³University of Canberra, Integrated Catchment Assessment and Management Centre, Australia. ⁴University of Potsdam, Institute for Geoecology, Germany. ⁵Lisec NV, Genk, Belgium. ⁶Forschungszentrum Jülich, ICG IV Agrosphere, Germany. ⁷Hydrologic Solutions, Pantymwyn, United Kingdom. ⁸University of Washington, USA. ⁹USGS, Denver, Colorado, USA. ¹⁰Swedish Meteorological and Hydrological Institute, Norrköping, Sweden. ¹¹Stockholm University, Department of Physical Geography and Quaternary Geology, Sweden. ¹²CSIRO Land and Water, Canberra, Australia. ¹³University of Leuven, Land Management, Hydraulics Laboratory, Belgium.

Corresponding author: Helge Bormann, email: helge.bormann@uni-oldenburg.de

ABSTRACT

This paper presents results of the LUCHEM project (“Assessing the impact of Land Use Changes on Hydrology by Ensemble Modelling”). In the framework of LUCHEM ten different hydrological catchment models are applied to the same data set from the central German Dill basin (693 km²). The models encompass a large range in complexity and input requirements. Calculating simple ensembles such as arithmetic mean or median value of all model results for every time step in simulations, which are comparable or even better than the best model for both, calibration and validation period. Quality measures of the ensembles such as root mean squared deviation, model efficiency and bias outperform the best single model in particular for the validation period. When applied to several projected land use change scenarios, there is broad agreement among the models on the expected hydrological change. An ensemble prediction of the effect of land use change well represents the mean behaviour of all models and eliminates the deviating behaviour of outlying models. Resuming, it can be stated that model ensembles can significantly reduce the predictive uncertainty in hydrological model application.

Keywords: model ensembles, catchment models, uncertainty, simulation quality, land use change

Introduction

Ensemble modelling, whereby predictions from several models are pooled to improve the accuracy of model predictions, has often been successfully applied in atmospheric sciences. One of the key aims of the ensemble approach is to reduce uncertainty in the simulation results. Most studies of the accuracy of multi-model ensemble forecasts in weather prediction report that they tend to outperform individual models (Georgakakos et al., 2004) and that multi-model ensembles tend to perform better than single-model ensembles (Ziehmann, 2000). Ensemble modelling has, however, received little attention in hydrology, where most modelling studies use only one model. There have been several studies comparing predictions from various hydrological models (e.g., Diekkrüger et al., 1995; Ye et al., 1997; Perrin et al., 2001). In general, these studies have been limited to describing how different models and modelling approaches can affect prediction accuracy, but usually have not considered the issue of pooling model predictions to arrive at some consensus prediction. Recently, some new cooperative initiatives such as DMIP in the United States and the international HEPEX project have begun to explore ensemble modelling in hydrology. Georgakakos et al. (2004) assessed predictions from seven distributed models applied to six catchments in the United States. They found that a simple mean of the five best models in each catchment consistently outperformed the best individual model, but that a weighted mean

ensemble, while usually better than the best model, was inferior to the simple mean ensemble. To date, none of these projects have considered ensemble modelling of the hydrological impacts of land use change. This paper describes the application of ten catchment models to the German Dill catchment and the quantification of land use change impacts within LUCHEM. The study was initiated by the Working Group on Resources Management of the University of Gießen (Germany).

Catchment models

Ten different models are applied to the Dill catchment. All of them have already been applied to environmental change studies and should have the capability to predict the impacts of land use change. In approximately decreasing order of complexity, they are: DHSVM (Wigmosta et al., 1994), MIKE-SHE (Refsgaard and Storm, 1995), TOPLATS (Peters-Lidard et al., 1997), WASIM-ETH (Niehoff et al., 2002), SWAT (Arnold et al., 1998), PRMS (Leavesley and Stannard, 1995), SLURP (Kite, 1978), HBV (Bergström, 1995), LASCAM (Sivapalan et al., 1996) and IHACRES (Jakeman et al., 1990). In terms of their spatial resolution and the overall number of model parameters, the models represent a broad cross-section of complexity ranging from fully distributed, physically-based models (DHSVM, MIKE-SHE) to lumped, conceptual models (e.g. IHACRES). Each model is driven by common digital maps of elevation (25 m resolution), soil type (soil map 1:50 000) and land cover (Landsat based). Daily precipitation (15 sites) and weather (2 sites) data are available. Rainfall interpolation and temperature lapse rate are standardised. The calibration methods and objective functions are different from model to model. All models are calibrated using observed discharges for the period 1983–1989, and model predictions are developed for the validation period 1990–1998. Three years of additional weather data (1980–1982) are available for model initialisation.

Study area

The Dill River in central Germany is a tributary of the Lahn River, which ultimately flows into the Rhine River. The Dill River at Asslar has a catchment area of 693 km². The topography of the catchment is characterised by low mountains and has an altitude range of 155–674 m. The mean annual precipitation of the Dill catchment varies from 700 mm in the south to more than 1100 mm in the higher elevation areas in the north. Just over half of the catchment is forested (with nearly even proportions of deciduous and coniferous species), while 21% is pasture, 9% is fallow, 6% is cropped (winter rape, winter barley, oats) and the remaining 10% is either urban or water. However, the pattern of land use across the catchment is highly fragmented, with an average field size of about 0.7 ha. Social, political and economic pressures are slowly transforming land uses away from cropping and leading to increasing pasture and forest cover. Streamflow in the Dill catchment is generated primarily from interflow with relatively little baseflow and surface runoff. Mean annual streamflow for the period 1983–1998 is 438 mm/a (about 48% of catchment-averaged precipitation).

Results

A time series of simulated discharges is shown in Fig. 1 for a part of the calibration period. Qualitatively, the models prove good predictions of the observed streamflow in terms of timing and magnitude of events. The envelope defined by the range of model predictions of all applied models encompasses the observed streamflow on 96% of days, with only little difference between calibration and validation periods. Scatter plots for two of the performance statistics (daily Nash-Sutcliffe efficiency and bias) for each of the models are shown in Fig. 2. Statistically, the best models are those with efficiencies approaching 1.0 and biases near 0%. For the calibration period, all but two of the models have negative biases. However, no model has an absolute bias as high as 10%. The calibration efficiencies range from about 0.6 to 0.9, with the less complex models tending to have higher values. For the validation period the relative positions of the models remain largely unchanged. However, most models show increased biases, to the extent that they are all now overpredicting. Most models also show increased efficiencies in the validation period. Ensemble predictions may be derived in

a number of ways. Two simple ensembles are the arithmetic mean and the median of the every day's model predictions. A third method is to select a number of models performing best in terms of model efficiency by again taking the arithmetic mean of these best models.

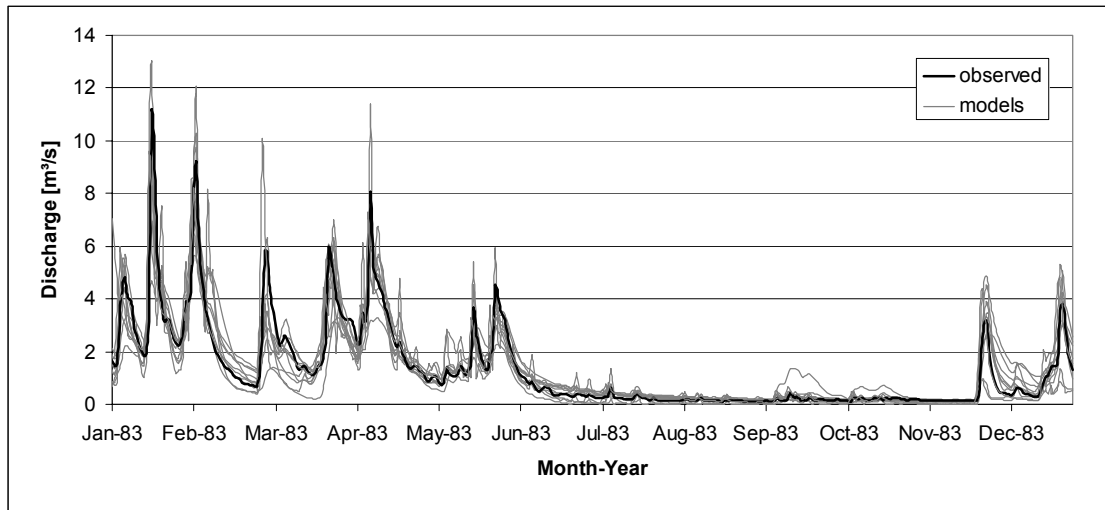


Fig. 1: Time series of observed streamflow (black line) in the Dill catchment, calibration period 1983, together with the various model predictions (grey lines - each line represents a different model).

The prediction capabilities of the introduced ensembles compared to those of the single models are shown in Fig. 2. For both calibration and validation periods in particular the simple ensembles perform as good as or even better than the best single model. In the calibration period the ensemble composed of the best three or five single models perform superior. But in the validation period the median ensemble performs as good as the ensemble constructed of the best performing three single models.

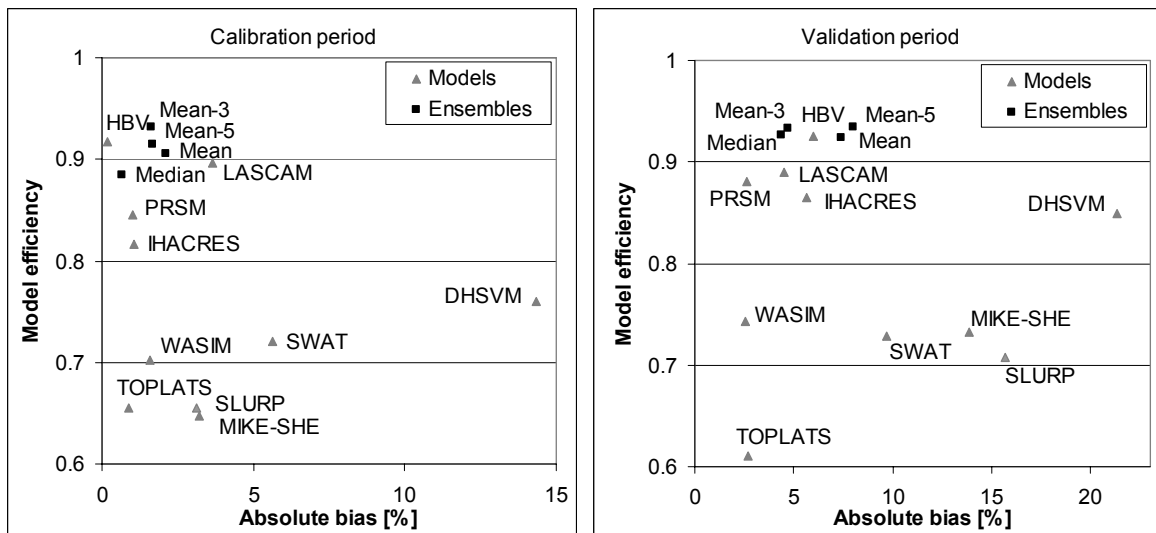


Fig. 2: Absolute bias and model efficiency of model predictions (grey triangles) and ensemble predictions (black squares) for the calibration (left) and validation period (right).

It can be concluded that the median ensemble is robust against outliers. The errors of the single models seem to be mostly symmetrically distributed around the observations. This indicates that statistically the median of the simulations is at least as good as the best performing model. The ensemble derived from the best five models

does not show an advantage compared to the arithmetic mean of all models. This indicates that large ensembles are more robust than small ensembles even if the small ensembles consist of the better performing models. These results are confirmed by application of further two quality measures (Fig. 3; coefficient of determination against root mean squared deviation, RMSD). For the validation period all simple model ensembles are at least as good as the best model with respect to the root mean squared deviation.

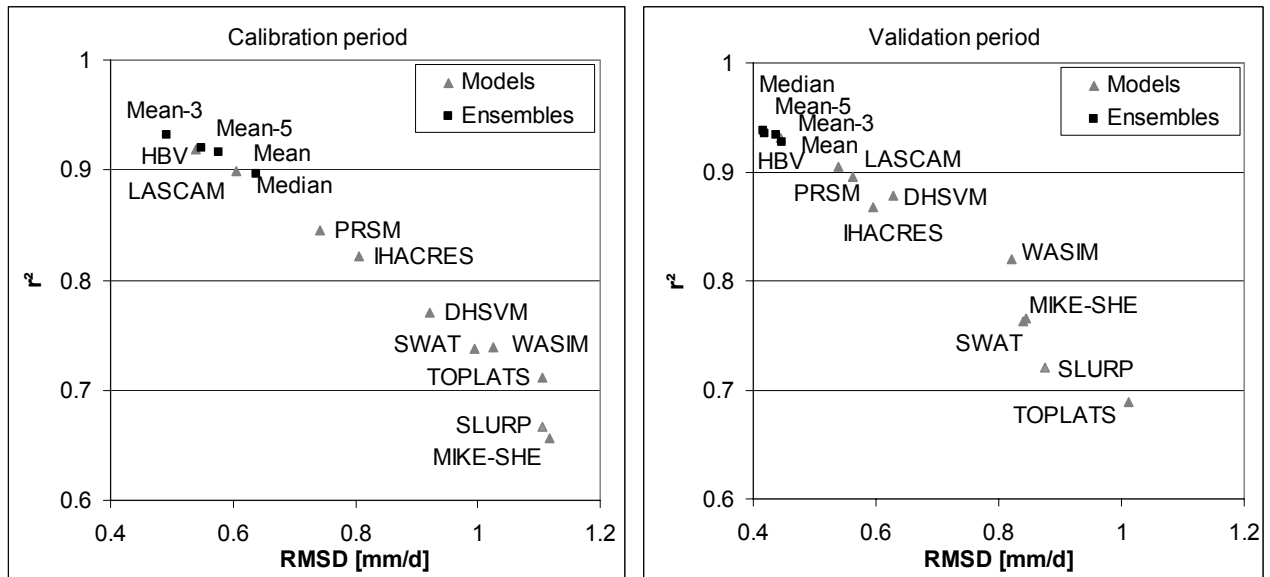


Fig. 3: Root mean squared deviation (RMSD) versus coefficient of determination (r^2) of model predictions (grey triangles) and ensemble predictions (black squares) for the calibration and validation period.

The median seems to be the best model ensemble for most of the quality measures for the validation period. The performance of the simple ensembles improves for mean and median ensembles from calibration to validation periods. The described advantages of simple model ensembles compared to single models are also valid for the prediction of extreme flows. The analysis of the annual high flows of the whole period (1983-1998) revealed that both peak flow rates and the discharge volume of peak flow events could be better predicted by simple model ensembles than by single calibrated models (Bormann, 2006). One reason for this behaviour might be that calibrating catchment models often focuses on the calibration of extreme events, e.g. using the Nash-Sutcliffe efficiency as the objective function. Then it can be assumed that the simulation results of the peak flow events, simulated by the ten different models, are normally distributed around the observations. If this assumption is valid, means and medians are close to the observations, and simple model ensembles outperform single models also for extreme events. Finally the question arises how many models are needed for reliable multi-model ensemble predictions. Fig. 4 gives an idea on the answer to this question for LUCHEM. A number of six models seems to be sufficient to obtain reliable predictions. Increasing the number of models does not considerably improve the performance of the worst ensemble.

Land use change scenarios

Three spatially distributed scenarios of land use change are considered and are based on land use simulations involving different field sizes. The three scenarios reflect predicted land uses associated with target field sizes of 0.5 ha, 1.5 ha and 5.0 ha (Weinmann et al., 2006). In general, increasing field sizes are associated with intensified land use and therefore with decreasing areas of forested land and increasing areas of cropland. The impacts of land use change are assessed by running all models calibrated for current land uses with the changed land use scenarios. Weather input from the period 1983-1998 and data sets on soils and topography are used.

The resulting annual discharge predictions for the Dill catchment are presented in Fig. 4. The slopes of the thin grey lines in Fig. 5 representing the 10 individual models are quite similar. This indicates that all models predict a similar relative increase in streamflow as field size increases.

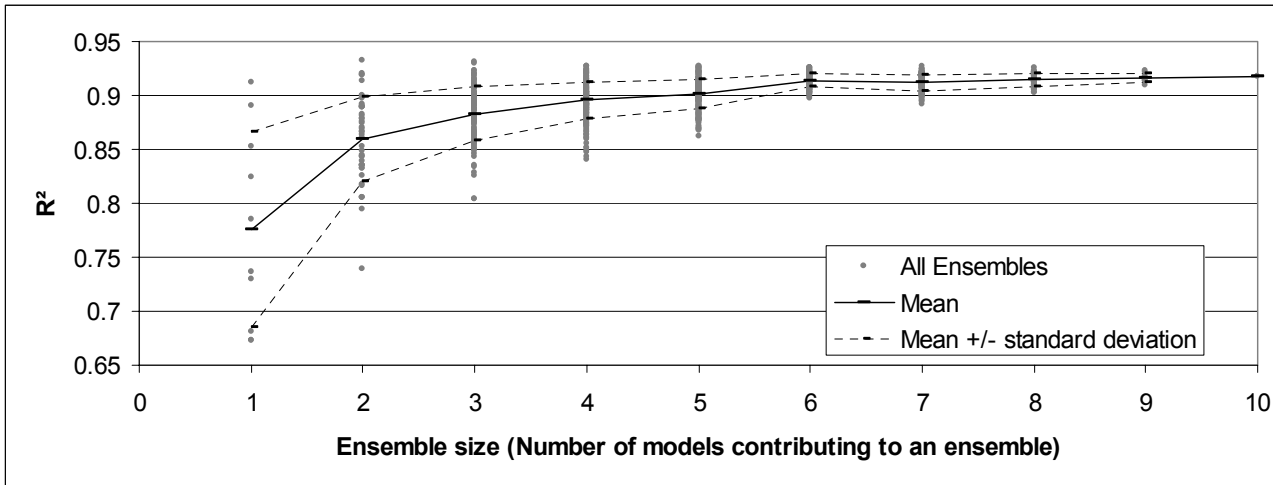


Fig. 4: Quality of ensemble predictions depending on the number of ensemble members (“mean” ensemble).

However, two of the ten models show simulated discharges that are substantially offset either above or below the majority of models. Computing the two simple model ensembles introduced before (arithmetic mean and median) leads to predictions which are within the majority of models. This confirms the hypothesis that large ensembles are more robust to outliers. In both median and mean cases, the offsets of the outlying models are compensated in the ensemble. For all 10 models the mean changes in mean annual streamflow, relative to the baseline case, for each of the three scenarios are 7 mm/a, 13 mm/a and 27 mm/a, respectively. For the third scenario, this represents an increase of about 6%. In percentage terms, the increases tend to be greater in summer (11% for the third scenario) than winter (5%), but the patterns of change among models and among scenarios for summer and winter (not shown) are similar to those for the entire year.

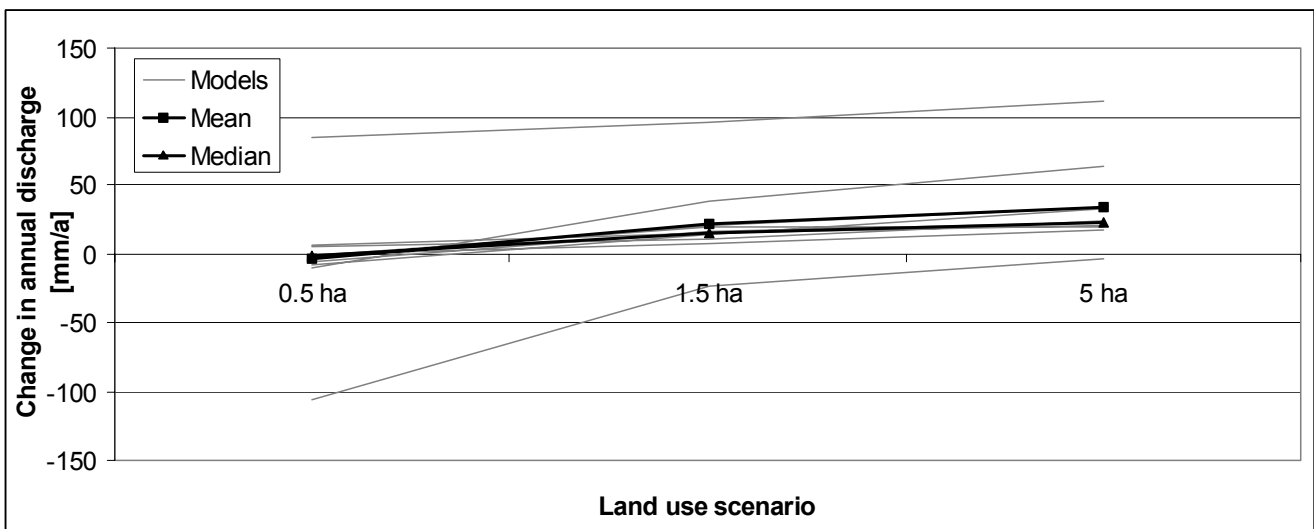


Fig. 5: Changes in predicted mean annual discharge for the three land use change scenarios relative to the current land use. Each line represents a different model.

Concluding remarks

In this investigation ten different models were applied to the same data set. All models provided good to moderate predictions for streamflow in the mesoscale Dill catchment. Calculating simple multi-model ensembles revealed that simple ensembles such as the median of daily simulated water flows outperformed the best single models in terms of objective functions. In the ensemble, the deficiencies in one model may be masked by the strengths in others or even by a compensating weakness in another model. That leads to the fact that predictive uncertainty is reduced by sampling models with a range of structural uncertainties, and plausibility of the model predictions is increased by ensemble calculation. In this study 96% of observed daily flows of the ensembles fall within the envelope defined by the daily range of predictions. This suggests that this envelope might be an approximate representation of the 95% confidence interval. Many other, more sophisticated ensembles can be readily envisaged. An obvious example would be a weighted mean ensemble with weights depending on calibration statistics (e.g. efficiency), so that the stronger models have a greater impact on the ensemble. However, it was not the aim of this study to find the best ensemble but to prove that already simple ensembles are helpful instruments for the reduction of predictive uncertainty. But, of course ensembles that do not include “well performing” models are not necessarily “good” ensembles. The study has demonstrated the advantages of a multi-model approach to reduce predictive uncertainty for the simulation of mean and extreme catchment outflow and to predict the impacts of land use change. Although the predicted streamflow changes in this study are quite small, there is strong agreement among the models on the direction and magnitude of change for each scenario.

Acknowledgements

This study has been supported by the German Science Foundation within the scope of the Collaborative Research Centre (SFB) 299.

References

- Arnold J.G., Srinivasan R., Muttiah R.S., Williams J.R. (1998). Large area hydrologic modelling and assessment. Part I: Model development. *Journal of the American Water Resources Association*, 34: 73-88.
- Bergström S. (1995). The HBV Model. In: V.P. Singh (Ed.), *Computer Models of Watershed Hydrology*, Water Resources Publications, Highland Ranch, Colorado, USA. 443–476.
- Bormann H. (2006). Verbesserung der Prognosequalität hydrologischer Modelle durch den Einsatz von Modell-Ensembles für die Simulation von Hochwasserereignissen. *Forum der Hydrologie und Wasserwirtschaft*, 15: 87-98.
- Diekkrüger B., Söndgerath D., Kersebaum K.C., McVoy C.W. (1995). Validity of agroecosystem models – A comparison of results of different models applied to the same data set. *Ecological Modelling*, 81: 3-29.
- Georgakakos K.P., Seo D., Gupta H., Schaake J., Butts M.B. (2004). Towards the characterization of streamflow simulation uncertainty through multimodel ensembles. *Journal of Hydrology*, 298: 222-241.
- Jakeman A.J., Littlewood I.G., Whitehead P.G. (1990). Computation of the instantaneous unit hydrograph and identifiable component flows with application to two small upland catchments. *Journal of Hydrology*, 117: 275-300.
- Kite G.W. (1978). Development of a hydrological model for a Canadian watershed. *Canadian Journal of Civil Engineering*, 5: 126-134.
- Leavesley G.H., Stannard L.G. (1995). The precipitation runoff modeling system — PRMS. In: V.P. Singh (Ed.), *Computer Models of Watershed Hydrology*, Water Resources Publications, Highland Ranch, Colorado, USA. 281–310.

- Niehoff D., Fritsch U., Bronstert A. (2002). Landuse impacts on storm-runoff generation: scenarios of land-use change and simulation of hydrological response in a meso-scale catchment in SW Germany. *Journal of Hydrology*, 267: 80-93.
- Perrin C., Michel C., Andréassian V. (2001). Does a large number of parameters enhance model performance? Comparative assessment of common catchment model structures on 429 catchments. *Journal of Hydrology*, 242: 275-301.
- Peters-Lidard C.D., Zion M.S., Wood E.F. (1997). A soil-vegetation-atmosphere transfer scheme for modeling spatially variable water and energy balance processes. *Journal of Geophysical Research*, 102: 4303-4324.
- Refsgaard J.C., Storm B. (1995). MIKE SHE. In: V.P. Singh (Ed.), *Computer Models of Watershed Hydrology*, Water Resources Publications, Highland Ranch, Colorado, USA: 809-846.
- Sivapalan M., Ruprecht J.K., Viney N.R. (1996). Water and salt balance modelling to predict the effects of land-use changes in forested catchments. 1. Small catchment water balance model. *Hydrological Processes*, 10: 393-411.
- Weinmann B., Schroers J.O., Sheridan P. (2006). Simulating the effects of decoupled transfer payments using the land use model ProLand. *Agrarwirtschaft*, 55: 248-256.
- Wigmosta M.S., Vail L.W., Lettenmaier D.P. (1994). A distributed hydrology-vegetation model for complex terrain. *Water Resources Research*, 30: 1665-1679.
- Ye W., Bates B.C., Jakeman A.J., Viney N.R., Sivapalan M. (1997). Performance of conceptual rainfall-runoff models in low-yielding catchments. *Water Resources Research*, 33: 153-166.
- Ziehm C. (2000). Comparison of a single-model EPS with a multi-model ensemble consisting of a few operational models. *Tellus*, 52A: 280-299.

STORM RUNOFF ESTIMATION BASED ON THE SOIL CONSERVATION SERVICE – CURVE NUMBER METHOD WITH SOIL MOISTURE DATA ASSIMILATION

L. Brocca, F. Melone & T. Moramarco

National Research Council, IRPI, Via Madonna Alta 126, 06128 Perugia, Italy.

Corresponding author: Luca Brocca, email: brocca@irpi.cnr.it

ABSTRACT

The estimation of the antecedent wetness conditions is one of the most important issues for event-based rainfall-runoff modeling. This study investigated the use of near-surface soil moisture observed in a small experimental plot to estimate the soil retention capacity parameter of the Soil Conservation Service - Curve Number (SCS-CN) method. The accuracy of the modified SCS-CN method coupled to a unit hydrograph transfer function was tested through a rainfall-runoff event that occurred in a small catchment in Central Italy where the plot is located. In particular, a linear relationship between the observed near-surface soil moisture and the soil retention capacity was detected with a high determination coefficient ($R^2=0.84$). Assimilating the observed soil moisture in the rainfall-runoff model both the runoff volume and the peak discharge were well predicted with errors less than 20%. The use of this simple rainfall-runoff model can be useful to address the prediction in poorly gauged catchments.

Keywords: soil moisture, antecedent wetness condition, rainfall-runoff modelling, SCS-CN method

Introduction

The simple assessment of parameters through rainfall data and easily available watershed characteristics has made the SCS-CN method for rainfall abstraction a widely applied approach in event-based rainfall-runoff modeling for estimating the outlet response in small watersheds and, more recently, it has been integrated into several models (Michel et al., 2005) such as SWAT (Arnold et al., 1990) and AGNPS (Young et al., 1994).

One of the greatest uncertainties of the method is linked to the assessment of the initial soil saturation known as the Antecedent Moisture Condition (AMC) (Ponce and Hawkins, 1996). In particular, Hawkins (1993) illustrated that the estimated runoff is more sensitive to the chosen CN than to the depth of the rainfall event. When the SCS-CN method is used to transform a rainfall frequency distribution to a runoff frequency distribution, the importance of the knowledge of AMC for estimation of the flood quantiles was highlighted by De Michele and Salvadori (2002). Moreover, Melone et al. (2001) found that the classical formulation based on the antecedent precipitation of 5 days furnished poor results with errors in the volume of direct runoff up to 100% in magnitude for five basins of the Upper Tiber river (Central Italy) ranging between 57 and 272 km². On this basis, an improved characterization of this variable can greatly enhance rainfall-runoff prediction (Goodrich et al., 1994).

Because soil moisture is the most important factor defining the initial abstraction of the CN method, an alternative solution to characterize the AMC would be to use direct measurements, or estimated values, of soil moisture prior to a rainfall event, rather than using antecedent rainfall. In particular, Jacobs et al. (2003), during an intensive field experiment (SGP97) for soil moisture and runoff monitoring, used remotely sensed soil moisture to adjust the CN for estimating runoff for five watersheds, ranging from 2.8 to 601.6 km², and characterized by a sub-humid climate. Assimilating the remotely sensed soil moisture a reduction of nearly 50% in the root mean square error on runoff volume was obtained. Recently, Huang et al. (2006), for four experimental plots characterized by different vegetation cover in the Loess Plateau of China (~250 m²), developed a relationship between CN and measured gravimetric soil moisture for 98 plot runoff events that

occurred in a 10-year period. Results indicated that the standard CN method underestimated runoff depths. On the contrary, considering the soil moisture-CN relationship a very significant increase in the model efficiency was obtained by the authors. As can be deduced, the above mentioned investigations required great efforts for soil moisture monitoring, whereas a methodology based on more easily available soil moisture data should be employed.

The objective of this work is to investigate the reliability of the SCS-CN method to simulate flood events in a small experimental catchment located in Central Italy where the AMC is estimated through the near-surface soil moisture continuously observed in a small inner plot.

Theoretical background

The partitioning of rainfall to runoff using the SCS-CN approach for a storm as a whole relies on the following empirical equation:

$$E = \frac{(P - F_a)^2}{P - F_a + S} \quad P \geq F_a \quad \text{Eq. 1}$$

where F_a is initial abstraction, S is potential maximum retention, E is effective rainfall depth and P is rainfall depth, all in length unit. The quantity F_a is assumed as a fraction of S with 0.2 S as the SCS standard value (Ponce and Hawkins, 1996). In particular, the potential maximum retention is estimated through rainfall-direct runoff data or by using the classical procedure based on a dimensionless curve number (CN) assessed as a function of land use, hydrological soil group and the total precipitation of the previous five days, API_5 .

Equation (1) is extended for the time evolution of effective rainfall rate, e , within a given storm as (Chow et al., 1988):

$$\begin{cases} e(t) = \frac{dE}{dt} = \frac{p(t)(P(t) - F_a)(P(t) - F_a + 2S)}{(P(t) - F_a + S)^2} & P(t) \geq F_a \\ e(t) = 0 & P(t) < F_a \end{cases} \quad \text{Eq. 2}$$

where p is the rainfall rate and $P(t) = \int_0^t p(\tau) d\tau$.

The discharge hydrograph at the basin outlet is given by the convolution of e and the geomorphological instantaneous unit hydrograph such as proposed by Gupta et al. (1980) where the lag-time is given by the empirical relationship proposed by Melone et al. (2002):

$$L = \eta 1.19 A^{0.33} \quad \text{Eq. 3}$$

with L lag-time (in hours), A the drainage area (in km²) and η a parameter to be calibrated. This relationship with $\eta=1$ was obtained for 26 watersheds in Central Italy ranging in extension between 12.4 to 4147 km². This result refers to the effective rainfall hyetographs determined by using the extended form of the two-term Philip infiltration equation in conjunction with a volume balance analysis (Corradini et al., 1986).

Study area and data

The Colorso experimental catchment is located in an inland region of central Italy and covers an area of 12.9 km² (see Fig. 1). The elevation ranges between 798 and 312 m a.s.l. at the outlet with a mean slope of 28%.

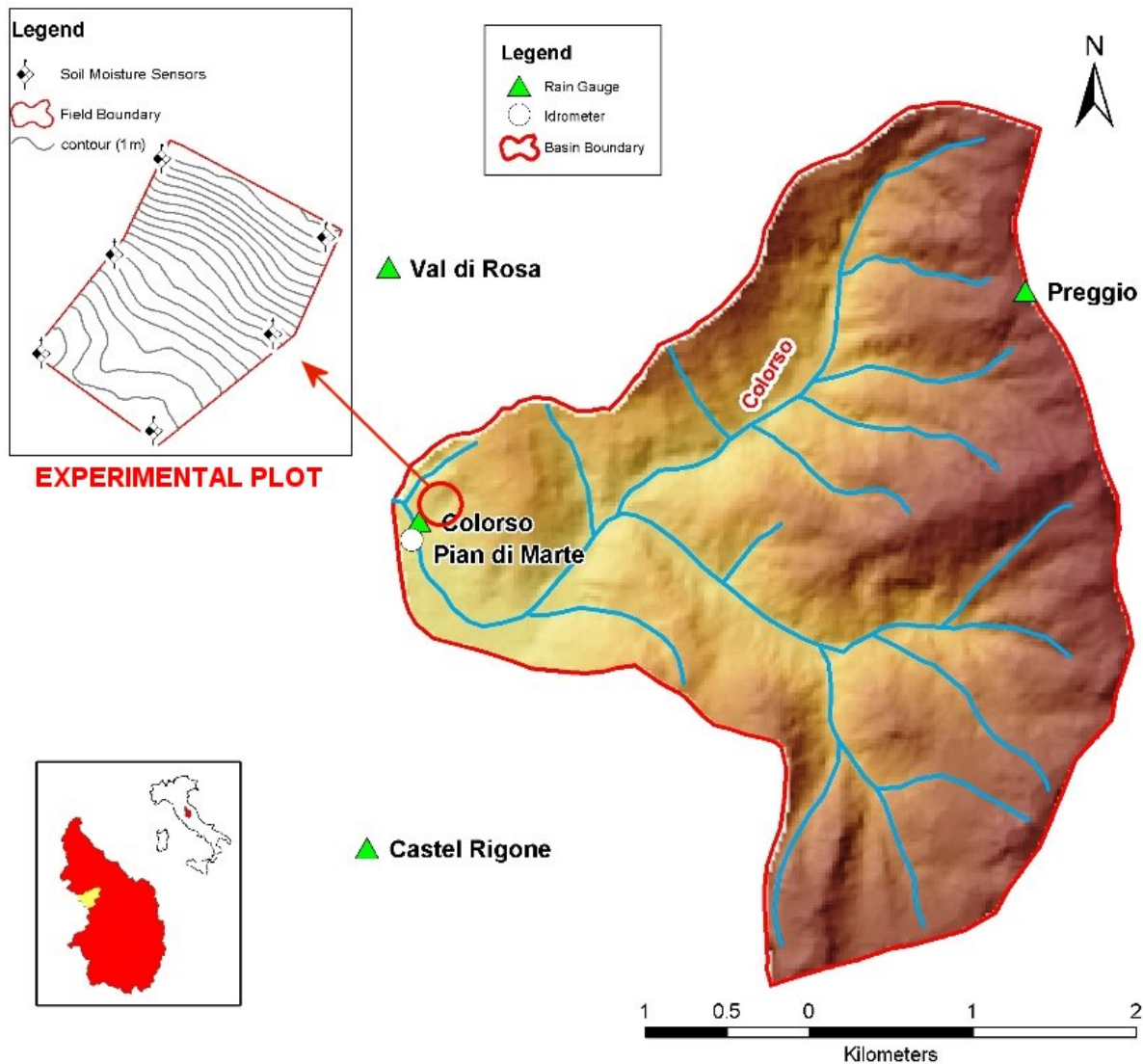


Fig. 1: The Colorso catchment with the location of the hydro meteorological stations and of the experimental plot for soil moisture monitoring.

The basin is characterized by a Mediterranean climate with a mean annual rainfall of ~ 930 mm. The lithology is a flysch formation and the land use is mainly forested and pasture. From these characteristics the catchment Curve Number for normal surface conditions was estimated to be 78.

Since July 2002, an experimental plot of nearly 1 ha for continuous soil moisture monitoring was set up inside the catchment near the outlet and close to the river (Brocca et al., 2004). The plot, covered by grass (permanent pasture), is characterized by a variable slope gradient, with mean and maximum slope of 12.6% and 70.0%, respectively. On the basis of the textural analysis, the soil was classified as sandy-loam to a depth of 0.3 m and silty-loam to a depth of 1.5 m (*Typic Haplustept*). In particular, the mean of the measured values by the six sensors buried at 10 cm depth are considered as the "observed" near-surface soil moisture. Four rain gauges and one hydrometric gauge are also operating in the basin (see Fig. 1).

Fifteen rainfall-runoff events were selected for this study and their main characteristics are summarized in Table 1. Specifically, the first ten of them were used for calibration and the remaining for model testing.

Table 1: Main characteristics of the selected rainfall-runoff events. P rainfall depth, p_{max} maximum rainfall intensity over 30 minutes, D rainfall duration, R_c runoff coefficient, R_d runoff depth, Q_p peak discharge and L lag time.

Date	Rainfall			Runoff			L (h)
	P (mm)	p_{max} (mm/h)	D (h)	R_c	R_d (mm)	Q_p (m ³ /s)	
Dec 17, 2002	18.3	3.7	10	0.09	1.58	0.86	8.6
Dec 28, 2002	14.9	12.4	3.5	0.05	0.81	0.75	7.1
Dec 31, 2002	19.7	3.6	12.5	0.08	1.57	0.57	8.2
Nov 27, 2003	24.3	8.6	11	0.08	1.96	1.34	4.5
Feb 19, 2004	30.5	3.6	21	0.06	1.75	0.49	3.3
Feb 22, 2004	16.0	3.4	11.5	0.12	1.89	1.05	3.9
Feb 26, 2004	24.5	10.6	7	0.22	5.42	3.18	3.0
Mar 7, 2004	18.5	5.3	12	0.11	2.00	0.98	3.4
Apr 17, 2004	8.2	8.4	2.5	0.04	0.34	0.40	5.5
Apr 19, 2004	35.7	11.0	12.5	0.29	10.23	7.09	2.2
Apr 11, 2005	27.4	7.2	9.5	0.12	3.38	2.31	4.1
Apr 16, 2005	29.5	5.5	11.5	0.14	4.03	2.15	3.6
Dec 3, 2005	19.0	11.9	7	0.24	4.64	6.01	3.1
Dec 6, 2005	16.6	4.5	7.5	0.25	4.17	3.16	3.6
Dec 9, 2005	26.4	3.9	15.5	0.27	7.17	3.12	1.9

Results and discussion

For each calibration event the optimal value of parameter η for the lag-time was computed along with the potential maximum retention assuming the knowledge of the direct runoff volume. As can be seen from Table 1, the lag-time exhibits a substantial variability but it was found to be dependent on the runoff magnitude in a physical consistent way. Fig. 2 shows that the lag-time is decreasing from small to large floods as the latter involve higher water depths and therefore large velocities. Moreover, floods of appreciable magnitude are characterized by a relatively small variability of the lag-time (Boyd, 1982). To make the model easier, a constant value of η equal to 0.8, corresponding to the more relevant floods, was derived from the calibration events.

The relation of S with the antecedent moisture condition is shown in Fig. 3. In particular, S was determined through the rainfall-runoff data and is denoted henceforth as "observed" potential maximum retention. The antecedent moisture condition was estimated by the API_5 index and by the saturation degree obtained through the near-surface soil moisture "observed" at the experimental plot, θ_i , and expressed as:

$$\theta_e = (\theta_i - \theta_r) / (\theta_s - \theta_r) \quad \text{Eq. 4}$$

where θ_r and θ_s are the residual and at saturation soil moisture, and fixed as the minimum and maximum "observed" value. As reported in previous investigations carried out in different regions (Brocca et al., 2005; 2007), a very weak relationship with the API_5 was observed, whereas with θ_i a determination coefficient of 0.84 was found (see Fig. 3). In particular, the relation between S and the "observed" soil moisture is given by (Chahinian et al., 2005):

$$S = (S_s - S_r)\theta_e + S_r \tag{Eq. 5}$$

where S_r and S_s are, respectively, the potential maximum retention for $\theta_i = \theta_r$ and $\theta_i = \theta_s$. Through the calibration events, S_r and S_s were found equal to 202.0 mm and 17.2 mm, respectively. These values are consistent with the S values corresponding to the dry and wet AMC ($S[CN(I)]=170.5$ mm, $S[CN(III)]=31.1$ mm) as derived with the CN method. Eq. (5) was used to compute the value of S from the soil moisture "observed" at the beginning of each event of the verification set.

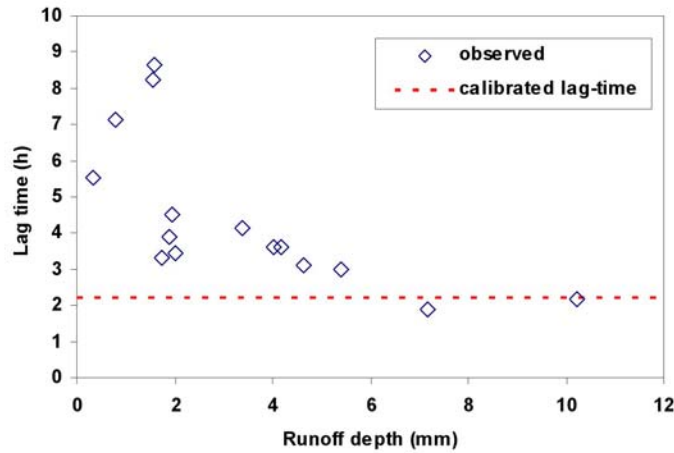


Fig. 2: Relationship between lag-time and runoff depth for the selected rainfall-runoff events.

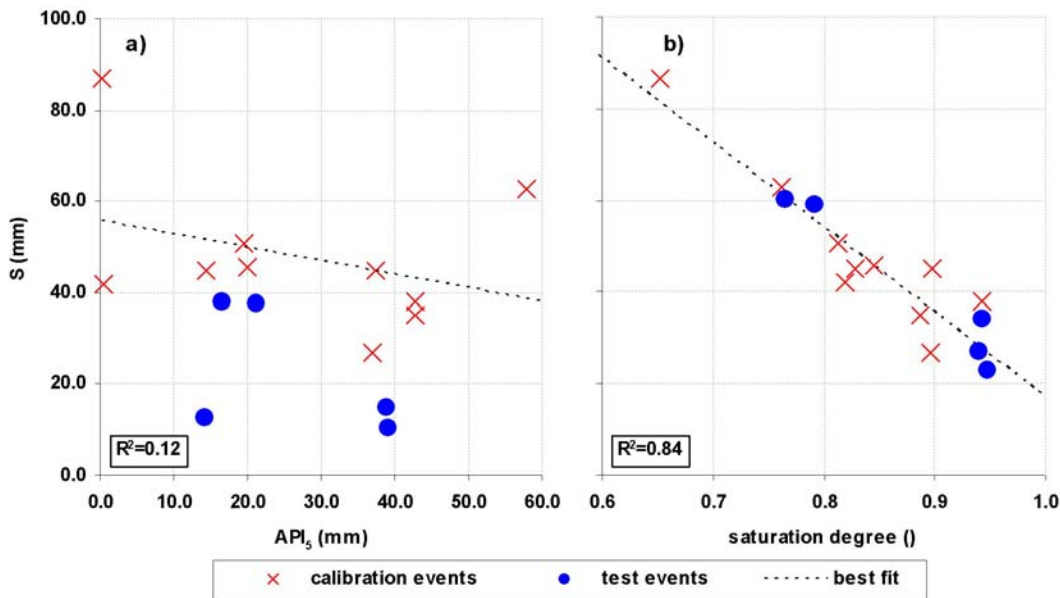


Fig. 3: "Observed" potential maximum retention, S , versus: a) antecedent precipitation index, API_5 , and b) saturation degree observed at the plot. The determination coefficient, R^2 , of best fit line for the calibration events is also shown.

Fig. 4 shows the observed and simulated direct runoff hydrographs for some of the calibration and test events. Model performance is shown in Table 2 in terms of error in direct runoff depth, direct peak discharge, peak time along with the Nash-Sutcliffe coefficient and the root mean square error. Table 2 reports also the value of

the potential maximum retention "observed" and estimated by eq. (5) along with the antecedent moisture condition used (API_5 and θ_i). We point out that some events of the calibration set show an overestimation of peak runoff and accordingly an underestimation of time to peak. It can be ascribed to the lag-time, which is considered constant, whereas this assumption is correct only for large flood events as discussed before (see Fig. 2).

Considering the test events, the model can be considered reliable in predicting both the runoff volume and the peak discharge with errors less than 20%. A very high efficiency, as expressed by the Nash-Sutcliffe coefficient, was observed for the whole set of events with a mean value of 83.5%. We note that the model performance remained almost accurate also for double peak and lower events, which were usually more difficult to predict. In order to show the advantages when using θ_i instead of API_5 , Fig. 2 reports also the estimated discharge through the model based on API_5 which may be affected by large errors with the Nash-Sutcliffe coefficient ranging between -120% and 87%.

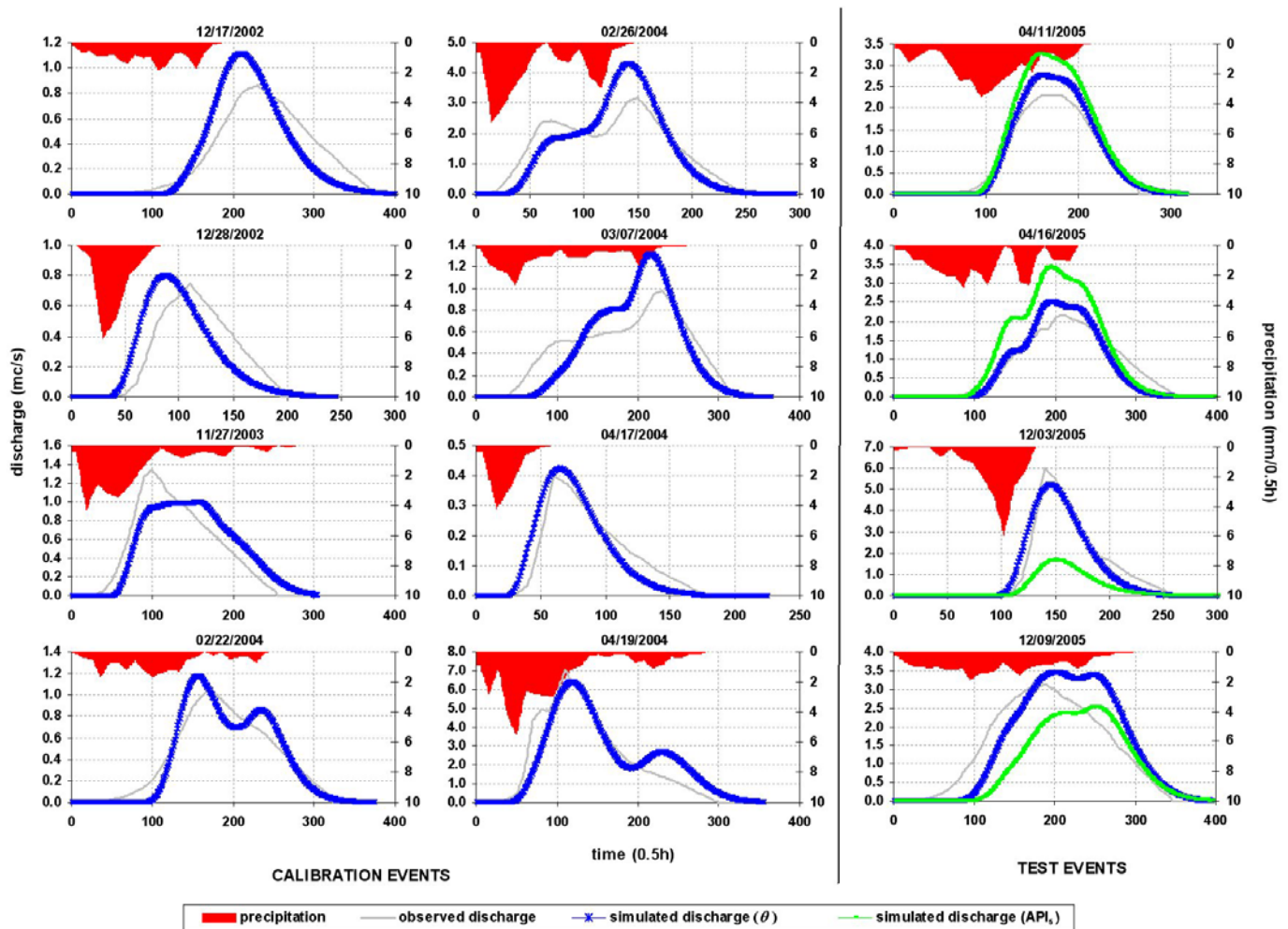


Fig. 4: Comparison of observed and simulated direct runoff hydrographs. For the test events the simulated discharge both using θ_i and API_5 is shown. The half-hourly rainfall pattern is also shown.

Table 2 : Errors on time to peak, ε_{tp} , direct peak discharge, ε_{Qp} , and direct runoff depth, ε_{Rd} , along with the Nash-Sutcliffe coefficient, NS, and the root mean square error, RMSE. The maximum potential retention given by eq. (5), S_{sim} , and computed with rainfall and runoff data, S_{obs} , is also reported. (For the other symbols see text)

date	S_{obs} (mm)	S_{sim} (mm)	API_5 (mm)	θ_i (cm ³ /cm ³)	ε_{Rd} (%)	ε_{Qp} (%)	ε_{tp} (h)	NS (%)	RMSE (m ³ /s)
Dec 17, 2002	45.6	45.6	20.0	36.6	/	29.8	-2.0	81.2	0.16
Dec 28, 2002	44.9	48.8	14.4	36.0	/	7.2	-2.3	67.8	0.16
Dec 31, 2002	50.6	51.7	19.6	35.5	/	55.5	-0.9	78.1	0.14
Nov 27, 2003	62.7	61.1	57.8	34.0	/	-25.6	5.7	76.8	0.19
Feb 19, 2004	86.8	81.4	0.3	30.6	/	44.5	0.4	73.9	0.11
Feb 22, 2004	35.0	37.9	42.9	37.8	/	12.9	-1.4	92.1	0.11
Feb 26, 2004	38.1	27.7	42.8	39.5	/	35.1	-0.9	82.6	0.57
Mar 07, 2004	41.9	50.4	0.4	35.8	/	35.2	-1.4	78.3	0.20
Apr 17, 2004	26.7	36.4	36.9	38.1	/	5.8	0.5	89.3	0.05
Apr 19, 2004	44.8	36.1	37.5	38.1	/	-9.5	0.9	82.4	0.82
Apr 11, 2005	59.0	55.7	16.4	34.9	12.7	19.8	-0.9	95.7	0.22
Apr 16, 2005	60.0	60.4	21.1	34.1	-1.4	17.3	-1.6	91.4	0.26
Dec 03, 2005	27.2	28.2	14.1	39.5	-4.5	-13.0	0.5	94.4	0.39
Dec 06, 2005	22.9	24.8	39.0	40.1	-9.7	13.0	0.8	88.6	0.41
Dec 09, 2005	34.1	32.1	38.9	38.8	7.5	10.9	1.2	80.3	0.61

Conclusion

The antecedent wetness condition at the catchment scale estimated through the knowledge of the near-surface soil moisture in a small area can be considered reliable in estimating the hydrological response in terms of both runoff volume and peak runoff. Moreover, the extreme values of the potential maximum retention were found consistent with those derived by the classical CN method. Based on these results, the plot could be representative of the experimental basin but this needs to be verified using, for example, the remote sensing technology. This issue will be addressed through further investigations along with the analysis on the catchment area for which the experimental plot can be considered representative.

References

- Arnold J.G., Williams J.R., Nicks A.D., Sammons N.B. (1990). In *SWRRB - A Basin Scale Simulation Model for Soil and Water Resources Management*. Texas A&M University Press: College Station, Texas.
- Boyd M.J. (1982). A linear branched network model for storm rainfall and runoff. In: Singh V.P. (ed.), *Rainfall-Runoff Relationship*, Water Resources Publications, Littleton, Colorado. 111-124.
- Brocca L., Melone F., Moramarco T. (2004). Soil water content monitoring in an experimental basin in Central Italy. *Proceedings of the Euromediterranean Conference ERB 2004*, 13-17 Ottobre 2004, Torino. *UNESCO IHP-VI Technical Documents in Hydrology*, 77: 48-51.
- Brocca L., Melone F., Moramarco T. (2005). Empirical and conceptual approaches for soil moisture estimation in view of event-based rainfall-runoff modeling. *UNESCO -IHP - VI, Technical Documents in Hydrology* 77: 1-8 .
- Brocca L., Melone F., Moramarco T. (2007). On the estimation of antecedent wetness conditions in rainfall-runoff modelling. *Hydrological Processes*, in press.
- Chahinian N., Moussa R., Andrieux P., Voltz M. (2005). Comparison of infiltration models to simulate flood events at the field scale. *Journal of Hydrology*, 306: 191-214.

- Chow V.T., Maidment D.R., Mays L.W. (1988). *Applied Hydrology*. McGraw-Hill. Chap. 5.2.
- Corradini C., Melone F., Singh V.P., Ubertini L. (1986). Geomorphologic approach to synthesis of direct runoff hydrograph from the Upper Tiber River basin. In: V.K. Gupta, I. Rodriguez-Iturbe, E.F. Wood (Eds.), *Scale Problems in Hydrology*. Reidel, Dordrecht. 57-79.
- De Michele C., Salvadori G. (2002). On the derived flood frequency distribution: analytical formulation and the influence of antecedent soil moisture condition. *Journal of Hydrology*, 262: 245-258.
- Goodrich D.C., Schmugge T.J., Jackson T.J., Unkrich C.L., Keefer T.O., Parry R., Bach L.B., Amer S.A. (1994). Runoff simulation sensitivity to remotely sensed initial soil water content. *Water Resources Research*, 30: 1393-1405.
- Gupta V.K., Waymire E., Wang C.T. (1980). A representation of an instantaneous unit hydrograph from geomorphology. *Water Resources Research*, 16: 855-862.
- Hawkins R.H. (1993). Asymptotic determination of runoff curve numbers from data. *Journal of Irrigation and Drainage*, 199: 334-345.
- Huang M., Gallichand J., Dong C., Wang Z., Shao M. (2006). Use of soil moisture data and curve number method for estimating runoff in the Loess Plateau of China. *Hydrological Processes*, in press.
- Jacobs J.M., Myers D.A., Whitfield B.M. (2003). Improved rainfall/runoff estimates using remotely sensed soil moisture. *Journal of the American Water Resources Association*, 4: 313-324.
- Melone F., Corradini C., Singh V.P. (2002). Lag prediction in ungauged basins: an investigation through actual data of the upper Tiber River valley. *Hydrological Processes*, 16: 1085-1094.
- Melone F., Neri N., Morbidelli R., Saltalippi C. (2001). A conceptual model for flood prediction in basins of moderate size. In: M.H. Hamza (Ed.), *Applied Simulation and Modelling*, IASTED Acta Press, Marbella (SP): 461-466.
- Michel C., Andreassian V., Perrin C. (2005). Soil conservation service curve number: how to mend wrong soil moisture accounting procedure? *Water Resources Research*, 41: W02011.
- Ponce V.M., Hawkins R.H. (1996). Runoff curve number: Has it reached maturity? *Journal of Hydrologic Engineering*, 1: 11-19.
- Young R.A., Onstad C.A., Bosch D.D., Anderson W.P. (1994). *AGNPS User's Guide. Agricultural Nonpoint Source Pollution Model*, version 4D03, July. USDA-NRS-NSL, Oxford, MS.

RAINFALL–STREAMFLOW MODELS FOR UNGAUGED BASINS: UNCERTAINTY DUE TO MODELLING TIME-STEP

I.G. Littlewood

Centre for Ecology and Hydrology, Wallingford, OXON, OX10 8BB, United Kingdom.

Corresponding author: Ian Littlewood, email: ianlittlewood505@btinternet.com

ABSTRACT

The extent to which the five parameters of a unit-hydrograph-based rainfall–streamflow model vary with modelling time-step is demonstrated for a 10.6 km² catchment in Wales. As the data time-step decreases from 24 hours to one hour, the calibrated parameters change by between 52% and 81%. The impact of time-step-dependent model parameters on the uncertainty in statistical relationships linking a model parameter and catchment properties is discussed. A simple method is described for normalising the parameters to give time-step-independent values. The results are discussed in terms of model parameter regionalisation towards estimation, from rainfall, of continuous streamflow in ungauged (flow) basins. Possible future work is outlined to compare the normalised model parameters presented in the paper with similar results from a modelling methodology presented by other authors that yields time-step-independent model parameters directly from analysis of discrete data.

Keywords: continuous rainfall-streamflow modelling, regionalisation, uncertainty, ungauged basins, unit hydrographs

Introduction

A popular approach to systematic estimation of river flows from rainfall in ungauged (flow) basins, regionally or nationally, has four main steps (omitting finer detail in the interests of brevity). In Step 1, a rainfall–streamflow model (m parameters) is calibrated for many (n) catchments. Statistical relationships (sample size n) are established in Step 2 between the m th model parameter and a few well-chosen catchment properties such as stream density, slope, etc. A different set of catchment properties might be used for each of the m statistical relationships. In Step 3, rainfall–streamflow model parameters for ungauged (flow) catchments are estimated using the regionalisation relationships established in Step 2. Flow in an ungauged catchment is estimated in Step 4 from rainfall and the rainfall–streamflow model parameters estimated from catchment properties in Step 3. Sefton and Howarth (1998) give an example of applying Steps 1 to 4.

Sources of uncertainty in a regionalisation scheme derived by Steps 1 to 4 include rainfall and streamflow measurement errors, the structure of the rainfall–streamflow model and uncertainties in its parameters, choice of catchment properties, and uncertainties in the regionalisation equations in Step 2.

The International Association of Hydrological Sciences (IAHS) Prediction in Ungauged Basins (PUB) Decade (<http://pub.iwmi.org>) has ‘reduction of predictive uncertainty’ as a cross-cutting objective, so all sources of uncertainty in regionalisation schemes are targets for better understanding and reduction of their impacts. In the context of gauged and ungauged UK catchments, the author has already discussed some aspects of uncertainty in (a) regionalised unit hydrographs for flood event hydrology and (b) the parameters of a continuous simulation rainfall-streamflow model (Littlewood, 2003; 2004). This paper addresses an aspect of uncertainty in rainfall-streamflow model parameter regionalisation that has, to date, received little attention in the hydrological research literature, i.e. the dependency of rainfall–streamflow model parameters on the data time-step employed for model calibration.

Constraints on the resources available for deriving regionalisation schemes for systematic estimation of continuous hydrographs at ungauged sites (e.g. Sefton and Howarth, 1998) have often led to the use of readily available daily data for calibrating rainfall–streamflow models in Step 1 (e.g. the use of flow data from the UK

National River Flow Archive, <http://www.ceh.ac.uk/data/nrfa/index.html>). A given model structure calibrated using a given data time-step will, of course, have different parameters for different catchments exhibiting different rainfall-streamflow dynamics. However, a discrete-time model calibrated for a particular catchment will yield different parameters according to the data time-step employed. When a common data time-step is used for all catchments for which rainfall-streamflow models are calibrated (Step 1), a source of uncertainty therefore arises in the statistical relationships between a model parameter and catchment properties (Step 2). As a contribution to PUB via its Top-Down modelling Working Group (<http://www.stars.net.au/tdwg/>), this paper demonstrates the extent to which the parameters of a rainfall-streamflow model, for a small research catchment, vary with the time-step of the data used for model calibration. A simple method is then outlined for normalising the model parameters to render them independent of the data time-step used for model calibration. The paper discusses implications of the data time-step-dependency of rainfall-streamflow model parameters in the context of uncertainty in flows in ungauged basins estimated systematically from catchment properties.

The catchment and modelling scheme

The Wye at Cefn Brwyn is a 10.6 km², predominantly open moorland, catchment draining the headwaters of the River Wye in mid-Wales (Fig. 1). It is one of the wettest gauged basins in England and Wales; mean annual rainfall is about 2490 mm, of which about 87% leaves the catchment as streamflow (NERC, 2003). The catchment is one of the Plynlimon research basins operated by the Centre for Ecology and Hydrology (e.g. Brandt et al., 2004; Robinson and Dupeyrat, 2005).

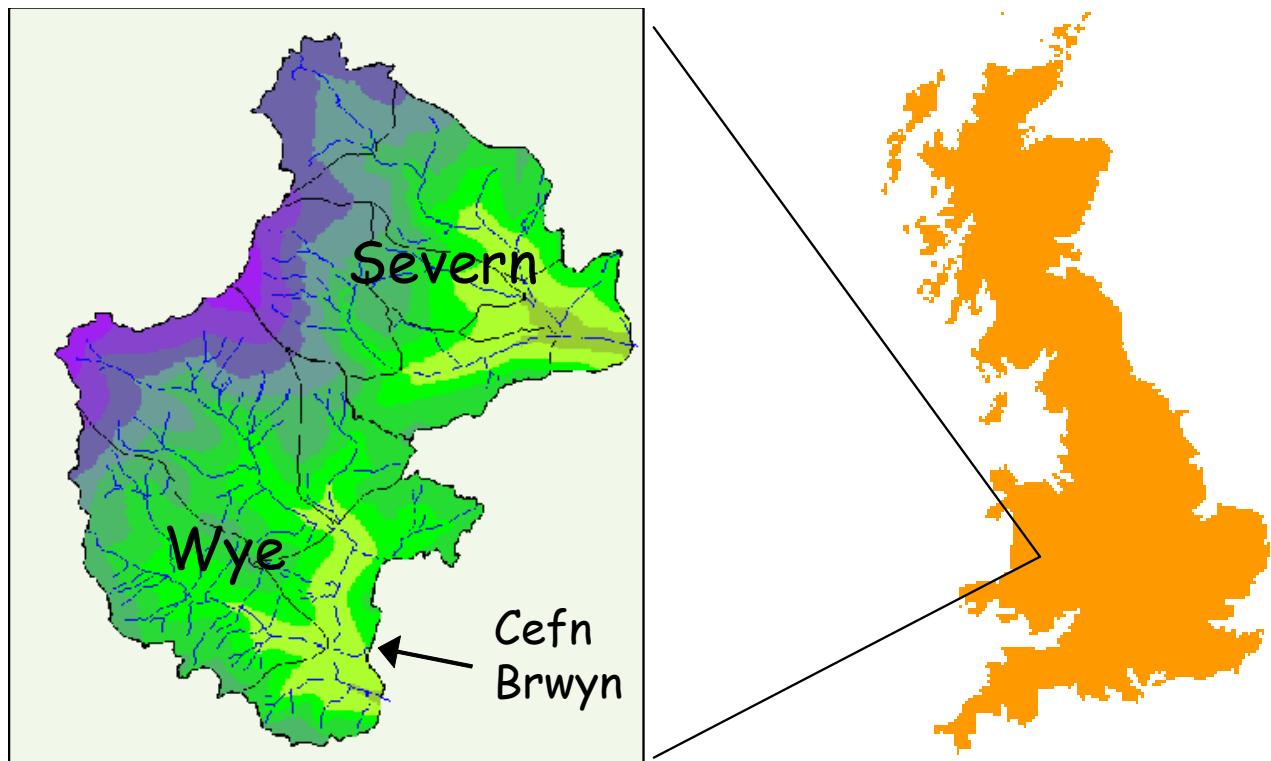


Fig. 1: Location of the Wye at Cefn Brwyn.

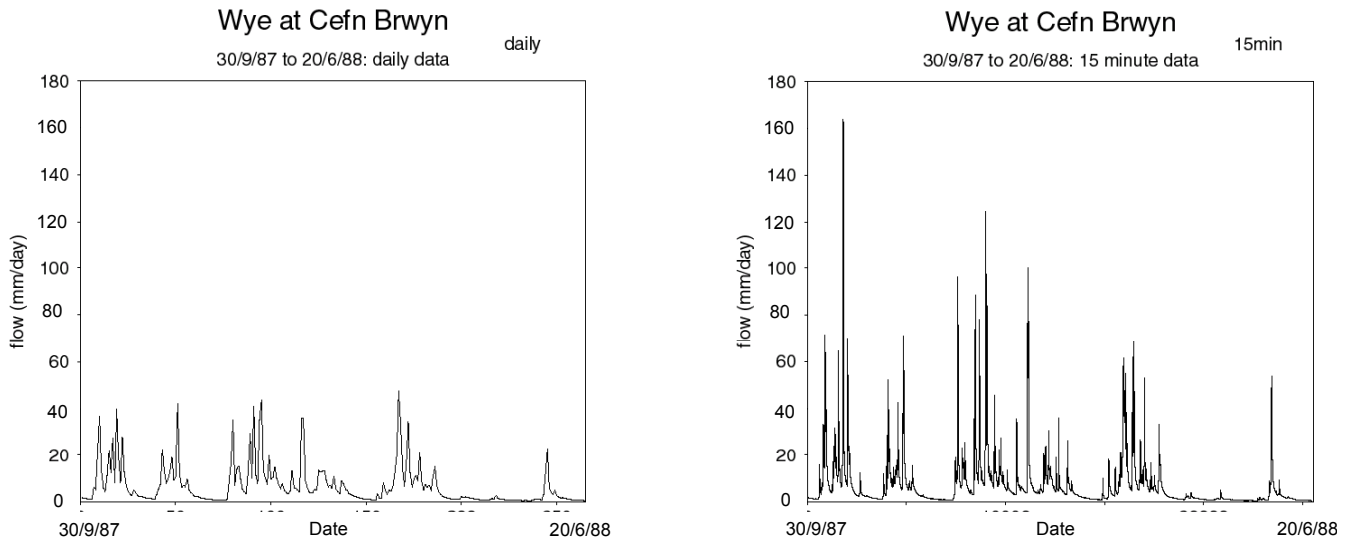


Fig. 2: Wye at Cefn Brwyn 24-hourly (left) and 15-minute (right) hydrographs.

Fig. 2 shows daily (265 points) and 15-minute (25,440 points) hydrographs from 30 September 1987 to 20 June 1988, indicating the extent to which a daily time-step hydrograph masks the highly dynamic flow regime at Cefn Brwyn. The available hydrometric data comprised 15-minute flow data and hourly catchment rainfall data, from which 1-, 2-, 4-, 6-, 12- and 24-hourly time-step rainfall-streamflow datasets were prepared. Using each dataset in turn, a rainfall-streamflow model was calibrated over the period from 6 December 1987 to 2 July 1988. The model employed was the spatially-lumped, unit-hydrograph-based, IHACRES (Identification of unit Hydrographs And Component flows from Rainfall, Evaporation and Streamflow data) model (Jakeman et al., 1990; Littlewood and Jakeman, 1992; 1994). The software used was IHACRES Classic Plus (Croke et al., 2006). Fig. 3 is a schematic of the model, giving outline descriptions of its six dynamic response characteristics (DRCs), f , c , τ_w , $\tau^{(q)}$, $\tau^{(s)}$ and $v^{(s)}$ (dimensions in square brackets). At time-step k , rainfall (r_k) and air temperature (t_k) are input to the loss module, which produces effective rainfall (u_k). The unit hydrograph module produces streamflow (x_k) from u_k . When f is set to zero, it plays no part in the model and air temperature (t_k) is not used. The models in this paper were thus constrained to have five DRCs.

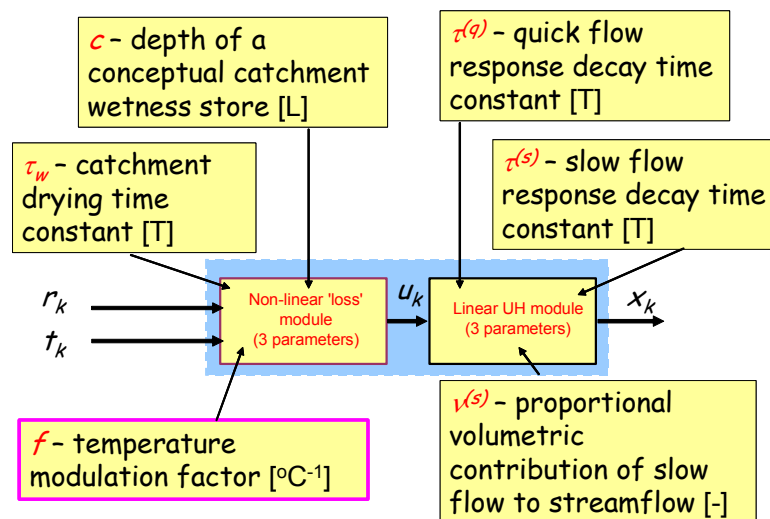


Fig. 3: IHACRES model structure and dynamic response characteristics (DRCs).

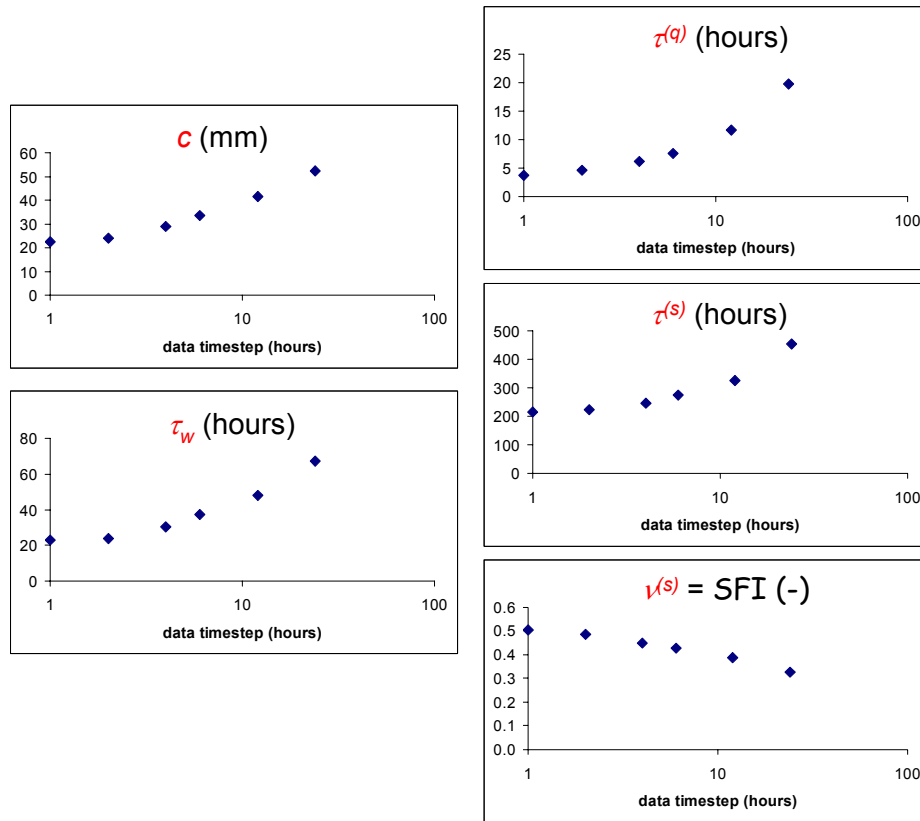


Fig. 4: Dynamic response characteristics against logarithm of modelling time-step.

Results

Fig. 4 shows each of the five DRCs, c , τ_w , $\tau^{(q)}$, $\tau^{(s)}$ and $\nu^{(s)}$ plotted against the logarithm of the data time-step (1-, 2-, 4-, 6-, 12- and 24-hours) used for corresponding model calibrations. The figure shows a systematic relationship for each DRC between its modelled value and the data time-step employed for model calibration. As the data time-step decreases from 24 hours to 1 hour, DRCs c , τ_w , $\tau^{(q)}$ and $\tau^{(s)}$ decrease by 66%, 81%, 52% and 57% respectively, and $\nu^{(s)}$ increases by 55%; substantial changes for each DRC. Other catchments, having different streamflow dynamics, will exhibit different relationships between each DRC and data time-step. Therefore, the use of a given data time-step for all n rainfall-streamflow models calibrated in Step 1, towards establishing a model parameter regionalisation scheme, is inappropriate and will cause some of the uncertainty in statistical models linking DRCs and catchment properties established in Step 2. What is required in order to eliminate, or at least reduce, this component of uncertainty is a method of normalising the DRCs so they are independent of data time-step. DRCs corresponding to a data time-step of zero would fulfil this objective (see next section). Although the problem has been illustrated here using IHACRES, the parameters of other conceptual-metric (Wheater et al., 1993) rainfall-streamflow models calibrated using temporally discrete data are also likely to be dependent on the data time-step employed (but see later discussion of this point).

Each of the models (using 1-, 2-, 4-, 6-, 12-, and 24-hourly data) was calibrated on the basis of a trade-off between a high value for a coefficient of determination (D) given by equation (1) and a low average relative parameter error ($ARPE$) for the unit hydrograph component of the model, as described by Jakeman et al. (1990) where details of how $ARPE$ is calculated are given. In equation (1) Q_0 and Q_m are observed and modelled flow respectively. As the data time-step decreases from 24 hours to 1 hour, D increases from 0.895 to about 0.907, and $ARPE$ decreases from 0.142 to 0.001, giving increasing confidence in the estimated DRCs as data time-step decreases.

$$D = 1 - \frac{\Sigma(Q_0 - Q_m)^2}{\Sigma(Q_0 - \overline{Q_0})^2} \quad \text{Eq. 1}$$

Rainfall–streamflow model parameter normalisation

The curves for c , τ_w and $\tau^{(s)}$ in Fig. 4 reach asymptotes at a data time-step of 1 hour, and for $\tau^{(q)}$ and $v^{(s)}$ nearly so, suggesting that modelling at sub-hourly data time-steps is required to reach asymptotes for those DRCs for the Wye at Cefn Brwyn (this requires additional data preparation and has not been attempted for this short paper). The asymptotes are effectively values of the DRCs at a data time-step of zero and, being thus independent of data time-step, provide a superior characterisation of rainfall–streamflow dynamic behaviour than time-dependent DRCs. From Fig. 4, normalised DRCs, c' , τ_w' , $\tau^{(q)'}$, $\tau^{(s)'}$ and $v^{(s)'}$ for the Wye at Cefn Brwyn are, respectively, about 20 mm, 20 hours, 3 hours, 200 hours and 0.51 (dimensionless). The DRCs $\tau^{(q)'}$, $\tau^{(s)'}$ and $v^{(s)'}$ are instantaneous unit hydrograph parameters for total streamflow and, by analogy, the DRCs c' and τ_w' are instantaneous loss module parameters. Taken together, the five normalised DRCs give an instantaneous rainfall–streamflow model for the Wye at Cefn Brwyn.

Discussion

The structure of the unit hydrograph module employed here comprises two linear stores acting in parallel, representing dominant quick- and slow-response, catchment-scale, streamflow generation processes respectively. Experience with IHACRES has shown that, from information in the rainfall–streamflow records typically available at a sufficient number of locations for regionalisation studies, two linear stores in parallel are usually an appropriate unit hydrograph structure (e.g. better than two similar stores in series). It is possible, however, that a more detailed unit hydrograph structure still having conceptual appeal (e.g. three stores in parallel, requiring an additional two model parameters) might be identifiable from small time-step data (e.g. hourly) for the Wye at Cefn Brwyn. Investigation of this possibility was considered to be unimportant for the theme of this paper and remains to be undertaken.

The first application of the IHACRES methodology was to two small (<1 km²) catchments in Wales located about 40 km south of Plynlimon (Littlewood, 1989; Jakeman et al., 1990), using hourly data. The flow regimes of those small basins, situated in the headwaters of the Llyn Brianne catchment, are not too different to the flow regimes observed in the headwaters of the Wye. The work presented in the current paper (for the Wye at Cefn Brwyn), supports the title “Computation of the *instantaneous* unit hydrograph ...” (italics added) of the Jakeman et al. (1990) paper, because the unit hydrograph DRCs for the Llyn Brianne catchments were derived using hourly data and are likely to be good approximations of the asymptotic values (Fig. 4) that would have been obtained if modelling had been undertaken using a range of sub-daily data time-steps. Data for the Llyn Brianne catchments are not readily available to the author, so this idea has not been tested here.

However, in the wettest regions of the United Kingdom the dynamics of many headwater flow regimes can be severely masked by a daily mean flow hydrograph, in which case modelling at sub-daily time-steps will be required to identify time-independent DRCs. Indeed, this will be the case whenever the quick-flow response time is close to, or less than, one day. The unit hydrograph DRCs $\tau^{(q)}$, $\tau^{(s)}$ and $v^{(s)}$ derived using daily data for UK catchments having areas of tens to hundreds of km² and highly dynamic flow regimes (e.g. Sefton and Howarth, 1998; Littlewood, 2003) may not be optimal for subsequent parameter regionalisation, because they are unlikely to be good approximations of time-independent DRCs. Loss module parameters c and τ_w , (and f , when included) for such catchments will also be sub-optimal. Rainfall–streamflow model parameter regionalisation should consider carefully the possible impact, in terms of uncertainties, of using a single modelling time-step for all catchments. Dependency of model parameters on modelling time-step should be assessed in each case and, when necessary, the model parameters should be normalised to be time-independent.

In order to estimate flows in an ungauged catchment using discrete-time rainfall data, a set of normalised DRCs (f' , c' , τ_w' , $\tau^{(q)'}$, $\tau^{(s)'}$ and $v^{(s)'}$) will need to be de-normalised to DRCs corresponding to the time-step of the available rainfall data. How to execute this back-transformation for ungauged catchments is beyond the scope of the current paper but there will, inevitably, be uncertainty associated with this step. It remains to be established whether or not the uncertainty in flows estimated via normalised DRCs is less than if time-dependent DRCs were used.

The method for estimating time-independent (normalised) DRCs presented in this paper, based on analysis of data from just one catchment, required preparation of datasets at different time-steps, and was demanding in terms of repetitive application of the modelling software. With (a) enhancements to database facilities, e.g. making high temporal resolution (sub-daily) data available and (b) further development of the modelling software to automate compilation of different time-step datasets and management of the repetitive modelling process using those different time-step datasets, it would be possible to implement the method systematically.

Further work is required to investigate whether or not the simple method for normalising IHACRES model parameters presented in this paper, for the Wye at Cefn Brwyn, will work well for other catchments (Littlewood and Croke, submitted). At least one other method of model parameter normalisation should also be evaluated. Young and Garnier (2006) describe data-based mechanistic (DBM) methods for deriving continuous-time models from discrete-time input data, where the calibrated model parameters are independent of the time-step of the input data. Since IHACRES is a special case of a DBM model, an extension of the work described above would be to apply DBM methods to the Wye at Cefn Brwyn and other catchments, and to compare the estimates of time-step-independent model parameters thus obtained with the normalised IHACRES DRCs presented in this paper.

Concluding remarks

Rainfall-streamflow model parameters (DRCs) for the Wye at Cefn Brwyn, estimated by the IHACRES methodology, have been shown to vary substantially with the data time-step used for model calibration. At a data time-step of 1 hour, each relationship between a DRC and the logarithm of modelling time-step reaches, or approaches, an asymptote that reasonably can be expected to be a better characterisation of the catchment rainfall–streamflow dynamic behaviour than a DRC corresponding to a larger data time-step. For regionalisation studies the technique would have to be applied to many gauged catchments. It is expected that there will be a better statistical link between a normalised DRC and catchment properties than between a time-step-dependent DRC and catchment properties. Further work is required to test this idea. Further work is also required to (a) compare DRCs normalised as described in this paper with time-step-independent model parameters derived by continuous-time DBM models corresponding to IHACRES and (b) devise a method of back-transforming normalised (time-independent) model parameters to time-step-dependent model parameters for the estimation, from discrete rainfall data, of flows in ungauged catchments.

References

- Brandt C., Robinson M., Finch J.W. (2004). Anatomy of a catchment: the relation of physical attributes of the Plynlimon catchments to variations in hydrology and water status. *Hydrology and Earth System Sciences*, 8: 345-354.
- Croke B.F.W., Andrews F., Jakeman A.J., Cuddy S.M., Luddy A. (2006). IHACRES Classic Plus: a redesign of the IHACRES rainfall-runoff model. *Environmental Modelling and Software*, 21: 426-427.
- Jakeman A.J., Littlewood I.G., Whitehead P.G. (1990). Computation of the instantaneous unit hydrograph and identifiable component flows with application to two small upland catchments. *Journal of Hydrology*, 117: 275-300.

- Littlewood I.G. (1989). *The Dynamics of Acid Runoff from Moorland and Conifer Afforested Catchments Draining into Llyn Brienne, Wales*. PhD Thesis, University of Wales (Swansea), 338 pp.
- Littlewood I.G. (2003). Improved unit hydrograph identification for seven Welsh rivers: implications for estimating continuous streamflow at ungauged sites. *Hydrological Sciences Journal*, 48: 743-762.
- Littlewood I.G. (2004). Unit hydrographs and regionalization of United Kingdom river flows: comments on some estimation uncertainties. In: C. Pahl-Wostl, S. Schmidt, A.E. Rizzoli, A.J. Jakeman (Eds), *Complexity and Integrated Resources Management, Transactions of the 2nd Biennial Meeting of the International Environmental Modelling and Software Society*, Manno, Switzerland, iEMSs, 2004, 3: 1153-1158.
- Littlewood I.G., Croke B.F.W. (submitted). Towards an instantaneous rainfall-streamflow model for ungauged basins: parameter dependency on data time-step. *Hydrological Sciences Journal*.
- Littlewood I.G., Jakeman A.J. (1992). Characterisation of quick and slow streamflow components by unit hydrographs for single- and multi-basin studies. In: M. Robinson (Ed.), *Proceedings of the Fourth General Assembly of the European Network of Experimental and Representative Basins*, Oxford, September 29 - October 2, published as Institute of Hydrology Report 120.
- Littlewood I.G., Jakeman A.J. (1994). A new method of rainfall-runoff modelling and its applications in catchment hydrology. In: P. Zannetti (Ed.), *Environmental Modelling (Volume II)*, Computational Mechanics Publications, Southampton, UK: 143-171.
- NERC (2003). *Hydrological Data UK: Hydrometric Register and Statistics 1996-2000*. Centre for Ecology and Hydrology, Natural Environment Research Council, 208 pp.
- Robinson M., Dupeyrat A. (2005). Effects of timber harvesting on streamflow regimes in the Plynlimon catchments, mid-Wales. *Hydrological Processes*, 19: 1213-1226.
- Sefton C.E.M., Howarth S.M. (1998). Relationships between dynamic response characteristics and physical descriptors of catchments in England and Wales. *Journal of Hydrology*, 211: 1-16.
- Wheater H.S., Jakeman A.J., Beven K.J. (1993). Progress and directions in rainfall – runoff modelling. In: A.J. Jakeman, M.B. Beck, M.J. McAleer (Eds.), *Modelling Change in Environmental Systems*, John Wiley & Sons Ltd. 99-130.
- Young P.C., Garnier H. (2006). Identification and estimation of continuous-time, data-based mechanistic (DBM) models for environmental systems. *Environmental Modelling and Software*, 21: 1055-1072.

APPLICATION OF FUZZY LOGIC SYSTEMS FOR THE ELABORATION OF AN OPERATIONAL HYDROLOGICAL WARNING SYSTEM IN UNGAUGED BASINS

S. Matreata & M. Matreata

National Institute of Hydrology and Water Management, Sos. Bucuresti - Ploiesti, no. 97, Bucharest, Romania.

Corresponding authors: S. Matreata & M. Matreata, email: simona.matreata@hidro.ro, marius.matreata@hidro.ro

ABSTRACT

Fuzzy logic modelling systems offer the potential for a more flexible approach of hydrological processes modelling. They have already proven to be suited as substitutes for the classical rainfall – runoff models, and also as tools for the real time updating of hydrological forecasting models and especially for the multimodel approach. We have selected a Fuzzy Logic System approach for rainfall-runoff modelling in ungauged basins. This approach relies on the tuning of the parameters used in the pre-processing of the input data (the maximum values for the input and output variables used in the normalization operations), the statistical estimation of precipitation and discharge with a certain return period, respectively the estimation of the basin concentration time, for which detailed methodologies and the necessary regionalization relations have been previously established.

The proposed Fuzzy Model provides reasonably good estimations of the possibility of flood occurrences and at the same time an estimation of the associated uncertainty.

Keywords: fuzzy logic, rainfall-runoff models, ungauged basins, hydrological warnings

Introduction

All rainfall-runoff models that are currently in use are approximating hydrological processes taking place. None of these models are able to completely describe those processes. This is mainly due to the lack of detailed knowledge of the processes involved in the generation of runoff from precipitation.

Conceptual models with an *a priori* specified structure based on the hydrologist's perception of the relevant processes and with parameters calibrated against observed time-series, are still the most commonly used.

Fuzzy logic modelling systems offer the potential for a more flexible, less assumption-based approach in hydrological processes modelling. They have already proven to be good substitutes for classical rainfall – runoff models (Stuber et al., 2000; Alvisi et al., 2005; See et al., 1998; Mahabir et al., 2002).

Prediction in ungauged basins (PUB) is defined as the prediction or forecasting of the hydrological response (e.g. of streamflow, groundwater, sediments, nutrients, etc.) of ungauged or poorly gauged basins, and its associated uncertainty, using all datasets, i.e. climatic inputs (observed, forecast or otherwise specified), soils, vegetation, geology and topography, including any predicted or expected future climatic or land-use changes, but without the benefit of past observational time series of the particular hydrological response that is being predicted, i.e. with no possibility or allowance for direct calibration (Definition based on the documents of the IAHS Decade on Predictions in Ungauged Basins initiative).

Fuzzy Logic Models

The origin of the fuzzy logic approach dates back to 1965 with the introduction of the fuzzy-set theory and its applications (Lotfi Zadeh's, 1965). In the fuzzy logic approach the Boolean logic is extended to handle the concept of partial truth which implies that the truth takes a value between a completely true value and a completely false value.

The fuzzy logic approach is a tool for dealing with problems related to uncertainties and imprecise information.

In general, a fuzzy model relies on the following application steps (Sen, 2004):

1. Fuzzy sets definitions for the input and output variables.
At the base of any fuzzy logic application we have the fuzzy sets and the corresponding membership functions, which use some general information about the values domain for each variables, in order to define some category boundary (like small, medium, high, etc.). The most used membership functions are: triangular, trapezoidal and gaussian.
2. Fuzzification of the input and output variables.
Fuzzification of the input and output variables is done using the previously defined fuzzy sets and the corresponding membership functions.
3. Construction of rules.
Construction of rules can be based on the expert knowledge, on the available theory and data. The rules relate the combined linguistic subsets of input variables to the convenient linguistic output subset. Any fuzzy rule includes statements such as "IF-THEN" with two parts:
 - The first part starts with IF and ends before THEN is referred to as the predicate (premise, antecedent), which combines the subsets of input variables.
 - After the THEN comes the consequent part, which includes the convenient fuzzy subset of the output based on the premise part. This implies that there is a set of rules each of which is valid for a specific portion of the input variation domain. The input subsets within the premise part are combined most often with the logical "and" conjunction whereas the rules are combined with the logical "or".In general, the fuzzy models used for hydrological forecasting are based on a fuzzy rule base describing the hydrological behaviour of the river basin.
Expert knowledge about specific discharge situations combined with precipitation information and soil moisture conditions can be transformed directly in IF ... THEN ... rules, using linguistic entities like: previous discharge=low AND precipitation=high AND soil moisture=high THEN discharge=high and thus building up an initial rule base.
Optimization procedures could then be used to adapt the rule base on the basis of data from former flood events in order to achieve an optimal forecast model.
4. Apply the fuzzy inference, and defuzzification of the output.
There are two main types of fuzzy inference: Mamdani and Sugeno:
 - Mamdani-type inference, in which the output membership functions are fuzzy sets. After the aggregation process, there is a fuzzy set for each output variable that needs defuzzification, in which usually we integrate across the two-dimensional function to find the centroid.
 - Sugeno-type inference can be used to model any inference system in which the output membership functions are either linear or constant. This is sometimes known as a *singleton* output membership function, and it can be thought of as a pre-defuzzified fuzzy set. It enhances the efficiency of the defuzzification process because it greatly simplifies the computation required by the more general Mamdani method.

The output defuzzification represents the transformation from a fuzzy set to a crisp number. It is a reverse process of fuzzification, and it is not a unique operation as different approaches are possible: smallest of maximal, mean of maximal, centroid, largest of maximal, etc. (Sen, 2004).

Fig. 1 shows the general block diagram of a fuzzy inference system structure, with the relations between the different main steps/components.

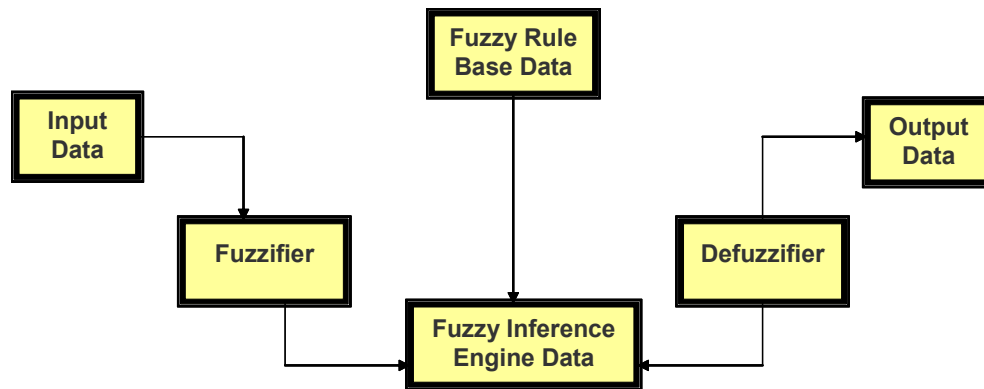


Fig. 1: General block diagram of a fuzzy inference system.

Proposed methodology and fuzzy model structure

Building a new model and the corresponding parameter regionalization relations is a very complex and time-consuming process.

Our primary objective was to build a simple model, which can provide an estimation of a flood occurrence probability and an estimation of the corresponding flood severity; information that can be used in the decision process of issuing hydrological warnings for ungauged basins, without very intensive requirements in terms of input data.

Regarding the regionalization relations for the model parameters, the objective was to build a model with parameters that can be derived for an ungauged basin based on other hydrologically related “variables” that can be computed for any ungauged basin using already existing regionalization relations and/or methodologies.

We have selected a Fuzzy Logic System approach for the rainfall-runoff process modelling in ungauged basins, relying on the tuning of the parameters used in the pre-processing of the input data (the maximum values that are used in the normalization operations for the input and output variables), using statistical estimations of precipitation and discharge with a certain return period, and estimations of the basin concentration time, for which standard methodologies and the necessary regionalization relations are already existing.

The fuzzy model is an event model, and has two processing modules:

1. The first module computes an index of the soil moisture state, expressed as a fuzzy set.

Input data for computing the index at a given moment are different time period precipitation accumulations:

- $P(t-24 \text{ hours} \rightarrow t)$;
- $P(t-72 \text{ hours} \rightarrow t-24 \text{ hours})$;
- $P(t-144 \text{ hours} \rightarrow t-72 \text{ hours})$;
- $P(t-240 \text{ hours} \rightarrow t-144 \text{ hours})$;

Output data:

- Soil Moisture Index (t)

2. The second module is a rainfall-runoff model which computes the maximum discharge produced by a rain event, presenting the result as a fuzzy set (Mamdani type inference).

Input data for computing the maximum discharge fuzzy set:

- $P(t \rightarrow t + T_p)$ – predicted rainfall at time t;

- Soil Moisture Index (t) – computed by the first module;
 - Tp – predicted rainfall duration in hours;
- Output data:
- Maximum discharge that could be produced by the predicted rain event, expressed as a fuzzy set.

Pilot implementation

The pilot basin that was used to apply and test the methodology is the hydrometric station Ranusa – Representative Basin Moneasa, situated in the western part of Romania – in the Crisul Alb River Basin (Area = 76.2 km², H = 586 m).

For the software implementation of the fuzzy model a dedicated software application was used: FisPro 3.0 – *Fuzzy Inference System Professional*, Cemagref – France, which is an open source software, available on the Internet at: <http://www.inra.fr/bia/M/fispro>.

Fig. 2 shows an example of the program interface, for a particular computation of the maximum discharge fuzzy value. Each row represents a fuzzy rule, and the black sections of triangles represent the different membership degree values, for input and output variables. The soil moisture input value is the simulated output from the first fuzzy API type model, which is used together with the predicted amount and duration of the precipitation in the rainfall – runoff model. On the right side of the first row, we can see the combined result for all the fuzzy rules, indicating the membership degree of the simulated discharge to each of the categories on the maximum discharge fuzzy set. As we can see in the combined fuzzy result, the rainfall – runoff model indicates that the simulated maximum discharge is in the “Minor Flood”, respectively “Flood” categories, but with the greater membership degree value in the “Flood” category. Based on the model result we could thus issue a hydrological warning.

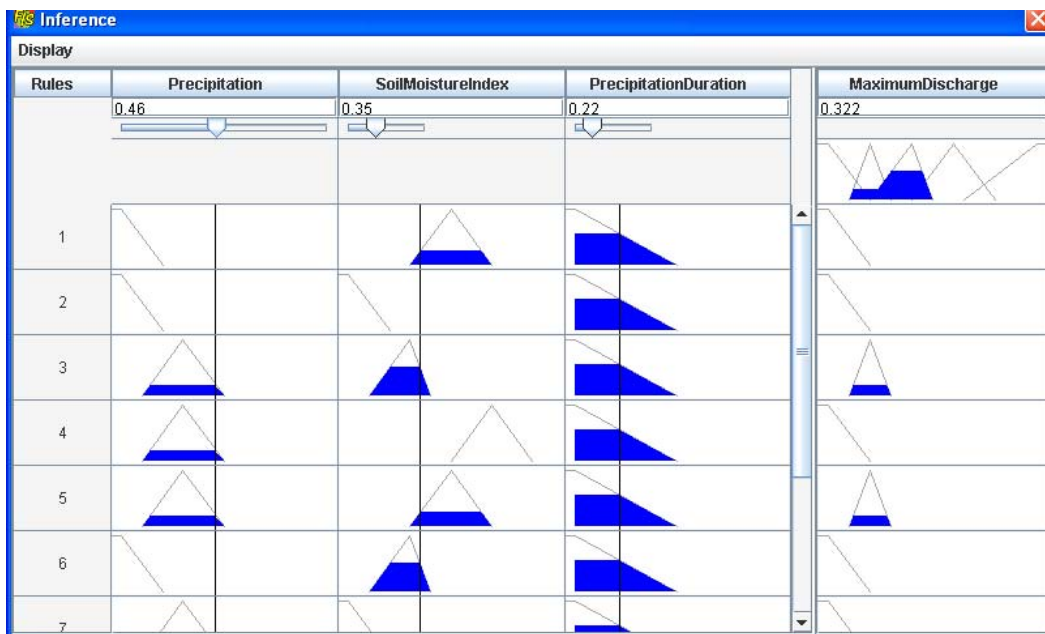


Fig. 2: Example of the FisPro graphical user interface for the inference results for the maximum discharge estimation fuzzy model (rainfall – runoff model).

Fig. 3 shows the scatter-plot of the defuzzified simulated maximum discharge values versus the maximum discharge observed values, for some historical test events. The defuzzified simulated maximum discharge is not really used if the model is applied to an ungauged basin, and it is not really used in the decision process of

issuing hydrological warnings. The comparison between those simulated values and the observed values, are just useful as a detailed model validation in the process of the model configuration and tuning processes.

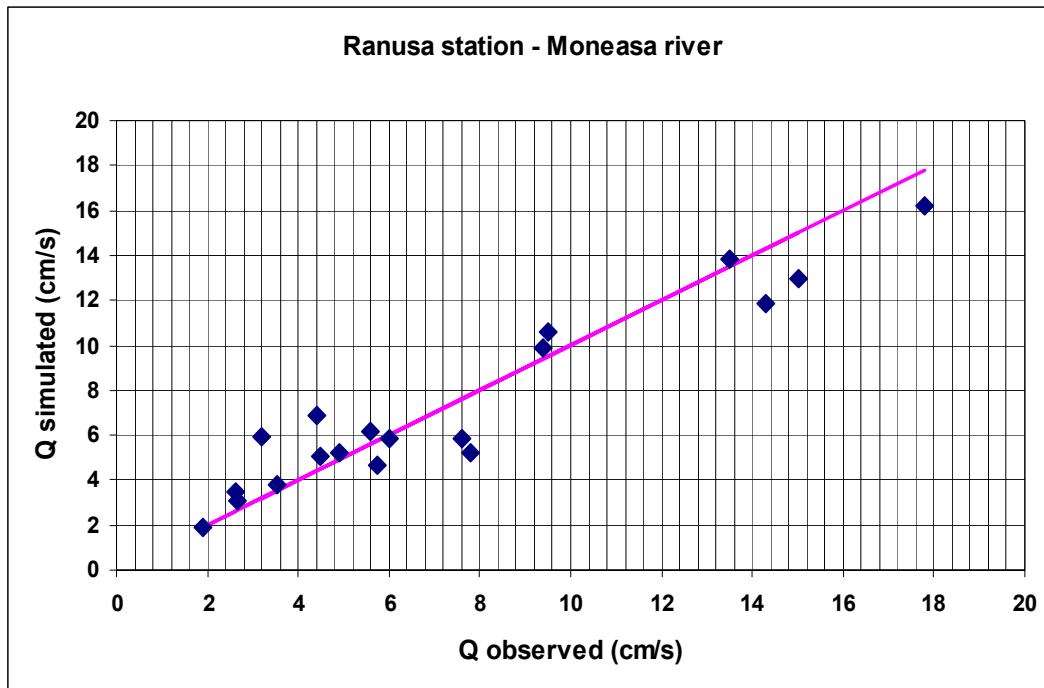


Fig. 3: Simulated maximum discharge crisp values obtained by defuzzification, compared with the observed values (after the fuzzy rules optimization based on historical data).

Observations and conclusions

Even though the proposed fuzzy model is rather simple, it provides reasonably good estimations of the likelihood of flood occurrence and at the same time an estimation of the associated uncertainty, expressed by different membership degree values to the different flood categories, within the simulated discharge fuzzy set (no flood, minor flood, flood, high flood, very high flood).

In order to apply the model to an ungauged basin we need the following information:

- An estimation of the 24-hour precipitation for that basin with a return period of 100 years (that value is used to normalize the precipitation values).
- An estimation of the time of concentration (t_c) for that basin. The value of $2 \cdot t_c$ is used to normalize the precipitation duration values.
- An estimation of the maximum discharge for a 100-year return period, which is used in the defuzzification of the simulated fuzzy sets discharges.

The main model assumption is that for all the basins within a region (established based on the regions defined from the previous statistical precipitations and maximum discharge regionalization analysis) the fuzzy set memberships functions and the fuzzy rule set defined for the normalized values of all the inputs and output variables are the same.

Before applying the model to a new region, it is recommended to make some validation tests on some gauged basins from that region, and to make the necessary adjustments to the fuzzy rules and/or to the membership functions. The model can only be used for small basins up to the scale of a few hundred square kilometers.

Plans for the future

In a near future there will be further testing of the model assumptions, as well as comparisons with the classic uncertainty analysis methods using the probability theory, and a linear regression model relying on the same input data.

A more complex fuzzy system is also to be implemented, corresponding to a continuous hydrological model, with the explicit modeling of different “standard conceptual reservoirs” – fuzzy reservoirs (work recently started; for the software implementation we use the open source JFS development environment for the programming language JFL, which is a special-purpose language used to write functions that utilize fuzzy logic and machine-learning techniques, combined with features from traditional programming languages, created by Jan E. Mortensen, <http://inet.uni2.dk/~jemor/download.htm>).

References

- Alvisi S., Mascellani G., Franchini M., Bardossy A. (2005). Water level forecasting through fuzzy logic and artificial neural network approaches, *Hydrology and Earth System Science Discussions*, EGU.
- Zadeh L. (1965). Fuzzy sets. *Information and Control*, 8: 338-353.
- Mahabir C., Hicks F.E., Fayek A.R. (2002). Forecasting ice jam risk at Fort McMurray, AB, using fuzzy logic. *Proceedings of the 16th IAHR International Symposium on Ice*, Dunedin, New Zealand.
- See L., Abrahart R.J., Openshaw S. (1998). *An Integrated Neuro-Fuzzy-Statistical Approach to Hydrological Modelling*. School of Geography, University of Leeds, UK.
- Sen Z. (2004). *Fuzzy Logic and System Models in Water Sciences*. Turkish Water Foundation, Istanbul.
- Stuber M., Gemmar P., Greving M. (2000). Machine supported development of fuzzy - flood forecast systems. *European Conference on Advances in Flood Research*, Potsdam, PIK Report Nr. 65.

FLOOD FORECAST METHOD USING DATA FROM REPRESENTATIVE BASINS

P. Mita, C. Corbus & S. Matreata

National Institute of Hydrology and Water Management, Bucuresti - Ploiesti 97, 013686 Bucharest, Romania.

Corresponding author: Pompiliu Mita, email: pompiliu.mita@hidro.ro

ABSTRACT

The main objective of this paper was the elaboration of a flood forecast method on rivers with surfaces larger than 500-600 km² by using data from representative basins (R.B.). It is considered that the existence of such basins within certain larger river basins allows a faster and more precise elaboration of flood forecasts. The approach relies on the fast determination in the R.B. of the main elements of the flood wave (starting moment, increase time, maximum discharge, depth of runoff) based on relations obtained between these elements and precipitation characteristics. For the determination of the flood wave elements in the ungauged small basins, the synthesis relations of these elements as a function of event rainfall and basin characteristics are used. For large rivers, the knowledge of the flood wave elements in small rivers that form in the end the large river basins is very useful.

Keywords : representative basins, flood analysis, hydrological modelling

Introduction

Major floods occurred in the last years on the Romanian rivers and many institutions in the country have been involved in the development of mitigation strategies. The main goal of this study was to find some mitigation methods for the flooding effects. The proposed flood forecast method is part of this effort.

The elaboration of a flood forecast method for big rivers, with areas larger than 500 - 600 km², uses the data from representative basins (R.B.), which are small basins, covering less than 100 km². The R.B. are used as warning basins.

The paper has the following goals:

- Establish a methodology for the determination of the flood wave elements from hydrometrical stations.
- Elaborate synthesis relations for the determination of the flood wave elements for ungauged river basins.
- Establish a method for the determination of the flood wave hydrograph in sub-basins and their aggregation and routing in the forecast points in the main rivers.

It is considered that the existence of such warning basins within certain big rivers basins enables a faster and more precise elaboration of flood forecasts. The fast determination in the R.B. of the main elements of the flood wave (starting moment, increase time, maximum discharge, runoff depth) based on relations obtained between these elements and precipitation characteristics is taken into consideration. But the authors are aware that the flood forecast elaborated for small rivers is not sufficient alone due to the very quick reaction of small basins to the precipitation factor, most of the times in a few hours. In these conditions, even when information is rapidly transmitted, the possibility to take the necessary measures is minimal. However, for large rivers, the knowledge in advance of the flood wave elements on small rivers that make up large river basins is very useful.

Methodology

The calculation methodology of flood forecasts using data from representative basins relies on 6 steps, which will be presented here below with an example of the Crisul Alb river basin.

Topological modelling: In the first step a schematic representation of the way in which flow into a river basin is formed, called topological modelling of the basin, is realized. This modelling takes into account the fact, that a successive integration process on the slope and riverbed forms the runoff. The topological modelling of river basins supposes the division of the basin and hydrographic network into homogeneous units, considering certain criteria. The river basin will be divided into homogeneous areas (sub-basins) from the point of view of the variability of factors that condition runoff: topography, vegetation, soils and geology (Fig. 1).

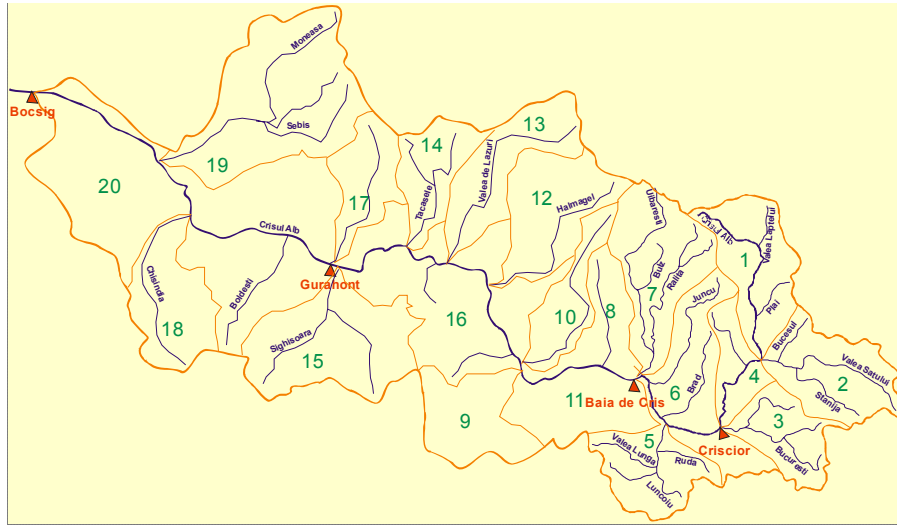


Fig. 1: Topological modelling of the Crisul Alb river basin.

The hydrographic network will have discrete sectors, taking into account the following criteria: the homogeneity of hydraulic and morphometric characteristics of the low-flow channel and the flood channel; runoff type (one-dimensional or two-dimensional); the degree of stability of the riverbed (Fig. 2).

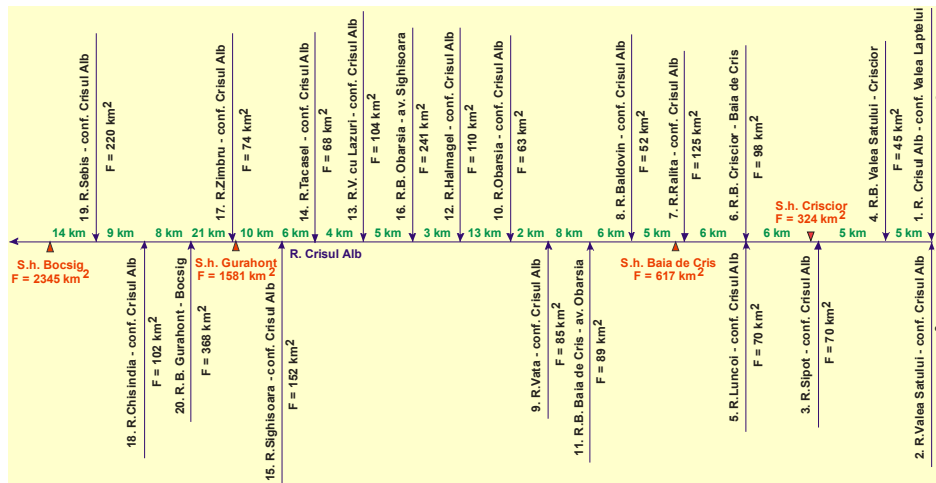


Fig. 2: Flood routing scheme for the Crisul Alb river, reach spring - Bocsig (Topological modelling of the Crisul Alb hydrographic network).



The topological modelling of river basins and of their hydrographic network also takes into account the following elements: quality and quantity of available data, the purpose of the modelling and required accuracy, type and importance of the reservoirs that influence runoff.

Morphohydrographical characterisation: The second step is the determination of morphohydrographical characteristics (area, length, mean altitude, basin slope, river slope, etc) and the characteristics of the environment (soil, relief, vegetation) for all sub-basins. The example on Fig. 3 is for R.B. Moneasa. These characteristics were also determined for all R.B.

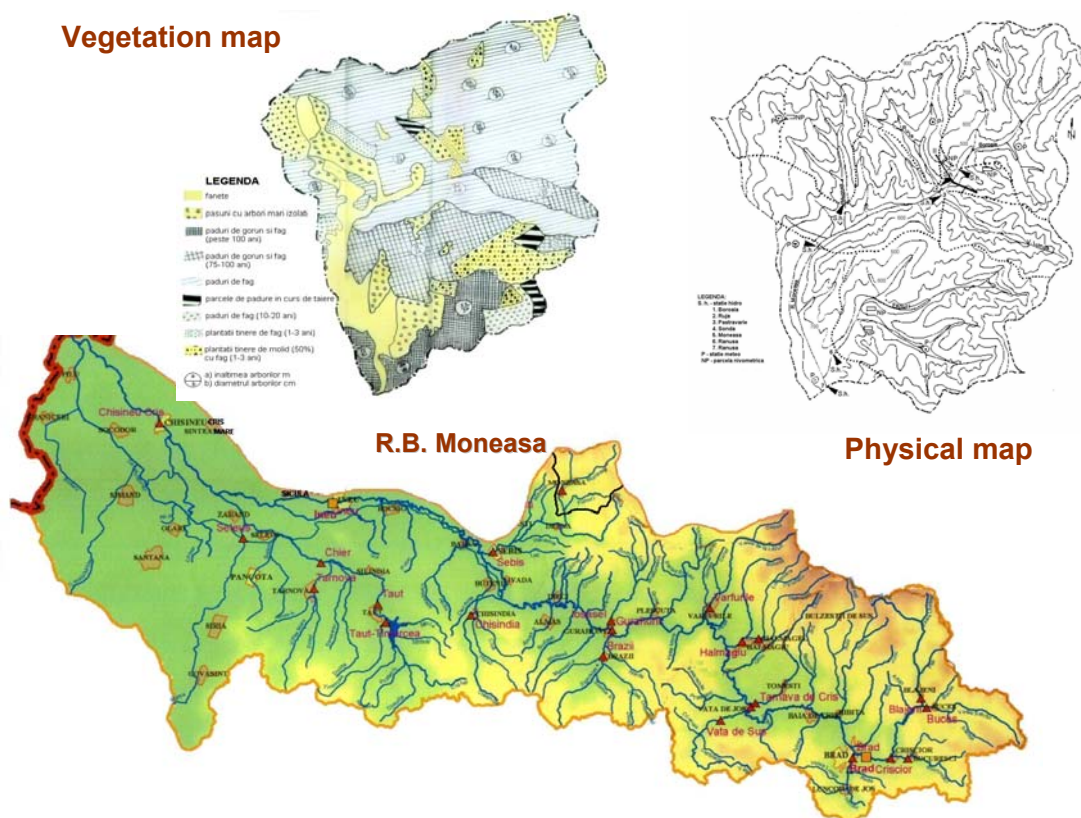


Fig. 3: The determination of morphohydrographical characteristics for all sub-basins.

The purpose of the determination of these characteristics for all small river basins was to transmit (extrapolate) data (flood wave elements) from the R.B. to the other river basins, which have similar runoff conditions. When these basins have different characteristics than the R.B. from the respective river basin, data from the R.B. from another river basins will be used.

Relation between flood wave elements and precipitation characteristics: The relation between the flood wave elements (maximum discharge Q_{max} ; the increase duration/time t_{cr} ; decrease duration/time t_d) and precipitation characteristics (quantity, duration, intensity) obtained at hydrometric stations (the third step) are presented for certain hydrometric stations within the Moneasa representative basin (Crisul Alb basin).

Fig. 4a shows the relation between maximum discharge and precipitation characteristics for the Ranusa hydrometric station: precipitation intensity i_p (mm/min), total rainfall duration T_p (min), the antecedent precipitation recorded 10 days before (computed with the API model, API_{10} in mm). For this hydrometric station the following values were determined: $Q_{max} = 69 \text{ m}^3/\text{s}$ when $i_p = 1.2 \text{ mm/min}$, $T_p = 90 \text{ min}$ and $API_{10} = 20 \text{ mm}$.

Fig. 5a shows the relation between the increase duration t_{cr} (min) and total duration of the rainfall T_p (min) for the sub-basins of the Moneasa R.B.

From these relations it can be concluded that the ascending time t_{cr} accordingly increases with T_p . The relation between the decrease duration of the wave, t_d and the total duration of the rainfall; T_p and the total amount of rainfall, P , are shown in Fig. 6a.

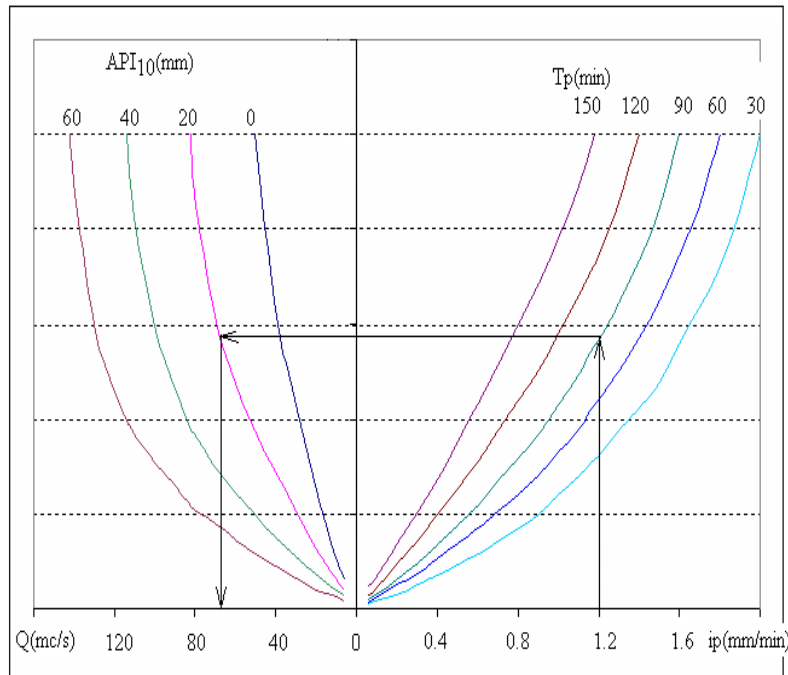


Fig. 4.a) The determination of the maximum discharge (Q_{max}). Ranusa hydrometric station.

To determine the beginning of the flood, the interval between the beginning of the rainfall and the beginning of the flood (t_1) is determined. In Fig. 7, the relation between t_1 and the intensity of the precipitation fallen in the t_1 interval, i_{x1} , and API_{10} are presented.

Determination of synthesis relations: Within the fourth step the synthesis relations of the flood wave elements (Q_{max} , t_{cr} , t_d) obtained on the basis of data at hydrometric stations are presented. This synthesis relation uses for referenced elements the area of the river basin, S (km^2). The main advantage of the synthesis relations is the determination of the flood wave elements for the ungauged small basins.

The computed synthesis relations rely on the following physiographic characteristics of the environment: forest cover coefficient $C_p=80-100\%$; slope of the river basin, $I_b=20-25\%$; soil texture, medium.

Fig. 4b shows the synthesis relation for the maximum discharge, Q_{max} (m^3/s). In this example the following values were determined: $Q_{max}=69 m^3/s$ for one basin with an area $S=75 km^2$, when: $i_p=1.0 mm/min$; $T_p=90 min$; $API_{10}=30 mm$. Q_{max} is determined in a similar way for all sub-basins with areas up to $100 km^2$ and for different conditions regarding i_p , T_p , API_{10} .

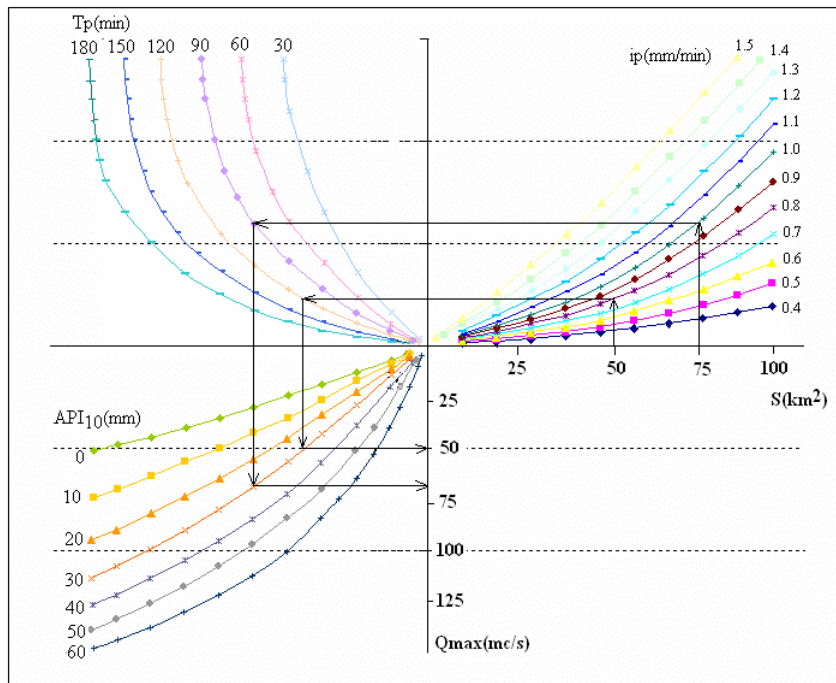


Fig. 4.b) The determination of the maximum discharge (Q_{max}). Synthesis relation.

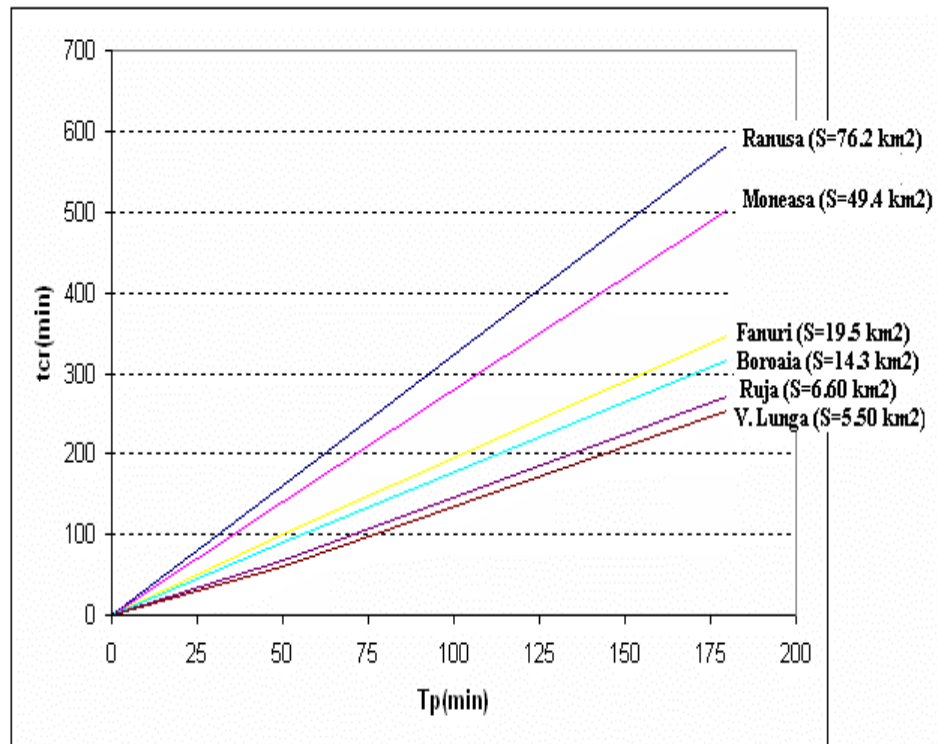


Fig. 5.a) The determination of the increase time of the flood wave (t_{cr}). Moneasa R.B.

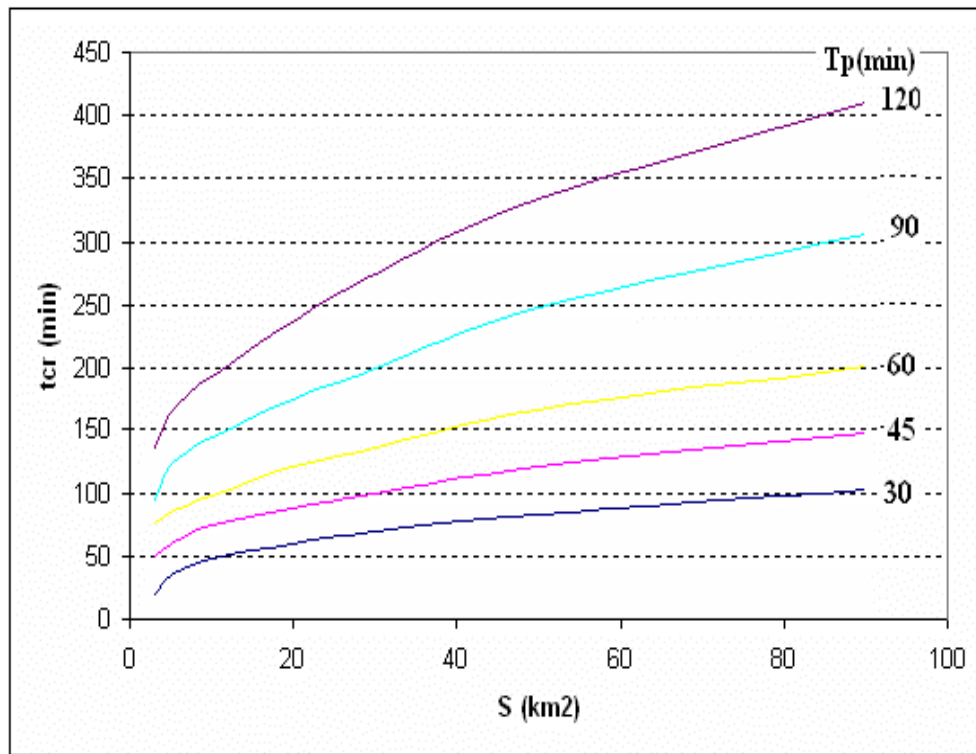


Fig. 5.b) The determination of the increase time of the flood wave (t_{cr}). Synthesis relation.

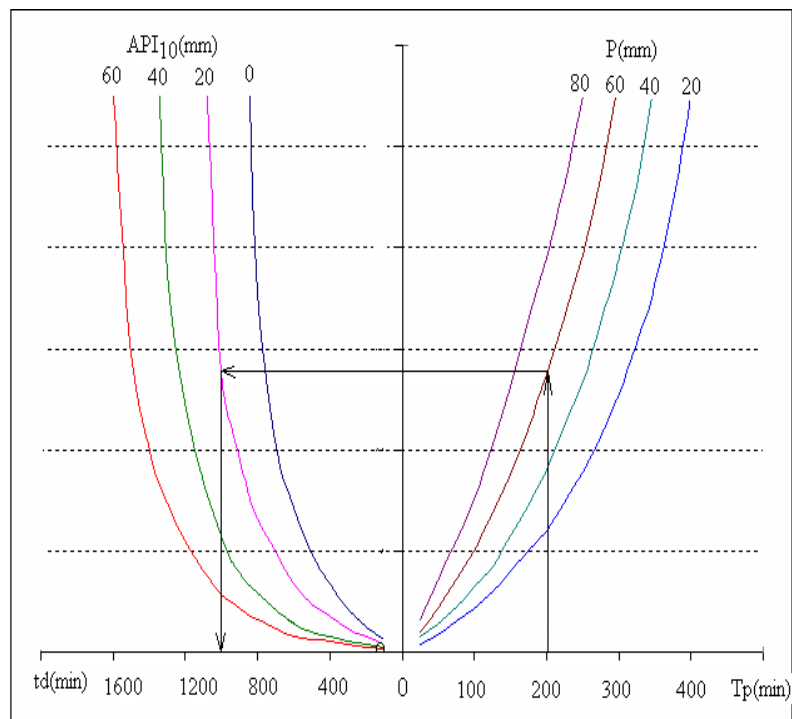


Fig. 6.a) The determination of the decrease time of the flood wave (t_d). Ruja hydrometric station.

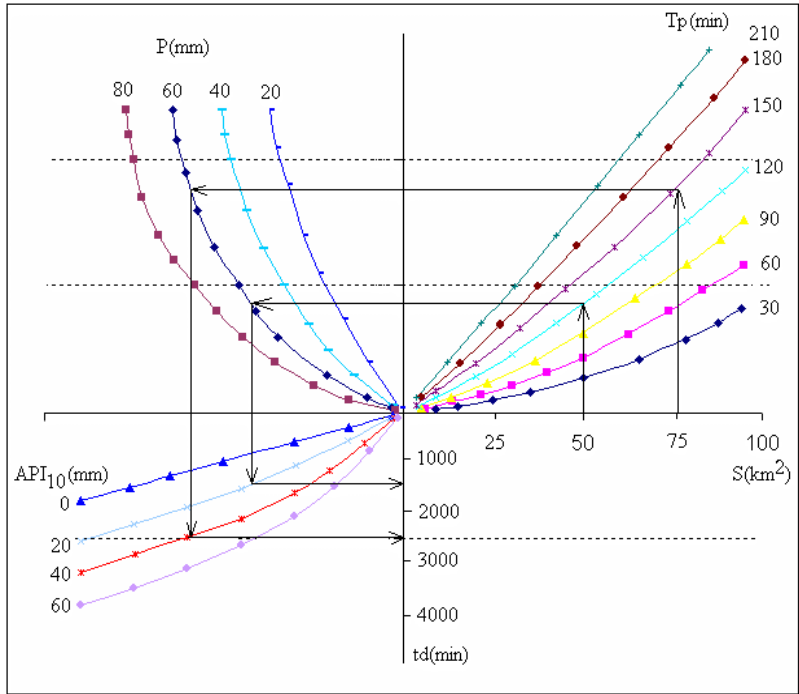


Fig. 6.b) The determination of the decrease time of the flood wave (t_d). Synthesis relation.

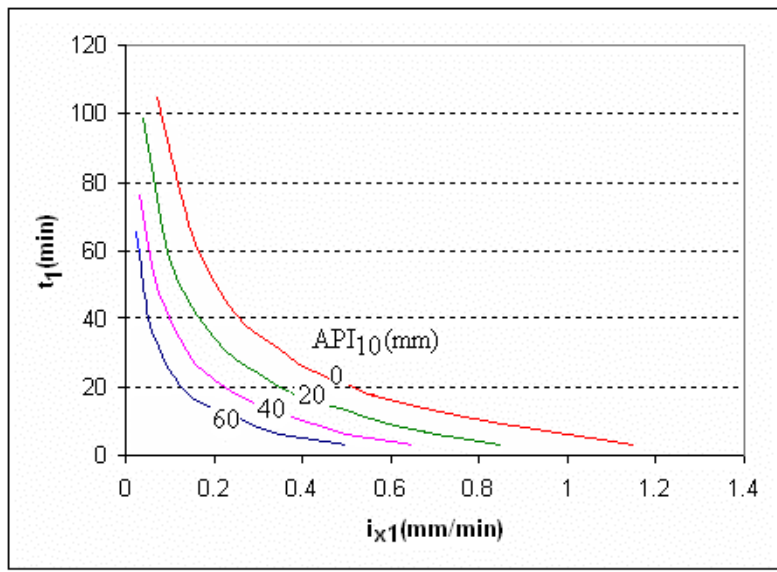


Fig. 7: The determination of the intensity fallen in the t_1 interval (i_{x1}).

Fig. 5b shows the synthesis relation for the increased duration of the wave, t_{cr} , where T_p is classified in 30, 45, 60, 90 and 120 min.

Fig. 6b shows the synthesis relation for the decrease duration of the wave, t_d . The relation used for the determination of the t_d values is shown for a basin of 75 km^2 . The obtained values for $t_d=2500$ min (42 hours) are: $T_p=150$ min; $P=60$ mm; $API_{10}=40$ mm.

Calculation of the characteristics: The fifth step is the calculation of the characteristics of the flood waves for all ungauged sub-basins, based on the synthesis relations determined before.

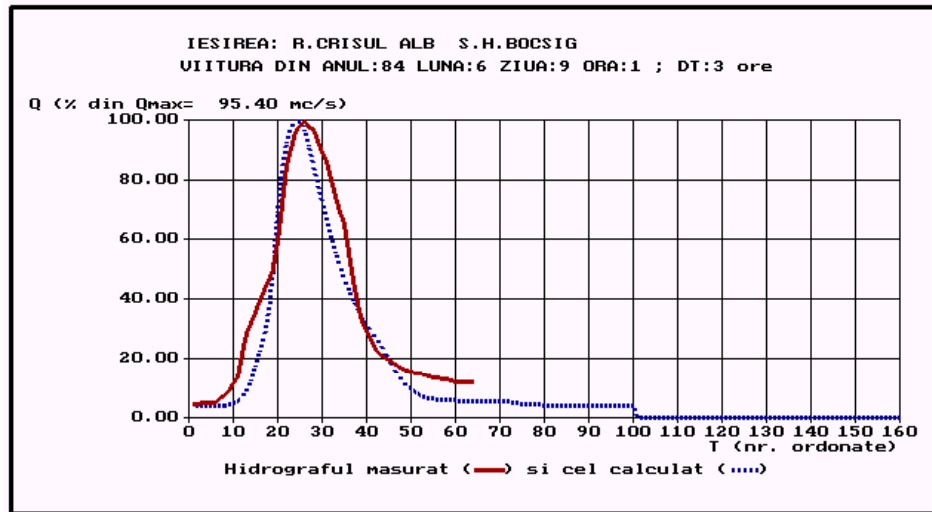


Fig. 8: Discharge hydrographs (red line – measured; dotted blue line – computed) at the Bocsig hydrometric station on the Crisul Alb River.

Determination of flood waves for the sub-basins: The sixth step is the determination of flood waves on all sub-basins, and also their building and propagation in the forecast sections on the main river. For the aggregation and propagation of the flood waves the Muskingum method is used, and for the attenuation through reservoirs, a mathematical algorithm is used, which is based on the PULS method. Once the flood waves of the sub-basins are determined, with the method presented before, the model of the building of the flood wave in a certain section on the main river can be applied in certain conditions regarding rain distribution on the whole basin area: uniform rain on the basin; rain with different distribution on different areas of the basin; rain concentrated upstream or downstream of a reservoir; rain having the occurrence direction from upstream to downstream or vice-versa.

Fig. 8 shows the results obtained at the Bocsig hydrometric station by applying the presented methodology in the Crisul Alb River basin.

Conclusions

- The proposed methodology is adequate when we have in real time information about the flood wave formation, upstream of the forecast point.
- The data from the representative river basins have provided a solid support for the determination of the model relations, for constructing the flood waves.
- The method efficiency is due to the fact that, unlike other methods, the needed precipitation input data are represented by the total predicted rainfall amount, without requiring information about the rainfall distribution.

References

- Diaconu C. (1976). Flood forecasting based on warning small basins. *Meteorology and Hydrology*, 1, Bucharest, Romania.
- Mita P., Corbus C. (1998). A model for determining flood waves in small basins up to 100 km². *Proceedings of*

the Seventh Conference of the European Network of Experimental and Representative Basins, Liblice, Czech Republic.

Mita P., Corbus C., Matreata M. (2004). A method for determining flood hydrographs in small river. *Proceedings of the 10th ERB Conference, Turin, Italy.*

CONTINUOUS HYDROLOGIC MODELING OF MIDDLE URUGUAY TRIBUTARY FLOWS

M. Uriburu Quirno, J. Borús & D. Goniadzki

Instituto Nacional del Agua (National Water Institute). Autopista Ezeiza-Cañuelas, Tramo J. Newbery, km 1.62. 1804- Ezeiza, Prov. de Buenos Aires, República Argentina.

Corresponding author: M. Uriburu Quirno, email: muriburu@ina.gov.ar

ABSTRACT

A continuous lumped hydrologic model has been calibrated and validated for the catchments of three tributaries of the Middle Uruguay River: the Ibicui River basin (42,900 km²), the Ijui River basin (9,400 km²), and the Piratinim River basin (5,300 km²), all in Brazilian territory. The simulations were good in terms of correlation, volumes and timing between observed and modeled discharge series. Therefore, a suitable forecasting tool has been built. As such, it requires both observed and predicted inputs, for the warm-up period and for the lead time, respectively. Forecast of daily rainfall may be extracted, for instance, from outlooks for South America, made available by the National Centers for Environmental Prediction of the United States, whereas daily potential evapotranspiration may be estimated empirically.

Keywords: hydrologic model, continuous modeling, hydrologic forecasts, Uruguay river basin

Introduction

The National Water Institute of Argentina (INA) is responsible for the operation of a hydrological warning system for the Del Plata Basin. With an area of 3.1 million sq. km, this basin is shared by Brazil, Paraguay, Bolivia, Uruguay and Argentina. Its main rivers are some of the largest in the world and their floods can have a tremendous socio-economic impact. The INA's warning system was developed after the devastating floods of 1982-83 and has been providing a permanent service ever since. It is committed to operational hydrometeorology, basin monitoring, and short-, medium- and long-term hydrological forecasts.

Table 1. Study basins features

Feature	Ibicui basin	Ijui basin	Piratinim basin
Basin area (sq. km)	42,900	9,400	5,300
Centroid location (Lat-Lon)	-29° 40', -55° 20'	-28° 27', -53° 55'	-28° 45', -54° 40'
Elevation range (m amsl)	100 - 550	200 - 480	100 - 530
Time of concentration (days)	5.1	2.4	1.8
Annual rainfall (mm)	1,600	1,650	1,650
Annual potential evapotranspiration (mm)	900	860	860
Annual runoff (mm)	650	855	855
Annual flow rate (m ³ .s ⁻¹)	880	254	143
Ratio mean annual flow: rainfall	40%	52%	52%

Consolidation of the system was achieved by improving data collection, diagnosis and forecast and by strengthening the relationship with users. As part of these efforts, this study presents the application of hydrologic modeling to three basins: (a) Ibicui basin, (b) Ijui basin, and (c) Piratinim basin, all in Brazil. These rivers are tributaries of the Middle Uruguay River, a bi-national boundary across which a large hydropower dam is set downstream from the three confluences (Salto Grande Dam) and a second hydropower dam is in

project, upstream from the confluence with the Ibicui River (Garabi Dam). A continuous lumped conceptual physically-based hydrologic model (based on the differential approach of the Sacramento model) has been calibrated, fed by areally-averaged rainfall and air temperature. In order to use the model as an operational forecasting tool, forecast inputs are needed. Various sources for weather forecast are available, with different lead times and resolutions. Precipitation forecast, as well as rainfall and temperature outlooks for South America, issued by the National Centers for Environmental Prediction (US-NCEP) are possible solutions. The main characteristics of the three study basins are summarized in Table 1. Fig. 1 shows the basins in the context of South America.



Fig. 1: Study basins in southeastern South America.

Model description

The model simulates the processes of rainfall-runoff and flow routing. It is based on the differential version of the Sacramento Soil Moisture Accounting Model (Burnash et al., 1973), described in different papers (e.g. Bae and Georgakakos, 1994; Guetter, 2000). Yet a conceptual spatially-lumped two-layer model of the soil vertical profile as is the Sacramento, this version reduces its complexity, gaining in robustness and ease of use for operational purposes. The main modifications are: (a) the differential formulation in the state space and (b) the addition of a flow routing component.

The model is structured in two components: (1) Rainfall-runoff component, which simulates for a soil column, the soil moisture balance resulting from two fluxes through the soil-atmosphere interface, i.e. rainfall and evapotranspiration. The soil column is divided into two layers, a fast-responding upper layer and a slow-responding lower one. Precipitation is the primary source of water for both layers (directly into the upper layer and through percolation into the second one). Water losses are accounted for by evapotranspiration: as evaporation from the upper layer and transpiration from the lower one. Unlike the Sacramento model, no sub-processes are considered within the two layers. Tension and free water contents are not considered separately. This formulation tends to reduce flexibility for applications of fine temporal resolution (order of hours), such as those required for small and steep fast responding catchments. However, it is sufficiently adequate for a time scale in the order of days, such as that of the study basins. (2) Flow routing component, which simulates the routing process along the drainage network by means of a conceptual two-equal-linear-reservoir cascade. Following the notation by Guetter (2000), the state equations governing the processes read:

$$\frac{dX_1}{dt} = P - SR - PC - ET_1 - INT \quad \text{Eq. 1} \quad \frac{dX_2}{dt} = PC - ET_2 - GW \quad \text{Eq. 2}$$

$$\frac{dX_3}{dt} = (SR + BF) - \alpha X_3 \quad \text{Eq. 3} \quad \frac{dX_4}{dt} = \alpha X_3 - \alpha X_4 \quad \text{Eq. 4}$$

where X_1 / X_2 is the volume of water in the upper/lower soil layer $[L]$ (state variables), X_3 / X_4 is the water stored in the first / second linear reservoir of the cascade $[L]$ (state variables), P is the rainfall intensity $[L.T^{-1}]$, SR is the surface runoff $[L.T^{-1}]$, PC is the percolation rate $[L.T^{-1}]$, ET_1 is the evaporation rate from the upper soil layer $[L.T^{-1}]$, INT is the interflow, i.e. the flow from the upper soil layer to base flow $[L.T^{-1}]$, ET_2 is the transpiration rate from the lower soil layer $[L.T^{-1}]$, GW is the groundwater flow $[L.T^{-1}]$, BF is the base flow $[L.T^{-1}]$ and α is the inverse of the reservoir recession constant $[T^{-1}]$.

a) Surface runoff is a direct response to rainfall, produced only by the upper soil layer. It is computed as:

$$SR = P.(X_1 / X_1^0)^{m_1} \quad \text{Eq. 5}$$

where X_1^0 , the water-holding capacity of the upper soil layer $[L]$, and m_1 , the surface runoff exponent [dimensionless], are two of the model parameters. The other variables are as defined above.

b) Surface evaporation rate from the upper soil layer is computed as the product of the potential evapotranspiration rate and the water availability in the layer:

$$ET_1 = PET.(X_1 / X_1^0) \quad \text{Eq. 6}$$

where PET is the potential evapotranspiration rate $[L.T^{-1}]$ along the computational time step.

c) The process of percolation, which represents the water transfer from the upper soil layer to the lower one, is computed as a non-linear function of their storages, such that:

$$PC = C_3.X_2^0.(1 + C_2.(1 - X_2 / X_2^0)^{m_2}).(X_1 / X_1^0) \quad \text{Eq. 7}$$

where X_2^0 is the water-holding capacity of the lower soil layer $[L]$, C_3 is the base flow recession rate $[T^{-1}]$, C_2 is the percolation function coefficient [dimensionless] and m_2 is the percolation function exponent [dimensionless]. These four variables are model parameters while the others are as previously defined.

Subsurface flow $C_3.X_2^0$ corresponds to the lower layer outflow in saturation conditions. The parameters C_2 and m_2 control the percolation rate when the lower layer is unsaturated. Percolation increases with the ratio X_1 / X_1^0 , that is, with soil moisture in the upper layer approaching its water-holding capacity.

d) Interflow is taken proportional to the first state variable, such that:

$$INT = C_1 X_1 \quad \text{Eq. 8}$$

where C_1 , the interflow recession coefficient $[T^{-1}]$, is a model parameter. The other variables, as previously defined.

e) Transpiration from the soil lower layer is computed as:

$$ET_2 = (PET - ET_1).(X_2 / X_2^0)^{m_3} \quad \text{Eq. 9}$$

where m_3 is a model parameter that represents the transpiration function exponent [dimensionless], and the other variables are as previously defined.

f) The groundwater flow is calculated (with predefined variables) as:

$$GW = C_3 \cdot X_2 \quad \text{Eq. 10}$$

g) The base flow is proposed as a function of both interflow and groundwater flow, yielding:

$$BF = (1 + \mu)^{-1} \cdot GW + INT \quad \text{Eq. 11}$$

where μ [dimensionless] is a model parameter such that $GW/(1 + \mu)$ contributes to the base flow and $GW \cdot \mu/(1 + \mu)$ recharges the aquifer. The other variables are as defined above.

h) The flow routing process along the drainage network is modeled by a two-equal-linear-reservoir cascade, so that:

$$\frac{dX_3}{dt} = (SR + BF) - \alpha X_3 \quad \text{Eq. 12}$$

$$\frac{dX_4}{dt} = \alpha X_3 - \alpha X_4 \quad \text{Eq. 13}$$

$$Q_i = \alpha X_i, \quad i = 3, 4 \quad \text{Eq. 14}$$

where Q_3 and Q_4 [$L \cdot T^{-1}$] are the outflows from the first and the second conceptual reservoirs respectively, and α , the inverse of the reservoir recession constant, is a model parameter. The other variables, as defined above.

Model implementation and numerical integration

The time step adopted for the modeling is one day, in accordance with data availability, catchment time scales and duration of significant storm events (two to four days). Due to the dominant climate in the region, snowmelt is clearly not a process to be modeled. Similarly, the absence of frozen ground effects do not interfere percolation and interflow. Only daily precipitation as rainfall and daily potential evapotranspiration are inputs. A 4th-order Runge-Kutta Method was applied for integration of the differential equations. Daily time steps were split into subintervals so that precipitation in each one is less than 2 mm (with at least 2 subintervals). This has been done for the sake of precision since the equations are highly non-linear.

Data requirements

The model requires daily potential evapotranspiration and mean areal rainfall along the simulation period. In the absence of daily field measurements of pan (or other) evaporation, estimates were based on the empirical Thornthwaite formula (Thornthwaite, 1948). Its main independent variable, the monthly mean air temperature was estimated through reanalysis made by NOAA's NCEP/NCAR (National Center for Atmospheric Research). Monthly values of PET were simply divided by the number of days of the month in order to obtain daily PETs. Regarding daily mean areal precipitation, rain-gauge data are available from a set of telemetric stations in the region, belonging to the Brazilian Water Agency (ANA). Mean areal values were computed using Thiessen Polygons. Flow rates were computed with available rating curves. ANA records water stages twice daily. After transformation to flow rate and averaging, the three daily streamflow series were obtained for the period from 09/01/2004 to 01/31/2006.

The operational mode requires both observed and predicted inputs, for the warm-up period and for the lead time, respectively. Forecast daily rainfall may be extracted, for instance, from outlooks for South America,

made available by the NCEP or from the results of the Southern South-America version of the ETA model (Mesinger et al., 1988; Janji, 1990; Collini et al., 1997). Since the hydrologic model proved not very sensitive to daily potential evapotranspiration, empirically computed climatic values are sufficiently good as inputs for the lead-time.

Calibration and validation

Ten model parameters were calibrated for each basin. The model performance criterion was a weighted quadratic error that reflects the extent to which the model is successful in reproducing observed flow rates. The sum of squares of differences between the observed and the simulated discharges was used, each term affected by a weighting function that gives preference to the accurate reproduction of observed peak flows. Minimization of this objective function resulted in the optimal set of parameters. The minimization was performed with an automatic procedure, the Downhill Simplex Method (Nelder and Mead, 1965), while parameter constraints were dealt with by a Penalty Function Method (Heath, 2002). The penalty function method computes an approximate solution to a constrained optimization problem by successive unconstrained optimization of a weighted combination of the original objective function and a function that penalizes violation of the constraints.

For calibration and validation, data are available along the period 09/01/2004 to 01/31/2006. The period was split into three fourths and one fourth, respectively. Ten significant flood waves occurred, with peaks well above the normal discharge, and three periods of low waters were observed. Table 2 presents the optimized values of the ten parameters.

Table 2. Calibrated parameters

Parameter	X_1^0	X_2^0	m_1	C_1	C_2	C_3	μ	α	m_2	m_3
Units	[mm]	[mm]	[1]	[1/day]	[1]	[1/day]	[1]	[1/day]	[1]	[1]
Ibicui basin	194.1	397.3	1.55	0.00322	235.67	0.0010	4.87	0.251	1.23	1.35
Ijui basin	350.0	427.5	3.50	0.00496	47.59	0.0050	6.00	0.464	2.20	3.68
Piratinim basin	350.0	104.9	3.17	0.00019	192.92	0.0182	4.35	0.455	2.20	4.27

Beyond the objective function applied to optimize the parameters, the model performance was also assessed through other statistics: (a) relative error in mean discharge, (b) relative error in standard deviation of discharge, (c) correlation coefficient of modeled and observed series, and (d) SPEDS (Special Directional Symmetry), a measure of the phase shift between the two series. SPEDS sums up one for every time both observed and simulated incremental quotients have the same sign, along the simulation period, and zero otherwise. It is expressed as percentage of the total number of time steps. The model performance is presented in Table 3. Hydrographs are shown in Figs. 2 through 7.

Table 3. Model performance

Statistic	Calibration
(a) $\frac{\bar{Q}_{sim} - \bar{Q}_{obs}}{\bar{Q}_{obs}}$	-0.27%
(b) $\frac{S_{Q,sim} - S_{Q,obs}}{S_{Q,obs}}$	-2.10%
(c) r	96.74%
(d) $SPEDS$	83.5%

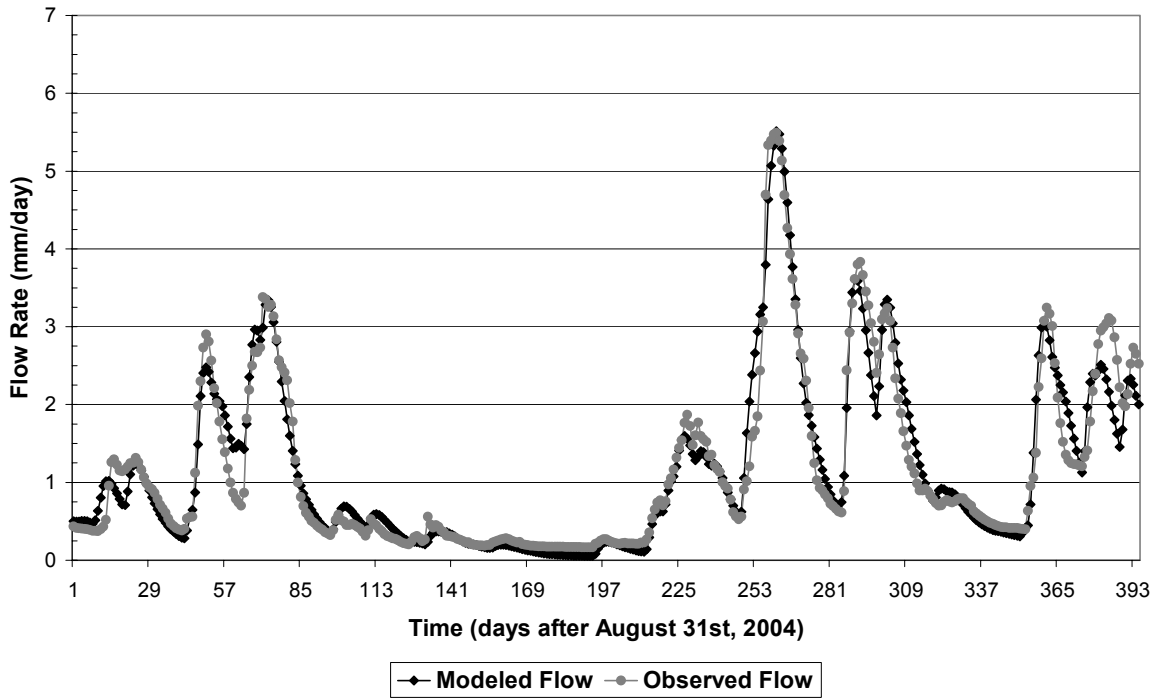


Fig. 2: Ibicui River. Calibration. (1mm/day = 497 m³.s⁻¹)

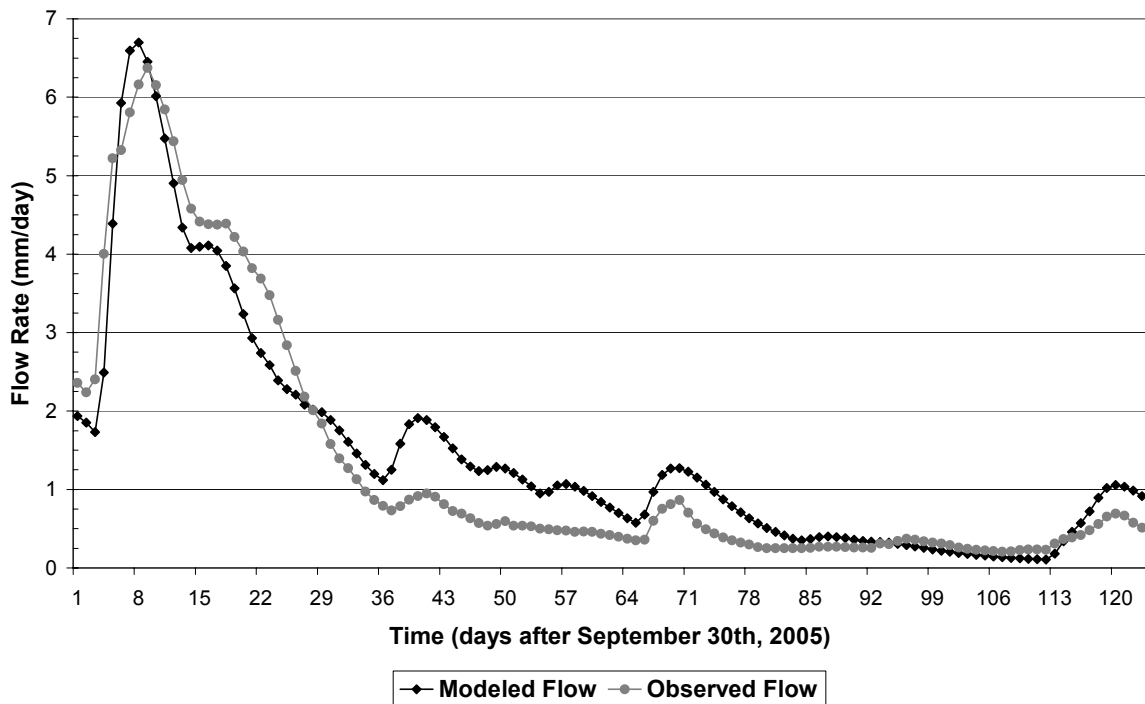


Fig. 3: Ibicui River. Validation. (1mm/day = 497 m³.s⁻¹)

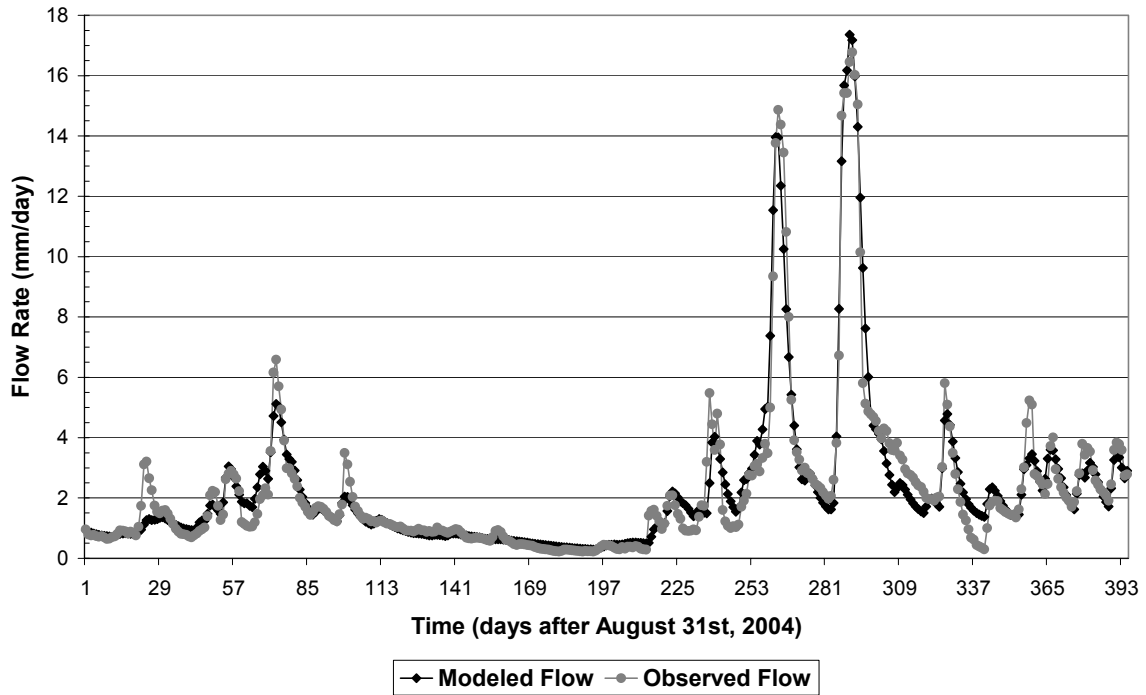


Fig. 4: Ijui River. Calibration. (1mm/day = $109 \text{ m}^3 \cdot \text{s}^{-1}$)

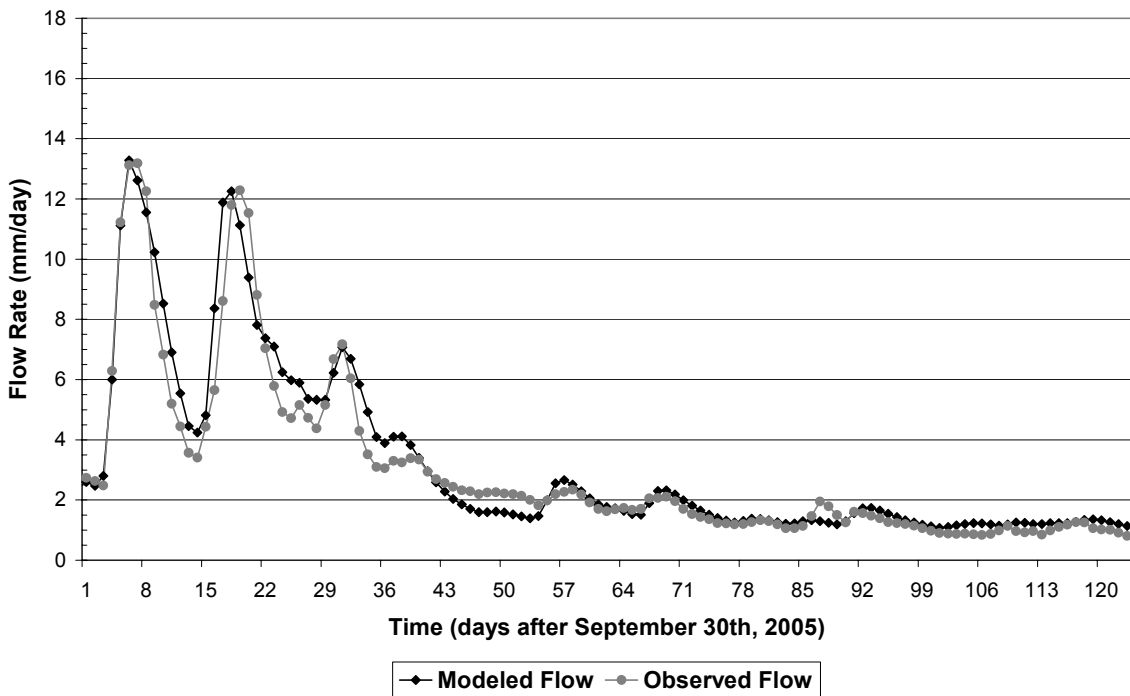


Fig. 5: Ijui River. Validation. (1mm/day = $109 \text{ m}^3 \cdot \text{s}^{-1}$)

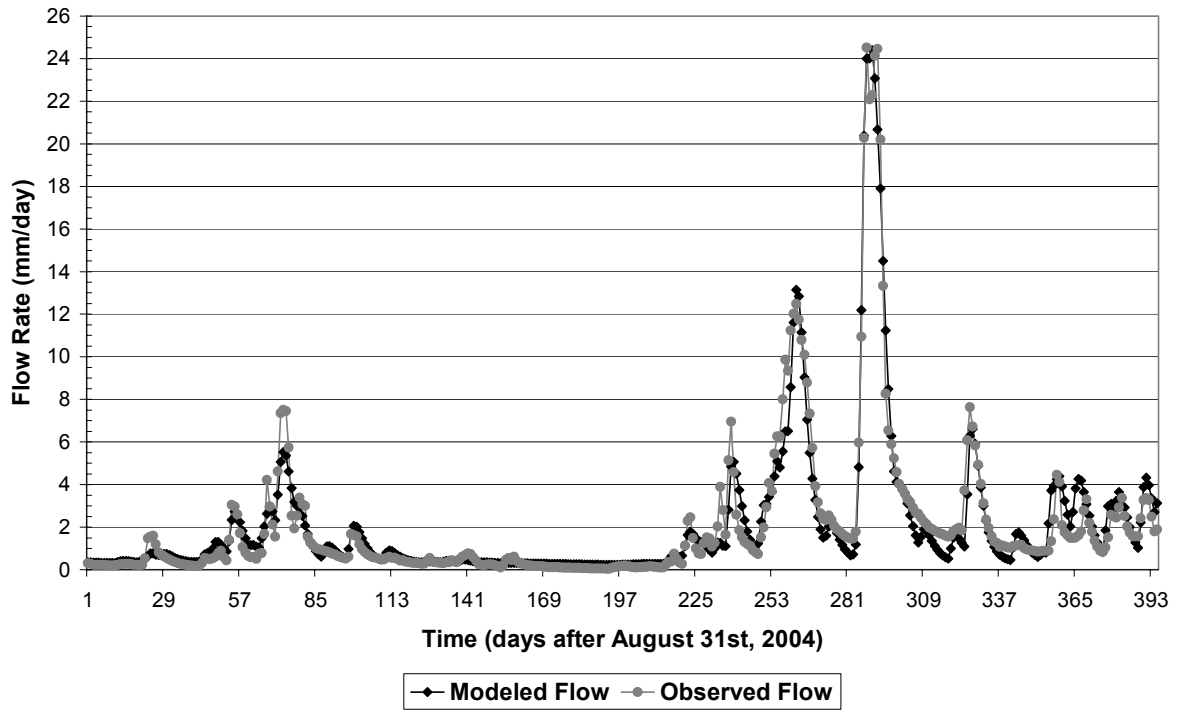


Fig. 6: Piratinim River. Calibration. (1mm/day = $61 \text{ m}^3 \cdot \text{s}^{-1}$)

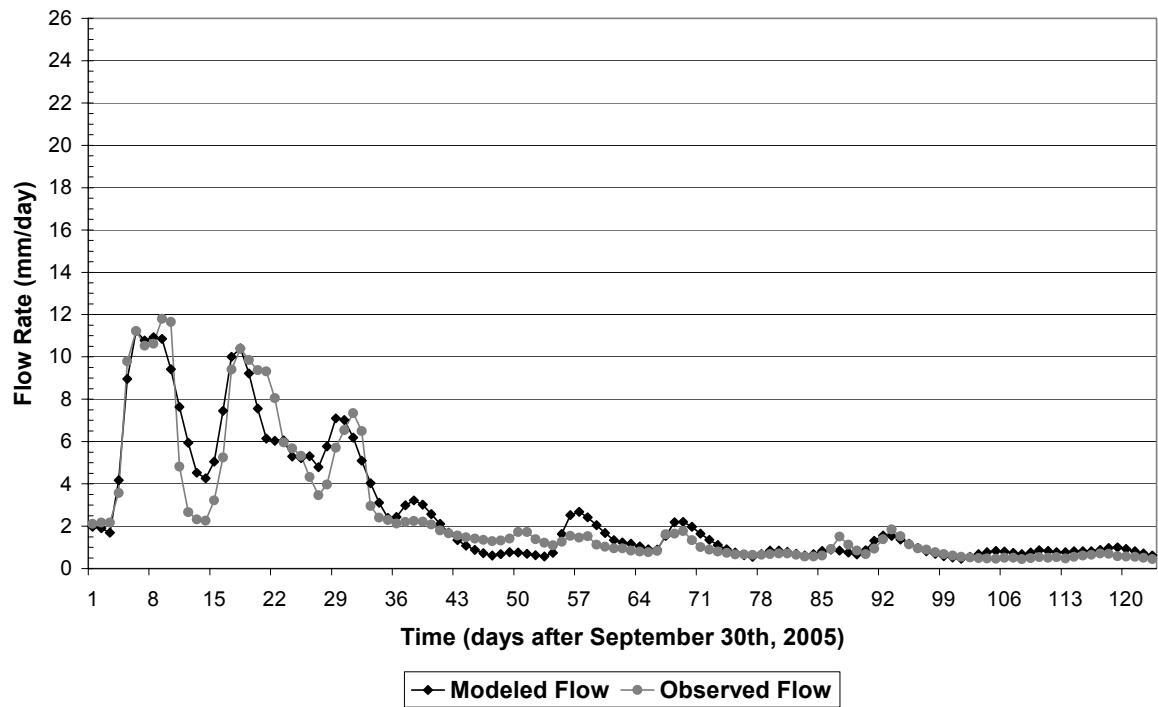


Fig. 7: Piratinim River. Validation. (1mm/day = $61 \text{ m}^3 \cdot \text{s}^{-1}$)

Conclusions

The model performed very well for the three basins, both in calibration and validation. It faithfully represented the physical processes and the daily water balance. It simulated adequately the streamflows, both during floods and low waters, with daily resolution. The model showed a fast reaction to heavy-rain events, especially when the precipitation pattern affected the entire catchment. The peak error was reduced and the timing was always tightly reproduced, important features particularly when the focus is set on operational forecasting of flood waves, as is the case. Additionally, the agreement was also very high during low flow regimes and the total volume was well quantified. Therefore, it is concluded that the model is suitable for operational use.

Although the time series is relatively short (only 17 months), which would invite to future recalibrations when longer records become available, it is worth noting that receding limbs are almost all very well simulated, an indication of a close representation of the soil layer characteristics. Rather, future efforts will be devoted to investigate possible improvements in the representation of the spatial distribution of the daily precipitation field. However, it should be remembered that, even with a 'perfectly' calibrated model, the quality of the flood forecasts is tightly dependent on that of the quantitative precipitation forecast along the lead time, which normally loses reliability quickly after a few days.

References

- Bae D.H., Georgakakos K.P. (1994). Climatic variability of soil water in the American Midwest: Part 1. Hydrologic modeling. *Journal of Hydrology*, 162: 355-377.
- Burnash R.J.C., Ferral R.L., McGuire R.A. (1973). *A Generalized Streamflow Simulation System - Conceptual Modeling for Digital Computers*. U.S. Department of Commerce, National Weather Service and State of California, Department of Water Resources.
- Collini E.A, Berbery E.H., Rogers E. (1997). Application of the Eta Model to the Southamerican Region. *Proceedings of the Fifth International Conference on Southern Hemisphere Meteorology and Oceanography*. April 7/11, 1997, Pretoria, South Africa.
- Guetter A.K. (2000). *Hydrological Modeling and Hydrological Warning Systems*. Lecture Notes (in Portuguese). Advanced Course in Numerical Modeling, Lima, Perú, 03-14/July/2000.
- Heath M.T. (2002). *Scientific Computing, An Introductory Survey*, 2nd edition, McGraw-Hill, New York.
- Janji Z.I. (1990). The step-mountain coordinate: Physical package. *Monthly Weather Review*, 7: 1429-1443.
- Mesinger F., Janji Z.I., Nikovi S., Gavrilov D., Deaven D.G. (1988). The step-mountain coordinate: Model description and performance for cases of alpine lee cyclogenesis and for a case of an Appalachian redevelopment. *Monthly Weather Review*, 116: 1493-1518.
- Nelder J.A., Mead R. (1965). A simplex method for function minimization. *Computer Journal*, 7: 308-313.
- Thornthwaite C.W. (1948). An approach toward a rational classification of climate. *Geographical Review*, 38: 55-94.

SEARCHING FOR AN OPTIMUM LEVEL OF SPATIAL DISTRIBUTION AND COMPLEXITY IN REGIONAL MODELLING

R. van den Bos, P. Matgen & L. Pfister

Department Environment and Agro-Biotechnologies, Public Research Center-Gabriel Lippmann, 41 rue du Brill, L-4422 Belvaux, Grand-Duchy of Luxembourg.

Corresponding author: R. van den Bos, email: vandenbo@lippmann.lu

ABSTRACT

The dominant processes concept has been used to develop a regionally applicable rainfall-runoff model. Conceptual models with variable complexity were developed to monitor the level of spatial distribution of first order controls on the runoff processes that is needed to accurately represent the hydrological processes. For each model structure the runoff signals were calibrated against the hourly-recorded discharge series of 10 sub-basins, with model performance, parameter sensitivity and correlation analysis outlining the justification of the level of complexity in the model structure. Validation against another set of 8 sub-basins indicated the level of complexity, at which the performance of the model is robust in regional applications. Due to an up-scaling effect, inducing variations in the dominance of particular runoff processes, some anomalies were found in the performance of individual runoff characteristics. In this respect, limiting the application of the model to the investigated spatial scale gives a high reliability of the prediction of the dynamics of hourly runoff in ungauged basins within the study area. This analysis depends on two factors, being the amount of representative data available and the homogeneity of the basin characteristics within the area of interest. Hence, the results are always regionally conditioned.

Keywords: Alzette river basin, dominant processes concept, model complexity analysis, PUB, top-down approach

Introduction

Within the framework of the Predictions in Ungauged Basins (PUB) Decade (Sivapalan et al., 2003), the demands have been expressed to investigate the possibilities of developing hydrological models with the explicit characteristic to have high potential in predicting hydrograph behavior in non-monitored basins. Much effort has been put in a structural approach that combines findings of different studies with various model structures into a general assessment of the potential of these models for global application (e.g. Perrin et al., 2001; Croke et al., 2006). However, since the hydrological processes that generate the volumes and timing of the runoff reaction are always based on a local compilation of the natural system (depending on the geologic, pedologic, land cover and climatologic attributes of the research area), the conceptual representations of these processes are hard to establish in a single, general model structure. Two approaches are generally applied to solve the problem of spatial variability of runoff generating processes, being the top-down approach and the bottom-up approach. The top-down approach tries to link specific model structures and their parameter values to the characteristics of the basins of interest, whereas the bottom-up approach focuses on the development of models that are capable of representing the physical background of the flowpaths of the basin of interest (Littlewood et al., 2003). Examples of both approaches can often be found in literature, but it goes beyond the scope of this paper to give a complete overview.

In an effort to overcome the problem of spatial variability of dominant controls on the runoff generating processes we decided to investigate the possibility of developing a regionally applicable model that is capable of representing the hydrological processes that dominate the runoff behavior in the vicinity of the Alzette river basin only. This investigation started already several years ago, but due to the growing information content of the measured runoff data within the area, new model structures were repeatedly being tested in a search for an

accurate representation of the spatial and temporal behavior of the hydrographs of the main rivers and their tributaries. This paper will give an overview of the previous efforts to develop such a regionally applicable model and it will give an assessment of the accuracy of the model and its representation of the dominant processes.

Study area

The Alzette river basin (1175 km²) is mainly located in the Grand Duchy of Luxembourg and contains a dense network of over 20 discharge measurement locations, whereby five tributaries are considered in more detail, being the Petrusse (45 km²), the Eisch at Hagen (49 km²), the Mamer at Mamer (18 km²), the Mierbech (7 km²) and the Bibeschbach (11 km²). These measurements are accompanied by a raingauge network with an average station density of one per 30 km². Since the spatial correlation in rainfall is difficult to capture for small time steps, lumped rainfall values are estimated for each basin, according to the weights of the Thiessen polygon configuration of the surrounding raingauge stations. Potential evapotranspiration (PET) values are estimated with the Hamon equation. Marls form the most important lithological formations, dominating approximately 60% of the basin area.

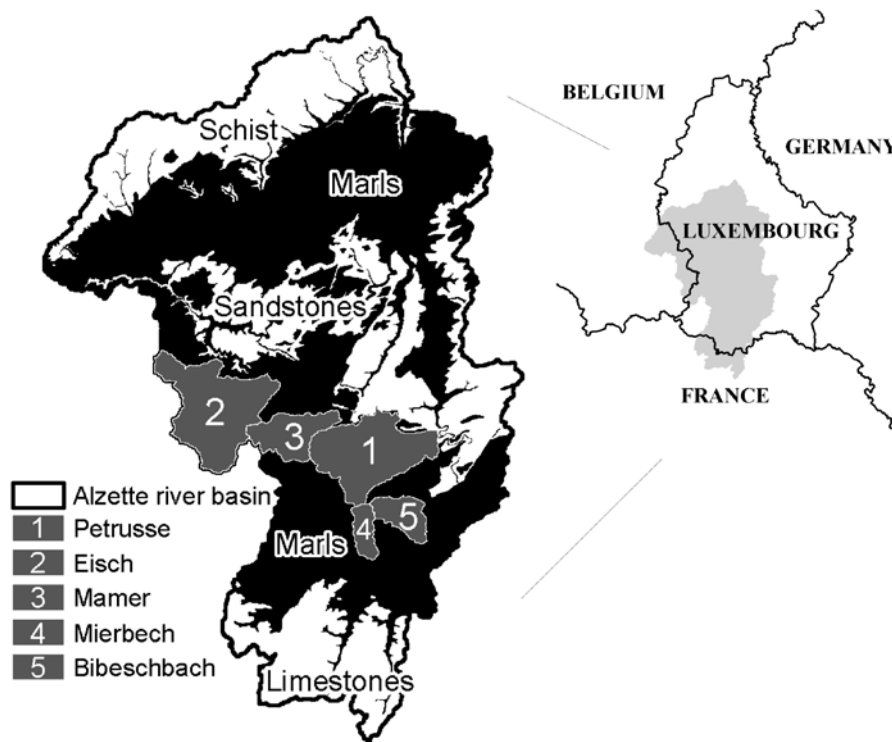


Fig. 1: The Alzette river basin and its lithological units with the five basins of which the discharge series are used for the model complexity analysis.

Initial model structures and performances

Six years ago, a parsimonious conceptual rainfall-runoff model HRM (4 parameters) was applied on the River Alzette and its monitored tributaries (Drogue et al., 2002). After a calibration and validation procedure, the optimal parameters of the model were compared with the basin attributes of the different basins. This top-down analysis resulted in a significant correlation between some of the model parameters and the permeability of the geology of the basin. Incorporating the spatial distribution of permeable and impermeable substrata in the

model structure improved the simulations for a set of independent basins, using the optimal parameter sets of the calibration basins.

Independent from the previously mentioned study, a second investigation with a different model was performed. This model, SOCONT, which had only three parameters, was applied on the same basins with the same calibration techniques and procedures (Hoffmann et al., 2004). However, this time the link between model parameters and basin attributes (slope, percentage of impermeable substrata and basin area) was obtained through stepwise regression analysis. The analysis of some distinctive objective functions showed that for the calibration as well as the validation basins, the HRM model performed significantly better than the SOCONT model. Especially the efficiency value (R_{eff} , Nash and Sutcliffe, 1970) clearly demonstrated this fact (Table 1). Hence, the model with more complexity was superior to the other, if we consider the number of parameters as indication of complexity.

After the collection of another two years of discharge data and the experimental investigation on the runoff characteristics in different geological formations a totally new approach was undertaken to achieve a better representation of the spatial distribution of the dominant hydrological processes (Van den Bos et al., 2006). Based on the experimental knowledge gained and the information content of physio-geographical maps, a bottom-up analysis of the process representation was performed and transformed into conceptual model structures for different lithological units (the ALZETTE model). This means that the processes are not described in a physically based way, but in a parsimonious conceptual way, which gives this approach a more hybrid bottom-up character (see Littlewood et al., 2003). Again, a similar calibration and validation procedure was performed, however with a different set of basins, because instead of daily, hourly data could be used for this purpose. The regional parameter sets were estimated with the calibration basins, which were chosen as most representative for the four different lithological units. Through a river routing module the runoff of the different units could be combined into a hydrograph signal at any location in the study area. Table 1 also shows the results of this modelling exercise, displaying a significant improvement in consistency of the regional model performance. With the regional performance the performance of the transferred calibration parameters is meant.

Table 1 : Average performances of the different modelling exercises.

Model	Calibr. basins	Valid. basins	
	average R_{eff}	average R_{eff}	regional R_{eff}
HRM (Drogue et al., 2002)	0.81	0.79	0.72
SOCONT (Hoffmann et al., 2004)	0.76	0.70	0.63
ALZETTE (Van den Bos et al., 2006)	0.81	0.83	0.79

Model complexity analysis

Although the unit-based ALZETTE model was giving good results, some concerns could be expressed on the performance potential of the parsimonious model structures of the different units. Since these structures were derived from process knowledge and simplified into conceptual representations, the performance of these structures depends on how well we understand the processes. If any misinterpretation of the dominance of certain processes occurred, the model will show higher accuracy if 'better' model structures are used. This can be either a more simplistic representation or a more complex one. We therefore applied a total number of 64 model structures of different complexity and with different interactions between the storage reservoirs of the model. These model structures are generated from a combination of modules. It goes beyond the scope of this paper to explain each flux in the model modules, but the visualization of Fig. 2 is a good impression of the used complexities.

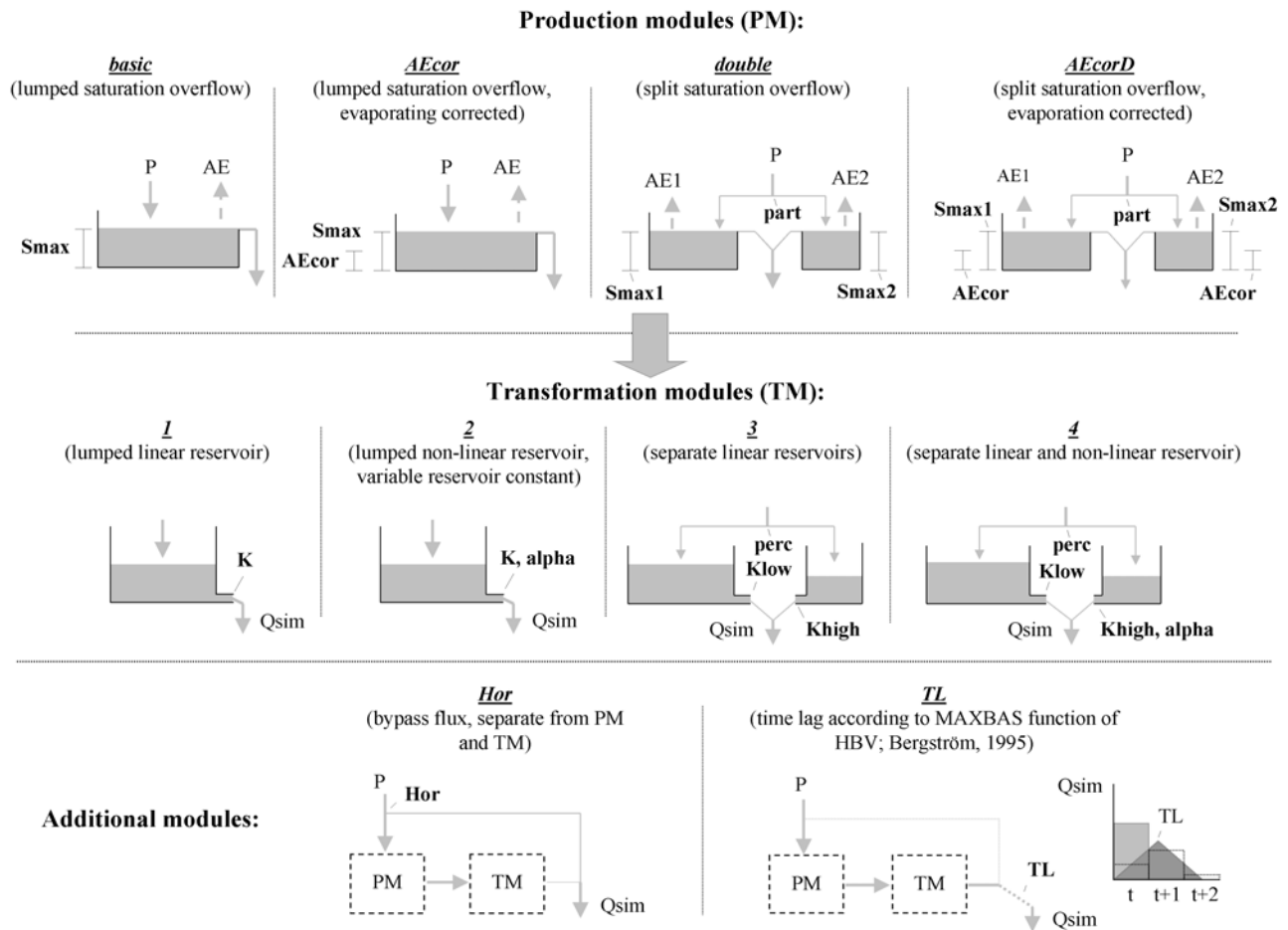


Fig. 2: Pragmatic overview of the model modules that together form 64 possible model structure combinations.

Since not enough data sets are available for each unit to perform such an analysis, we only applied this approach to the more extensively measured unit of marls, having the availability of five basins with hourly discharge data (see Fig. 1). The results are therefore indicative only for how well we were able to capture the runoff behaviour of the marls unit into a simple model structure. In principle, however, these results have no general meaning for the whole model.

Looking in detail at the R_{eff} -values of the different combinations of modules and for each of the five basins, it can be seen that the runoff reaction of the unit is far from being homogeneous over the five basins (Fig. 3). Each basin shows an optimum performance for a different combination of modules, meaning that apparently some processes dominate the runoff reaction in one location more than in another.

The results of the Mierbech basin indicate that the good model performance is mainly based on the non-linear transformation structure ('2_TL'), more than on the differentiated linear reservoirs ('3_TL'). The Eisch basin on the other hand shows the opposite, where transformation structure '3_TL' performs just as accurate as structure '4_TL', whereas structure '2_TL' lacks in accuracy. The Mamer basin only gives most accuracy if both modules are involved ('4_TL'). The results of the Petrusse basin mainly depend on the presence of the combination of 'TL' and 'Hor' in the model structure. This is a clear indication that compared to the other basins, its large percentage of urban area influences the runoff generation significantly. Finally, the

Bibeschbach basin is somewhat sensitive to an increasing amount of complexity, which could also mean that the maximum complexity for accurate simulations could be even higher.

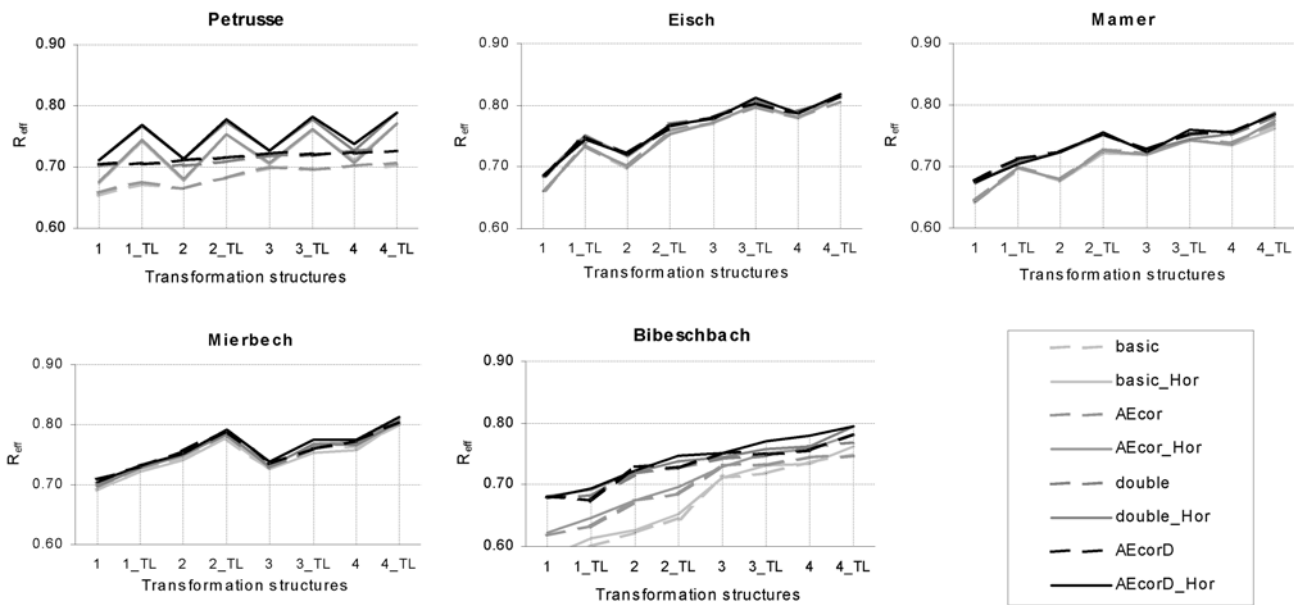


Fig. 3: R_{eff} -values for the optimum parameter sets for each basin and for the different combinations of model modules.

However, if we consider the regional performance of the five basins, which is the average performance of all basins using one single model and parameter set, it appears that the best combinations perform just as well as the ALZETTE model structure that has been defined through bottom-up process analysis. The best regional performance for both approaches (top-down and bottom-up) has a R_{eff} -value of 0.75. Also the similarity between these two model structures is striking, with only a difference in the interceptive storage module of the model and some discrepancy in the routing functions of the two model structures (Fig. 4).

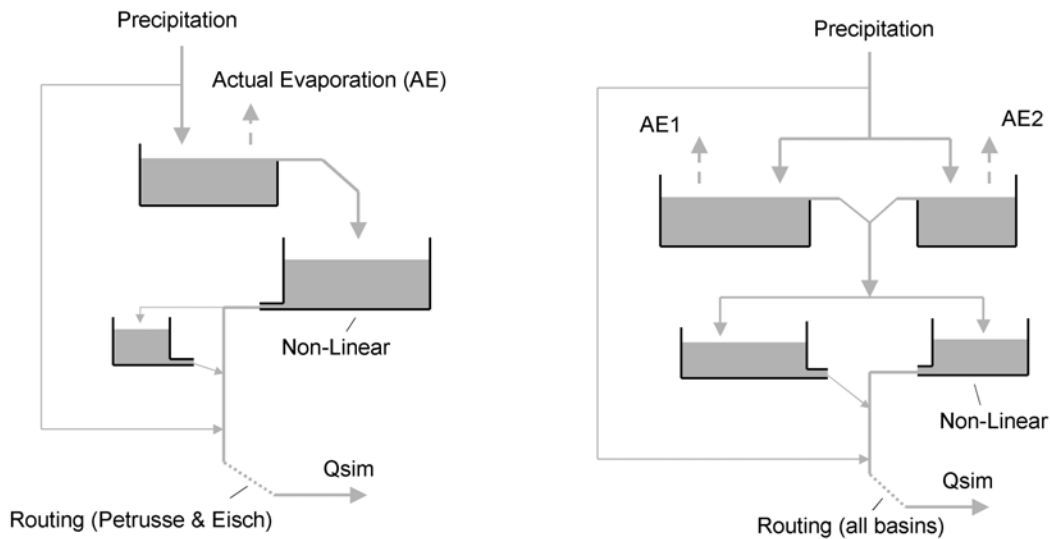


Fig. 4: Comparison between the marls unit of the ALZETTE model structure (left) and the optimal performing model structure of the complexity analysis (right).

Discussion

We found that when we applied a top-down model analysis on the marls unit, the local performance increased compared to the bottom-up defined model structure. However, we also found that the regional performance was not affected by changing model complexity levels. These facts strongly suggest that even more spatial distribution is needed within the total model structure to obtain better regional performances. However, this is impossible to implement, since not enough calibration and validation data is available to verify the correctness of such an additional model distribution. On the other hand, these results also suggest that the process representation, as it was found in the bottom-up approach, was appropriate on a regional basis, which makes us more confident about the accuracy of the model representation of the other units, although the results can only be considered as an indication of the model structure correctness. Finally, it can be argued that the model complexity analysis itself is a very useful tool to better understand the variability in the runoff behaviour of different basins. It clearly identified the distinctive runoff reactions of the basins and even gave some information on what these differences look like. This can be very useful information if a new study is started in the future on the same topic with, again, more data available. It would help finding the distinctive processes and their dominance and it would contribute to the identification of their spatial distribution. However, this will certainly take another few years of taking measurements as well as it needs a higher number of monitored locations.

References

- Croke B.F.W., Littlewood I.G., Post D.A. (2006). Rainfall-streamflow-air temperature datasets (and catchment information) available internationally to assist with PUB Decade top-down modelling. In: A. Voinov, A.J. Jakeman, A.E. Rizzoli (Eds.), *Proceedings of the iEMSs Third Biennial Meeting: Summit on Environmental Modelling and Software*. International Environmental Modelling and Software Society, Burlington, USA, July 2006.
- Drogue G., Pfister L., El Idrissi A., Iffly J.-F., Hoffmann L., Leviandier T., Guex F., Hingray B., Humbert J. (2002). The applicability of a parsimonious model for local and regional prediction of runoff. *Hydrological Sciences Journal*, 47: 905–920.
- Hoffmann L., El Idrissi A., Pfister L., Hingray B., Guex F., Musy A., Humbert J., Drogue G., Leviandier T. (2004). Development of regionalized hydrological models in an area with short hydrological observation series. *River Research Applications*, 20: 243-254.
- Littlewood I.G., Croke B.F.W., Jakeman A.J., Sivapalan M. (2003). The role of ‘Top-Down’ modelling for Prediction in Ungauged Basins (PUB). *Hydrological Processes*, 17: 1673-1679.
- Nash J.E., Sutcliffe J.V. (1970). River flow forecasting through conceptual models. Part I: a discussion of principles. *Journal of Hydrology*, 10: 282-290.
- Perrin C., Michel C., Andreassian V. (2001). Does a large number of parameters enhance model performance? Comparative assessment of common catchment model structures on 429 catchments. *Journal of Hydrology*, 242: 275-301.
- Sivapalan M., Takeuchi K., Franks S., Schertzer D., O’Connell P.E., Gupta V.K., McDonnell J.J., Pomeroy J.W., Uhlenbrook S., Zehe E., Lakshmi V. (2003). IAHS Decade on Prediction in Ungauged Basins (PUB), 2003-2012: Shaping an exciting future for the hydrological sciences. *Hydrological Sciences Journal*, 48: 857–880.
- Van den Bos R., Hoffmann L., Juilleret J., Matgen P., Pfister L. (2006). Regional runoff prediction through aggregation of first-order hydrological process knowledge: a case study. *Hydrological Sciences Journal*, 51: 1021-1038.

ANNEX

POSTERS PRESENTED AT THE CONFERENCE

SESSION 1: 'UNCERTAINTIES IN HYDRO-CLIMATOLOGICAL MEASUREMENTS'

Álvarez-Mozos, J., Larrañaga, A., Gastesi, R., Casalí, J., González-Audicana, M. :
UNCERTAINTIES IN SURFACE STORAGE CAPACITY AS INFLUENCED BY RANDOM ROUGHNESS
SPATIAL VARIABILITY

Berakovic, B., Berakovic, M., Cesarec, K. :
UNSTEADY FLOW IN A NATURAL RIVER CAUSED BY HYDROELECTRIC POWER PLANTS:
MEASURES AND THEIR CONTROL

Buytaert, W., Célleri, R., De Bièvre, B. :
THE IMPACT OF SPATIAL VARIABILITY ON AREAL RAINFALL ESTIMATION IN SMALL
MOUNTAIN CATCHMENTS

Célleri, R., Willems, P., Buytaert, W., Feyen, J. :
SPATIAL RAINFALL VARIABILITY IN THE PAUTE RIVER BASIN FROM THE ECUADORIAN
ANDES

Jakubowski, W. :
DOES THE THRESHOLD LEVEL SELECTION HAVE AN INFLUENCE ON THE LOW FLOW
EXTREME INDICES DISTRIBUTIONS ?

Mezghani, A., Hingray, B., Musy, A. :
STOCHASTIC GENERATION OF WEATHER VARIABLE FIELDS FOR FUTURE CLIMATE CHANGE
SCENARIOS USING CIRCULATION INDICES FOR THE ALZETTE WATERSHED, LUXEMBOURG

Poyatos, R., Villagarcía, L., Domingo, F., Llorens, P. :
PARAMETERISATION AND APPLICATION OF A TWO-SOURCE EVAPOTRANSPIRATION MODEL
IN A SCOTS PINE (*PINUS SYLVESTRIS L.*) STAND UNDER MEDITERRANEAN MOUNTAIN
CONDITIONS (VALLCEBRE, EASTERN PYRENEES)

Rubio, C., Llorens, P., Gallart, F. :
EFFICIENCY OF DIFFERENT METHODS TO PREDICT THE SOIL WATER RETENTION CURVE
FROM DIRECT DETERMINATION TO PEDOTRANSFER FUNCTIONS

SESSION 2: 'REDUCTION OF UNCERTAINTIES IN MODEL CONCEPTS USING EXPERIMENTAL DATA'

Bieroza, M.Z., Nowicka, B. :
UNCERTAINTY IN LAKE NET GROUNDWATER FLOW ASSESSMENT IN THE RIVER-LAKE
SYSTEMS (THE WATER BUDGET METHOD)

Casper, M., Gemmar, P., Gronz, O., Johst, M., Stüber, M. :
ENHANCEMENT IN FLOOD PREDICTION FOR SMALL BASINS BY USING SOIL MOISTURE
OBSERVATIONS IN HIGH SPATIAL AND TEMPORAL RESOLUTION AND FUZZY LOGIC SYSTEMS

Dohnal, M., Dusek, J., Vogel, T., Sanda, M. :
THE EFFECT OF SPATIO-TEMPORAL VARIABILITY OF HYDRAULIC PROPERTIES ON THE
SIMULATED DEVELOPMENT OF SOIL WATER PRESSURE IN THE UHLIRSKA WATERSHED

Kriauciuniene, J., Kopustinskas, V., Vileiniskis, V., Kaliatka, A., Gailiusis, B. :
CALIBRATION OF HYDRODYNAMIC MODEL OF THE KAUNAS RESERVOIR, LITHUANIA

Neruda, M., Neruda, R., Kudova, P., Fiedlerova, K. :
RAINFALL-RUNOFF MODELLING WITH ARTIFICIAL NEURAL NETWORKS IN THE SAZAVA
BASIN

Timbe, L., Willems, P. :
UNCERTAINTY ON SIMULATION OF SYNTHETIC HYDROGRAPH EVENTS IN RIVER FLOOD
MODELS

Zhang, G.P., Gerrits, A.M.J., Savenije, H.H.G., McDonnell, J.J. :
EFFECTS OF INTERCEPTION ON SUBSURFACE BEHAVIOUR: A VIRTUAL EXPERIMENT IN THE
HESPERANGE CATCHMENT, LUXEMBOURG, USING THE REW APPROACH

SESSION 3: ‘CALIBRATION OF HYDROLOGICAL MODELS: COPING WITH CONCEPT SHORTCOMINGS AND DATA UNCERTAINTIES’

Llorens, P., Gallart, F., Latron, J., Poyatos, R., Rubio, C., Garcia-Pintado, J. :
SIMULATING THE WATER BALANCE OF CATCHMENTS WITH DIVERSE VEGETATION TYPES
WITHIN THE TOPMODEL FRAMEWORK

Goegebeur, M., Pauwels, V.R.N. :
IMPROVEMENT OF THE PEST PARAMETER ESTIMATION ALGORITHM THROUGH EXTENDED
KALMAN FILTERING

SESSION 4: ‘NEW IDEAS, DEVELOPMENTS AND EXPERIENCES IN SMALL BASIN RESEARCH’

Alvera, B. :
SNOW DEPTH AND SNOW COVER IN A SMALL PYRENEAN WATERSHED

Bíba, M., Jarabác, M., Oceánská, Z., Vícha, Z. :
FINDINGS AFTER FIFTY TWO YEARS LONG FOREST-HYDROLOGICAL RESEARCH FROM TWO
SMALL EXPERIMENTAL WATERSHEDS IN THE BESKYDY MTS., CZ

Bubenicková, L., Ricicová, P., Kulasová, A. :
MODELLING OF FLOOD WAVES IN THE JEZDECKA EXPERIMENTAL BASIN

Fucik, P., Bystricky, V., Lexa, M. :
MONITORING THE WATER QUALITY OF AGRICULTURAL DRAINAGE SYSTEMS IN THREE
SELECTED REGIONS OF THE CZECH REPUBLIC IN CONNECTION WITH THE ACTUAL NITRATE
MONITORING PROGRAMME PRACTISED FOR PURPOSES OF THE EC NITRATES DIRECTIVE
(91/676/EEC) IN SMALL WATER COURSES

Halmova, D., Miklanek, P., Pekarova, P. :
OBSERVATION AND CALCULATION OF DAILY RAINFALL INTERCEPTION OF THE HORNBEAM FOREST

Lana-Renault, N., Latron, J., Regüés, D., Serrano, P., Nadal, E., Martí-Bono, C. :
TEMPORAL VARIABILITY OF THE HYDROLOGICAL RESPONSE IN A SMALL HUMAN DISTURBED CATCHMENT IN THE CENTRAL SPANISH PYRENEES

Martínez-Carreras, N., Krein, A., Iffly, J-F., Salvia-Castellví, M., Pfister, L., Hoffmann, L., Gallart, F. :
SUSPENDED SEDIMENT TRANSPORT AND DYNAMICS IN THE ATTERT RIVER BASIN (GRAND-DUCHY OF LUXEMBOURG)

Moquet, A., Matgen, P., Hoffmann, L., Pfister, L. :
TEMPORAL RADAR SERIES, A TOOL TO INVESTIGATE EVOLUTION OF SOIL MOISTURE CHARACTERISTICS DURING WINTER IN AN AGRICULTURAL BASIN?

Nadal-Romero, E., Regüés, D., Latron, J., Martí-Bono, C., Serrano-Muela, M.P., Lana-Renault, N. :
HYDROLOGICAL AND SEDIMENT DYNAMICS IN A SMALL CATCHMENT WITH BADLAND AREA (CENTRAL SPANISH PYRENEES): INSTRUMENTATION AND PRELIMINARY RESULTS

Rafailova, E. :
ROLE OF SATURATION OF THE CATCHMENT AREA IN RUNOFF FORMATION

Rusjan, S., Brilly, M., Mikoš, M., Padežnik, M., Vidmar, A. :
HYDROLOGIC AND WATER CHEMISTRY CHARACTERISTICS OF THE PADEZ STREAM

Sebin, M., Pekarova, P., Pekar, J. :
LONG-TERM PREDICTION OF MONTHLY NITRATE CONCENTRATION IN THE RYBARIK MICROBASIN

Serrano-Muela, P., Regüés, D., Latron, J. :
RAINFALL INTERCEPTION UNDER DIFFERENT FOREST COVERS IN THE CENTRAL SPANISH PYRENEES

Soler, M., Regüés, D., Gallart, F. :
AUTOMATIC SAMPLER CALIBRATION TO ESTIMATE THE COLLECTION CAPACITY OF SUSPENDED SEDIMENT

Uhlířová, J. :
SURVEY OF EFFICIENCY OF EROSION AND FLOOD CONTROL MEASURES

Westhoff, M.C., Luxemburg, W.M.J, Van de Giesen, N.J. :
HIGH RESOLUTION TEMPERATURE OBSERVATION FOR QUANTIFICATION OF LATERAL INFLOW: A TEST CASE FOR THE MAISBICH RIVER

Klotz, S., Mathys, N., Olivier, J.-E. :
SEDIMENT TRANSPORT OBSERVATION IN THE DRAIX FIELD LABORATORY: MEASUREMENT PROCEDURE AND INVENTORY OF THE SOURCES OF UNCERTAINTIES

Ferrero, A., Lisa, L., Lipiec, J. :
MONITORING RUN-OFF AND SOIL LOSSES FROM SLOPING VINEYARDS IN A HILLSIDE CATCHMENT

Maca, P., Torfs, P., Pavlasek, J., Pech, P. :
EVALUATION OF THE ROLE OF TEMPORAL RAINFALL DISTRIBUTION IN RUNOFF PROCESS

Redinova, J., Pavlasek, J., Maca, P., Skalska, P., Roub, R. :
REAL-TIME FLOOD FORECASTING

Skalska, P., Pavlasek, J., Maca, P., Redinova, J. :
OUTFLOW DURING SPRING SNOWMELT PERIOD ON MODRAVA EXPERIMENTAL CATCHMENTS

Pavlasek, J., Maca, P., Redinova, J., Skalska, P., Hanel, M. :
MODRAVA EXPERIMENTAL WATERSHEDS

Horacek, S., Maca, P., Pavlasek, J., Rednova, J. :
APPLICATION OF CHOSEN EVENT BASED RAINFALL RUNOFF MODELS ON THE SMALL
MOUNTAIN CATCHMENT MODRAVA